Studies in archaeometry

Edited by
Mario Ramírez Galán
Ronda Sandifer Bard

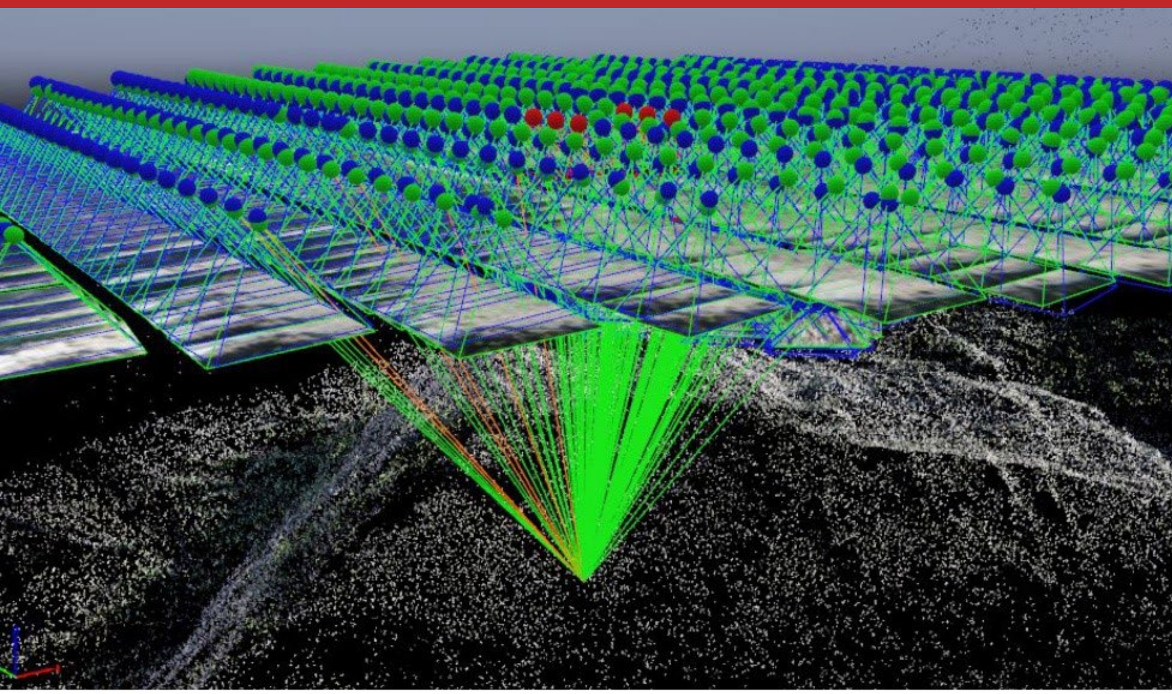

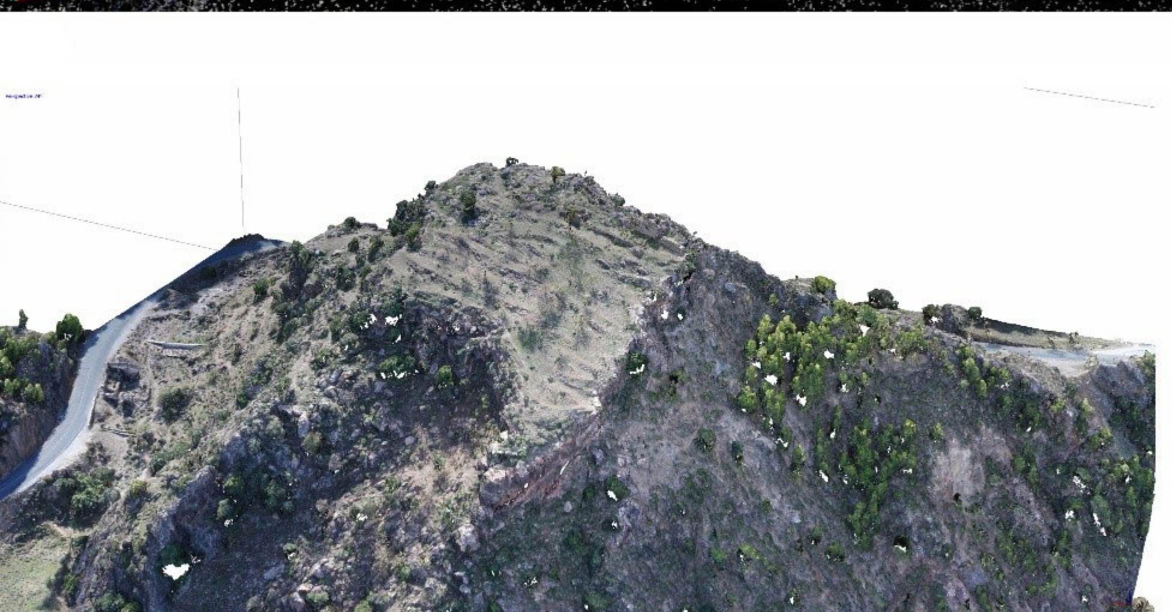

Access Archaeology

Archaeopress Access Archaeology

About Access Archaeology

Access Archaeology offers a different publishing model for specialist academic material that might traditionally prove commercially unviable, perhaps due to its sheer extent or volume of colour content, or simply due to its relatively niche field of interest. This could apply, for example, to a PhD dissertation or a catalogue of archaeological data.

All *Access Archaeology* publications are available as a free-to-download pdf eBook and in print format. The free pdf download model supports dissemination in areas of the world where budgets are more severely limited, and also allows individual academics from all over the world the opportunity to access the material privately, rather than relying solely on their university or public library. Print copies, nevertheless, remain available to individuals and institutions who need or prefer them.

The material is refereed and/or peer reviewed. Copy-editing takes place prior to submission of the work for publication and is the responsibility of the author. Academics who are able to supply print-ready material are not charged any fee to publish (including making the material available as a free-to-download pdf). In some instances the material is type-set in-house and in these cases a small charge is passed on for layout work.

Our principal effort goes into promoting the material, both the free-to-download pdf and print edition, where *Access Archaeology* books get the same level of attention as all of our publications which are marketed through e-alerts, print catalogues, displays at academic conferences, and are supported by professional distribution worldwide.

The free pdf download allows for greater dissemination of academic work than traditional print models could ever hope to support. It is common for a free-to-download pdf to be downloaded hundreds or sometimes thousands of times when it first appears on our website. Print sales of such specialist material would take years to match this figure, if indeed they ever would.

This model may well evolve over time, but its ambition will always remain to publish archaeological material that would prove commercially unviable in traditional publishing models, without passing the expense on to the academic (author or reader).

Archaeopress Access Archaeology

Studies in archaeometry

Proceedings of the archaeometry symposium at NORM 2019, June 16-19, Portland, Oregon, Portland State University.Dedicated to the Rev. H. Richard Rutherford, C.S.C., Ph.D

Edited by

Mario Ramírez Galán

Ronda Sandifer Bard

Access Archaeology

Archaeopress Access Archaeology

Archaeopress Publishing Ltd
Summertown Pavilion
18-24 Middle Way
Summertown
Oxford OX2 7LG
www.archaeopress.com

ISBN 978-1-78969-734-6
ISBN 978-1-78969-733-9 (e-Pdf)

This book is available direct from Archaeopress or from our website www.archaeopress.com

A mis padres y hermanos, por estar siempre ahí

y apoyarme en mi sueño.

Index of contents

Identification of iron and wood through the effects of microstructures in timber-laced walls of the Celtic Iron Age of the Iberian Peninsula. Luis Berrocal-Rangel, Rosario García-Giménez, Raquel Vigil de la Villa, Carmen Gutiérrez-Sáez, Lucía Ruano & Marcos Osório **1**

Traction or hybrid trebuchet? The use of physical calculations to classify trebuchets. Mario Ramírez Galán, María Benítez Galán, Rafael Montalvo Laguna, Reina Inlow & Ronda S. Bard **23**

Blue-and-white porcelain in early South Thailand maritime trade. Angelica Kneisly, William Ayres & Maury Morgenstein.. **45**

Archaeometallography: a new look at old issues in the history of the iron industry. N. N. Terekhova & V. I. Zavyalov.. **66**

Falling from the sky. Aerial photogrammetry and LiDAR applied to the archaeology of architecture and landscape: two fortifications from the Alpujarra (Granada, Spain). Jorge Rouco Collazo, José Antonio Benavides López & José María Martín Civantos **87**

Early Roman Iron Age jewellery in the Northern Barbaricum: between stylistic and technological simplicity and luxury. Audronė Bliujienė, Gediminas Petrauskas, Jurga Bagdzevičienė, Sergej Suzdalev & Evaldas Babenskas **175**

The application and evaluation of remote sensing techniques to household archaeology on the Northwest Coast. William T. D. Wadsworth, Andrew Martindale, Colin Grier & Kisha Supernant............................**218**

Identification of iron and wood through the effects of microstructures in timber-laced walls of the Celtic Iron Age of the Iberian Peninsula

Luis Berrocal-Rangel (*Autonomous University of Madrid*), Rosario García-Giménez (*Autonomous University of Madrid*), Raquel Vigil de la Villa (*Câmara Municipal de Sabugal*), Carmen Gutiérrez-Sáez (*Autonomous University of Madrid*), Lucía Ruano (*Autonomous University of Madrid*), Marcos Osório (*Câmara Municipal de Sabugal*)

Abstract

Vitrified forts in the European Iron Age is a well-known phenomenon with different causes and interpretations but with a similar effect: the vitrification of an enormous amount of stones, used as masonry for the construction of the ramparts. Among the many causes, the most supported one is the fire of a wall which was built with an inner timber laced structure and a massive use of stones. This proposal can be defended by the construction systems of walls between the Gaullish peoples of Central Europe, such as *murus gallicus*. This system consisted in a combination of an armed wooden structure linked by iron nails and masonry. Thus, archaeological excavations of this type of walls provide vitrified stones beside iron nails and wood timber remains. Over the last two decades, several vitrified forts have been found in the Celtic territories of Western Iberia. Recently, we have studied these cases and we have been able to find evidences of the use of iron nails and wooden timbers, thanks to the analysis of microstructures in combination with microphotography of the vitrified stones.

Keywords

Vitrified forts; Ramparts; Fortification; Architectural Archaeology; Microstructures

1. Introduction

The existence of a defensive architecture with timber laced structures and a massive use of stones in Celtic Iberia during the Iron Age has been discussed for decades, looking for the connection between some classical Greek and Roman written testimonies and archaeological remains, but without clear conclusions (Esparza 1982: 401-402; Moret 1996: 76; Berrocal-Rangel & Moret 2007: 24-26). To solve this polemical subject, we have included it in the objectives of a research project, supported by the Spanish

Ministry of Science.[1], which has allowed us to analyse it through archaeometry techniques, applied to the raw materials used to build the Iron Age ramparts of Spain and Portugal.

We have studied a short number of archaeological sites, such as the hillfort of Chao Samartín, at the Asturias country, north-western Spain, and a growing number of vitrified ramparts that have been located along the Spanish and Portuguese frontier lands. In the last issue of the *Journal of European Archaeology*, we have published a synthesis with the first geochemical analyses and proposed a chronological context between the end of the Bronze Age and the end of the Iron Age for these archaeological remains (Berrocal-Rangel *et al.* 2019). In this paper, we have used the archaeological record not only to understand the causes of the vitrification of these ramparts in Western and Northern Europe, the subject that it is usually investigated, but mainly to advance our technical knowledge about the existence of an architecture with timber laced structures in Iberia, similar to the well-known ramparts of the Gaullish peoples (e.g., Fichtl 2010; Ralston 2006).

With this target, we have face new facts that support the hypothesis of the existence of this type of architecture by proving the use of beams, timbers and nails that were burnt in a vitrification process. And these results, crossed with other analyses, are included in the historical context of the Roman Conquest of the Iberian Peninsula, during the last two centuries before Christ (Dobson 2008; Curchin 2014). This was a period in which the circumstances of the war forced the Celtic peoples of Iberia to use *oppida*-refuges, just as it would happen in Gaul a century later (Deyber 2013; Gruel and Buchsenschutz 2015; Moret 2017: 171-180).

2. The uncertainty of the Classical testimony

Iberian building traditions were among those of the Mediterranean cultures, over a masonry architecture: the use of compartmented ramparts, built with mud bricks and, even, with earth-laying fills is well-known in the Mediterranean Spain, the land that was inhabited by the true Iberian people (Sanmartí 2009; Ruiz and Molino 1998; Moret 1996).

But most of the Iberian Peninsula was not inhabited by Iberian but Celtic people, so architecture traditions could be very different (Almagro-Gorbea 2014). And the Classic testimonies, those ought to the Roman and Greek writers, support these differences, mainly by some few quotations about this use of a timber laced architecture in the northern and western Peninsula. For example, the text of the Greek historian Appian of Alexandria, in the First book of *Roman Civil Wars*, 112, says: *While Pompey was laying*

[1] 'Late Prehistory Architecture in the Western Spanish Plateau. Archaeotecture and Archaeometry about the built heritage of the Vettones hillforts' (HAR2016-77739-P). Ministry of Economy, Industry and Competitiveness of the Kingdom of Spain.

siege to Pallantia and underrunning the walls with wooden supports, Sertorius suddenly appeared on the scene and raised the siege. Pompey hastily set fire to the timbers and retreated to Metellus (Appian, The Civil Wars, I, 112)[2]. *Pallantia* was a celebrated *oppidum* of the strongest Celtic peoples of the Vaccei, located in Northern Castile, Spain (Balado and Martínez 2009; Sacristán 2011: 190). The site was a stronghold of *Sertorius*, the rebel Roman general who raised against Rome from 80 to 72 BC. He could have entrenched between the indigenous peoples of nowadays Celtic Spain and Portugal, peoples such as the Lusitanians and Vettones not even totally controlled by Roman legions. Therefore, the quote serves to characterize a timber defensive and indigenous architecture, because the Greek text refers literally *destroyed the walls* [built] *with timbers...*

3. The weakness of the Archaeological record

The archaeological record provides few but clear evidences and remains, such as the quoted hillfort of Chao Samartín (Asturias, North-western Spain), the oldest testimony of the Spanish Archaeology dated in the Late Bronze Age.

Chao Samartín is in the edge of a steep plateau, with a wall three metres wide, which was built with large upright timber beams in two parallel rows and a fill of stones (figure 1.1). This rampart was protected outside with a V profile ditch (Villa 2007). Both can be dated at the end of the 8th century BC. Near the wall, a big quadrangular building was discovered. Inside, a sword, one cauldron and fragments of a big bronze riveted disc, that we identified as a shield, were located, which proves the importance of this site. We have not doubt that timber laced ramparts of this type should have been frequent along the Late Bronze Age and Iron Age in the whole northern and Atlantic zone of the Iberian Peninsula, where the environment is adequate for this type of constructions, due to the abundance of timber. But it is true that we do not known another example as clear as this.

[2] Horace White (ed.), Loeb Classical Library, Consulted April 20th 2019: http://remacle.org/bloodwolf/historiens/appien/index.htm 73.

Figure 1. 1. Foundation of the LBA rampart of the hill-fort of Chao Samartin (Asturias, NW Spain), with two parallel rows of holes in the lithic subtract, related to big vertical timbers. 2. Foundations of the two LBA ramparts of the hill-fort of Ratinhos (Alentejo, Southerm Portugal). In the bottom line, two width holes were found with other remains of a burnt wall.

Building ramparts in the Iron Age of the Castilian plateau, and of the Atlantic coast of Iberia, is misunderstood, only because a short number of sites has been dug: most of them are old excavations, from the middle of the 20th century, and weather in the Spanish plateau does not facilitate the preservation of ancient wood implements. Only by the identification of timber prints, holes and carbonized remains, we can find the traces of this type of structures.

However, an authentic tradition of timber laced building can be identified between the *Vaccei*, the quoted strong people of the Northern Spanish plateau: they constructed walls with a wooden formwork and a fill of mud bricks or, simply, mud layers (figure 1.2) - (Sanz Mínguez et al. 2003; Blanco 2015; Ruiz Zapatero 2018: 338-339).

The hillfort of Soto de Medinilla (Valladolid) shows a rampart of mud bricks. This wall has an inside face made with a palisade, a row of upright poles. Their imprints are preserved in a hard clay floor, burnt by a fire. Inside, four or five rows of holes, each half metre deep, would have been supported a parapet walk or, even, the own wall. This rampart was well dated along the 6th century BC (Delibes 1995: 149-150).

The hillfort of Padilla de Duero, also in the province of Valladolid, was the *oppidum* of *Pintia*, one of the richest Vaccei towns, well dated between the 5th and 1st century BC. Wall and households were built with a system like that of the Early Iron Age of Soto de Medinilla, but with rectangular plans: wooden facings and a filling of mud bricks. In the houses, vertical and horizontal inner beams every metre or half a metre formed laced structures, filled with mud layers or mud bricks (Sanz Mínguez et al. 2003).

Therefore, in the Northern Spanish plateau and, probably, along the Bay of Biscay coast, there was a tradition of timber laced architecture since the end of the Bronze Age. This tradition is similar to the ramparts of Central Europe if we change stones for mud or earth as raw materials for the fill and elevation of walls, mainly because there are no stones in this region: the central basin of Douro river is composed by sand and clay, where the only stones are sedimentary rocks, sandstones, conglomerates and lutites, all of them too soft for a lasting construction (Santiesteban et al. 1996: 188-187).

But, at the Western plateau, and at the North-western Iberian Peninsula too, hard stones such as granites, quartzites and slates are more abundant than clay rocks (Valladares et al. 2002: 10-12; Liñán et al. 2002: 23). However, people in these regions followed prehistoric building techniques, according to the principle of stacking (figure 2.1). Most of excavations in Galicia, Asturias and Northern Portugal have dug ramparts of massive dry-stone elevations, with a few exceptions such as the so-called *murallas de módulos* (Berrocal-Rangel 2004: 53-54).

Anyway, regarding the poor and scanty record of building wood in the excavations of the Western Iberia, we have open new paths of research about the use of wood in the construction of the ramparts: we have studied the phenomenon of vitrified walls, identifying mineral components and using them as geo-thermometers. In addition, we have identified possible traces of timbers on the masonry blocks and mud bricks and, furthermore, we are working on photogrammetry and 3D modelling for the virtual reconstruction of these buildings. With this methodology we have been able to identify timber imprints and iron nail traces, thanks to the geochemical analyses and microphotography.

Figure 2. 1. Bastion, or tower, beside the main gate of the Iron Age hill-fort of Yecla la Vieja (Salamanca, Western Spain). 2. Mud brick and earth fills of the Iron Age rampart of Cauca, over a masonry slate and quartzite foundations (Segovia, Central Spain). Photography by F. Blanco García.

4. The contribution of Geochemistry

Vitrified ramparts have a long history of research in Northern and Western Europe (Youngblood et al. 1978; Buchsenschutz and Ralston 1981; Kresten et al. 1993; Cook et al., 2016...). Dry-stone masonry, with clear effects of the action of fire such as vitrification, calcination or reddening were known from Scandinavian countries to Southern Portugal (Berrocal-Rangel et al. 2019: 187, figure 1). These remains do not give evidence of a single historic, cultural or functional phenomenon, but they could be reflecting a specific building tradition.

In the Iberian Peninsula, after the first case was discovered at the *oppidum* of Monte Novo (Alto Alentejo, Central Portugal), several examples of new vitrified stones have come to light thanks to surveying works. They were sometimes identified as remains of metallurgical ovens but, also, as burnt walls, such as Ratinhos and Monte Novo (both in Southern Portugal) and Sabugal Velho (Central Portugal).

The hillfort of Ratinhos was the first site with a vitrified wall to be dug (figure 2.2). Fired remains were in the main entry of the acropolis, the upper platform of this fortified settlement of the Late Bronze Age, that was defended by three rampart lines. At the end of the occupation, dated in the first half of the 8th century BC, the whole acropolis was destroyed by a large-scale fire and, then, abandoned. The fire affected the indoor facade of the rampart, a facing wall of stones with a wooden laced framework. These timbers were supported by big vertical posts, that were identified by holes of 50 x 40 cm, diameter and deepness. These posts were the central axis of other, smaller, that were fixed over them transversally. Some fragments of fired clay pieces show the imprints of these poles and sticks.

We published these stratigraphical results in detail, but this preliminary study lacked the geochemical analyses (Silva et al. 2013). Later, we have used samples from those building materials, both stone and silt, to test our methodology: first, we identified the lithic substrate of this site, that is a grey-greenish slate at Ratinhos. Then, we analysed a sample from this substrate, free of fire traces, just to identify the mineral composition of this protolith. This identification is made through two steps: first, by a visual reconnaissance of thin-films in microscope and, second, through X-Ray diffraction (XRD), using a SIEMENS D-5000 with a Cu anode, operating at 30 mA and 40 kV, using divergence and reception slits of two millimetres and 0.6 mm, respectively. We used the powder method for the bulk sample and the oriented slides method for the <2 μm fraction. The XRD profiles were measured in 0.04 2θ goniometer steps for 3s.

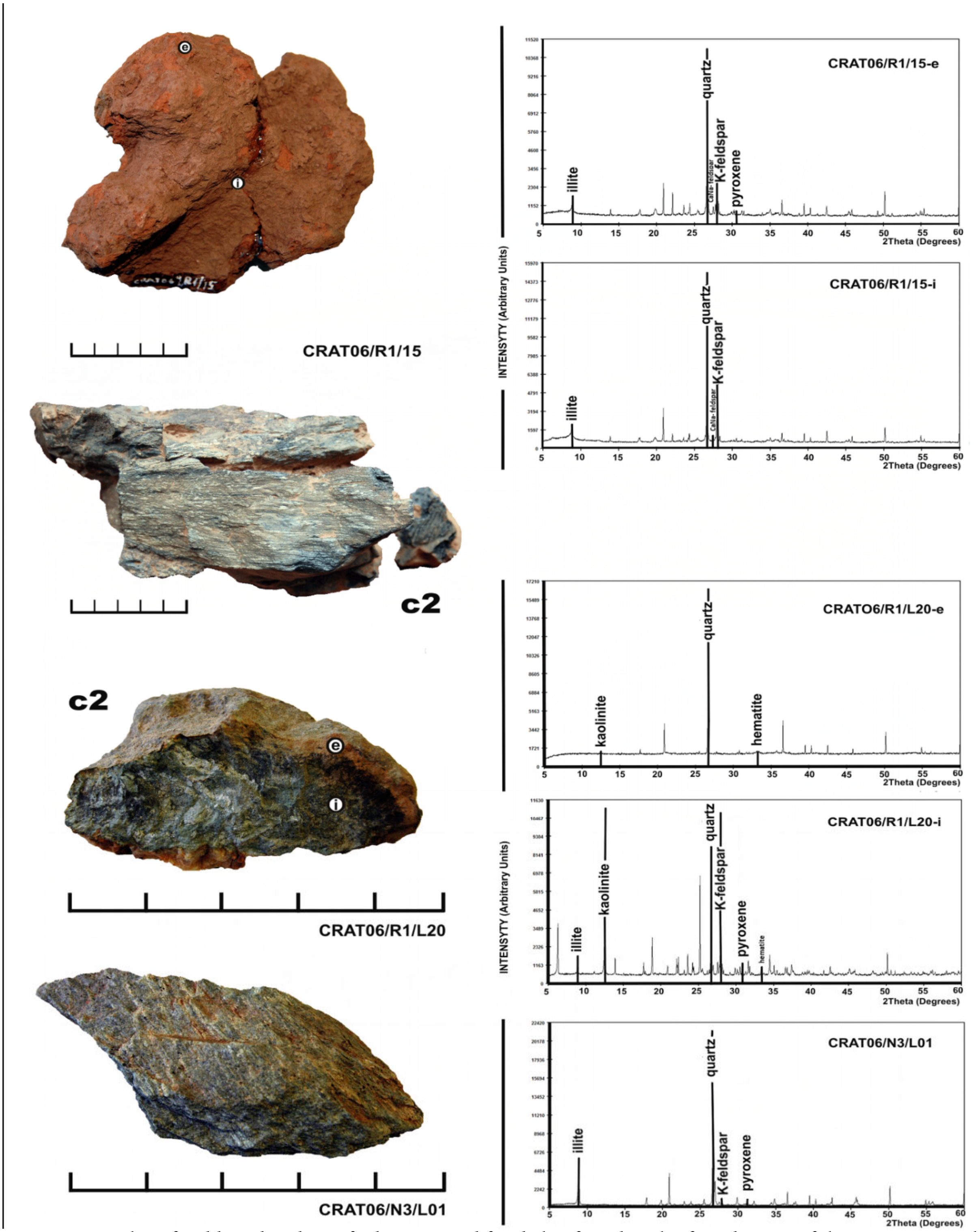

Figure 3. Samples of reddened and vitrified stones and fired clay found in the foundations of the LBA inner wall line of Ratinhos (Alentejo, Southern Portugal), with diffractograms.

The method is based on the comparation between the protolith and the vitrified, calcined or reddened samples from the wall, looking for the presence or absence of minerals and using them as geothermometers (Berrocal-Rangel et al. 2019: 192-194). When the rock shows two different structures, usually with two different colours, we take samples from both zones, core and surface. The same process is made for fired clay pieces such as R001/L15, where the imprint of sticks and poles can be easily view. By confirming the presence or absence of these minerals, we can determine temperatures and, so, types of fires, both reducing or oxidant (figure 3).

The fired samples of Ratinhos show grey-greenish cores and red-orange surfaces, without traces of vitrification or micro-vacuoles. But they were exposed to a fire that burnt a great vertical post and left a layer of fired earth, coal, ashes and fragments of clay lumps with imprints of poles. The analysis of the stone samples reflects the presence of pyroxene, feldspars, illite and quartz. In the cores, great quantities of K-feldspars are significant, because this mineral becomes clay minerals over 1000º C (Sayanam et al. 1989). Also, the presence of kaolinite supports this deduction, because it changes over 650º C (Frías et al. 2013). Similar results were obtained in the surface, which was exposed to a similar temperature. The colour diversity between cores and surfaces do not prove a great difference in temperature, between 650 and 600º C. This rank is not enough to vitrify the stones but to made redden the surfaces. And these results are like those obtained from the fired clay pieces, such as R1/L15.

Therefore, at Ratinhos, the Archaeology and the Geochemistry prove the presence of a simple slate wall that was built with an inner laced timber, at the beginning of the Early Iron Age. This case seems to have parallels in the same region, such as Passo Alto and Azenha da Misericordia. The fire was located in a specific point of the wall, the main entrance, and was related to a large-scale fire that affected the whole upper enclosure of the settlement, the acropolis. It is coherent to see a war cause in this destruction, with a localized fire that cooked mud bricks but only reddened the stones.

The *oppidum* of Monte Novo, in the same Portuguese region of Alentejo, is a quite different example, but very significant. The presence of true vitrified stones is located along a big stretch of the rampart. This settlement was defended by three lines of walls, enclosing a surface of more than 20 ha (Correia 1995). According to the superficial remains, it is dated in the Late Iron Age or along the Sertorian Wars, contemporary to the case of *Pallantia* and the previous quotation of Appian of Alexandria. The third and outer wall has provided fired mud bricks and vitrified stones. The wall must have been built with mud bricks over a dry-stone base: a fire along 300 metres must have affected the whole rampart (Burgess et al. 1999: 142-143).

The analysis of one shale stone from the wall, MN002, shows micro-vacuoles and a clearly vitrified surface, both of them proof of a strong and concentrated fire: the illite is found on the surface sample, but not in the core, where temperature must have been over 1000º C, because the illite disappears between 900 and 1000º C (figure 4). Also, the presence of pyroxene in the core proves temperatures over 1100º C (García-Giménez et al. 2016).

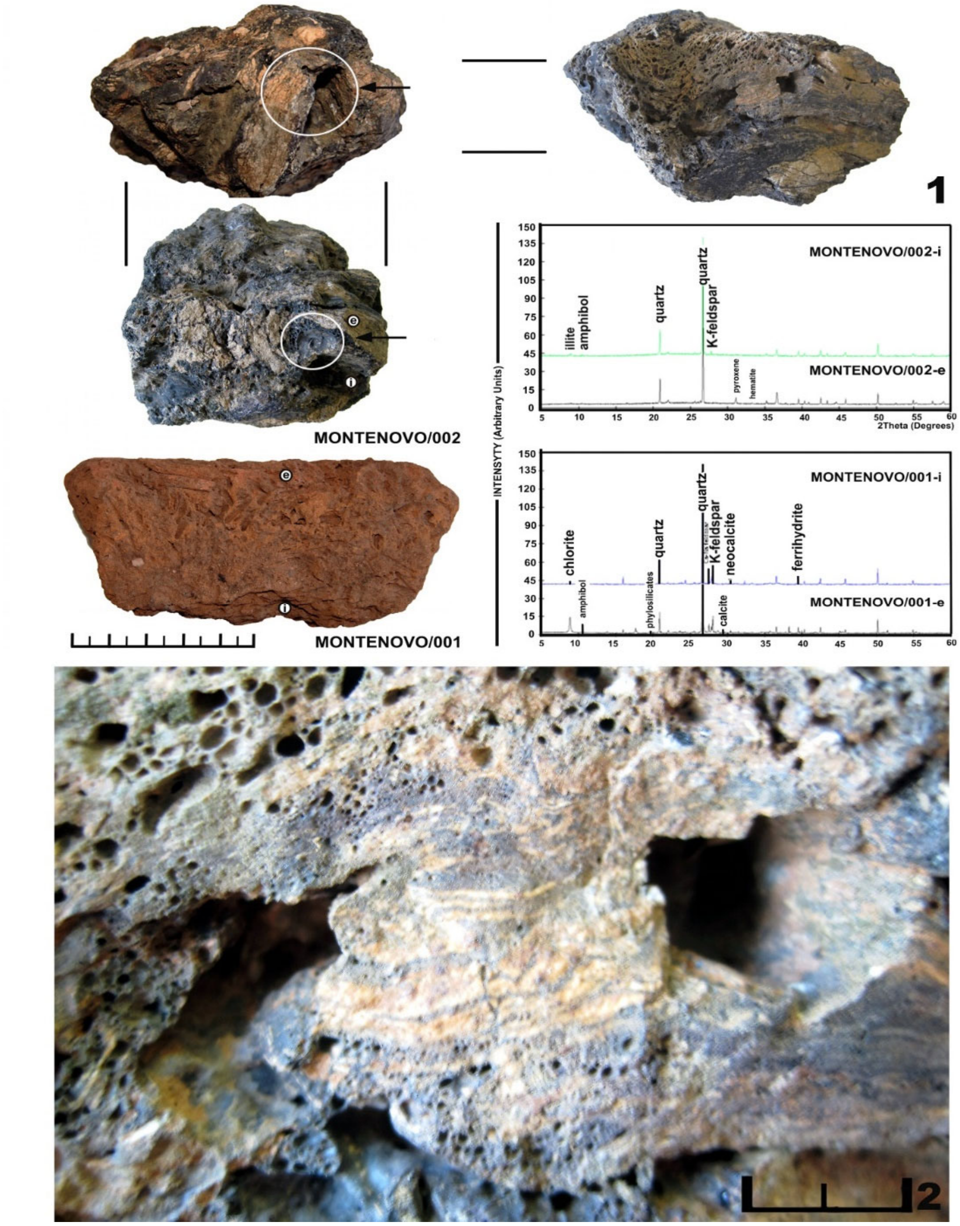

Figure 4.1. Samples of vitrified stones and fired mud brick found in the Iron Age wall of Castelos de Monte Novo (Alentejo, Southern Portugal), with diffractograms. 2. Detail of the stone sample nº 1, MONTENOVO/002, with two prismatic holes.

In the same vein, the analysis of the mud brick MN001 has provided very significant results, with the presence of chlorite, secondary calcite and ferrihydrite. A big quantity of chlorite supports a lower temperature than the stones, since hydroxyl groups of the structure change between 600 and 700º C in favour of chlorite and the conversion of calcite into secondary calcite happens between 600 and 850º C. (García-Giménez et al. 2016: 64). This behaviour matches a fire that started as reducing in the stone plinth and grew as oxidant over the whole wall of mud bricks.

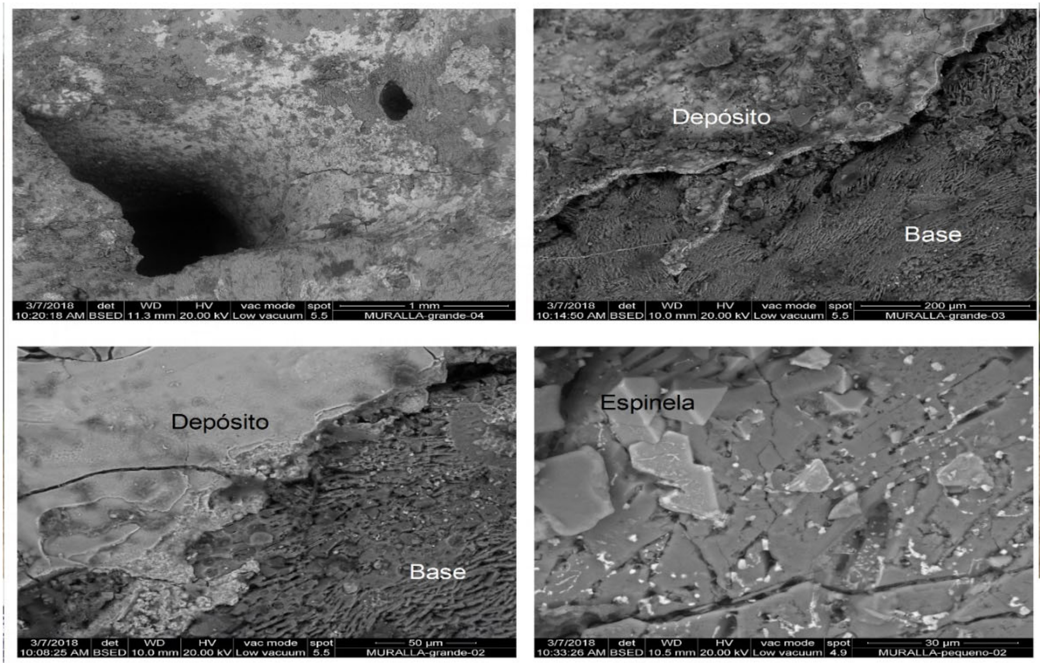

oxides (%)	Clay support	Deposits	Spinel
Na_2O	1.45	-	-
MgO	0.63	0.47	10.52
Al_2O_3	21.88	3.96	**38.60**
SiO_2	51.51	7.09	14.07
P_2O_5	1.32	3.21	0.37
SO_3	-	0.42	-
K_2O	8.20	0.73	1.58
CaO	5.64	0.83	0.72
TiO_2	1.08	0.30	1.19
MnO_2	-	0.68	0.75
Fe_2O_3	8.28	**82.32**	**32.20**

Figure 5. Analysis of the internal wall of one of these holes, with Scanning Electron Microscopy (SEM), and the two found covering layers: the inner one of clay, similar to the mud bricks (Clay depostis = Depósito); the outer one, composed by iron minerals, between them, octahedral crystals as ferric spinel (Spinel = Espinela).

But the sample MN002 gave us another significant fact: there were two prismatic holes of one cm side each. We analysed the internal walls of one of these holes, looking for possible remains thanks to the Scanning Electron Microscopy (SEM), and we found two covering layers: the inner one of clay, similar to the mud bricks. This material is laminar and is composed by an aluminium silicate with magnesium, sodium, potassium and calcium (figure 5). There were also small quantities of iron, phosphate and titanium, anomaly concentrated. But the outer layer was composed by iron minerals. It is possible to identify octahedral crystals as ferric spinel. The spinel is a double oxide that appeared at temperatures over 650º C, reaching 1300º C, according to composition and structure (Özden & Dunlop 2000; Kumar Sinha et al. 2015; Ponomar et al. 2018). Therefore, we could prove the presence of an iron mineral inside one of these holes, a mineral which is produced at temperatures to 1300º C. We propose that these holes are the imprints of iron nails, that could have partially melted during the fire.

The hill-fort of Sabugal Velho, Central Portugal, was a Late iron Age fortification, contemporary to the preceding Monte Novo (Osório and Pernadas 2011). At this place, the rampart was fired, and remains of vitrified rocks have been recovered from superficial surveying but also from scientific excavations. In them, we have been able to identify vacuoles, micro-vacuoles, true vitrified surfaces, and also, we can find vitrified stones with this singular pair of holes! (figure 6).

But we are curious about the interesting regular shapes that it is easy to identify on the surfaces of these stones. As a new line of research, we are now considering the possible existence of regular patterns, that could reveal prints of timbers.

Although we are still studying such possibility, we can advance some results: for example, the distributions of vacuoles are clearly related to the proximity of the deepest zone of the marks, usually with regular edges (figures 6.3 and 7.2-4). Along this area, there are not vacuoles, probably because the intensity of the fire avoided all kind of gas release to the atmosphere. When we move away from the cores, vacuoles appear and progressively became bigger and more separated, as the result of the gas release (Pullen 2011: 729).

Figure 6. 1. Main gate of the earth and stone Iron Age wall of the hill-fort of Sabugal Velho (Central Portugal), with the places where vitrified stone are found; 2. Vitrified stone as it was found beside the wall; 3 and 4. Marks with regular edges, supposed to be wooden traces; 5. Two prismatic holes in one vitrified stone.

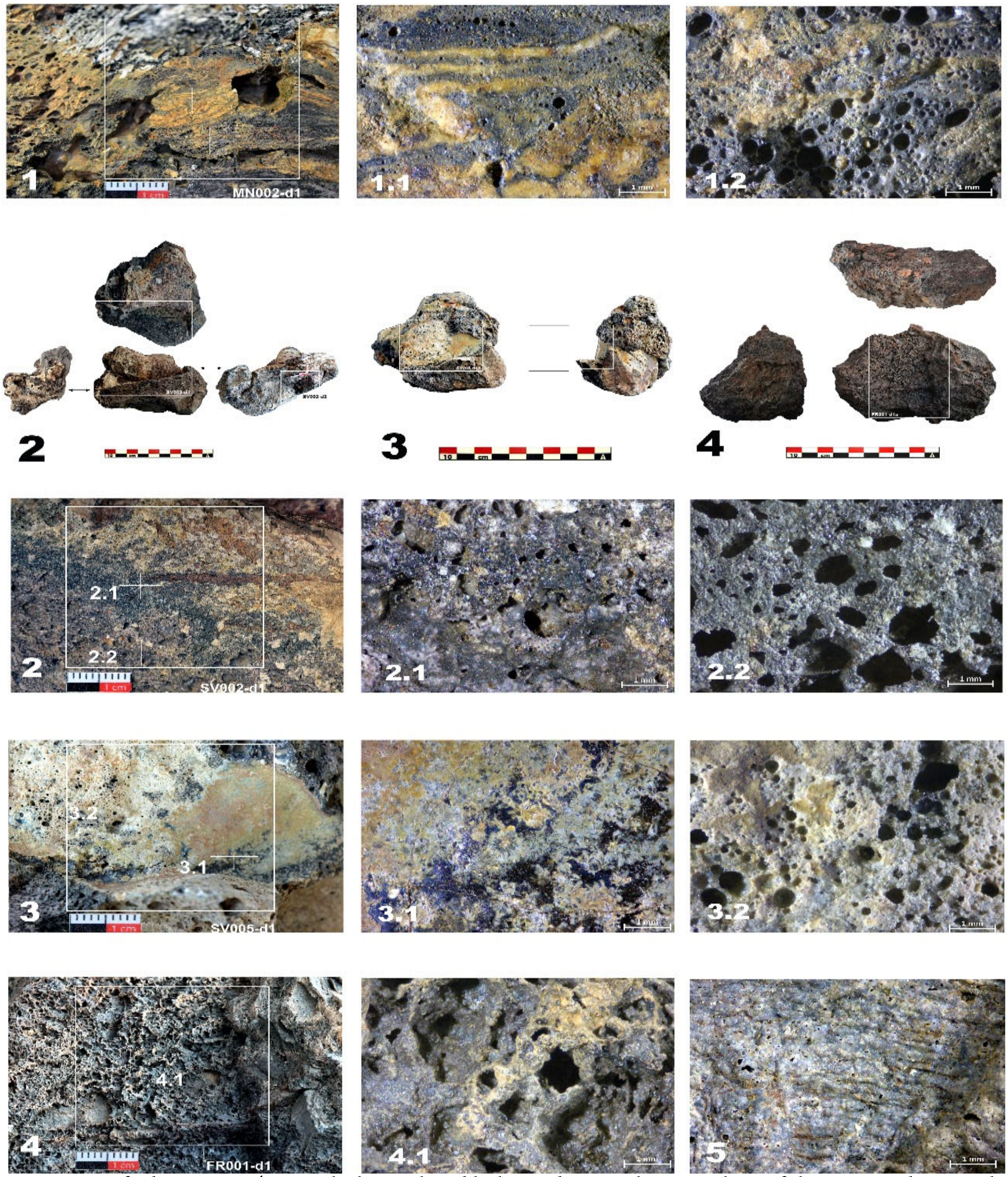

Figure 7. 1. Vitrified stone MN/002 with the analysed holes and microphotographies of the surround's vacuoles in the crossed point (1.1) and 2 cm. away (1.2); 2 and 3. Samples SV002 and SV005 from vitrified stones of Sabugal, with vacuoles in the crossed points (2.1 and 3.1) and 2 cm. away (2.2 and 3.2); 4. A vitrified stone from a metallurgical oven from Iron age site of Fraga de Romualdo (Huelva, SW Spain) and vacuoles in the crossed point (4.1); 5. Detail of supposed wooden marks in the sample SV007 of Sabugal.

In the sample MN002, we can find many small vacuoles near the pair of holes, with an average of 0.2 x 0.2 mm, while the vacuoles are bigger and spherical just 2 cm away, reaching 0.4x0.4 mm[3]. This pattern is the same that we can find in the sample SV002, where microvacuoles are 0.2x0.2 mm in the edge of the possible imprint. They measure 0.4 x 0.2 mm and show tubulars profiles 2 cm away from this edge, reaching 0.8x0.6 mm with spherical shapes, 3 cm away (figure 7). When we study a truly vitrified surface, as the example SV005, we cannot observe vacuoles, only surface radial cracks, while few centimetres away very small vacuoles are identified, of 0.1 x 0.2 mm and smaller.

By contrast, the same approach made to a stone, FR001, from a metallurgical oven found at the Iron Age site of Fraga do Romualdo (Huelva, Soutwestern Spain) threw very different results: the vacuoles are irregularly spread by all the surface of the stone, and they are bigger and regular in size, of a diameter of one millimetre (figure 7.4).

5. The infography to the rescue

Our third line of research is the use of LiDAR images, photogrammetry and 3D restitutions of walls, with which we have obtained really good results.

This is the case of the main gate of the big fortified settlement of La Mesa de Miranda, at the Avila country, Central Spain (Álvarez-Sanchís 2007: 239-240; Fabián 2005: 36-37). We have made a photogrammetric study of this interesting building thanks to which we have obtained a 3D model that is being used in an on-going virtual reconstruction (figure 8).

Thanks to this study, we could find regular notches between the big blocks of the plinth, with a measurement of one or two Hellenistic foot unit of 27 cm in width, known as *Osco foot*, which was used in Western Europe and the Mediterranean along the Late Iron Age (Peterse 1984; Gabba 2003; Stieglitz 2006). And we could prove that there is a connection between the notches of the inner and the outer facings of the building, raising the possibility of a timber laced building at the end of the Iron Age.

[3] We use a binocular microscope Stemi305-N ZEISS, with a 8-80X objective and zenithal light. We took the pictures with a built-in digital camera AXIOCAM ERc 5 s ZEISS.

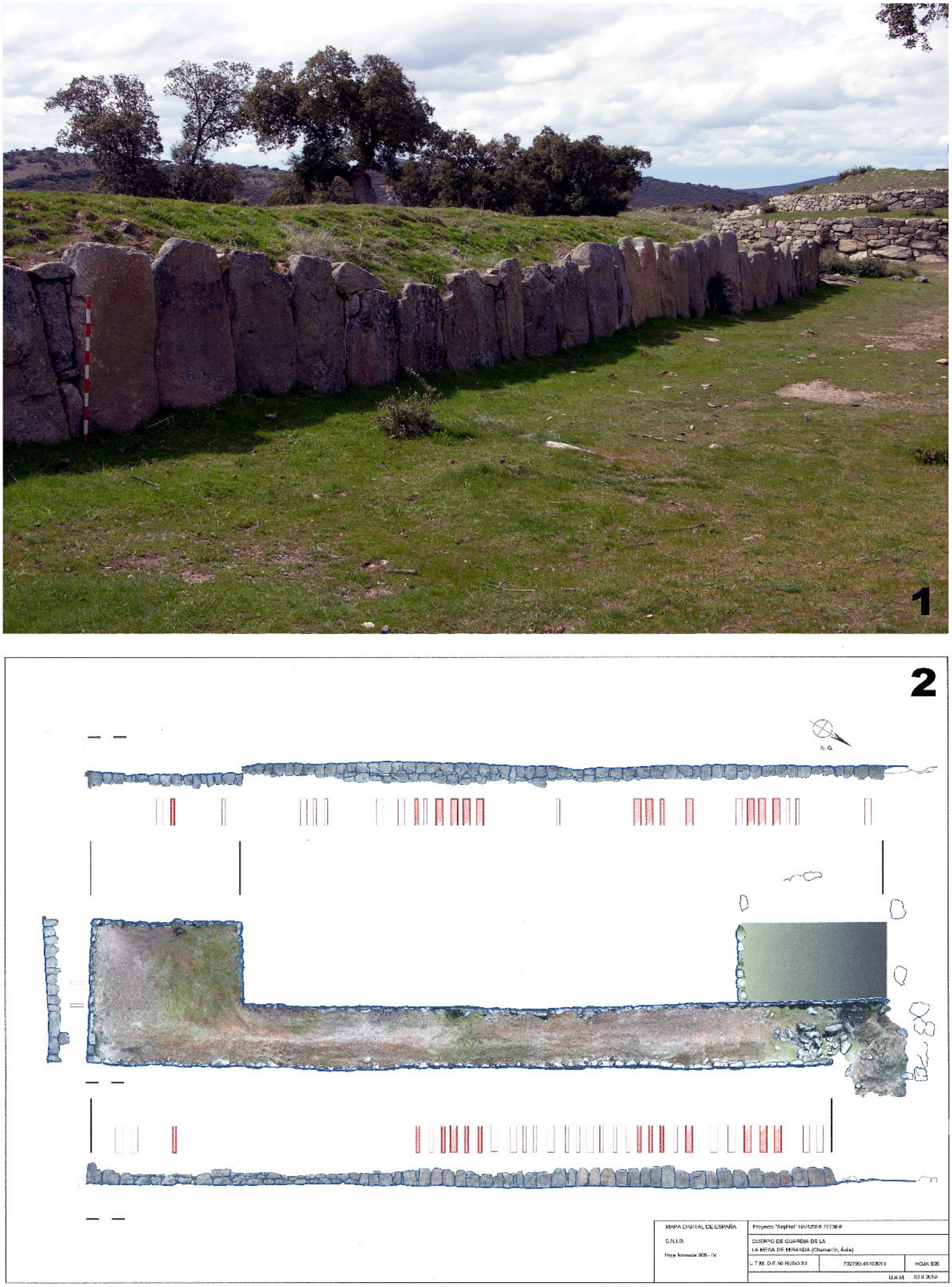

Figure 8. 1. Main gate of the oppidum of La Mesa de Miranda (Ávila, Central Spain), with cyclopean masonry foundations. View from the North; 2. Orthophotography of this gatehouse building, with the alignments of supposed timber marks.

6. Conclusions

This research wants to defend the existence of a timber laced architectural tradition between the Celtic people of the Iberian Peninsula. That was a very debated subject because of the uncertainty of the Classical testimonies and the weakness of the Archaeological record, but thanks to the geochemical analyses and the microphotography, beside the Photogrammetry and the 3D restitution of some constructions, we can defend new ways of approaching the knowledge about these building techniques. Based on these results, we support the existence of ramparts in the West and North of the Iberian Peninsula that could have been constructed following a similar system that the well-known *murus gallicus* during the 1st century BC in Central Europe.

7. References

Almagro-Gorbea, M. (ed) 2014. *Protohistory of the Far West of Europe: From Neolithic to Roman Conquest.* Burgos: Universidad de Burgos & Fundación Atapuerca.

Álvarez-Sanchís J.R. 2007. El poblado fortificado de la Mesa de Miranda (Chamartín, Ávila) y su relación con el poblamiento prerromano del Valle Amblés. In L. Berrocal-Rangel & P. Moret (eds) *Paisajes fortificados de la Edad del Hierro*: 237-254. Madrid: Bibliotheca Archaeologica Hispana 28 - RAH.

Balado, A. & A.B. Martínez 2009. Excavaciones arqueológicas en la Capilla de los Reyes de la Catedral de Palencia: nuevos datos sobre el origen de la Pallantia romana. *Sautuola* XV: 311-326.

Berrocal-Rangel, L. 2004. La defensa de la comunidad. Sobre las funciones emblemáticas de las murallas protohistóricas en la Península Ibérica. *Gladius* XXIV: 27-98.

Berrocal-Rangel, L. & Moret P. 2007. Las fortificaciones protohistóricas de la Hispania céltica. Cuestiones a debate. In L. Berrocal-Rangel & P. Moret (eds) *Paisajes fortificados de la Edad del Hierro*: 169–330. Madrid: Real Academia de la Historia, Casa de Velázquez.

Berrocal-Rangel, L.; García-Giménez, R.; Ruano, L. & Vigil de la Villa R. 2019. Vitrified Walls in the Iron Age of Western Iberia: New Research from an Archaeometric Perspective. *European Journal of Archaeology* 22.2: 185-209. DOI: https://doi.org/10.1017/eaa.2018.69

Blanco, J.F. 2015. Piedra y barro. La muralla de la ciudad vaccea de Cauca. *Vaccea Anuario* 8: 38-46.

Blanco-González, A. 2018. De cabañas a casas. Estrategias sociales en la Prehistoria Final de la Meseta (1400-400 AC). In A. Rodríguez Díaz; I. Pavón & D. M. Duque (eds) *Más allá de las casas. Familias, linajes y comunidades en la Protohistoria peninsular*: 297-361. Cáceres: Universidad de Extremadura.

Burgess, C.; Gibson, C.; Correira, V.H. & I. Ralston 1999. Hillforts, Oppida and Vitrification in the Évora Area, Central Portugal, 1986–1988. A Preliminary Report. *Northern Archaeology* 17/18: 129–47.

Correia, V.H. 1995. The Iron Age in South and Central Portugal and the Emergence of Urban Centres. In B. Cunliffe and S. Keay (eds) *Social Complexity and the Development of Towns in Iberia*: 237–262. Oxford: Oxford University Press for British Academy.

Curchin, L.A. 2014. *Roman Spain. Conquest and Assimilation.* Abingdon and New York: Routledge.

Delibes, G.; Romero, F. & Ramírez, M.ª L. 1995. El poblado 'céltico' de El Soto de Medinilla (Valladolid). Sondeo estratigráfico de 1989-1990. In G.Delibes, F. Romero & A. Morales (eds) *Arqueología y Medio Ambiente. El primer milenio a.C. en el Duero medio*: 149-177.Valladolid: Junta de Castilla y León.

Deyber, A. 2013. Oppida en action. Libres réflexions sur le rôle militaire de l'oppidum gaulois (58-51 a.C.). In S. Krausz, A. Collin, K. Gruel, I. Ralston & Th. Dechezleprêtre (eds) *L'Âge du Fer en Europe. Mélanges offerts à Olivier Buchsenschutz*: 661-670. Bordeaux: Ausonius.

Dobson, M. 2008. *The Army of the Roman Republic: The 2nd century BC, Polybius, and the Camps at Numantia.* Oxford: Oxbow Books.

Esparza, A. 1982. Reflexiones sobre el castro de Monte Bernorio (Palencia). *Publicaciones de la Inst. Tello Téllez de Henares* 47: 393-408.

Fabián García, F. J. 2005. *Guía del Castro de la Mesa de Miranda.* Ávila: Cuadernos de Patrimonio Abulense, 2.

Fichtl, S. (ed) 2010. *Murus celticus. Architecture et fonctions des remparts de l'âge du Fer* (Collection Bibracte, 19). Glux-en-Glenne: Centre archéologique européen.

Frías, M.; Vigil de la Villa, R.; García, R.; Sánchez de Rojas, M.I. & Juan, A. 2013. The Influence of Slate Waste Activation Conditions on Mineralogical Changes and Pozzolanic Behavior. *Journal of the American Ceramic Society* 96: 2276–2282. <https://doi.org/10.1111/jace.12387>.

Gabba, E. 2003. *Misurare la terra: centuriazione e coloni nel mondo romano*, vol. 1: Modena: Edizioni Panini.

García-Giménez, R.; Vigil de la Villa, R.; Rubio, V. & M. Frías 2016. The Transformation of Coal-Mining Waste Minerals in the Pozzolanic Reactions of Cements. *Minerals* 6/64: 333–343. <https://doi.org/10.3390/min6030064>.

Gibbons, W. & T. Moreno 2002. *The Geology of Spain*. London: The Geological Society.

Gruel K. & O. Buchsenschutz 2015. La civilisation des oppida. In O. Buchsenschutz (ed.) *L'Europe Celtique à l' Âge du Fer. VIIIe – Ier siècles*: 295-371. Paris: Nouvelle Clio. PUF.

Kumar Sinha, P.; Kiran Kumar, M. & V. Kain 2015. Effect of microstructure of carbon steel on magnetite formation in simulated Hot Conditioning environment of nuclear reactors. *Journal of Nuclear Materials* 464: 20-27.

Liñan E.; Gozalo, R.; Palacios, T.; Gámez, J.A.; Ugidos, J.M. & E. Mayoral 2005. Cambrian. In W. Gibbons & T. Moreno (eds) *The Geology of Spain*: 17-30. London: The Geological Society.

Moret, P. 1996. *Les fortifications ibériques. De la fin de l'âge du Bronze à la conquête romaine*. Madrid: Casa de Velázquez.

Moret, P. 2017. The purpose of Gallic Oppida Ramparts: A Reappraisal. In A. Ballmer; M. Fernández-Götz & D.P. Mielke (eds) *Understanding Ancient Fortifications. Between Regionality and Connectivity*: 171-180. Oxford: Oxbow Books.

Osório, M. & P. Pernadas 2011. Indícios de vitrificação da muralha proto-histórica do Sabugal Velho. In M.A. Rodrigues; A.C. Lima & A.T. Santos (eds) *Actas do V Congresso de Arqueologia do Interior Norte e Centro de Portugal*: 219-238. Porto: Caleidoscópio/ Direcção Regional de Cultura do Norte.

Özdemir, Ö. & D. J. Dunlop 2000. Intermediate magnetite formation during dehydration of goethite. *Earth and Planetary Science Letters* 177 (1-2): 59-67.

Peterse, C. 1984. Der oskische Fuss in pompejanischen Atrien. *Babesch (Bulletin Antieke Beschaving)* 59: 9-30.

Ponomar, V.P.; Dudchenko, N.O. & A.B. Brik 2018. Synthesis of magnetite poder from the mixture consisting of siderite and hematites iron ores. *Minerals Enginneering* 122: 277-284.

Pullen, D.J. 2011. *The Early Bronze Age Village on Tsoungiza Hill.* Dexter: American School of Classical Studies at Athenes.

Ralston, I. 2006. *Celtic Fortifications*. Stroud: Tempus.

Ruiz Zapatero, G. 2018. Casas, "hogares" y comunidades: castros y oppida prerromanos en la Meseta. In A. Rodríguez Díaz, I. Pavón & D. M. Duque (eds) *Más allá de las casas. Familias, linajes y comunidades en la Protohistoria peninsular*: 325-361. Cáceres: Universidad de Extremadura.

Ruiz, A. & M. Molinos 1998. The archaeology of the Iberians. Cambridge: Cambridge University Press.

Sacristán, D. 2011. El urbanismo vacceo. *Complutum* 22.2: 185-22.

Sanmartí, J. 2009. From the archaic states to romanization: a historical and evolutionary perspective on the Iberians. *Catalan Historical Review* 2: 9-32. < http://revistes.iec.cat/chr/>.

Santisteban, J.I.; Mediavilla, R.; Martín-Serrano, A. & C. J. Dabrio 1996. The Duero Bsin: a general overview. In P. F. Friend & C. J. Dabrio (eds) *Tertiary Basins of Spain. The Stratigraphical Record of Crustal Kinematics*: 183-187. Cambridge: Cambridge U.P. (World and Regional Geology 6).

Sanz Mínguez, C.; Romero, F.; Velasco, J. & I. Centeno 2003. Lo cotidiano en Pintia: El poblado de Las Quintanas. In C. Sanz Mínguez & J. Velasco (eds) *Pintia. Un oppidum en los confines orientales de la región vaccea*: 69-123. Valladolid: Universidad de Valladolid.

Sayanam, R.A.; Kalsotra, A.K.; Mehta, S.K.; Singh, R.S. and G. Mandal 1989. Studies in Thermal Transformations and Pozzolanic Activities of Clay from Jammu Region (India). *Journal of Thermal Analysis* 35: 99–106. <https://doi.org/10.1007/BF01914268>.

Silva, A.C., Berrocal-Rangel, L. & V. M. Rodero 2013. Le rempart vitrifié du Castro dos Ratinhos (Moura, Portugal) et la question de la vitrification dans les fortifications protohistoriques dans la Péninsule Ibérique. In S. Krausz, A. Colin, I. Ralston & T. Dechezlepetre (eds) *L'âge du Fer en Europe. Mélanges offerts à Olivier Buchsenschutz*: 167-181. Bordeaux: Ausonius.

Stieglitz, R. 2006. Classical Greek measures and the builder's instruments from the Ma'agan Mikhael shipwreck. *AlA (American Institute of Archotects Journal)* 110: 195-203.

Valladares, M.I.; Barba, P. & Ugidos, J.M. 2002. Precambiran. In Gibbons, W. & T. Moreno (eds) *The Geology of Spain*: 7-16. London: The Geological Society.

Villa Valdés. A. 2007. El Chao Samartín (Grandas de Salime, Asturias) y el paisaje fortificado en la Asturias protohistórica. In L. Berrocal-Rangel and P. Moret (eds.) *Paisajes fortificados de la Edad del Hierro. Las murallas protohistóricas de la Meseta y la Vertiente atlántica en su contexto europeo*: 191-212. Madrid: Real Academia de la Historia - Casa de Velázquez.

8. Acknowledgement

These authors would like to thanks comments, suggestions and photographies from Dr. Francisco Blanco García and Dr. Gregorio R. Manglano, both from the Autonomous University of Madrid; to the staff of the museum of Sabugal (Portugal) and Dr. Francisco Fabián and Dr. Nicolás Benet, from the *Servicio de Arqueología* of Castile and Leon region.

9. Biographies of the authors

Luis Berrocal-Rangel obtained his PhD in 1992 from the Autonomous University of Madrid, where he is now Professor of European Prehistory. He specializes in Celtic archaeology, mainly of the Celts in the Iberian Peninsula, and in Late Bronze Age and Iron Age architecture. He is Principal Researcher of the project 'Late Prehistory Architecture in the Western Spanish Plateau.' He is member of the European Association of Archaeologists since its foundation in 1993 and became a member of the Real Academia de la Historia of the Kingdom of Spain in 2002.

Address: Department of Prehistory and Archaeology, Universidad Autónoma de Madrid, Carretera de Colmenar Viejo, Km 15, Campus de Cantoblanco, 28049 – Madrid. [email: luis.berrocal@uam.es].

Rosario Garcia-Giménez has PhD degrees in chemistry, legal history, and physical geography. She is Professor of Geology and Director of the Department of Geology and Geochemistry at the Faculty of Sciences of the Autonomous University of Madrid. She specializes in XRD and polarization optical microscopy. Her main research areas are in archaeometry, pozzolanic additions to cement using waste, gemology, loess, mineralogy, and ceramic materials. She coordinates the 'Applied Geochemistry Clays, Cements, and Ceramics' research group.

Email: rosario.garcia@uam.es.

Raquel Vigil de la Villa has a PhD degree in Chemistry. She is Reader of Materials Science and Crystallography at the Autonomous University of Madrid. She specializes in XRD and SEM/EDX. Her main research areas are in archaeometry, materials analysis, mineralogy, and ceramic materials. She is a member of the Geomaterials group with the Cement Institute of the Consejo Superior de Investigaciones Científicas.

Email: raquel.vigil@uam.es.

Lucía Ruano is a PhD researcher at the Autonomous University of Madrid, specializing in the Iron Age of the northern Iberian Peninsula. Her research seeks to use architecture and the use of space to understand long-term processes of change and continuity, as well as to acquire tools from other disciplines, such as ethnography, to better understand aspects of daily life.

Email: lucia.ruano@uam.es.

Carmen Gutiérrez-Sáez obtained his PhD degree in Prehistory by the University of Salamanca (Spain). She is Reader of Prehistory in the Department of Prehistory and Archaeology of the Authonomous University of Madrid. He has a well-reputated trajectory in Micro-traceology and other Archaeometric disciplines.

Email: carmen.gutierrez@uam.es.

Marcos Osorio works as archaeologist in the museum of Sabugal (Central Portugal) and he is director of the excavation of the Medieval and Iron Age site of Sabugal Velho. He is PhD student of Archaeology in the University of Coimbra (Portugal) and he has conducted many excavations in protohistoric archaeological sites of Portugal.

Email: arkmarcos@hotmail.com.

Traction or hybrid trebuchet? The use of physical calculations to classify trebuchets.

Mario Ramírez Galán (*University of Portland*), María Benítez Galán (*University of Granada*), Rafael Montalvo Laguna (*Archaeologist*), Reina Inlow (*Graduate of University of Portland*), and Ronda Bard (*University of Portland*)

Abstract

Trebuchets and siege engines are very difficult to find in an archaeological context because they were made using mostly perishable materials, specifically wood. The preservation of those elements is quite complicated and for that reason we may find a reduced number of components, like stone or rock projectiles.

According to historical sources, in the siege of Alcalá la Vieja, which took place in 1118 in Alcalá de Henares (Spain), these engines were used by the Christian army to besiege the Muslim fortress. However, the information and data provided by them are short, brief, and in some cases unreliable.

With this paper, we want to illustrate how the use of physical calculations, using the four stone projectiles found around the castle and the historical descriptions about them, can determine the type of trebuchet

Keywords

Archaeology, medieval warfare, physics, trebuchets.

1. Introduction

The fortress of Alcalá la Vieja (figure 1) is located at an enclave watching over the route between what is now Toledo and Zaragoza. This location was the perfect place to build the fortress because they had a great visibility of the area, it was situated near the Henares river, providing them with a source of water, and it was protected by natural defenses. The two sides of the castle, oriented to the North, had two vertical cliffs where access to the fortress was completely impossible.

It has been argued that the outlying neighborhood was gradually depopulated until abandoned in the fourteenth century. The fortress was probably completely abandoned around the sixteenth century.

Only 472 meters away we find the base of Malvecino hill, an elevation that reaches an altitude of 698 meters. This hill has different terraces, some of them natural, others resulting from recent replanting work. Archaeological remains and features were documented according to the archaeological map of the Autonomous Community of Madrid. Those remains were from several time periods, showing a continuous occupation of that location in different ages.

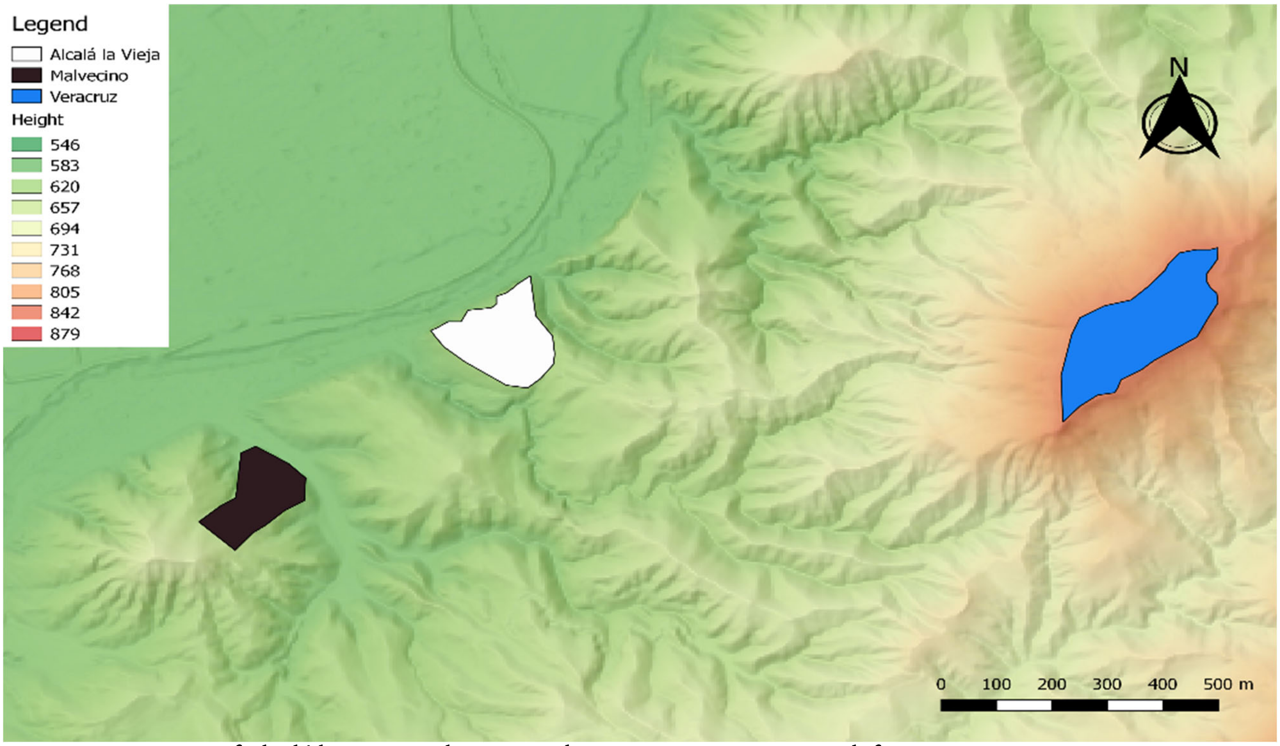

Figure. 1. Location of Alcalá la Vieja, Malvecino and Veracruz. Derivative work from MDT5 2015 CC-BY scne.es

Two archaeological surveys were taken. The first prospection was conducted by Fernández-Galiano, who confirmed the presence of materials and structures in Malvecino (Fernández-Galiano and Garcés-Toledano 1990). However, they were not located in the exploration undertaken in 1989-1990 by S. Rascón Marqués and A. Méndez Madariaga.[4]

Ever since Juan Zozaya (1983: 411-529) began his archaeological explorations of the fortress during the 1960's, there have been other archaeological campaigns carried out regarding the fortress of Alcalá la Vieja (López, Presas, Serrano and Torra 2009, 2011 and 2013). These studies established a continuous occupation since the Al-Andalus period; however, the building date could never be specified. They could

[4] Rascón Marqués, S. & Méndez Madariaga, A. (1990): *Carta Arqueológica de la Comunidad de Madrid. Base de Datos de Bienes del Patrimonio Histórico*. Museo Arqueológico Regional, Comunidad de Madrid.

confirm, however, the structure's occupation in previous periods with structures belonging to recent pre-history and the Carpetian era.

The Alcalá la Vieja stronghold was part of the defensive system of the middle frontier. This defense, together with those of Guadalajara, Talamanca, Paracuellos, Maqueda, and Madrid, was an essential piece of the Al-Andalus protection system.

Following the Christian conquest in 1118, the fortress was transferred to the Christians. In 1129, King Alfonso VII and Doña Berenguela assigned this territory to the archbishop of Toledo, Don Raimundo (Fita 1885).

2. The siege of Alcalá la Vieja

When we started this research in 2016, we found a problem in the historical written sources (Echevarría 1990: 631). The issue was that the explanation of the siege development and all the factors related to this conflict was too short and brief, making it problematic in locating maneuvers and actions on the field. This could be the consequence of an absence of firsthand testimonies or direct evidence. Consequently, authors of secondary sources had to fill those gaps in the texts to explain what happened in 1118. For this reason, we had to use these sources to study the siege of Alcala la Vieja.

The closest written source, chronologically speaking, to the historical fact, is *De Rebus Hispaniae*[5] (HRH), written by the archbishop Don Rodrigo Jiménez de Rada. In that text, the author mentions the conquest of the Muslim fortress of Qal'at 'Abd al-Salam and he alludes to the construction of a castle on a hill to control the moor stronghold of Alcalá la Vieja (HRH Capítulo XXVIII). The elevation mentioned by Jiménez de Rada was that of Malvecino hill.

On the other hand, subsequent authors emphasize the location of a Christian post on the hill just mentioned. Furthermore, the scholar Portilla y Esquivel (1725: 148) gives detailed information about that place. For example, he explains its military role and the remains that he saw there during his visit. It is necessary to highlight that this source mentions the existence of a second Christian position in this siege, on Veracruz hill. He explains that this post was far away from the castle of Alcalá la Vieja and the siege would not be possible from Veracruz, even with the use of powder.

On his behalf, Ambrosio de Morales says in his work, *Opúsculos castellanos*, that Don Bernardo de Sedirac commanded that a fortress be built (de Morales 1793: 59) on an elevation near the fortress, where they

[5] http://fondosdigitales.us.es/fondos/

deployed the trebuchets to siege it. This information coincides exactly with Jiménez de Rada's explanation, previously mentioned.

After reading Azaña's work (1882: 127-128), we found nearly the same mention of the two Christian places around the stronghold of Qal'at 'Abd al-Salam. This information reinforces the presence of those posts during the siege carried out by the archbishop of Toledo, Don Bernardo de Sedirac in the twelfth century. The clearest reference to it is in Alcalá la Vieja, ensayo histórico o apuntes para una monografía de aquel castillo, written by Jose Demetrio Calleja. Within this source, the apostolic vicar says (1897: 18) that the Christian troops established their tents on Veracruz hill, today called Eccehomo hill. Furthermore, he indicates the existence of an advanced post in Malvecino, as do the rest of scholars.

To siege the enemy stronghold, the Christian army used trebuchets (Portilla 1725: 148; Demetrio 1897: 6, 17; Torres 1959: 165-166) to hurl rocks and stones from the elevation where they built the temporary fortress. In his work, Demetrio Calleja (1897: 17-18) says that the Christian army established another post in a different place. That site was Veracruz hill, and there they settled their main camp.

The Christians tried to take control of the castle several times, but they did not achieve their goal because of Alcalá la Vieja's defensive structures and its defenders, who fought very bravely, shooting arrowheads and rocks towards the Christians. According to tradition, when Don Bernardo de Sedirac's army was discouraged, a miracle happened. A bright cross appeared over the hill (Portilla, 1725: 149; Azaña, 1882: 128-129) where Christians had their camp (Veracruz hill), giving them motivation and strength to assault the stronghold. Obviously, the effect on Muslim soldiers was the opposite, and they tried to abandon the castle by crossing the river and even jumping off the cliffs around *Qal'at 'Abd al-Salam. Once the castle was under Christian control, the Muslims tried to recover it fighting in an open field close to the Henares river, but Christians defeated them again, and they pursued the Muslim soldiers until Daganzo de Arriba, where they were massacred. From then on, the place is known as Monte de la Matanza (Massacre Hill).*

3. Medieval siege engines in the siege of Alcalá la Vieja: trebuchets

Several authors mentioned the presence of trebuchets and other similar siege engines used to besiege the fortress of Alcalá la Vieja, but it was necessary to determine the variety, as there were different typologies.

According to Chevedden (2000: 99), the term trebuchet is composed of two parts: "*...the first part of the word is the prefix tri- (three), and the second part is the Latin noun bracchium (arm) or it cognates in medieval Latin (bracco), romance languages, or German. A tribacchium, or tribacho, literally means a device having three arms or branches.*" Thanks to the analysis of medieval codices, it is possible to corroborate his explanation and also see the evolution of these siege engines.

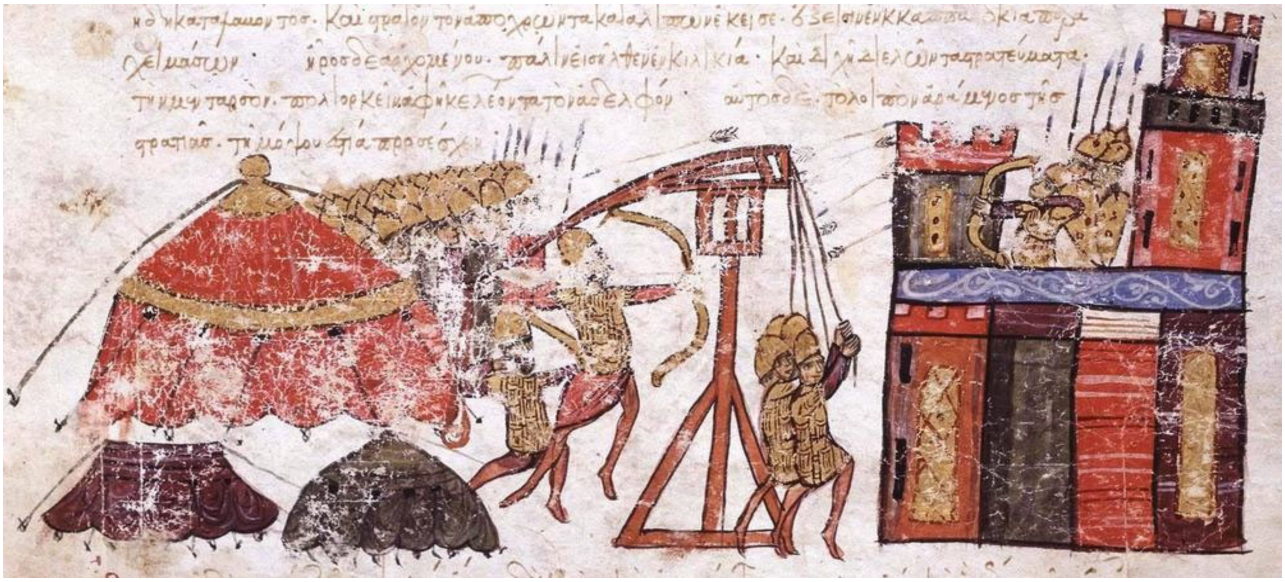

Figure. 2. Traction trebuchet. Historia Scylitzes, folio 151r. «Biblioteca Nacional de España»

During the Middle Ages, there were three different types of trebuchet: traction, hybrid, and counterweight. The traction trebuchet (figure 2) was created between the V and III centuries B. C. in China (Chevedden *et al.* 1995: 66-67; Chevedden 2000: 73; Tsurtumia 2015: 178) and its mechanism was a group of men pulling ropes to launch projectiles.

The second model was the hybrid trebuchet (figure 3) that started to replace the previous type at the beginning of the VIII century and expanded during the IX through the Middle East, Mediterranean world, and western Europe (Chevedden 2000: 74; Chevedden *et al*. 2000: 442-443). This mechanism was a combination of a group of men pulling ropes and a small counterweight (Chevedden *et al*. 2000: 456; Sáez Abad 2007: 103). According to Chevedden *et al.* (2000: 456), that counterweight was "*...to balance the beam forward of the axle at the moment of discharge.*"

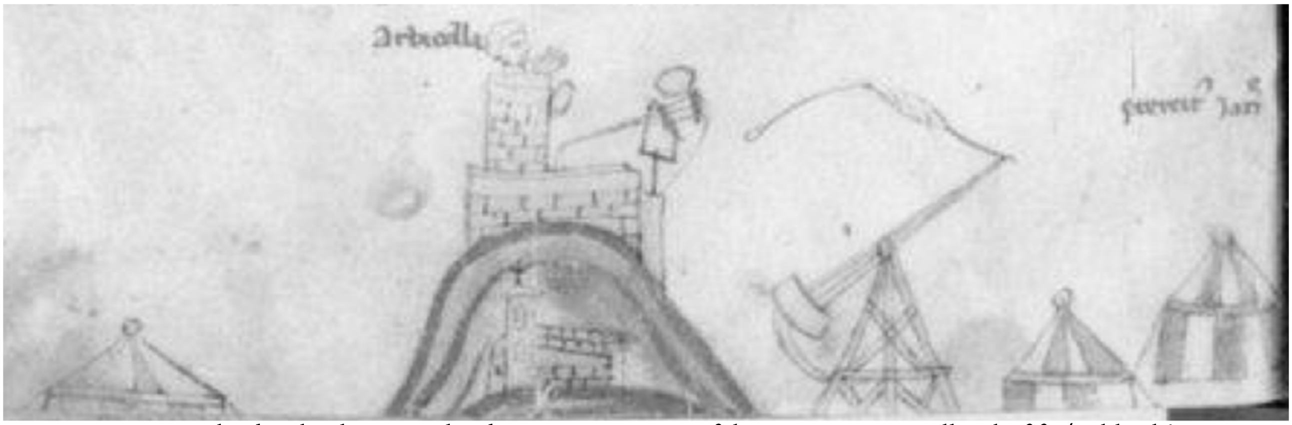

Figure 3. Hybrid trebuchet. Annales de Genes, Lat. 10136, folio 141v. «Sourcegallica.bnf.fr / Bibliothè quenationale de France»

The last model was the fixed counterweight trebuchet (figure 4), the most famous and widely known siege engine during the Middle Ages. This type appeared in the XII century, however several authors (Tarver 1995: 146, 167; Saimre 2006: 64; Tsurtsumia 2015: 180) cannot specify the exact date and moment of creation for the counterweight trebuchet. For example, one of author (Chevedden 2000: 76) believes that the origin could be at the end of XI century.

Figure 4. Counterweight trebuchet. Folio 94v. Histoire de la guerra sainte [par Guillaume, de Tyr] traduction et continuation. Date: 1201-1300. « Source gallica.bnf.fr / Bibliothèque nationale de France »

Basically, the mechanism was similar to the others but the human force was substituted with a very heavy counterweight to shoot the projectile. (Tarver 1995: 167; Chevedden *et al.* 2000: 435; Saimre 2006: 62; Gillmor 1981: 1; Chevedden 1998: 179 in Tsurtsumia 2015: 180) These large counterweights were filled with different materials like sand, stone, etc. (Sáez Abad 2007: 103-104)

This upgrade brought along positive consequences, however the most important aspect for our study was the shooting range. Different researchers, based on a military treatise written by Salah al-Din, say that the traction trebuchet could shoot a projectile between 80 and 120 meters. Other group of scholars mention data from a Chinese treatise (1044) where the shooting range is similar(Chevedden 2000: 74; Chevedden *et al.* 2000: 443). Unfortunately, we do not have any information about the hybrid trebuchet. However, the evolution of medieval warfare could provide an idea of the incremental change of range and precision that happened as the trebuchets advanced.

It is obvious that the counterweight trebuchet had the best upgrade thanks to the incorporation of the fixed counterweight. Experiments and experimental archaeology allowed us to attain valuable data to better understand this model. The beginning of these activities took place in the XIX century when Napoleon III ordered to build Ildefonso Favé a trebuchet. That model could only shoot four times (table 1) (Hansen 1992: 194 in Saimre 2006: 74; Sáez Abad 2007: 204).

Projectile	**Distance**
Cannon ball, 10.88 kg.	175 meters
Projectile, diameter 22 cm.	472 meters
Projectile, diameter 27 cm.	120 meters
Projectile[6], diameter 32 cm.	120 meters

Table 1. Shooting range.

Payne-Gallwey (1903: 309 in Saimre 2006: 66) came to the conclusion that the most powerful trebuchet had a maximum shooting range of 300 meters, using a 140 kilograms projectile and a 9.000 kilograms counterweight. Another scholar, Peter Veemming Hansen, made several trebuchets in order to figure out the shooting range. One trebuchet launched a 15 kilogram stone 168 meters with a 2 ton counterweight (Saimre 2006: 75). However, Hansen, based on physical calculations, concluded that this trebuchet model could have a shooting range of 490 meters.

[6] The projectiles 2, 3 and 4 were filled with sand.

3.1. Artifacts associated to the siege context: trebuchet projectiles

These artifacts (figure 5) were a casual find discovered in the vicinity of Alcalá la Vieja in 2017. The discovery of these materials signified a key asset to help understand the siege of the stronghold. Trebuchets and other siege engines do not leave remains in an archaeological site because they were made using perishable materials, such as wood, and the only possible remains would be the nonperishable components, like these projectiles.

ID Number	Dimensions	Weight
MAR-CE2017/42-1	33.5 x 30.5 cm.	50.8 kg.
MAR-CE2017/42-2	34 x 29.5 cm.	47.6 kg.
MAR-CE2017/42-3	28 x 29.5 cm.	32.8 kg.
MAR-CE2017/42-4	35 x 29.5 cm.	58.6 kg.

Table. 2. Projectiles' features.

One of our members, Rafael Montalvo Laguna, was able to study (table 2) them at the Archaeological Regional Museum in Alcalá de Henares, analyzing and measuring them.

The material used to make the four medieval projectiles was limestone, and each projectile has very similar dimensions. Their diameter has a range between 35 and 28 centimeters, with projectile number three (MAR-CE2017/42-3) having the smallest dimameter. Although the third projectile is the smallest, it is not unusual. In some medieval sieges, where other projectiles had been found after digging, some artifacts had smaller measurements. In our case, we can determine, after calculating the average, that the standard size was 34 x 29.75 cm, keeping in mind that we have more differences between their weights because the range coveres masses from 58,6 kg to 32,8 kg.

The craftsmen tried to create a round projectile to improve the function of the projectile's launch , and this is visible. However, their shape showes flattened and irregular parts, problably created by the erosive processes occurring since 1118 when the siege took place. Moreover, it is possible to observe the masonry marks that give them their round shape.

This type of rock is good for carving because it is "soft" and because of this, the process to make them was faster and easier. In our ongoing research, we found several limestone sources around the area, and some of them were very close to the Christian camp on Veracruz hill. Regarding materials, we can say that they were looking for a certain raw material with specific features and characteristics, but probably, their knowledge about rocks and stones may have been limited because of the projectile's differing weights. Those different weights may mean different rock compositions.

Figure 5. Trebuchet projectiles: MAR-CE2017/42-1 (A), MAR-CE2017/42-2 (B), MAR-CE2017/42-3 (C) & MAR-CE2017/42-4 (D) respectively. Photographs: Rafael Montalvo Laguna.

4. The use of physics to determine the type of trebuchet

The trebuchet converts the potential energy of the counterweight and the work executed by a group of men into kinetic energy. When men perform more strength and the counterweight is heavier, the projectile acquires more speed and the range will be greater.

Developing the equations to analyze the physics of the hybrid trebuchet is complex. This complex problem can be treated as a two-dimensional system, making the following assumptions:

- The trebuchet is rigid.
- There is no air resistance as the payload flies through the air.
- The trebuchet remains stationary on the ground during launch.

The difficulty of this study lies in the small amount of data (number of men, average strength of each man, length of beams, average weight of the counterweight ...) that there is on this type of machine and the physical description.

To avoid these difficulties, we will assume the validity of the physics that describes the trebuchet of the counterweight (figure 6) for its simplicity and we will presume that the machine used in this study is less effective. We will include that difference in the calculations. We can make this assumption since we will take as weight of the counterweight, the sum of the weight of the counterbalance of the hybrid machine and the force made by men.

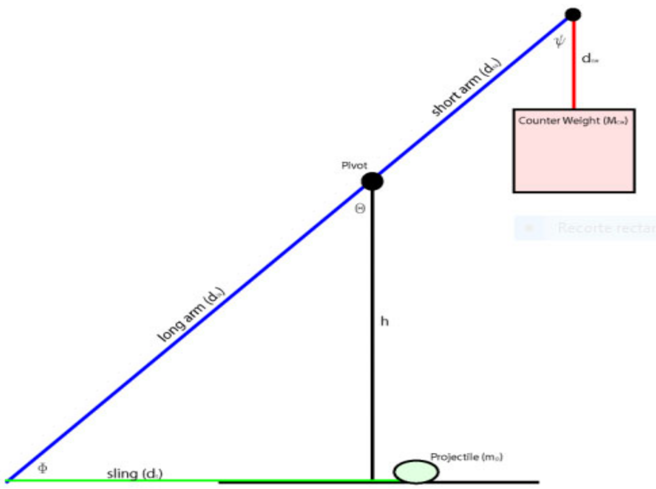

Figure 6. Schematic of a trebuchet.

4.1. Theoretical approach

As we said before the trebuchet is a device that converts potential energy and the manual force into kinetic energy. The amount of potential energy and the work done by a group of men are what define the power of a trebuchet. The potential energy can be obtained through

$$E_p = M_{CW} g h_{CW}$$

Where M is the counterweight mass, g is the gravity's acceleration, and hcw is the distance between the counterweight and the floor.

The work done through manual labor is given by

$$W_M = F_M h_{CW} \cos\alpha = M_{CW} g h_{CW} \cos\alpha$$

Where F is the strength made by men, a is the acceleration, and α is the angle with respect to the height of the counterweight.

The total initial mechanical energy is

$$E_{M_i} = E_p + W_M = M_{CW} g h_{CW} + M_{CW} g h_{CW} \cos\alpha = M_{CW} g h_{CW}(1 + \cos\alpha)$$

Summing up, we can approximate the operation of the machine as the conversion of potential energy into kinetic energy. Due to the conservation of mechanical energy

$$M_{CW} g h_{CW}(1 + \cos\alpha) = \frac{1}{2} m_p v_p^2$$

Where m_p is the projectile mass and $v_p$is the projectile velocity.

The height at which the counterweight is calculated from the length of the longest arm of the beam is as follows

$$h_{CW} = d_p \mathrm{sen}(\pi/4)$$

We calculate the maximum distance reached by the projectile from the velocity with which it is launched. We use the parabolic launch formulas.

The projectile reaches the distance that is given by

$$R = v_p \cos\theta\, t$$

Where θ is the launch angle and t is the time. To know the time it will take the projectile to fall, we will calculate the time it takes to travel half of the trajectory, since at that point we will only have velocity on the horizontal axis.

$$v_y = v_p \sin\theta - g\frac{t}{2} = 0$$

$$t = 2\left(\frac{v_p \sin\theta}{g}\right)$$

4.2 *Results*

The first step we take is to calculate the height of the counterweight. We do not know the exact value of the beam of the trebuchet used so we take several values (table 3).

LENGTH OF THE ARM (M)	HEIGHT OF THE CW (M)
8,5	6,01
9	6,36
9,5	6,72
10	7,07
10,5	7,42

Table 3. Height of the counterweight

The next step is to calculate the velocity of the projectile. The angle formed by the rope with which the group of men pulls with the vertical is unknown in its exact value, we will take a set of values that comprised of 0º, 30º and 45º. In the calculations we have made we can see that the projectiles reach higher speeds for angles close to zero.

Because we do not have exact values of these two variables (angle and height) the value of the speed will depend on both.

In this study we used the mass of four projectiles (Table 4.) that were discovered in the area.

Projectile 1 (m)	50,8
Projectile 2 (m)	47,6
Projectile 3 (m)	32,8
Projectile 4 (m)	58,6

Table 4. Mass of projectiles

We will calculate the speed by taking different lengths for the beam, since exact measurements are unknown. We will use two possibilities for the set of counterweights and the group of men, we will perform the calculations for a maximum and a minimum case. In choosing the mass of the counterweight, we chose to be guided by historical data gathered from other similar studies due to the lack of available data regarding the trebuchets.

From these lengths, the mass of the projectiles, counterweight, and the force made by men, we will calculate the velocity reached by the projectile. From the calculated speeds we will obtain the range that the four projectiles can reach.

For the first projectile, for the maximum strength of the counterweight, and the group of men (figure 7) we obtain minimum speeds of 35, 9 m / s and maximums of 41, 44 m / s. For these speeds, the range of distances reached that we obtained is as follows; 22 m for launch angles near zero degrees and 176 m for launch angles near forty-five degrees.

For the minimum strength we obtain velocities between 29, 37 m/s and 32, 63 m/s. The projectile barely reaches 110 meters (figure 8).

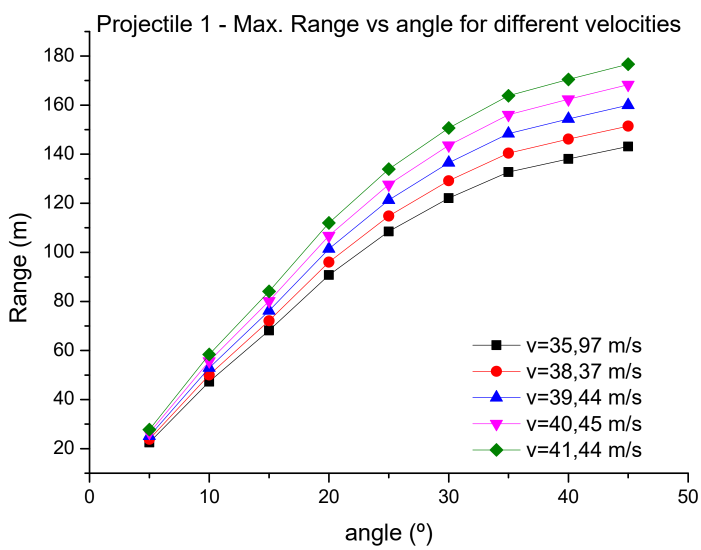

Figure 7. Representation of the range vs angle for different velocities for the projectile 1, maximum strength of the counterweight and the group of men.

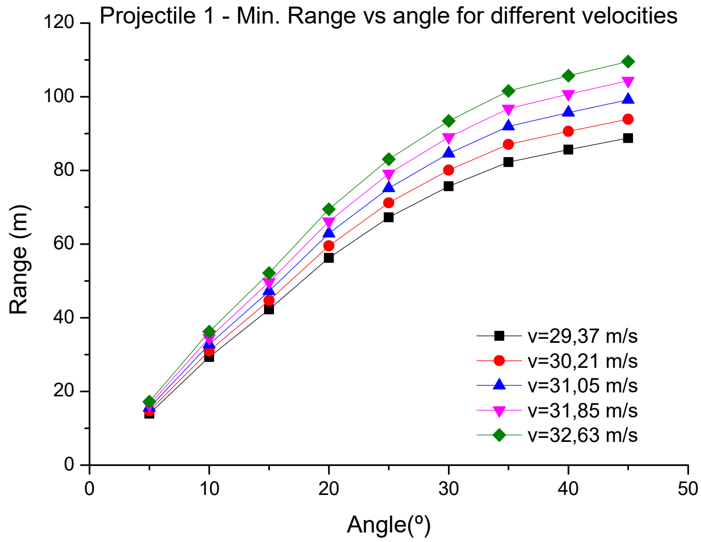

Figure 8. Representation of the range vs angle for different velocities for the projectile 1, minimum strength of the counterweight and the group of men.

The velocities obtained for the second projectile range from 38, 53 m/s to 42, 81 m/s for the maximum case of counterweight and group of men. With these speeds the projectile can reach maximum distances between 150 meters and 190 meters (figure 9).

For the case of minimum force, the range of speeds reached ranges from 31.46 m/s to 34.98 m/so that the maximum distances that the second projectile can reach are from 100 to 125 meters as seen in figure 10.

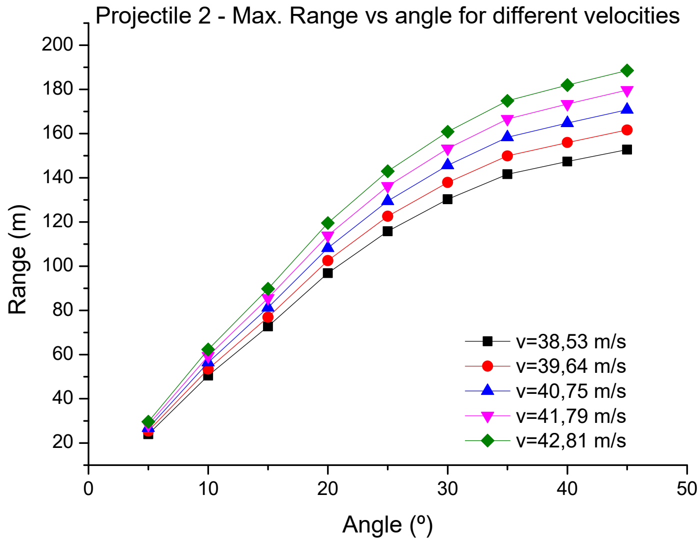

Figure 9. Representation of the range vs angle for different velocities for the projectile 2, maximum strength of the counterweight and the group of men.

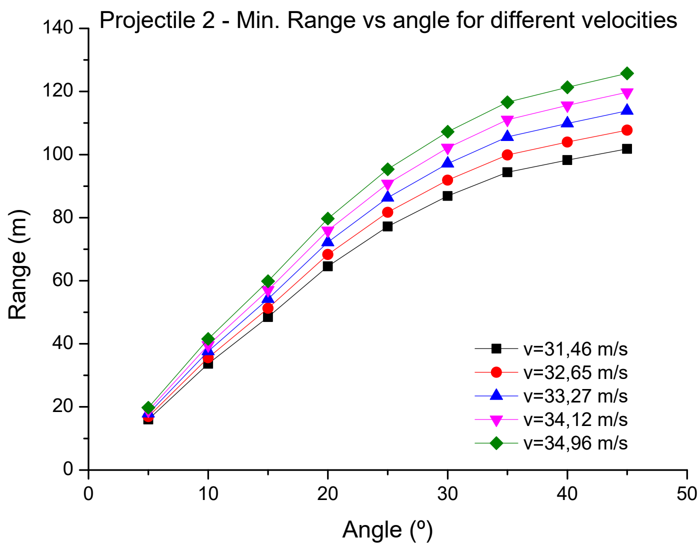

Figure 10. Representation of the range vs angle for different velocities for the projectile 2, minimum strength of the counterweight and the group of men.

With the third projectile for the case of maximum strength, (figure 11) the range of forces is 46 m/s at 52 m/s, it can reach maximum distances between 220 and 275 meters. On the other hand, for the minimum case (figure 12) the lower velocity reached is 37, 90 m/s and the maximum velocity is 42, 11 m/s can reach maximum distances between 147 and 185 meters.

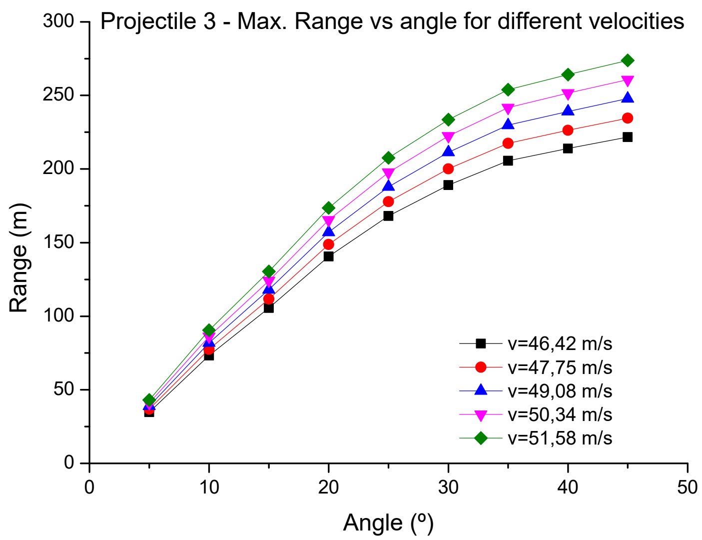

Figure 11. Representation of the range vs angle for different velocities for the projectile 3, maximum strength of the counterweight and the group of men.

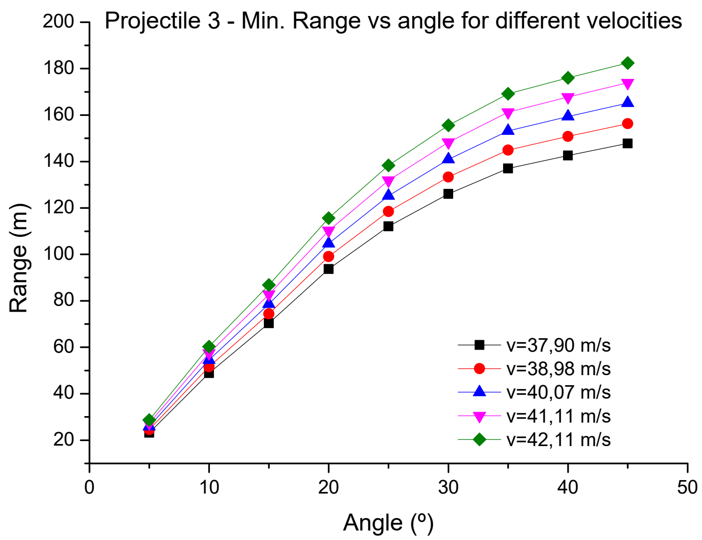

Figure 12. Representation of the range vs angle for different velocities for the projectile 3, minimum strength of the counterweight and the group of men.

The last, and heaviest projectile reaches a maximum distance of between 125 and 145 meters. While for the minimum force, the maximum distances reached are between 80 and 100 meters (figures 13-14).

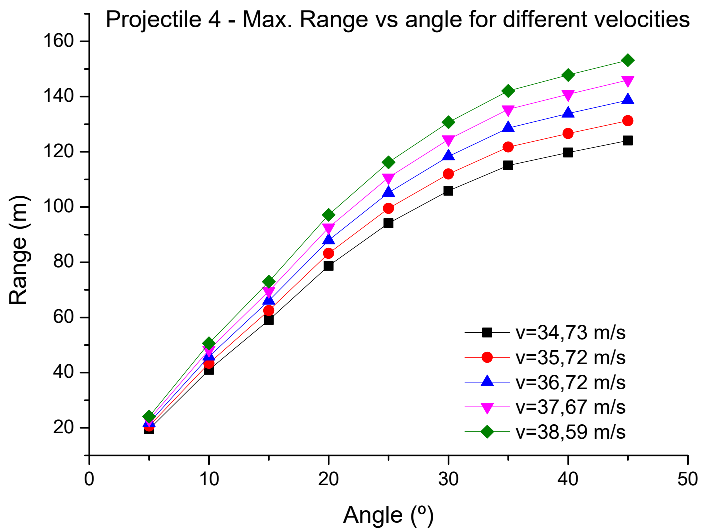

Figure 13. Representation of the range vs angle for different velocities for the projectile 4, maximum strength of the counterweight and the group of men.

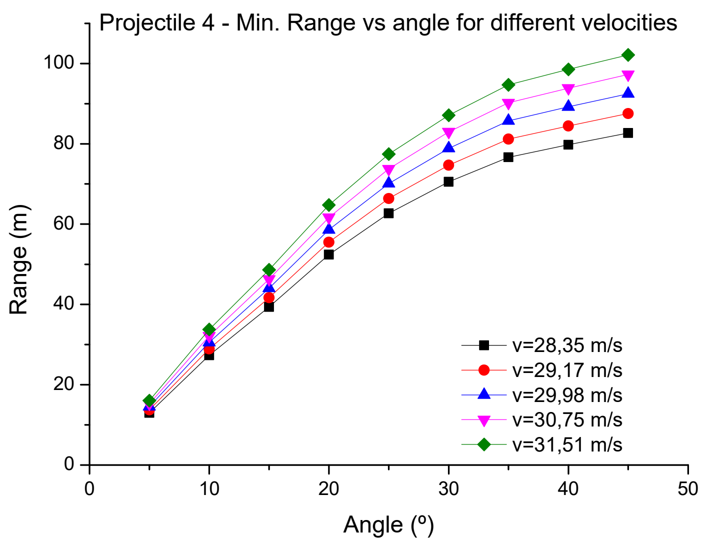

Figure 14. Representation of the range vs angle for different velocities for the projectile 4, minimum strength of the counterweight and the group of men.

5. Conclusions

In this paper we have investigated the use of physics to provide a new insight about the siege of Alcalá la Vieja, because documents had a great lack of information about the historical fact and medieval siege engines. The historical evidence from this study suggests that the Christian army could have used the hybrid trebuchet because the range of dates for this model fit with the time of the siege. This type of siege engine was expanded during the IX century and the next model appeared four centuries later.

Once we carried out the analysis of historical sources, the next step was to calculate the maximum and minimum distances for each projectile through physical calculations and determine the most likely type of trebuchet used during this siege. In order to do this, it was necessary to work with estimations and assumptions because of the lack of information that we have previously mentioned. After developing the equations and applying those estimations, we obtained a set of values for each stone projectile which gave a new perspective about the study of these medieval machines.

Based on previous studies, experiments, experimental archaeology, historical sources, and after comparison with our work, the findings of our study suggest that the possible model of trebuchet used during the siege of Alcalá la Vieja could be the hybrid.

Despite the fact that there are limitations due to the information, or lack thereof, provided from historical sources, we are confident that our results may improve knowledge about medieval siege warfare. Furthermore, we are confident that this paper has underlined the importance of interdisciplinary studies to solve problems and fill the informational gaps in historical documents.

6. References

Azaña, E. 1882. *Historia de Alcalá de Henares*. Alcalá de Henares: edición facsímil 1986.

Azuar Ruiz, R. 1995. Las técnicas constructivas en al-Andalus. El origen de la sillería y del hormigón de tapial, in J. I. de la Iglesia Duarte (ed.), *V Semana de Estudios Medievales (Nájera 1994):* 125-142. Logroño. Instituto de Estudios Riojanos.

Azuar Ruiz, R. 2005. Las técnicas constructivas en la formación de al-Andalus. *Arqueología de la arquitectura 4*: 149-160.

Basista, M. 2007. Hybrid or Counterpoise? A Study of Transitional Trebuchets, in C. Rogers, K. Devries, & J. France (eds.), *Journal of Medieval Military History*: 33-55. Boydell & Brewer.

Calleja Carrasco, J.D. (1897). *Alcalá La Vieja, ensayo histórico o apuntes para una monografía de aquel castillo.* Guadalajara: Guadalajara Imp. de Diputación Provincial.

Castillo Oreja, M.A. 1985. Alcalá de Henares, una ciudad medieval en la España cristiana (s. XIII-XV). *En la España Medieval 7:* 1059-1080.

Castro Priego, M. 2011. La problemática del registro arqueológico de Alcalá de Henares. Unpublished PhD dissertation, Universidad de Alcalá de Henares, Madrid, Spain. https://ebuah.uah.es/dspace/handle/10017/18541

Chevedden, P. E., Eigenbrod, L., Foley, V. & Soedel, W. 1995. The trebuchet. *Scientific American, July 1995:* 66-71

Chevedden, P. E. (1996): The Artillery of King James I the Conqueror, iIn P. Chevedden, D. Kagay & P. Padilla (eds.), *Iberia and the Mediterranean World of the Middle Ages: Essays in Honor of Robert I. Burns, S. J. vol. 2:* 47-97. Leiden: Brill.

Chevedden, P. E. (1998): The hybrid trebuchet: the halfway step to the counterweight trebuchet. In D. J. Kagay y T. M. Vann, *On the Social Origins of Medieval Institutios, Essays in Honor of Joseph F. O'Callaghan* (pp. 179-222). Leiden: Brill.

Chevedden, P. E. 2000. The Invention of the Counterweight Trebuchet: A Study in Cultural Diffusion. *Dumbarton Oaks Papers 54:* 71-116.

Chevedden, P. E., Shiller, Z., Samuel, R., Kagay, D. J. & Gilbert, S. R. 2000. The traction trebuchet: a triumph of four civilizations. *Viator 31:* 433-486. https://doi.org/10.1484/J.VIATOR.2.300774

Echevarría Arsuaga, A. 1990. Los castillos de Alcalá la Vieja y Santorcaz en la frontera cristiano-musulmana Española, in Universidad Complutense (eds.): *Congreso de jóvenes historiadores y geógrafos: actas I, celebrado en la Facultad de Geografía e Historia de la Universidad Complutense de Madrid del 12 al 16 de diciembre de 1988, Vol. 1, 1990*: 631-642. Madrid: Editorial de la Universidad Complutense.

Fernández-Galiano, D. & Garcés-Toledano, A. 1978. Problemática y estado actual de los yacimientos arqueológicos en el corredor Madrid-Guadalajara. *Wad-al-Hayara: Revista de estudios de Guadalajara 5*: 7-34.

Fita Colomé, F. 1885. Bula inédita de Honorio II. *Boletín de la Real Academia de la Historia vol. VII*: 336-338

Flórez de Setién & Huidobro, E. (1767). *Anales Toledanos I. España sagrada: Theatro geographico-histórico de la iglesia de España.* Tomo XXIII. Madrid.

Hill, D. R. 1973. Trebuchets, in J. France (ed.) *Medieval Warfare 1000-1300:* 99-114. London: Routledge.

Jiménez de Rada, R. 1989. *Historia de los hechos de España. Introducción, traducción, notas e índices de Juan Fernández Valverde*. Madrid: Alianza Editorial.

López Marcos, M. Á., Presas Vías, M. M., Serrano Herrero, E. y Torra Pérez, M. 2011. Excavaciones y conservación preventiva en la fortaleza de Alcalá la Vieja (Alcalá de Henares, Madrid), in Jornadas de Patrimonio Arqueológico en la Comunidad de Madrid, *Actas de las octavas jornadas de patrimonio arqueológico de la Comunidad de Madrid, 2011*: 235-246. Madrid: Dirección General de Patrimonio Histórico, Comunidad de Madrid, D. L.

López Marcos, M. Á., Presas Vías, M. M., Serrano Herrero, E. y Torra Pérez, M. 2013. La fortaleza de Qal'at 'Abd as-Salam. La recuperación de una dignidad perdida (Alcalá de Henares, Madrid). *Arqueología de la Arquitectura 10:* 1-19. doi: http://dx.doi.org/10.3989/arq.arqt.2013.017

Palacios Ontalva, J. S. 2001. Fortalezas y Guerra Santa. Un estudio comparado de algunos aspectos de su funcionalidad en las fronteras de la Cristiandad. *Espacio, Tiempo y Forma, Serie III, H.ª Medieval 14:* 193-217.

Palacios Ontalva, J. S. 2006. Castillos contra castillos. Padrastros y fortalezas de asedio en la España Medieval. *Arqueología y territorio medieval 13 (2):* 33-55

Portilla y Esquivel, M. (1725). *Historia de la Ciudad de Compluto*. Alcalá de Henares.

Presas Vías, M., Serrano Herrero, E. & Torra Pérez, M. (2009). Memoria de las excavaciones arqueológicas realizadas en el yacimiento de Alcalá La Vieja (Alcalá de Henares, Madrid).

Presas, M. M., Serrano, E. & Torra, M. 2009. Materiales cerámicos estratificados (siglos IX-XVI) en el Reino de Toledo, in Zozaya, J., Retuerce, M., Hervás, M. A. & De Juan, A (eds.), *Actas del VIII Congreso Internacional de Cerámica Medieval en el Mediterráneo (Ciudad Real y Almagro 2006):* 805-824. Ciudad Real: Asociación Española de Arqueología Medieval.

Purton, P. 2009. Shifting balances: The eleventh century, in *A History of the Early Medieval Siege, c.450-1200*: 155-208. Woodbridge: Boydell and Brewer. http://www.jstor.org/stable/10.7722/j.ctt14brvp6.14

Purton, P. 2009. The developing technology of attack and the response of the defence, in *A History of the Early Medieval Siege, c.450-1200*: 357-388. Woodbridge: Boydell and Brewer. http://www.jstor.org/stable/10.7722/j.ctt14brvp6.19

Rascón Marqués, S. & Méndez Madariaga, A. (1990). Carta Arqueológica de la Comunidad de Madrid. Base de Datos de Bienes del Patrimonio Histórico. Museo Arqueológico Regional, Comunidad de Madrid.

Ramírez Galán, M & Montalvo Laguna, R. 2017. Alcalá la Vieja: localizando un campo de batalla en el Parque de los Cerros de Alcalá. (Alcalá de Henares, Madrid), in *Congreso de Arqueología de los campos de batalla, 27 y 28 de octubre de 2017, Real Sitio de San Ildefonso (Segovia).* (Forthcoming).

Ramírez Galán, M., Montalvo Laguna, R. & Benítez Galán, Mª. (2018). The battle of Alcalá la Vieja. Location and understanding of a medieval battle, in Nikita Moreira, Michael Derderian & Ashley Bissonnette (eds.): *Fields of conflict 10th Biennial International Conference 26-30 September 2018, Mashantucket Pequot Museum & Research Center:* 27-44.

Retuerce Velasco, M. & Iglesias Picazo, P. 2005. "*Los "castillos" y "palacios" de Mora de Toledo, i*n José Manuel Tofiño Pérez (ed.) *Espacios fortificados en la provincia de Toledo, 2003:* 293-330. Diputación Provincial: Toledo.

Retuerce Velasco, M. 2014. La arqueología andalusí en la Comunidad de Madrid, in Jornadas de Patrimonio Arqueológico en la Comunidad de Madrid, *Actas de las décimas jornadas de patrimonio arqueológico en la Comunidad de Madrid, Alcalá de Henares, 2013:* 21-46. Madrid: Dirección General de Patrimonio Histórico, Comunidad de Madrid, D. L.

Rivera Recio J.F. (1966). Reconquista y Pobladores del Antiguo Reino de Toledo. *Anales Toledanos*. Toledo: Diputación de Toledo.

Saimre, T. 2006. Trebuchet-A gravity-operated siege engine. *Estonian Journal of Archaeology 10:* 61-80.

Serrano Herrero, E., Torra Pérez, M., Catalán Ramos, R. & Vigil-Escalera Guirado, A. 2016. La cerámica de los siglos VIII-IX en Madrid, Toledo y Guadalajara, in A. Vigil-Escalera Guirado & J. A. Quirós Castillo (coord.) *La cerámica de la Alta Edad Media en el cuadrante noroeste de la Península Ibérica (siglos V-X): sistemas de producción, mecanismos de distribución y patrones de consumo:* 279-313. Bilbao: Universidad del País Vasco.

Tarver, W. T. S. 1995. The Traction Trebuchet: A Reconstruction of an Early Medieval Siege Engine. *Technology and Culture 36 (1):* 136-167.

Torres Balbás, L. 1959. Complutum, Qal'at 'Abd al-Salam y Alcalá de Henares. *Boletín de la Real Academia de la Historia n.º CXLIV*: 155-188

Tsurtsumia, M. 2015. Medieval Georgian Poliorcetica. *Historia I ŚWIAT 4:* 175-204.

Turina Gómez, A. 1985: Alcalá medieval, in *I Curso de Historia, Arte y Cultura de Alcalá de Henares*. Alcalá de Henares.

Turina Gómez, A. 1990. El castillo de Alcalá de Henares, in Dirección General de Patrimonio Cultural (eds.), *Madrid del s. IX al XI: Madrid, octubre-noviembre 1990, Real Academia de Bellas Artes de San Fernando*: 189-194. Madrid: Comunidad, Dirección General de Patrimonio Cultural, D.L.

Vigil-Escalera Guirado, A. 2003. Arquitectura de tierra, piedra y madera en Madrid (ss. V-IX d. C.). Variables materiales, consideraciones sociales. *Arqueología de la arquitectura 2:* 287-291.

Zozaya Stabel-Hansen, J. 1983. Excavaciones en la fortaleza de Qal'at 'Abd-al-Salam (Alcalá de Henares, Madrid). *Noticiario Arqueológico Hispánico 17:* 411-529.

Zozaya Stabel-Hansen, J. 1991. Recientes estudios sobre la arqueología andalusí: la Frontera Media. *Aragón en la Edad Media 9:* 371-388.

Blue-and-White Porcelain in Early South Thailand Maritime Trade

Angelica Kneisly, William Ayres, and Maury Morgenstein (*Department of Anthropology, University of Oregon*)

Abstract

The Blue-and-White underglaze porcelain and stoneware found in ancient port towns in Southeast Asia can serve to identify the nature and scale of early global trade systems. Archaeological, X-ray fluorescence, and Raman analyses of a small sample of porcelain and stoneware sherds from coastal sites at Pattani, South Thailand, provide evidence of diverse ceramics as well as the relative importance of specific kiln production areas, especially ones in China since the 14th century.

Our compositional data, coupled with manufacturing characteristics of sherds from the Pattani site, document two main sources localized in modern-day China, at Jingdezhen, and to a lesser extent at another source, Zhangzhou. However, outside of the Jingdezhen clustering, diverse sources are evident for a subset of glazed pieces. Our conclusions about provenance are based principally on comparisons of Zr, Rb, and Sr values probed from glaze + paste of the sherds. Raman microprobe analysis of the Si-O stretching bond peaks on the glaze + paste offers additional perspective on the chronology of the sherds. Moreover, microscopic investigation provides critical information on the pottery manufacturing processes.

The range of vessel types and the preponderance of porcelain supports the identification of a trading center and reflects the larger global trade process. Over the long term, the Pattani site shows extensive local resource use for pottery production and distribution during the Neolithic, and after that this pattern is transformed through extra-regional contact with introduced religious concepts and sophisticated ceramic technologies. During the 15th-18th centuries CE, when Pattani was one of the Malay Muslim states, the extensive trade shifts to Chinese porcelain.

Keywords

Blue-and-white porcelain, provenance, pXRF, Raman Spectroscopy, Thailand archaeology

1. Introduction

Understanding porcelain's role in early Southeast Asian trade networks requires that we establish where it was produced as well as its distribution. Closely linked are issues of manufacture because this influenced how it became available as a trade item, how well its attributes would be preserved, and potential success in defining provenance and age. As well as issues about production, basic questions about the imports concern their age and social significance.

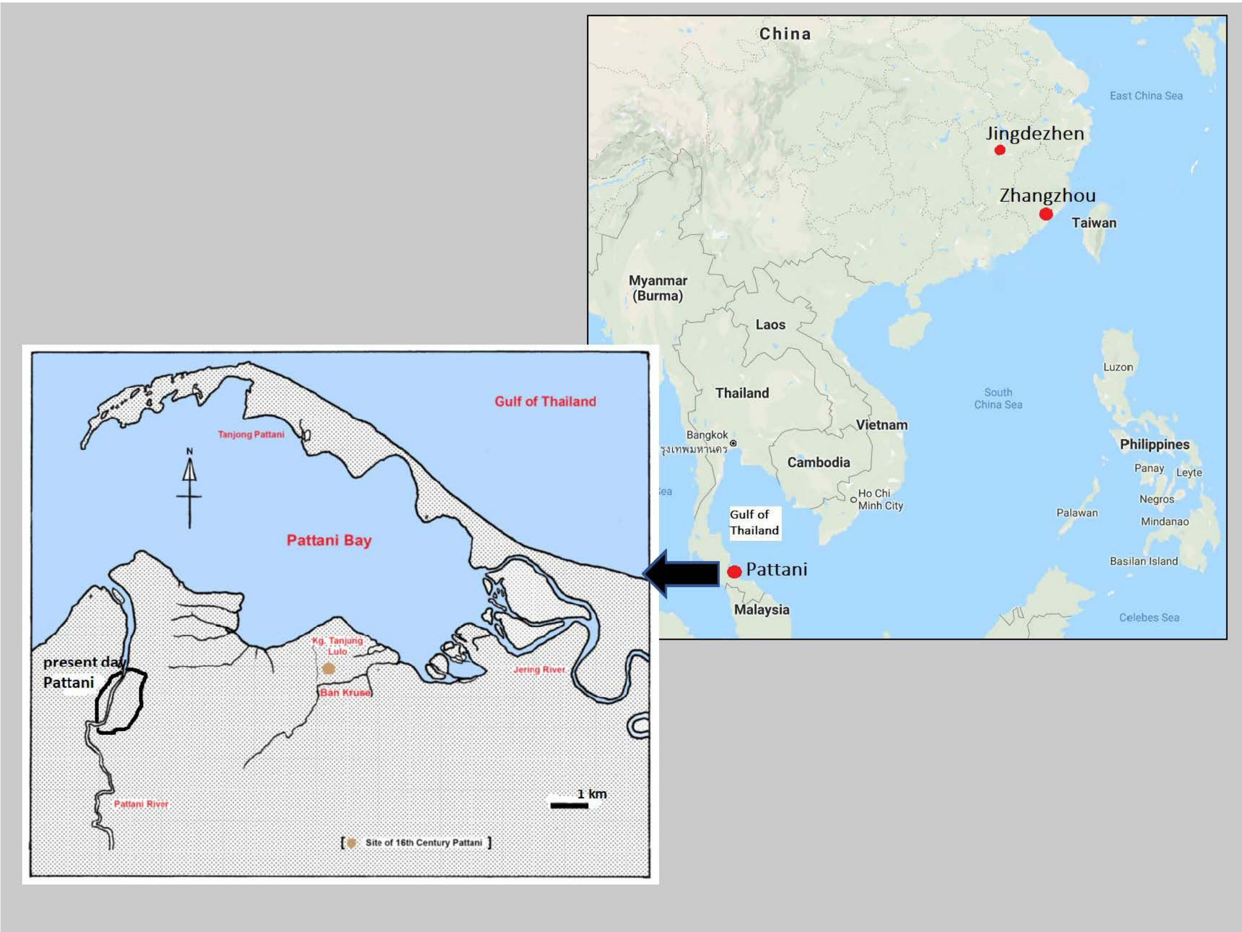

Figure 1. Map of the Pattani site (after Welch and McNeill 1989; Bougas 1990), and Southeast Asia.

The region of Pattani in southern Thailand was a nodal point for trade between the northern and southern parts of the Thai-Malay peninsula in the later prehistoric times, and especially during the early historic period for economic interaction between India, China, and the rest of Southeast Asia (Figure 1) (Welch and McNeill 1989). In the first half of the 15th century CE, trading between China and Southeast Asia had reached its highest point. The commerce during this period emphasized spices in return for silk and ceramics including underglaze blue-and-white, traded by Chinese merchants (Meilink-Roelofsz 1962).

Trade pottery, including Chinese manufactures, Changsha, is known in Southeast Asia from Tang Dynasty times; it is found especially in southern Thailand (Miksic 2009:72). The trade becomes more apparent during the subsequent Song and later dynasties (Crick 2010; Miksic 2009). The first of these trade wares associated with the Jingdezhen kiln complex, which we find important for our study of blue-and-white ceramics from Pattani, is the Qingbai stoneware (Scott 2002; Lim 2018); this was widely produced in China during this time frame. The underglaze blue-and-white refers to a cobalt blue-based decoration beneath the glaze layer.

Song Dynasty production continues during the Yuan and introduced green-glazed, Qingbai and white stoneware into Southeast Asia. Brown glazed stoneware storage jars from the southern Chinese kilns such as in Fujian were brought into Southeast Asian during this time as well (Crick 2010).

During the Yuan Dynasty, blue-and-white ceramic production centered around the Jingdezhen kiln sites of Hutian, Luomaqiao, and also Zhushan (Lim 2018:6). Subsequently, pottery produced in Southeast Asia--from Vietnamese, Thai, Cham, and Burmese kilns, in most of the fifteenth century AD (Brown 1988, 2009), replaced the Chinese product during the so-called “Ming Gap” and few examples of Ming (fourteenth to fifteenth century AD) ceramics are found in Southeast Asia (Crick 2010a: 223; Miksic 2009a: 84; Lim 2018: 8).

In later Ming times, in the sixteenth century, much Jingdezhen pottery was traded into the Southern Thai region. Crick (2010:224) reports this to be primarily robust, utilitarian vessels of bowl, small platter, cup, box and jar forms; we see these in the Pattani assemblage.

The blue-and-white exported through Southeast Asia during the 16th century was also intended for the emerging Islamic region. In the 16th century, Pattani experienced (1) conversion to Islam (2) involvement in overseas Chinese-European-South Asian trade networks (3) incorporation into the Thai sphere of influence (4) economic rise (Bougas 1990: 114). Pattani’s continuing role in Southeast Asian trade in the 16th century was also due to the arrival of European trading companies. In the early beginning of the 17th century (1602), Dutch East India Company established a trading post in Pattani (Bougas 1990). During the 16th and 17th century CE, Jingdezhen and Zhangzhou (Adhyatman 1999; Tan 2007) in China were the two main production centers for underglaze blue-and-white porcelain important for global trading.

Chinese blue-and-white has been widely investigated, including both typological attributes and chemical composition of the blue pigment, paste, and glaze for sourcing and technological manufacturing. However, most studies focused on complete vessels or pieces with known provenance.

In archaeological contexts however, most of the blue-and-white are small broken fragments. Therefore, distinguishing products from kiln sites is a challenge. In this research, combined typological characteristics and chemical composition of the Chinese blue-and-white sherds found in Pattani are investigated for provenance.

2. Research Issues

This research aims to establish the source of the South Thailand blue-and-white, as well as other presumably imported, high-fired ceramics. Written documents establish that export goods from China were being introduced into this region of the Thai-Malay peninsula during the 15th-18th centuries. Previous studies, for example, Fischer and Hsieh 2017 have documented through compositional XRF that blue-and-white sherds in Indonesia and the Philippines were derived from Jingdezhen and Zhangzhou. The issues of broader trade within Southeast Asia have been addressed by numerous authors (see in this regard, Guy 1986; Rinaldi 1989; Bronson 1996; Diem 1996; Melendres 2012; Bellina et al. 2014). Through provenance study using compositional analysis, we can identify the source areas within China for the Pattani sherds (for example, Peng et al. 2002), or perhaps other Southeast Asian regions such as North Thailand (Srisuchat 1994) or Vietnam.

3. Samples and Methods

3.1 Ceramic Samples

The samples are surface collections of diverse sets of glazed porcelain and stoneware found in the ancient trading port in Pattani, South Thailand. The sherds are dated to approximately 1300-1800 CE. Among these are the underglaze blue-and-white porcelain (n=17) and stoneware (n=5) sherds forming the core of our analysis. Figure 2 and Table 1 show the characteristics of the sherds.

Figure 2. Some of the porcelain and stoneware sherds that were analyzed from the larger Pattani collection.

Sample	Ceramic Type	Vessel Form	Part	Paste Texture	Glaze Attributes	Decoration	Other Characteristics
PAT 2	BW stoneware	bowl	base with ring foot	coarse	with crazing	spontaneous lines	
PAT 3	polychrome stoneware	bowl	body	coarse	White glaze	Floral, petal	
PAT 4	BW porcelain	bowl	rim	fine	Transparent glaze	Floral scrolls	
PAT 5	BW porcelain	Indeter-minate	indeterminate	fine	Transparent glaze with crazing	Floral/petals	Paste is reddish/brown
PAT 7	BW porcelain	bowl	rim	Fine	Transparent glaze	Floral scrolls	
PAT 9	BW porcelain	bowl	Base with ring foot	Fine	shiny, clear white glaze	Human/scholar	Four Chinese marks at the exterior base
PAT 12	BW porcelain	Indete-minate	body	Fine	Transparent glaze	indeterminate	
PAT 14	BW porcelain	bowl	body with rim	Fine	shiny, clear white	Floral scrolls	
PAT 16	BW porcelain	bowl	Body with rim	Fine	shiny, clear white glaze	Floral scrolls	
PAT 17	BW porcelain	small saucer	Body with rim	Fine	shiny, clear white glaze	Floral scrolls	
PAT 18	BW porcelain	plate	Body with ring foot	Fine	shiny, clear whiteglaze	Fish scale, medallions, floral	"Kraak style" and black-dark bluish pigment
PAT 19	BW porcelain	possible cup	body with rim	Fine	Transparent glaze	Floral scrolls	
PAT 20	BW porcelain	possible cup	Straight body with rim	Fine	Transparent glaze with crazing	Floral scrolls	
PAT 21	BW porcelain	bowl	Body with ring foot	Fine	Shiny, clear white	"Dotted points"	
PAT 22	BW porcelain	Indeter-minate	body	Coarse	Shiny, clear white glaze	cloud	Black-dark bluish pigment
PAT 23	BW porcelain	bowl	Body with flared rim	Fine	clear white	lotus	
PAT 24	BW porcelain	plate	body	Fine	clear white	Floral scrolls	
PAT 25	BW porcelain	jar	body with curvature	Fine	clear white	Floral scrolls	
PAT 26	BW porcelain	bowl	Body with indented ring foot	Coarse	white with light bluish tone	indeterminate	Overglaze brown enamel at the center

PAT 27	Stoneware	Indeter-minate	Body with base?	Coarse	Transparent glaze	indeterminate	Reddish, yellow green pigment
PAT 28	Stoneware	bowl	Body with corrugated rim	Coarse	Transparent green with crazing	Incised lattice pattern	Flared cavetto
PAT 29	Stoneware	bowl	Body with curvature	Coarse	Transparent green glaze	Incised lines on the exterior	

Table 1. Characteristics of the sherds from the Pattani site.

3.2. Method 1: Microscopic Analyses

A microscope was utilized to examine glaze and paste characteristics of the sherds. A petrographic microscope was used to examine minerals and non-plastic inclusions in the paste. The sherds were cut for thin sections (0.03mm) and were analyzed under a cross polarizing microscope (Leica DM4 P). In addition, the glaze thickness and attributes were investigated using similar microscope in transmitted mode. These analyses provide information about the manufacturing technology of the sherds that could be helpful in discriminating sources of manufacture.

3.3. Method 2: X-ray Fluorescence

A portable XRF spectrometer, Niton XL3t 950 GOLDD, equipped with a built-in camera was used to collect the major, minor and trace elements in parts per million. Each of the sherds was probed at the unpigmented area (clear glaze + paste) as the laser beam extends below the glaze and returns data from both the glaze and the paste. The camera was used in order to avoid the painted area of the sherds. The measurement was constrained by the size, thickness and shape of the sherds. For most sherds, the x-ray beam targeted the flat surface. For sherds with curvature, readings were obtained from the convex side to minimize the distance to the x-ray detector. The instrument operated at 50 kV with an acquisition time of 240 seconds. The collection of elemental data was performed in an open-air room, without a helium purge.

3.4. Method 3: Raman Spectrometer

A B&W BTR-111 532 nm Raman Spectrometer with a set focal length objective was used to collect Raman spectra data from glazed ceramic sherds. The sherds were wiped with a clean cloth prior to data acquisition; and in some cases, they were washed with water and then wiped dry. Standard data collection methods were used, including the subtraction of dark scan data and baseline correction. Peak height data were obtained using an Excel format.

4. Results and Analysis

4.1. Microscopic Analyses of the paste and glaze

Petrographic examination provides only limited information about non-plastic inclusions in the paste due to the fineness of the raw materials. However, it shows mineral inclusions and other details potentially valuable for provenance study. The paste of the blue-and-white porcelain samples show inclusions of high birefringent mineral (Figure 3). Typically, the firing temperature of the porcelain is between 1200-1400°C. In this case, it is possible this high birefringence mineral is muscovite which has a melting point of 1500°C. Because muscovite is commonly present in clays, this mineral alone is not sufficient to distinguish our porcelain samples as to geographic kiln productions.

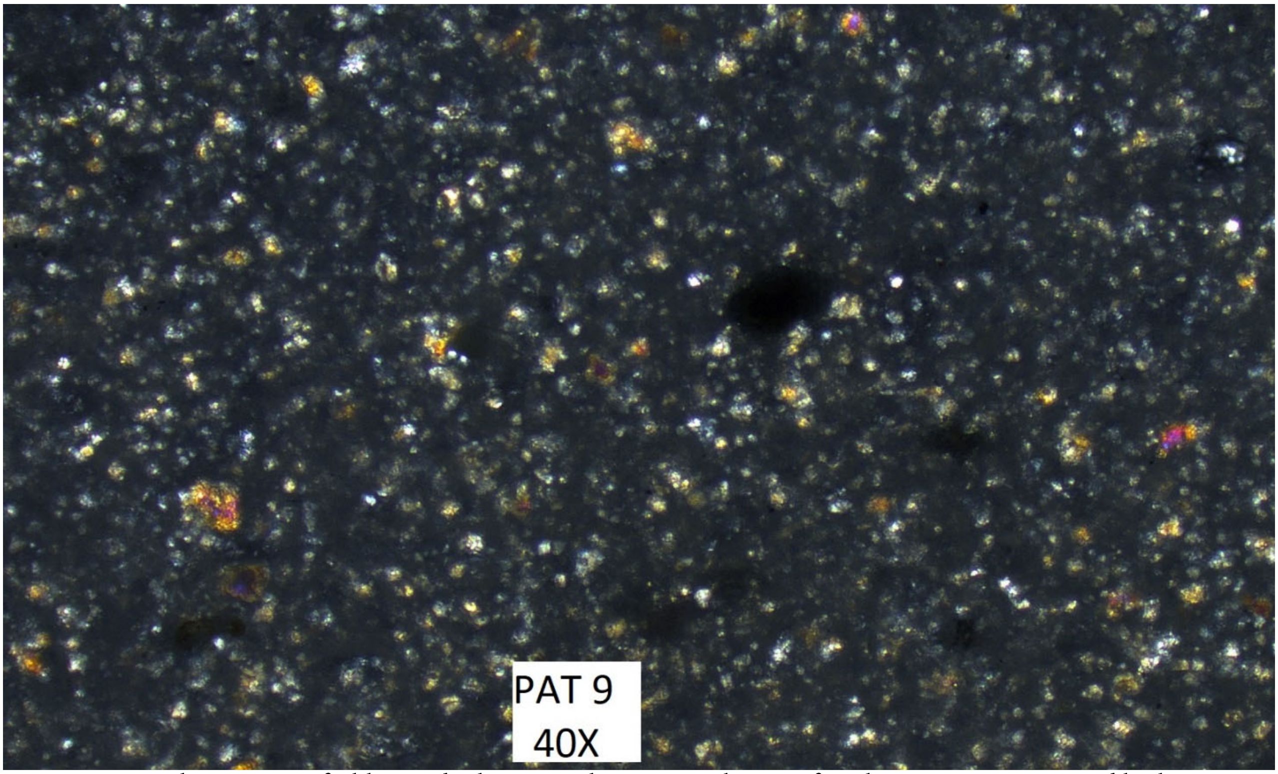

Figure 3. Thin section of a blue-and-white porcelain in XPL showing fine, homogenous paste and high birefringence mineral inclusions.

Further microscopic examination shows bubbles in the glaze for sherds stylistically identified as Zhangzhou and Jingdezhen production. The sherds show considerable variation in the quantities of bubbles, both small and large in size (Figures 4). This difference in bubble sizes was possibly controlled by the firing temperature (Qu et al. 2014). When the firing temperature is not regulated, it could create bubbles with different sizes. Whereas, a maintained firing temperature produces bubbles with a uniform size. Also, the bubbles could be produced by gas molecules due to the composition of the glaze. Prior research (Beals and Steele 1981) indicates that the size and distribution of bubbles may reflect chronological patterns.

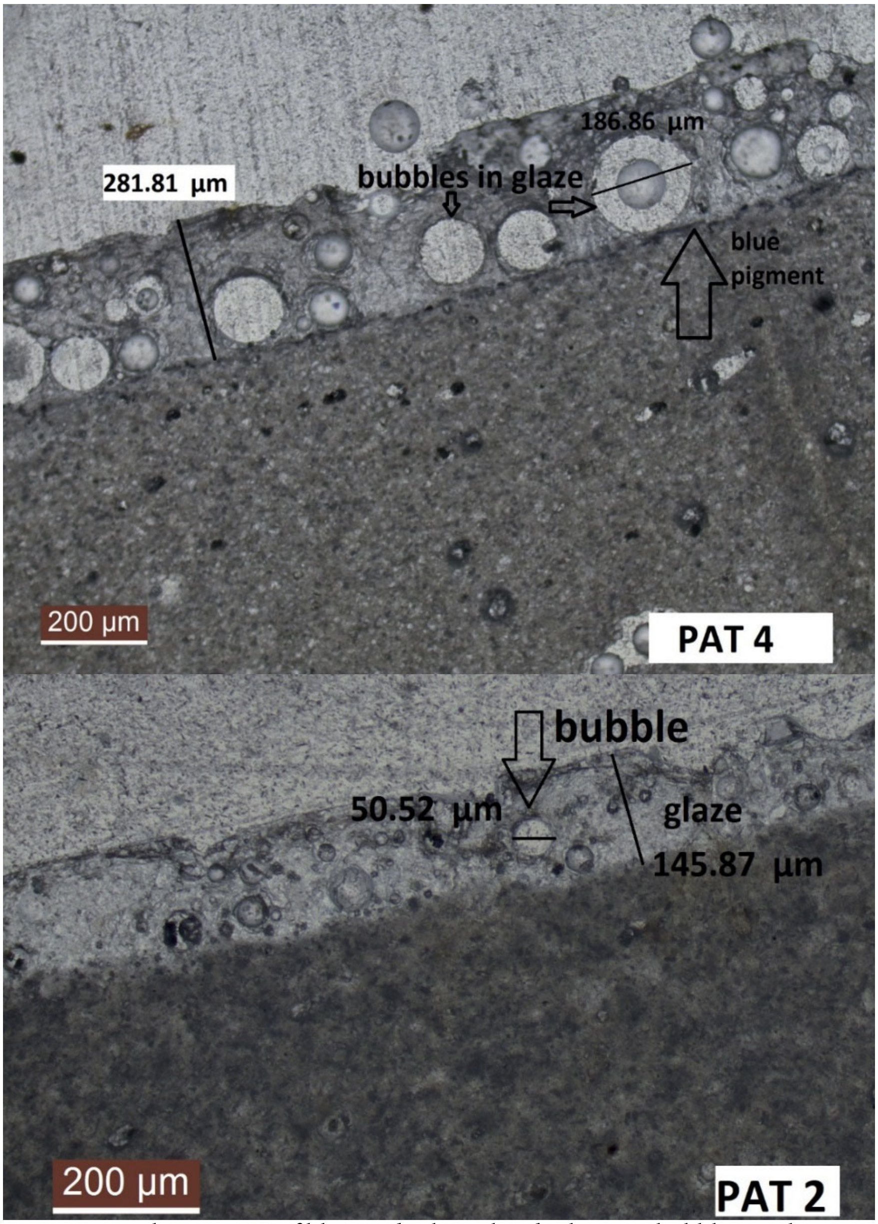

Figures 4. Thin section of blue-and-white sherds showing bubbles in glaze.

Blue-and-white ceramics from Jingdezhen are known for their fineness, including uniformity and thinness of the glaze, while Zhangzhou pieces have thicker glaze and other impurities (Tan 2007). Our microscopic measurements of the thickness of the glaze show that samples stylistically identified as Zhangzhou have a thinner glaze than the Jingdezhen ones. The Jingdezhen samples have relatively uniform thickness but are not necessarily thinner than sherds stylistically identified as Zhangzhou (Table 2). Glaze attributes such as thickness and bubbles are critical information for question of provenance, but because our samples are limited, this information it is not sufficient here to assign sherds to Jingdezhen, Zhangzhou and another possible kiln production. However, glaze attributes seen in our samples provide information on the manufacturing processes.

Sample no.	Paste (μm)	Glaze interior (μm)	Glaze exterior (μm)	Microscopic observations
PAT-2	3998.27	286.20	194.50	Exterior glaze is worn
PAT-3	5587.76	275.08	416.79	Glaze is worn
PAT-4	2601.04	488.16	441.67	Shows bubbles in the glaze
PAT-5	3792.78	605.73	625.18	Multiple layers of glaze, paste is reddish brown
PAT-7	2561.87	527.93	502.93	Bubbles in glaze
PAT-9	3609.40	338.99	386.22	Bubbles in the glaze
PAT-12	3262.07	252.85	333.43	Bubbles in the glaze, glaze is worn
PAT-14	4317.94	325.44	302.20	Bubbles in the glaze, glaze is worn
PAT-16	2999.06	255.70	348.69	Bubbles in the glaze
PAT-17	2161.86	326.27	185.97	Paste has voids (large and small)
PAT-18	----	----	---	No thin section
PAT-19	----	----	---	No thin section
PAT-20	2045.69	255.70	371.93	Paste has voids (large and small)
PAT-21	4257.65	389.00	416.79	Fine white paste with voids (large and small)
PAT-22	7187.49	302.59	391.78	Paste has voids (large and small); bubbles in the glaze
PAT-23	2705.10	370.62	335.53	
PAT-24	4819.65	403.46	232.89	Paste has voids (large and small)
PAT-25	6020.70	95.84	322.94	Glaze is worn
PAT-26	3184.76	488.72	488.72	Paste has voids (large and small); bubbles in the glaze

PAT-27	10620.04	333.35	229.30	Paste is fine, exterior glaze is deteriorated
PAT-28	5228.21	391.23	426.79	Paste has voids (large and small) and traces of organic materials; bubbles in the glaze
PAT-29	4488.95	326.91	340.94	Paste has voids (large and small) and traces of organic materials, rocks, bubbles in the glaze

Table 2. Measurements of the paste and glaze of the sherds from the Pattani site.

4.2. X-ray Fluorescence Analysis (glaze + paste)

The pXRF data on selected major, minor, and trace elements on the samples are shown in Table 3. For provenance, we focused on three trace elements: Zirconium (Zr), Rubidium (Rb), and Strontium (Sr) probed from glaze + paste. Zirconium is resistant to physical and chemical weathering and present in the main raw materials and therefore useful in provenance study. Rubidium is abundant element and it behaves similar to Potassium (K) which richly occurs in clays. Strontium occurs in sedimentary deposits and it behaves similar to Calcium (Ca) and Barium (Ba). Calcium is one of the main components in the glaze serving as flux. Therefore, Zr, Rb, Sr are the most helpful elements and they provided a useful distinct group distribution of the sherds shown in Figure 5.

Sample	Zr (+/-)	Sr (+/-)	Rb (+/-)	Th (+/-)	Pb (+/-)	Fe (+/-)	Mn (+/-)	Ti (+/-)	Ca (+/-)	K (+/-)	Al (+/-)	Si (+/-)
PAT-2	52.43 (2.71)	312.41 (4.89)	105.70 (2.90)	16.89 (2.89)	9.32 (3.91)	2.1K (0.1K)	734.13 (52.63)	454.64 (16.89)	78.1K (0.3K)	25.6K (0.3K)	41.8K (1.5K)	284.2K (1.6K)
PAT-3	32.2 (2.02)	69.46 (2.31)	450.84 (6.31)	BD	390.04 (11.55)	3.5K (0.1K)	260.37 (41.30)	422.64 (16.21)	25.8K (0.2K)	38.2K (0.3K)	50.1K (1.4K)	288.2K (1.5K)
PAT-4	34.96 (2.01)	65.06 (2.20)	136.84 (3.26)	10.69 (2.64)	BD	3.1K (0.1K)	679.82 (50.96)	413.8 (16.76)	80.1k (0.3K)	16.6k (0.2K)	46.4k (1.5K)	314.2k (1.6K)
PAT-5	84.16 (2.71)	123.28 (2.96)	135.54 (3.24)	26.98 (3.22)	6.75 (3.81)	3.0K (0.1K)	1.7K (0.1K)	549.89 (18.08)	30.7K (0.2K)	40.0K (0.3K)	42.2K (1.4K)	354.2K (1.7K)
PAT-7	33.29 (1.90)	48.14 (1.90)	235.08 (4.24)	2.77 (2.50)	4.16 (3.57)	3.4k (0.1k)	290.52 (40.25)	334.19 (14.60)	31.0k (0.2k)	45.8k (0.3k)	39.8k (1.4k)	316.0k (1.6k)
PAT-9	23.74 (2.07)	36.05 (2.00)	212.69 (4.74)	BD	5.71 (4.27)	2.9K (0.1K)	278.65 (46.63)	246.79 (14.62)	24.5K (0.2K)	13.1K (0.2K)	14.8K (0.9K)	204.2K (1.5K)
PAT-12	32.39 (1.92)	56.32 (2.03)	257.94 (4.47)	6.50 (2.69)	BD	3.6K (0.1K)	575.69 (47.55)	300.40 (14.01)	34.6K (0.3K)	34.2K (0.2K)	31.1K (1.3K)	258.6K (1.5K)

PAT-14	40.23 (2.01)	56.11 (2.01)	185.07 (3.72)	10.01 (2.67)	8.27 (3.72)	3.8K (0.1K)	357.82 (41.79)	392.45 (16.06)	45.3K (0.3K)	30.1K (0.3K)	41.7K (1.4K)	315.4K (1.6K)
PAT-16	28.63 (1.94)	55.90 (2.11)	220.69 (4.27)	BD	8.52 (3.86)	3.2K (0.1K)	311.53 42.88)	223.23 (11.90)	31.6K (0.2K)	26.7K (0.3K)	12.6K (0.6K)	136.4K (1.0K)
PAT-17	38.95 (1.96)	46.77 (1.86)	233.00 (4.19)	5.29 (2.57)	BD	3.7K (0.1K)	215.60 (37.31)	324.61 (14.55)	43.2K (0.3K)	31.0K (0.3K)	52.3K (1.6K)	348.7K (1.6K)
PAT-18	39.65 (2.09)	54.55 (2.08)	241.49 (4.48)	5.92 (2.77)	11.80 (4.05)	4.2K (0.1K)	389.98 (45.71)	305.31 (14.24)	52.3K (0.3K)	24.9K (0.3K)	40.9K (1.4K)	305.3K (1.6K)
PAT-19	30.04 (1.94)	70.49 (2.27)	158.86 (3.51)	8.30 (2.61)	10.14 (3.83)	2.9K (0.1K)	335.66 (42.21)	317.29 (14.43)	51.9K (0.3K)	38.4K (0.3K)	48.3K (1.5K)	327.5K (1.6K)
PAT-20	36.07 (1.93)	50.48 (1.91)	248.49 (4.31)	BD	21.90 (4.16)	3.3K (0.1K)	478.37 (44.45)	436.67 (16.11)	32.3K (0.2K)	53.2K (0.4K)	44.1K (1.4K)	312.7K (1.6K)
PAT-21	31.87 (1.96)	38.58 (1.82)	225.14 (4.35)	4.69 (2.69)	4.91 (2.29)	3.1K (0.1K)	371.22 (44.69)	404.03 (16.19)	43.6K (0.2K)	24.6K (0.2K)	35.5K (1.3K)	295.8K (1.6K)
PAT-22	43.01 (2.25)	79.92 (2.53)	156.17 (3.26)	10.77 (2.85)	10.62 (4.09)	6.5K (0.1K)	471.96 (49.46)	320.30 (18.88)	79.8K (0.4K)	18.1K (0.3K)	44.5K (1.5K)	306.1K (1.6K)
PAT-23	38.14 (2.04)	53.30 (2.04)	215.00 (4.15)	6.13 (2.74)	26.53 (4.51)	5.1K (0.1K)	368.53 (43.75)	295.78 (14.68)	41.1K (0.2K)	28.9K (0.3K)	44.7K (1.4K)	307.6K (1.6K)
PAT-24	33.79 (2.05)	72.07 (2.36)	205.70 (4.12)	8.19 (2.84)	29.07 (4.65)	3.4K (0.1K)	290.79 (42.52)	290.30 (13.93)	57.3K (0.3K)	34.3K (0.3K)	50.5K (1.6K)	325.5K (1.7K)
PAT-25	42.14 (2.14)	42.98 (1.92)	199.89 (4.11)	5.05 (2.73)	26.44 (4.62)	4.4K (1.1K)	303.18 (43.39)	277.36 (13.59)	14.6K (0.1K)	26.8K (0.1K)	32.9K (1.1K)	312.3K (1.7K)
PAT-26	32.05 (2.06)	88.28 (2.58)	197.07 (4.02)	4.70 (2.60)	BD	4.0K (0.1K)	899.91 (57.53)	345.01 (15.96)	65.0K (0.3K)	26.9K (0.3K)	48.2K (1.6K)	336.7K (1.7K)
PAT-27	31.72 (2.23)	78.18 (2.63)	140.60 (3.62)	13.86 (6.59)	1.8K (0.0K)	2.5K (0.1K)	265.44 (44.91)	335.19 (14.43)	26.4K (0.2K)	20.6K (0.2K)	27.7K (1.3K)	245.9K (1.6K)
PAT-28	98.35 (3.34)	304.32 (5.08)	100.01 (2.94)	6.62 (2.60)	BD	6.4K (0.1K)	762.32 (57.22)	1.0K (0.0K)	92.6K (0.4K)	20.08K (0.3K)	36.6K (1.5K)	233.8K (1.5K)
PAT-29	127.25 (3.77)	339.38 (5.53)	126.38 (3.42)	29.69 (3.76)	52.05 (5.84)	5.4K (0.1K)	3.5K (0.1K)	746.14 (24.34)	66.2K (0.3K)	28.3K (0.3K)	62.2K (2.1K)	358.8K (1.8K)

Table 3. Major, minor, and trace elements and standard deviations in parts per million in paste + glaze measured with portable XRF (BD=Below Detection).

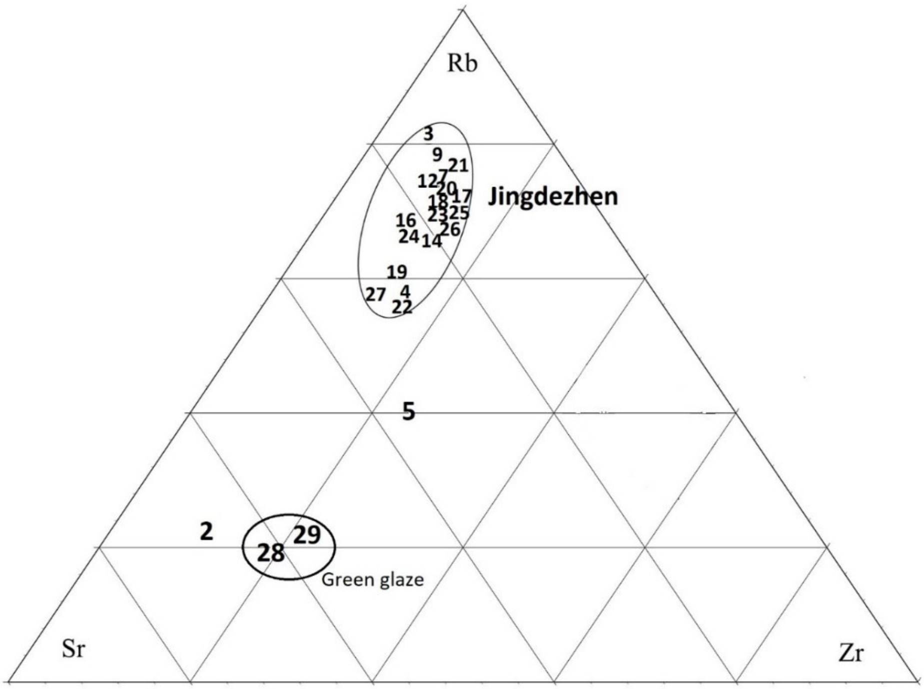

Figure 5. Ternary plot, Sr, Rb, Zr (ppm concentration) showing discrete distributions of the sherds.

The Rb, Zr, Sr ternary plot shows three group distributions of sherds, (1) Jingdezhen (2) Zhangzhou (3) Thai production. The blue-and white porcelain and stoneware sherds with high Rb, low Zr, lower Sr ppm content can be assigned to the Jingdezhen production. Within the general Jingdezhen group, the plot shows as least two groups (a) Jingdezhen core (b) Jingdezhen outliers. Although these sherds cluster in the Jingdezhen production, it shows that there is a slight compositional variation. This might be linked to many production kilns in the Jingdezhen area using different types of raw materials or changes in production technology over time.

Sample	**Polymerization Index Ip (Amax 500/Amax 1000)**	**Vmax Si-O Stretching Bond** cm-1
PAT-2	1.24	797
PAT-3	1.24	797
PAT-4	1.32	797
PAT-5	1.25	797
PAT-7	1.31	797
PAT-9	1.24	797
PAT-12	1.26	797
PAT-14	1.28	797

PAT-16	1.25	797
PAT-17	1.27	797
PAT-18	1.25	797
PAT-19	1.23	797
PAT-20	1.33	797
PAT-21	1.28	797
PAT-22	0.05	1086
PAT-23	1.34	801
PAT-24	1.24	797
PAT-25	1.37	801
PAT-26	1.27	801
PAT-27	1.24	801
PAT-28	1.26	797
PAT-29	1.25	801

Table 4. Si-O stretching bond and polymerization index data of the ceramic glaze + paste from Pattani measured with Raman Spectroscopy.

One sample (PAT-5) has relatively high Rb and Sr, and low Zr ppm concentration is an outlier in the plot. Based on the elemental data in the Table 4, provided by Fischer and Hsieh 2017, this sherd grouped to the Zhangzhou production (Figure 6).

The compositional variations for Jingdezhen and Zhangzhou sherds clearly suggest variation in raw materials in paste and glaze. The relatively high Strontium content for Zhangzhou may have reflected from the different species of wood ash mixed with porcelain stone in the glaze. The lower Strontium content in Jingdezhen may reflect using limestone as flux in glaze (Fischer and Hsieh 2017; 21, Reimann et al., 2008).

On the other hand, the stoneware sherds with highest Sr, high Rb, and very low Zr in ppm content cluster into one distinct group and can be assigned to a Thai production. Sherd samples PAT 28 and PAT 29 are stylistically similar having green glaze. These two sherds clusters together indicate they are similar in composition. Another reason we assigned these two as Thai productions is, they display a similar style to the Thai stoneware “Sawankhalok”.

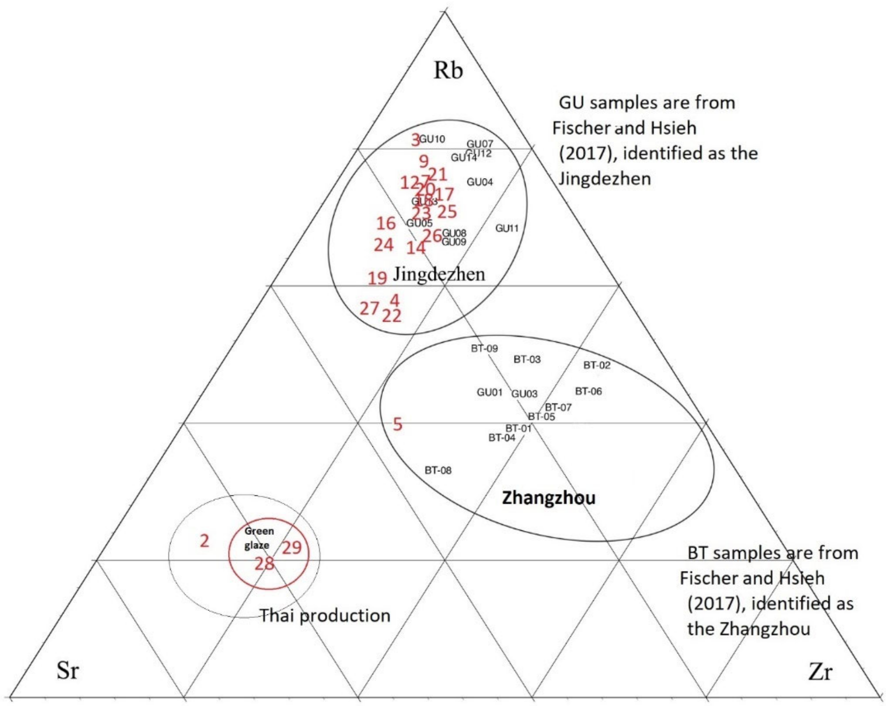

Figure 6. Ternary plot, Zr Sr, Rb, Zr (ppm concentration) showing three production groups (sherds in red are from the Pattani site).

However, the blue-and-white stoneware (PAT 2) clearly indicates that it is not a Zhangzhou production, in contrast to an identification based on stylistic attributes. In comparison to Chinese manufactured, this sherd has very different composition with high Sr, low Rb, very low Zr ppm content. Even though this sherd is blue-and-white, the composition does not correspond to a Chinese, but more so to a Thai manufacture. This is probably not unusual, because other kilns in Southeast Asia such as Thai and Vietnamese have also produced blue-and-white stoneware and porcelain to meet the demand during most of the 15th and 16th century CE (Lim 2018: 8).

4.3. Raman Analysis (glaze + paste)

In general, Raman spectroscopic analysis has been used to study the molecular and vibrational characteristics of the ceramic glazes, pigments and paste, including the paste mineralogy. It was found that most of the Pattani samples were well glazed and so that the comparative analysis reported here is for data collected from glazed ceramics and thus is glaze + paste data (as the laser beam extends below the glaze and returns data from both the glaze and the paste) with attempts to avoid pigments.

Ceramic glazes are made using three different components: a glass former such as silica, a flux to allow that glass to flow onto the ceramic surface such as ash, and a refractory to allow the glaze to stick to the ceramic such as clay or feldspar (aluminum silicates). Ceramic glazes are predominantly made of silica (quartz – SiO2), which forms a glass when it melted. Glass is a super cooled liquid that is ostensibly amorphous, but is actually composed of silica tetrahedra that are tied together in long chains. A glass that has well developed long chains is said to be well polymerized. The analysis used here to fingerprint the provenance-time of the ceramic glazes follows the determination of the degree of polymerization of the glazes, methodology used by Colomban et al., 2001; 2003; 2006.

Raman analysis used in this study (Colomban et al., 2001; 2003; 2006) looks at the SiO4 n-bridging oxygens (Q0-Q4) with respect to the number of bridging oxygens bonded per tetrahedron for the Si-O stretching range extending from 700 to 1300 cm-1. The maximum peak height from this range is obtained (designated ≈1000 max cm-1) and used in the determination of a polymerization index calculation when plotted against the maximum peak height Si-O bending peaks from 400-650 cm-1 (designated ≈500 max cm-1).

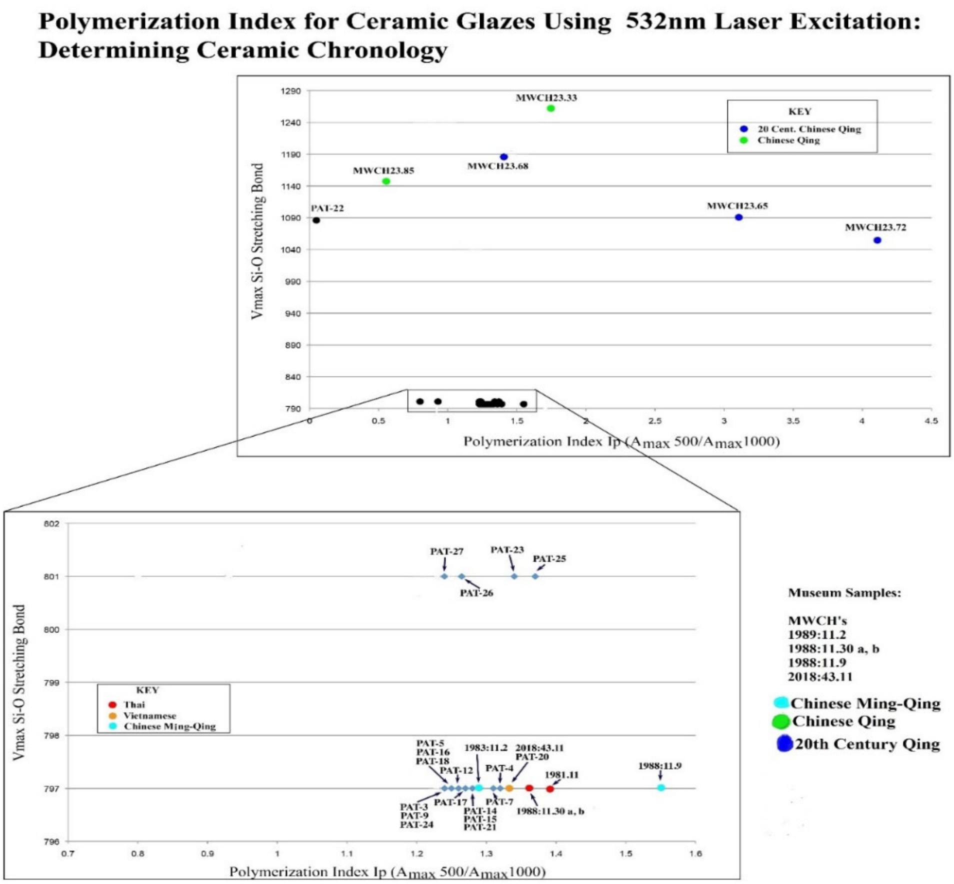

Figure 7. Plot of the Si-O stretching bond and polymerization index of the glaze for Pattani sherds and chronologically known vessels from the museum.

Figure 7 shows the Si-O stretching bond and polymerization index of the ceramic glaze + paste. The graph shows that most of our samples (n=21), the Si-O stretching vibrations are at 797 cm-1 and polymerization index between 1.24-1.25. In order to have chronological basis, we plotted our samples along with museum specimens dating Chinese Ming to 20th century Qing. The plot shows that most of our samples cluster in the Ming-early Qing time period. This is consistent to historical records where Pattani was an important site for local, Chinese and European traders, especially in the 16th-17th century (Meilink-Roelofsz 1962; Bougas 1990).

5. Conclusions

The scale of the maritime porcelain trade in South East Asia during the late 2nd millennium CE is understood primarily based on historical documents. When it comes to specific trading centers such as Pattani, South Thailand, information is limited. However, written documents and oral history about this early Malay state indicate that the scale of the trade endeavor was substantial during the Ming to early Qing periods in China, but identification and provenance information for the early blue-and-white porcelain is lacking. Our efforts to establish the sources of the import ceramics, as well as of other imported, high-fired ceramics, provide new evidence.

Methods of analysis found useful include stylistic assessment, petrography, and two primary techniques for deriving values of key compositional elements. Petrographic analysis provides perspective on the quality and production technology associated with blue and white porcelain found in Pattani. The Jingdezhen ceramics are typically fine and with homogeneous paste compared to stoneware in general and to the Zhangzhou production. The third set of sherds is of northern Thai style.

The portable EDXRF and the Raman instruments collect data in a non-invasive manner from the archaeological remains and do not damage the specimens. At the same time, for porcelain and glazed stoneware, a methodological issue exists in separating readings taken from glaze, glaze and underlying paste, and glaze and blue pigment. In this study, we have used primarily the glaze + paste compositional data to document variation among the sherds. Readings for key elements can be reliably acquired for all the sherds examined.

The precision of Raman laser sampling results in highly specific data relative to issues of paste, glaze and pigment. We collected glaze + paste evidence comparable to the XRF readings. Comparisons among samples of porcelain from museum vessels of known age and the Pattani sherd sample provide datable distributions showing that most of our samples cluster in the Ming-early Qing time period.

Through the compositional analysis based on XRF-derived elemental data, as well as stylistic attributes, we can identify three main sources for Pattani's early glazed wares. Elemental analysis of blue and white sherds from Pattani can be used to discriminate sources of manufacture between Jingdezhen and Zhangzhou area kilns. Particularly appropriate because of the nature of the specimens, pottery, Zr-Rb-Sr plots are most useful for differentiating sherd clusters as to manufacturing source. Comparison to results produced by Fischer and Hsieh (2017) for traded blue-and-white pottery in Banten, Indonesia and Cebu, Philippines show a high level of agreement. As well, it is clear that green-glaze stoneware made in northern Thailand is part of this trade interaction as well.

To fully investigate the compositional and elemental attributes of blue and white from two major production kilns, a larger sample set is needed, however, the Pattani sample aids in this endeavor and provides some convincing data. In sum, most of the blue-and-white sherds found in Pattani were produced in Jingdezhen and this reflects preferential trade routes and quality of goods.

6. Acknowledgments

Ayres wishes to acknowledge the efforts of Ajarn Khate Ratanajarana, the Rector's Office, and the Center for Southern Thai Studies, of the Prince of Songkla University, Pattani, Thailand, and also Ajarn Amara Srisuchat, for the original field study, which was sponsored by the Thai-US Fulbright Foundation. The authors acknowledge the Jordan Schnitzer Museum of Arts, University of Oregon, for providing some collections used for comparative study. Kneisly would like to thank Dr. Gyoung-Ah Lee, David Blackwell for microscopic access, and Sam Eat for his previous work in the earlier stage of this project while at the University of Oregon.

7. References

Adhyatman, S. 1999. Zhangzhou (Swatow) Ceramics Sixteenth to Seventeenth Centuries Found in Indonesia. Jakarta: The Ceramic Society of Indonesia.

Ayres, W., and K. Ratanajarana. 1985. Archaeology in Southern Thailand. In Rusamilae, pp. 83-86. Pattani: Prince of Songkla University (in Thai).

Bellina, B., P. Silapanth, B. Chaisuwan, et al. 2014. The development of coastal polities in the upper Thai-Malay Peninsula, in Before Siam: Essays in art and archaeology, eds. N. Revire & S. Murphy. Bangkok: River Books, 69–89.

Bougas, W. 1990. Pattani n the Beginning of the XVII Century. Archipel 39:113-138.

Bronson, B. 1996. "Chinese and Middle Eastern Trade in Southern Thailand During the 9th Century A.D."

181–200 in Ancient Trades and Cultural Contacts in Southeast Asia, edited by A. Srisuchat. Bangkok: ONCC.

Brown, R. 1988. The Ceramics of Southeast Asia: Their Dating and Identification. Kuala Lumpur: Oxford University Press.

Brown, R.M. & Siam Society, 2009. The Ming gap and shipwreck ceramics in Southeast Asia: towards a chronology of Thai trade ware, Bangkok, Thailand: Siam Society.

Colomban, Ph., Etcheverry, M-P, Asquier, M., Bounichou, M., and A. Tournie. 2006. Raman identification of ancient stained glasses and their degree of deterioration. Journal of Raman Spectroscopy, 37(5), pp.614–626.

Colomban, P., 2003. Polymerization degree and Raman identification of ancient glasses used for jewelry, ceramic enamels and mosaics. Journal of Non-Crystalline Solids, 323(1-3), pp.180–187.

Colomban, P., Sagon, G. & Faurel, X., 2001. Differentiation of antique ceramics from the Raman spectra of their coloured glazes and paintings. Journal of Raman Spectroscopy, 32(5), pp.351–360.

Crick, M. 2010a. Blue-and-white qinghua porcelain in South-East Asia. In Chinese trade ceramics for SouthEast Asia from the 1st to the 17th century. Collection of ambassador and Mrs Charles Muller, Geneve: Fondation Baur. 216.317.

Diem, A. 1996. Relics of a Lost Kingdom: Ceramics from the Asian Maritime Trade. Makati: Asia type, Inc.

Fischer, C., and E. Hsieh. 2017. Export Chinese Blue-and-white Porcelain: Compositional Analysis and Sourcing Using Non-invasive Portable XRF and Reflectance Spectroscopy. Journal of Archaeological Science 80: 14-26.

Guy, J. 1986. Oriental Tradeware Ceramics in Southeast Asia, 9th to 16th Centuries. Singapore: Oxford University Press.

Hsieh, E. and C. Fischer. 2014 Non-invasive Analysis of Chinese Blue-and-white Porcelain from Indonesia and the Philippines. The 40th International Symposium on Archaeometry, Los Angeles.

Jory, P. (ed). 2013. The Ghosts of the Past in Southern Thailand: Essays on the History and Historiography of Pattani. Singapore: NUS Press.

Lim, T.S. 2018. Chinese Ceramics in Southeast Asia. In: Smith C. (eds) Encyclopedia of Global Archaeology. Springer, Cham.

Ma, H., Zhu, J., Henderson, J. and Li, N., 2012. Provenance of Zhangzhou export blue-and-white and its clay source. Journal of Archaeological Science 39, 1218-1226.3.

Meilink-Roelofsz, M.A.P., 1962. Asian Trade and European Influence in the Indonesian Archipelago Between 1500 and About 1630. The American Historical Review. The Hague: Martinus Nijhoff. Pp. viii, 471. Glds. 29.75.

Melendres, R.G. 2012. Determination of Oriental Tradeware Ceramics: A Proposed System for Identifying and Documenting Pottery in Philippine Archaeological Sites. Hukay 17: 61-78.

Miksic, J. 2009a. Research in ceramic trade, within Southeast Asia and between Southeast Asia and China. In Southeast Asian Ceramics. New light on old pottery, ed. J.N. Miksic, 70–99. Singapore: Southeast Asian Ceramic Society.

Miksic, J., and G.Y. Goh. 2016. Ancient Southeast Asia. New York: Routledge.

Myo, T.T. and D. Rooney. 2001. Ancient Celadon in Myanmar: A New Ceramic Discovery. Orientations 32 (4): 57-61. Phivolcs Press.

Peng S., M. Peng, and P. Lam. 2002. Yuan and Ming Blue and White Ware from Jiangxi. Hongkong: Chinese University of Hongkong and Jiangxi Provincial Museum.

Perret, D., A. Srisuchat, and A. Sombatyanuchitand. 1999. Thaïlande. La Mission: Sites urbains anciens de la region de Pattani. In: Bulletine l'Ecole française 'Extrême-Orient. 86: 387-393.

Qu, Y. et al., 2014. Microstructure characteristics of blue-and-white porcelain from the folk kiln of Ming and Qing Dynasties. Ceramics International, 40(6), pp.8783–8790.

Rinaldi, M. 1989. Kraak Porcelain: London: Bamboo Publishing.

Scott, R. 2002. Introduction: Qingbai porcelain and its place in Chinese ceramic history. In Qingbai ware: Chinese porcelain of the Song and Yuan dynasties, ed. S. Pierson, 6–12. London: Percival David Foundation of Chinese Art

Srisuchat, A. 1994. "Discovering Chinese Yue and Longquan Green Glazed Wares and Reconsidering Their Socio-Economic Roles in the Development of Ancient Communities in Thailand". 213–228 in New Light on Chinese Yue and Longquan Wares—Archaeological Ceramics Found in Eastern and Southern Asia, A.D. 800–1400, edited by Ho Chuimei. Hong Kong: Centre of Asian Studies, The University of Hong Kong.

Tan, R. 2007. Zhangzhou Ware Found in the Philippines: “Swatow” Export Ceramics from Fujian 16th – 17th Century. Makati: Art Post Asia, Ltd.

Welch, D. J., and J. R. McNeill 1989. Archaeological Investigations of Pattani History. Journal of Southeast Asian Studies 19(1):27-41.

Archaeometallography: A New Look at Old Issues in the History of the Iron Industry

N.N. Terekhova (*Institute of Archaeology of the Russian Academy of Sciencies*) & V.I. Zavyalov (*Institute of Archaeology of the Russian Academy of Sciencies*)

Abstract

A traditional archaeological approach to the study of metal artifacts has some restrictions, because it is unable to expose the information contained inside them about the method of their production. The introduction of metallographic methods into archaeology has made it possible to obtain fundamentally new types of information. The analytical framework at the disposal of the archaeological metallography group of the Laboratory of Nature Sciences in Archaeology of the Institute of Archaeology of the Russian Academy of Sciences makes it possible to solve many problems in the formation and development of the iron industry, including some controversial issues.

Keywords

Archaeometallography, ferrous metal, bloomer process, meteoric iron, technological model

1. Introduction

Many great thinkers, beginning in antiquity, have noted the great significance of iron in the history of mankind. We may cite L. Morgan's famous words as the quintessence of remarks made on this topic: "The production of iron was the event of events in human experience, without a parallel, and without an equal, beside which all other inventions and discoveries were inconsiderable, or at least subordinate" (Morgan 1935, 28).

The traditional archaeological approach to the study of metal artifacts has some restrictions, because it is unable to expose the information contained inside them about the method of their production, i.e. about the knowledge and skills of the craftsman, and, ultimately, about the production culture of a certain society. The introduction of metallographic methods into archaeology has made it possible to obtain such information. Well-known Russian scientist Boris Aleksandrovich Kolchin (1914-1984) made an invaluable contribution to the adaptation of technical metallography to the study of archaeological objects.

The basis of the archaeometallographic method is the identification of the process flow of the object's manufacturing, which shows the nature of the raw material used and the sequence of technical operations. A generalization of the results of the research conducted makes it possible to advance to the construction of a historical and technological conception that sheds light on socioeconomic problems. In this way, metal artifacts become a full-fledged historical source. The significant potential of the method of archaeological metallography in this regard has been demonstrated by materials from sites of Ancient Rus' (Kolchin 1953; 1959).

2. Method

At present, the study of ancient iron artifacts continues in the Laboratory of Nature Sciences in Archaeology of the Institute of Archaeology of the Russian Academy of Sciences. Method of archaeological metallography (or archaeometallography) is the main one on studying of the problems of ancient metallurgy and metalworking. This method involves three sequential operations: microscopic determination of the metal structure, its interpretation, technological reconstruction of the artifact fabrication.

The specimens were prepared using standard metallographic techniques. Examined samples were cut from cutting-edges or from functional parts. The samples then mounted into Wood alloy, grinded and then polished by chromium oxide. The microstructures of iron objects were determined on an MMR-2R optical microscope after etching with nital reagent (3% solution of HNO3 in ethyl alcohol) at magnifications of 150x and 490x. The size of the grains was evaluated after Russian state standard (GOST 5639-82). Microhardness was measured on a microhardness machine PMT-3 with a diamond pyramidal indenter with 100 g load.

The generalization of the results of the mass series of obtained analytical data allows us to proceed to the construction of historical and technological concepts with access to social and economic problems. Thus, metal artifacts become a full-fledged historical source. In Russia, the method of archeometallography, began to be used from the late 40's XX c. In recent years the unique bank of metallographic data including more than 13000 analyzes was created. A number of projects are implemented on this basis. We give as an example a generalization of the history of blacksmith's craft in Eastern Europe. It was present a detailed analysis of archaeometallographical data and single out fundamental border lines which mark basic stages of development of iron metalwork in Eastern Europe.

The analytical framework allows many issues in the formation and development of the iron industry, including controversial ones, to be resolved.

3. Iron in the Bronze Age.

One of the key issues in the history of the study of ferrous metal is that of the conditions and timeframe of the discovery of the metallurgical method of iron production and the reasons for the transition from the bronze industry to the iron one. The set of archaeological and metallographic data available today allows the beginning of the harnessing of iron metallurgy to be attributed to be the last third of the 3rd millennium BC.

Most scientists currently considered the birthplace of iron industry Anatolia (Pleiner 2000; Buchwald 2005, 78; Snodgrass 1980; Yalçin 1999; Waldbaum 1978; 1980). All the necessary prerequisites existed for this in the indicated region: a purposeful search and awareness of the properties of ore minerals that can turn into metal, pyrotechnic structures, achievement of high temperatures due to artificial blasting, charcoal burning. Note that one-third of all known finds from iron dating from the Bronze Age comes from Anatolia (Waldbaum 1978, 23).

The hypothesis of the accidental obtainment of ferrous metal during the smelting of copper-sulphide ore is widely accepted in the matter of man's first acquaintance with metallurgical iron. This may have come about in the following way. The smelting of sulfide ore is complicated by the separation of metal from gangue. As a result of various experiments, ancient craftsmen could observe that the process of slagging goes more successfully if iron ore (hematite or limonite) is added to the charge (Wheeler, Maddin 1980, 115-116). Over the metallurgical process, iron, in the form of insignificant inclusions, could be reduced to a metallic state (Charles 1980, 166–167; Pleiner 2000 12; Wertime 1980, 13; Yalçin 1999, 185). T. Wertime (Wertime 1980, 14) and N. Gailhard (Gailhard 2012, 153) found a basis for this possibility over the course of experiments in the smelting of lead and copper ores.

However, it is difficult to imagine that the particles of iron obtained were suitable for the forging of even miniature articles, not to mention large artifacts. We will attempt to recreate the algorithm of actions on the path to understanding the new metal. Most likely, at first, metallurgists took the iron particles for white metal (tin? silver?), which was already known to them. One can imagine that, to obtain a sufficiently large piece of metal, ancient craftsmen may have tried to smelt the collected particles of iron and may have then noticed that the particles did not smelt, but, rather, sintered together in a monolithic block, which was suitable for the forging of small items (knives, awls, etc.). This was the first step towards ancient craftsmens' understanding of a new, promising metal – iron. The desire to obtain such a metal motivated craftsmen to carry out metallurgical experiments with a focus on iron ore. This allowed them to obtain ever greater volumes of ferrous metal, which contributed to the displacement of bronze from the production of tools and weapons.

As for the time of the appearance of the metallurgical method of iron production, it is demonstrated by large objects from Kaman-Kalehöyük, Alacahöyük (Anatolia), Tell Asmar (Mesopotamia), Buhen (Egypt), and Kültepe (Azerbaijan), which date to the second half of the 3rd millennium BC (Özgüç 1963, 15; Wertime 1973, 885; Frankfort 1950, 100; Waldbaum 1978, 22; 1980, 70).

With regard to the transition from bronze to iron, it is worth mentioning the three main hypotheses that explain the transition (Avilova, Terekhova 1989, 295).

One of them, the "ecological hypothesis," links the transition to iron to the insufficient fuel resources due to the felling of forests in the Mediterranean for the clearing of fields for terrace farming and due to the production of fuel for nonferrous metallurgy. Proponents of this hypothesis believe that iron metallurgy required less fuel and was thus more economical.

In our view, the "ecological" position does not hold up to criticism. It is contravened by calculations confirmed by experimental data that demonstrate that iron metallurgy required no less fuel than copper metallurgy. Up to 10-20 kg of charcoal are used to produce 1 kg of bloomery iron (not counting fuel used for pre-heating of the bloomery furnace and the heating of blooms during forging) (Kolchin, Krug 1965; Voss 1994; Crew 1991, 35; Gailhard 2012, 155), which is comparable with fuel usage for the smelting of 1 kg of copper with about 10% metal content in the ore. According to written sources, there is no evidence of a timber deficit in the late Bronze Age (Moorey 1994, 286). Thus, if the "ecological" factor had played a major role, it would have hampered the development of non-ferrous metallurgy no less than ferrous.

The basis of the "economic" hypothesis is the reduction of deliveries of tin to Middle Eastern trade centers and the resulting reduction of the amount of bronze produced. The bronze shortage is considered to have motivated metallurgists to switch to the production of iron.

Today, many researchers call the "economic hypothesis" into question: according to recent data, tin deposits existed on the territory of southeast Anatolia itself. In the view of J. Waldbaum, the lack of evidence of a reduction in the tin content in late Bronze Age articles also stands against the "economic hypothesis" (see: Avilova, Terekhova 1989, 295)

The "technological hypothesis" explains the transition from the production of bronze tools and weapons to the iron industry by the discovery of specific means of processing ferrous metal (carburizing and heat treatment), which increased the efficiency of iron articles many times over.

As a product of the bloomery process, iron is considered to be inferior in quality to bronze. Thus, only the discovery of means to improve its mechanical properties (carburizing, i.e. the artificial obtainment of steel) allowed it to displace bronze from the production of tools and weapons. Of course, this discovery was of major importance, but it was not the deciding factor. The data now at our disposal allows us to claim that the product of the bloomery process – metallurgical iron – was comparable with bronze in hardness. It was, essentially, not pure iron (with a structural component of ferrite), but bloomery steel (unevenly carburized). The results of numerous experiments and metallographic analyses of ancient iron products testify to this fact (Crew, Salter 1991, 21; Killick 1996, 259, 260; Kmošek 2015; Moorey 1994, 278; Pleiner 2000, 132; Snodgrass 1980, 338; Wang, Crew 2013, 400). According to the data of P.F. Tylecote, "the blade, which was really an inhomogeneous low-carbon steel, was harder than a cast tin bronze and far more ductile" (Tylecote 2002, 47). Thus, the decisive factor in the transition from the bronze industry to the iron industry, in our view, was the discovery of means of metallurgical production that allowed ferrous material to be produced in sufficient volumes. The prevalence and accessibility of iron ores themselves was also of considerable importance.

Thus, we have every reason to take a new look at the conditions, time, and reasons for the transition to the widespread use of iron.

4. The role of meteoric iron in the formation of the iron industry.

Some researchers believe that familiarity with meteoric iron played a decisive role in the formation of the iron industry. Moreover, it was recently proposed that all iron artefacts of the Bronze Age were of meteoric origin (Jambon, 2017). It is widely believed that familiarity with meteoric iron (which happened no later than in the second half of the 4th millennium BC) was a motivating factor for the desire to obtain a similar metal by metallurgical means. It is proposed that the particles of white metal obtained during the smelting of copper-sulphide ores as iron ore is added to the charge were associated by ancient metallurgists with meteoric iron.

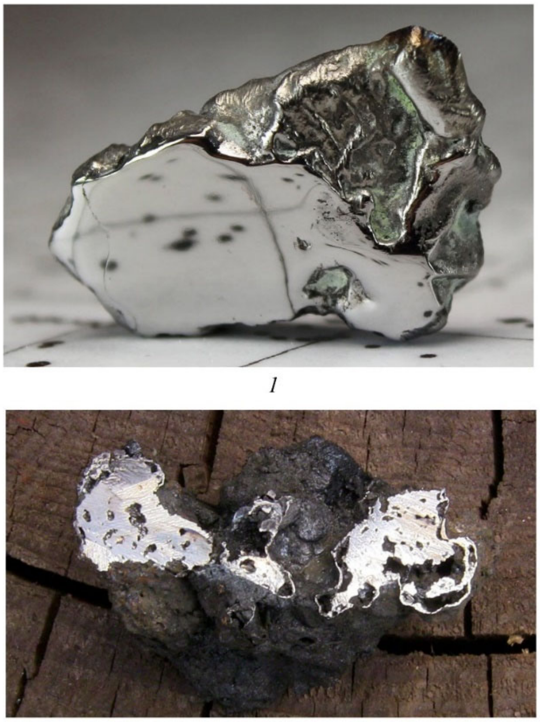

1

2

Figure 1. Meteoritic iron (1) and bloomery iron (2).

It should be noted that these materials are absolutely incomparable – not by their appearance (figure 1), nor form, nor mechanical properties. As a byproduct of the smelting of copper, metallic iron was particles of relatively soft metal, which was not suitable for the production of any kinds of articles. It required a whole series of further actions (sintering, forging, etc.) for a monolithic semi-manufactured product to be obtained. As for meteoric iron, it is a monolithic, fairly hard formation (comparable with high-carbon steel in hardness) of irregular form, which in no way resembles particles of light-colored metal embedded in the slag.

In our view, there are no grounds to connect the two processes: the processing of meteoric iron is just a mechanical transformation of the form, while the metallurgical process is a transformation of substances (ore–metal). The latter experience could be gained on the basis of non-ferrous metallurgy. The irregular nature of the use of meteoric iron should also be taken into account (Coghlan 1956). The extreme rarity of meteoric iron could not facilitate the formation and development of manufacturing traditions.

That is, it is clear that the processing of meteoric iron had no relation to the formation and development of ferrous metallurgy.

5. Ways of spreading technological knowledge and forming various production models (on the example of Eastern Europe).

For the early periods of the formation of the iron industry, the issue of the means of dissemination of technological knowledge is of particular importance. However, as a rule, researchers do not devote sufficient attention to this issue. In one work concerning ancient iron artefacts from Eastern European sites, no clear position is put forward regarding the character of the emergence of the iron industry in Eastern Europe: both the independent birth of ferrous metallurgy and the possibility of effects from foreign culture are accepted as versions (Grakov 1958, 9).

Collections of artifacts from the territory of Eastern Europe accumulated up to the present day, subjected to archaeometallographic research, allow the means of the iron industry's dissemination to be grounded technologically. Ancient articles made from ferrous metal appeared in Eastern Europe at the end of the 2nd millennium BC. They are single finds which testify to local tribes' first acquaintance with the new metal (Bidzilia et al. 1983; Grakov 1958; Chizhevskii 2012; Shramko et al. 1977; Shramko, Buinov 2012).

So far, there has been little archaeometallographic research of such finds. Only four objects from Ukraine have been studied: three knives and an awl. One knife (from the turn of the 2nd and 1st millenia BC) turned out to be forged whole from bloomery iron (Radzievska, Shramko 1980, 103). The second knife (11th-9th c. BC) was forged from iron with traces of accidental carburization (Bidzilia et al. 1983, 18), and the third (11th-9th c. BC) from crude bloomery steel (Buinov 2003, 6). An awl (13th c. BC) was made from bloomery iron, lightly carburized in places (Bidzilia et al. 1983, 15).

The transitional phase from the bronze industry to the iron industry in Eastern Europe can be dated to the 9th to the middle of the 7th century BC. It is recorded in materials from sites in the North Caucasus and northern Black Sea region. This phase was marked by significant growth in the number of ferrous metal articles and the expansion of the range of iron artifacts.

Data characterizing the technology using which the most ancient iron objects were manufactured makes it possible to conclude that, already at that time, various technological traditions were beginning to form in Eastern Europe (Terekhova, Erlikh 2002).

The "Eastern European tradition" formed in the steppe and forest steppe zones of the northern Black Sea region in the 11th-9th century BC. Its basis was the technical-technological standard,7 which was connected with the use of simple technological means – the creation of articles whole from iron or bloomery steel, that is, the direct product of the bloomery process. The use of special means to improve the mechanical properties of articles, which is typical for ferrous metal (carburizing and heat treatment), is only recorded on single articles.

Another tradition can be traced using materials from northern Caucasian sites. A specific characteristic of this technological tradition is the use of methods like carburizing and heat treatment, which are specific to the processing of ferrous metal. Moreover, heat treatment is presented in specific types, such as soft quenching and normalising (the structural expression of which is, respectively, sorbite and spheroidizing pearlite). The use of these methods, which were relatively high-tech for the early Iron Age, allowed the mechanical qualities of articles to be significantly enhanced.

The traditions noted formed the basis of two different technological models – respectively, the Eastern European and Caucasian.

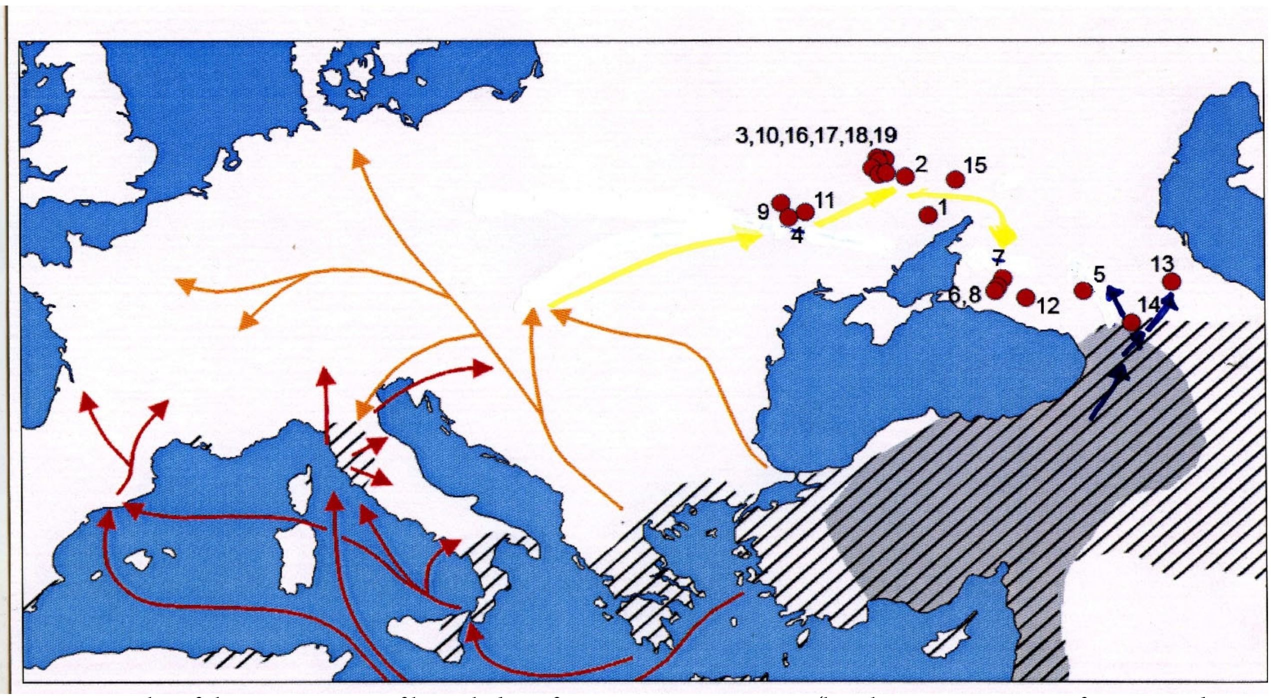

Figure 2. Paths of the penetration of knowledge of iron in Eastern Europe (by Pleiner 2000, 30–31, figure 8 and the authors – Zavyalov and Terekhova, 2018). The territory of initial development of iron industry marked by grey, shaded the zone of civilizations, mastered iron at the end of Bronze Age, red arrows mark West European

[7] By "technical-technological standard," we mean a certain set and balance of attributes characterizing the material, techniques and methods of manufacturing articles (*Zavyalov, Rozanova, Terekhova* 2009, 8).

path of the penetration of knowledge of iron, orange – Balkan and Central European path, yellow – East European path, blue – Caucasian path. Archaeological sites of the transitional phase from the bronze industry to the iron industry in Eastern Europe: 1 – Lubovka$ 2 – Oskol, 3 – Chervony Slyakh, 4 – Tashlyk 1, 5 – Klin-Yar, 6 – Pshish, 7 – Kubansky burial, 8 – Psekupski burial, 9 – Sofievka, 10 – Verkhniy Bishkin, 11 – Subbotovo, 12 – Fars, 13 – Serzhen-Yurt, 14 – Tli burial, 15 – Vishnevy Dol, 16 – Kicevka, 17 – Velikaya Topolyakha, 18 – Bondarikha, 19 – Timchenki.

It appears that the two models reflect the differing paths of the penetration of knowledge of iron in Eastern Europe from a single hearth, located in Southwest Asia (figure 2). One of them, the formative "Caucasian" model, came to the North Caucasus through Transcaucasia. The second path went through Greece and the Balkans and, later, onto the territory of Central and Eastern Europe (Zavyalov, Terekhova 2018a).

The formation of various technological models when there was only a single source for the dissemination of knowledge about iron working (Anatolia) requires explanation. The fact is that the discovery of advanced methods for the processing of ferrous metal, such as carburizing and heat treatment, date to the end of the 2nd millennium BC in Asia Minor. However, exactly at that time, as a result of the invasion of the "Sea Peoples" in the 13th-12th centuries BC, the connection between the states of Asia Minor and the population of the East Mediterranean was lost. Thus, innovative technological knowledge did not disseminate in the West or further in Eastern Europe. Meanwhile, there was no hindrance for contacts and the transmission of technological knowledge in the direction of Transcaucasia and the North Caucasus. Technological innovations in Transcaucasia and the North Caucasus, which were disseminated in a close cultural environment, long remained the professional secrets of local craftsmen. Until the middle of the first millennium BC, they did not exert significant influence on other regions of Eastern Europe.

Thus, our research allows us to argue that, in Eastern Europe, already at the early stages of the development of the iron industry, various technological models were formed, which served as the basis for the further development of local iron working.

6. Ferrous metal articles in the culture of early nomads

A key issue in the history of nomads is that of the source from which they obtained handicraft production. There are various opinions on this issue. One of them holds that nomads were capable of independently manufacturing the required forged products (Smirnov 1964, 60–62). Meanwhile, a different perspective holds that the nomad mentality and lifestyle did not allow for the formation of such complex processes in the local environment, as they require stationary conditions for work (long amounts of time spent to obtain raw materials and fuel, complex pyrotechnic structures, a set of tools, special devices, etc.). With a nomadic lifestyle, it was necessary to make do with instable means of obtaining handicraft production from the sedentary population (via trade, outright pillaging or tribute) (Zavyalov, Terekhova 2017; Moshkova 1989, 205).

Only when nomads transitioned to a settled lifestyle did the formation of iron production in the local environment become possible. The landmark event in this context is the emergence of such a site as the Kamenskoe hill-fort in the steppe zone of Eastern Europe (end of the 5th to the beginning of the 3rd century BC). The settlement is located on the left bank of the Dnieper. As a result of many years of excavations, significant and diverse material has been accumulated, which characterizes, among other things, the obtainment and processing of ferrous metal (Grakov 1954; Gavriliuk 1989). This has allowed researchers to come to the conclusion that "the Kamenskoe hill-fort was clearly a permanent settlement of settled craftsmen metallurgists in a country of nomad Scythians" (Grakov 1954, 123).

The preliminary analysis of metallurgic articles brought archaeologists to the conclusion that local iron production was not highly developed (Grakov 1954, 122). However, the use of archaeometallographic research methods of forged artifacts forces us to reconsider this conclusion.

We studied several dozen iron objects from the Kamenskoe hill-fort in the Laboratory of Nature Sciences in Archaeology of the Institute of Archaeology of the Russian Academy of Sciences (Zavyalov, Terekhova 2017). This has made it possible to speak to the existence of highly developed technologies for the processing of ferrous metals at the settlement (figure 3). This is evidenced by iron tools made using methods such as carburizing at the blades (obtainment of carburized steel) and the final product, as well as the differentiated use of heat treatment (soft quenching, quenching with self-tempering, normalising).

The methods listed testify to the existence of certain traditions that developed on the basis of extensive experience of work with ferrous metal. We will turn to Caucasian materials in the search for the possible roots of these manufacturing traditions. Data available today from archaeometallographic research demonstrates that all of the listed methods were already known to Transcaucasian craftsmen at the turn of the 2nd and 1st millennium BC (Tavadze et al., 1977) In the 8th century BC, the methods of carburizing and heat treatment (however, it should be emphasized that exclusively soft quenching and normalising were used) disseminated to the Central Caucasus (Voznesenskaya 1975), and, in the 7th-

6th c. BC, to the Northern Caucasus (Terekhova 2002; 2015). It can be said with a great degree of certainty that the artifacts we have studied in Steppe Scythia are the work of craftsmen who operated in the Caucasian producing traditions. Taking the aforesaid into account, there are grounds to assert that iron working in Scythia was not born of its own accord, but was imported.

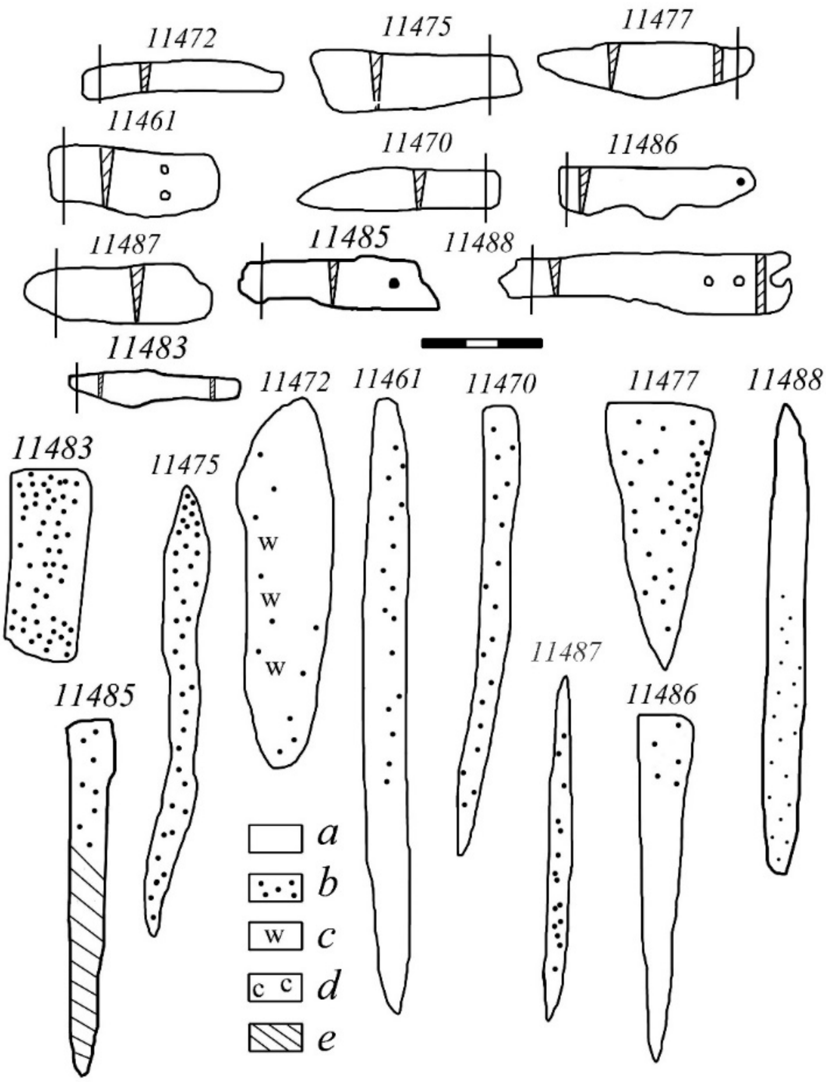

Figure 3. Technological schemes of iron knaves from Kamenskoe hillfort: a – iron, b – steel, c – widmanstetten structure, d – carburizing steel, e – tempered steel.

It is interesting to compare the results obtained with the specifics of the development of iron working handicraft in other regions of the Scythian world: in particular, among tribes of the forest steppe zone of Eastern Europe. On the basis of analytical materials from the Belskoe hill-fort (Northeast Ukraine), the largest site of this time, it has been established that here, as in the Kamenskoe hill-fort, there was a sufficiently high level of iron production. The wide use of methods for the artificial obtainment of steel and the methods of heat treatment and welding-on technologies testify to this. As a particularity of local iron working, we may note the use of hard quenching and methods of welding a steel blade onto the iron base of the tool. There are grounds to link the particularities indicated with the development of local blacksmithing of ancient manufacturing traditions (Pleiner 1969, 21; Kostoglou 2013).

The distinctive features revealed in the production of forged products give us reason to believe that various technological models existed in Forest Steppe and Steppe Scythia. The following reasons for the formation of these models can be put forward as a hypothesis. In one case (the Belskoe hill-fort), existing local blacksmithing was heavily influenced by highly-developed (most likely, Greek) manufacturing. In another (the Kamenskoe hill-fort), iron manufacturing arose in a situation without prior experience under the direct influence of Caucasian manufacturing traditions (Terekhova, Zavyalov 2019).

The issue of the spread of handicraft production among nomads is worth examining on the basis of other nomadic tribes – the Sarmatians, who lived on the steppe of the Volga region and the Ural region in the second half of the first millennium BC. Bladed weapons are a particularly vivid example of the material culture of the Sarmatians. To obtain the technical characteristics of these weapons, we conducted a series of archaeometallographic investigations. Four chronological periods can be distinguished in the history of the Sarmatians: the Scythian-Sarmatian period (6th-4th c. BC), early Sarmatian period (4th-2nd c. BC), middle Sarmatian period (end of the 2nd c. BC – beginning of the 2nd c. AD), and the late Sarmatian period (2nd-4th c. AD).

The distribution of the analytical results obtained by chronological periods allows us to assert that the technological standard in the production of the Sarmatian bladed weapon underwent major changes (figure 4). Thus, in the Scythian-Sarmatian period, a distinctive feature in the production of swords and daggers was the use of methods that were relatively high-tech for the early Iron Age, such as various types of carburizing (artificial obtainment of steel) and specific methods of heat treatment (soft quenching, 77ormalizing) of steel articles. Moreover, the high percentage of heat-treated artifacts is striking. The technical characteristics of weapons of the Scythian-Sarmatian period demonstrate, in our view, that the craftsmen who produced these weapons operated in the Caucasian production tradition.

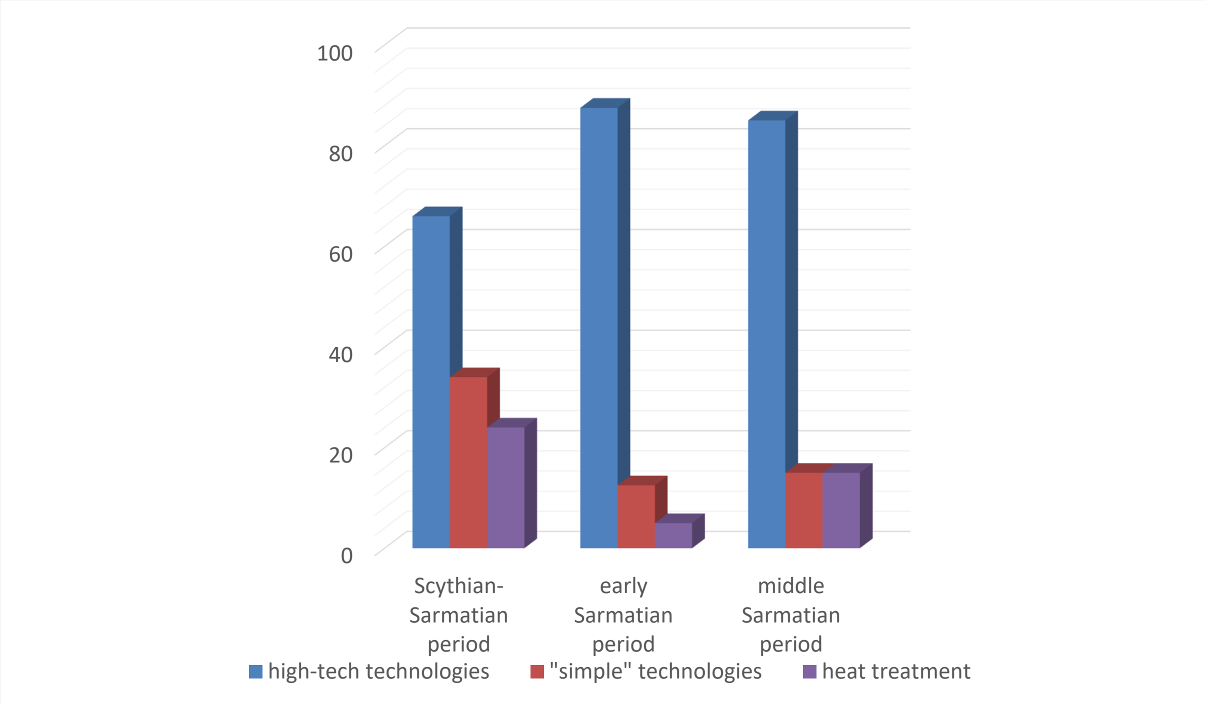

Figure 4. The distribution technologies of producing Sarmatian swords and daggers (in %) by chronological periods.

In the early Sarmatian period, some changes took place in the technical-technological standard, which was notable in comparison with the previous period. The type of swords and daggers changed (Zavyalov, Terekhova 2018b). Technologies that were advanced for the early Iron Age (artificial obtainment of carburized steel, heat treatment) disappeared. The characteristic technology of this method was the multilayer welding of the work piece. In the middle Sarmatian period, the tradition (use of simple technological methods, multilayer welding) noted in the early Sarmatian materials continued (Zavyalov, Terekhova 2018b).

There is reason to link the changes in the technical-technological standard in the production of Sarmatian bladed weapons to changes in the source of material for the manufacturing of forged products. This is confirmed by data from an X-ray fluorescent analysis: the percentage of trace elements such as Ni, Co, Mn demonstrate significant differences in the composition of Sarmatian and early Sarmatian metal.

A comprehensive analysis (archaeometallography, X-ray fluorescence) of the Sarmatian bladed weapon unambiguously demonstrates a change in source of ferrous metal articles in the early Sarmatian period (figure 5). At present, due to the lack of analytical materials for several archaeological cultures, it does not appear possible to localize that source. However, based on the data we have put forward, we can characterize its technical features: multilayer welding of the work piece and primary use of simple technologies (forging of objects whole from iron or crude steel).

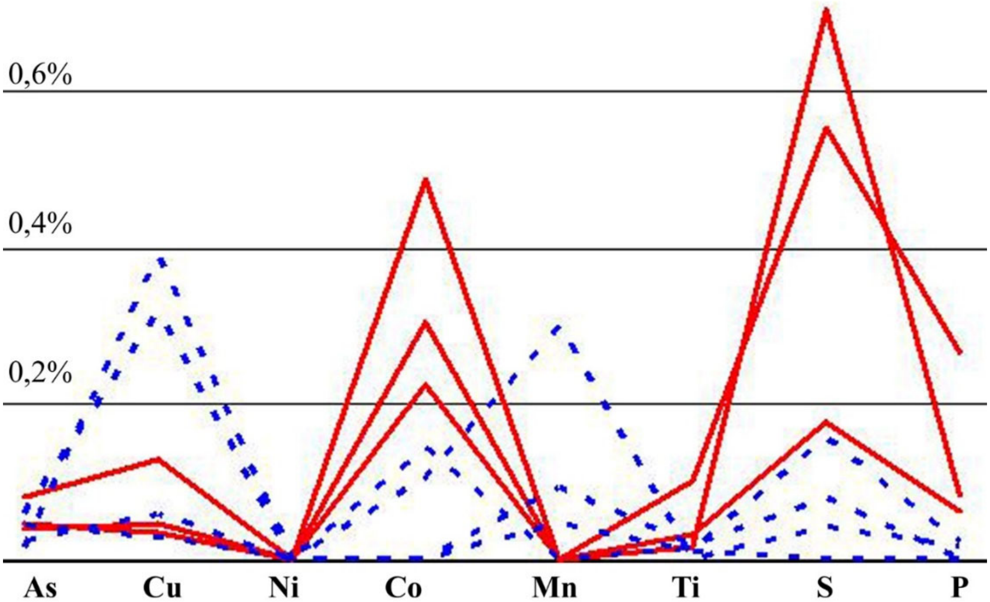

Figure 5. The distribution of trace elements (in wt %%) in metal of Scytho-Sarmatians (red) and early Sarmatians swords and daggers.

The technological method of multilayer welding of the billet is particularly noteworthy. It manifests itself distinctly in the early Sarmatian period and, in the following period (middle Sarmatian), it becomes one of the main methods in the production of Sarmatian bladed weapons.

In general, it must be said that a negative dynamic can be observed in the manufacturing of Sarmatian swords and daggers in the 4th–2nd centuries BC. This dynamic is attributable to the technological characteristics of the new source of ferrous metal articles. In this way, a direct dependency between the quality of the iron articles of nomads (in this case, Sarmatians) and the manufacturing traditions of their source of forged products.

7. The role of technological innovations in the formation of blacksmithing traditions in the feudal era

One of the major state entities of feudal Europe was Ancient Rus'. The issue of the formation of the leading sector of the medieval economy – blacksmithing – has long attracted specialists' attention. The great potential of archaeometallography was first demonstrated using precisely ancient Russian materials. On the basis of the analytical data, well-known Russian scientist B.A. Kolchin singled out chronological phases in the development of ancient Russian blacksmithing, underlining the fact that local manufacturing in this sphere was highly developed already in its early phase (9th–10th c.) (1953).

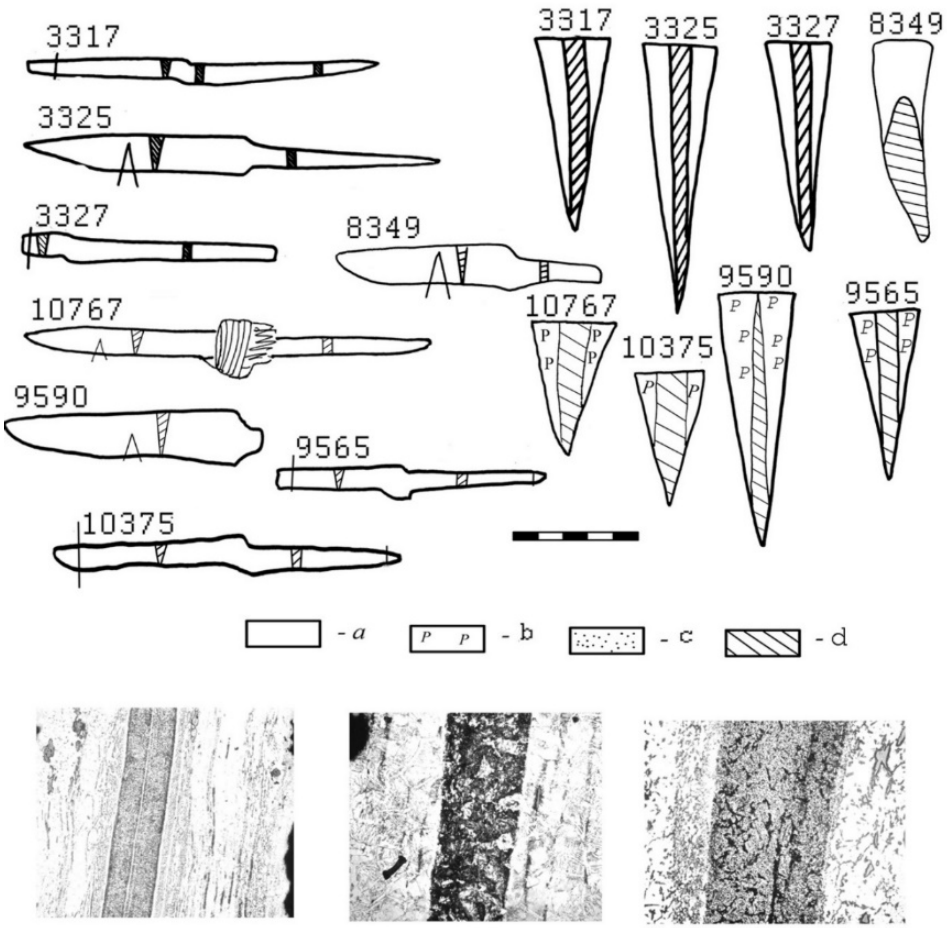

Figure 6. Technological schemes and microphotos of three-fold blades: a – iron, b – phosphoric iron, c – steel, d – tempered steel.

From a historical perspective, the period of the formation of the ancient Russian state coincides with the infiltration of numerous people coming from Scandinavia into the territory of Rus'[8], who exerted significant influence on various aspects of the life of the local population. Their important role in the history of Ancient Rus' was long considered to be controversial in Soviet historiography. In particular, their influence on the formation of urban blacksmithing was denied (Kolchin 1953, 207).

As analytic material was accumulated, it became necessary to correct this view. It has been established that a distinguishing trait of early urban blacksmithing in Ancient Rus' was the technology of three-fold welding (figure 6), which did not have local roots. At the same time, this technology is known from the materials of Scandinavian sites of the 7th century (Arrhenius 1970, figure 1, 3).

The appearance of three-fold articles in Eastern Europe is clearly linked to increased trade in the 9th century on the Volga trade route, in which the Varangians played a particular role. In Eastern Europe, the most ancient three-fold articles come from the Staraya Ladoga settlement in the vicinity of Lake Ladoga (Rosanova, 1994). Some specialists believe that the settlement was founded in the middle of the 8th century by people originating from Northern Europe (Nosov, 1999; Lebedev, 2005). It can be said with certainty that the three-fold welding technology was brought to the territory of Ancient Rus' from Scandinavia and, in the 10th to the first half of the 12th century, became the basis of local urban manufacturing. For example, in Novgorod, three-fold tools in the 10th century stratum make up more than 90% of all tools studied.

With the disappearance of the Scandinavian factor in ancient Russian history (end of the 11th c.), three-fold welding technology gradually ceased to be used in blacksmithing practice. The technology of welding a steel blade onto an iron base becomes a main tendency starting in the 12th century (figure 7).

A similar technology was already widespread in the Slavic world in the 7th-8th centuries. Articles manufactured using welding-on technology, were known in Great Moravia and the Slavic sites of the area between the Vistula and Oder rivers (Piaskowski 1974, 83–94; Pleiner 1967, 93, 138). In the last quarter of the first millennium AD, single articles made using welding-on technology appear in East Slavic sites as well (Voznesenskaya 1978, 64; Rosanova et al. 2008, 41). Gradually, welding technology became a distinctive feature of the East Slavic manufacturing tradition.

[8] In Europe, migrants from Scandinavia were called "Normans"; in Rus', they were called "Varangians."

In this way, contemporary archaeometallographic data suggest that the basis for the formation of ancient Russian blacksmithing consisted of two manufacturing traditions. The appearance of one tradition – the Scandinavian one, linked with the three-fold welding technology – was explosive, but it did not exert significant influence on the further development of iron manufacturing. It is no accident that, as the Scandinavian factor disappeared, the use of this technology in ancient Russian blacksmithing also ceased. Welding technology replaced three-fold welding in ancient Russian manufacturing culture. As analytical data demonstrate, it gradually spread and, in the second half of the 12th century, became a characteristic feature of blacksmithing in Ancient Rus'.

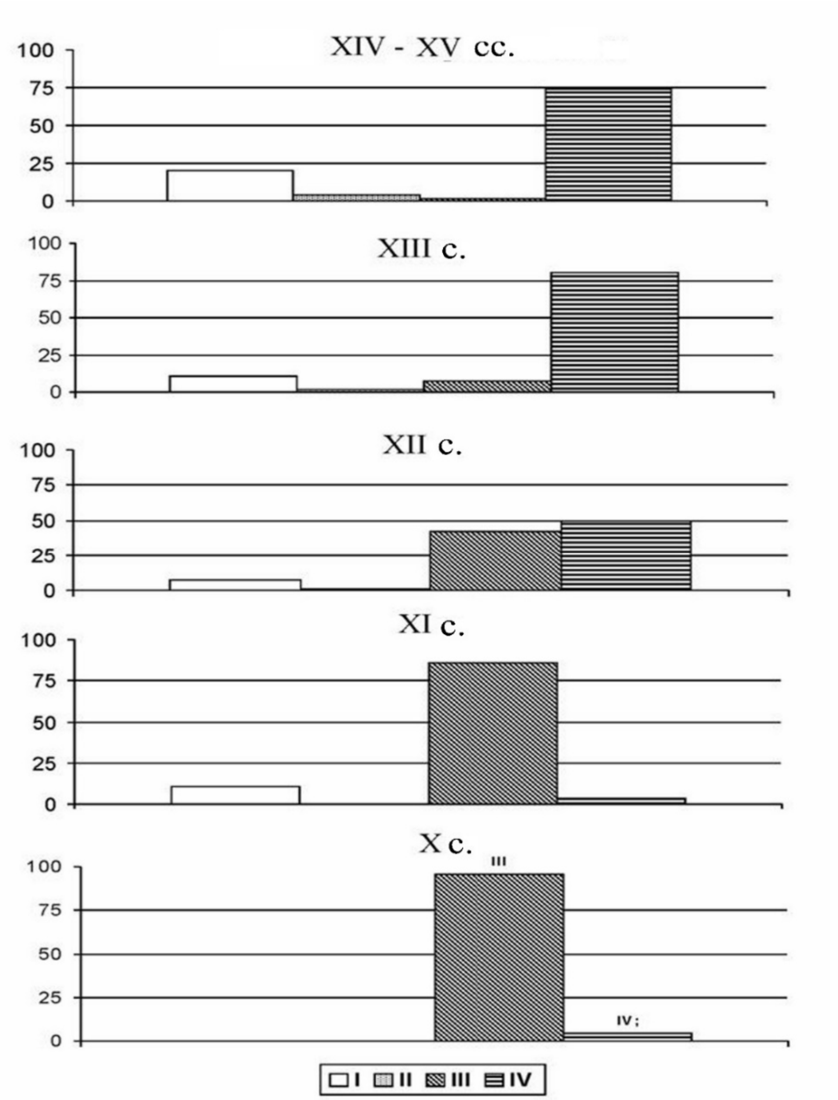

Figure 7. Chronological changes in using technologies in Russian blacksmith's craft (by Novgorod data): I – made from iron, II – made from steel, III – three-fold welding, IV – welding-on.

8. Conclusion

Thus, generalization and analysis of the archaeometallographic data obtained over the course of our work makes it possible to think about numerous processes of the formation and development of the iron industry in a new way. The findings from these investigations again demonstrate the great potential of the archaeometallographic method in addressing historical issues related not only to technology, but also to culture.

9. Acknowledgement

Article prepared with the financial support of the Russian Science Foundation, project 19-18-00144.

10. References

Akanuma, H. 2008. "The Significance of Early Bronze Age Iron Objects from Kaman-Kalehöyük, Turkey". *Anatolian Archaeological Studies*. Tokyo: Japanese Institute of Anatolian Archaeology. 17: 313–320.

Arrhenius, B. 1970. Knivas från Helgö och Birka. Fornvanner 65.

Avilova, L.I. and Terekhova, N.N. 1989. Sovetsko-amerikanskiy simpozium "Drevneishaya metallurgiya Starogo Sveta" (Tbilisi–Cignakhi). Sovetskaya arkheologiya 3: 290–296

Bidzilya et al. 1983. Bidzilya, V.I., Voznesenskaya, G.A., Nedopako, D.P., Pankov, S.V. Istoriya chyornoy metallurgii i metalloobrabotki na territorii UkSSR (III v. do n.e. – III v.n.e.). Kiev: Naukova dumka.

Buchwald V.F., 2005. Iron and steel in ancient times. København: Videnskabernes Selskabs. 378 p.

Buynov, Yu.V. 2003. Poselennye boundarykhinskoy kultury u s. Chervony Shlyakh na Kharkivshhyni. Vestnik Kharkovskogo gosudarstvennogo universiteta. Seriya Istoriya 35: 4–13.

Chizhevsky, A.A. 2012. K voprosu o nachale rannego zheleznogo veka v Volgo-Kame, Rossiyskiy arkheologicheskiy ezhegodnik 2: 383–399.

Coghlan, H.H., 1956. Notes on Prehistoric and early iron in the Old World. Oxford: University press.

Crew, P. and Salter, C.J., 1991. Comparative data from iron smelting and smithing experiments, Materiały archeologiczne XXVI 15–22.

Gailhard, N. 2012. Reflections on experimentation and innovation processes: The Origin of Iron in Anatolia, 8th International Congress on the Archaeology of the Ancient Near East: 149–162. Warsaw.

Gavriluk, N.A. 1989. Domashnee proizvodstvo i byt stepnykh skifov. Kiev: Naukova dumka.

Grakov, B.N. 1954. Kamenskoe gorodishche na Dnepre. Materialy i issledovaniya po arkheologii SSSR 36. Moskva: Akademiya nauk SSSR.

Grakov, B.N., 1958. Stareyshie nahodki zheleznyh veshchey v evropeyskoy chasti territorii SSSR. Sovetskaya arkheologiya 4: 3–9.

Jambon, A. 2017. Bronze Age iron: Meteoritic or not? A chemical strategy, Journal of Archaeological Studies 88: 47–53.

Kmošek, J. 2015. Archeometalurgický průzkum produktů z experimentální tavby železa v rekonstrukci šachtové pece se zahloubenou nístějí, Archeologia technica 24: 25–39.

Kolchin, B.A., 1953. Chyornaya metallurgiya i metalloobrabotka v Drevney Rusi. Materialy i issledovaniya po arkheologii SSSR 32. Moskva: Akademiya nauk SSSR.

Kolchin, B.A., 1959. Zhelezoobrabatyvayushchee remeslo Novgoroda Velikogo. Materialy i issledovaniya po arkheologii SSSR 65. Moskva: Akademiya nauk SSSR.

Kostoglou, M. 2013. Manufacturing techniques, technological traditions and social choices in ancient Greece, in: J. Humphrics and T. Rehren (eds) The World of Iron: 313–321. London: Archetype Publication Ltd.

Lebedev, G.S. 2005. Epoha vikingov v Severnoy Evrope i na Rusi. Sankt-Peterburg: Evraziya.

Moorey, P.R.S. 1994. Ancient Mesopotamian materials and industries. The Archaeological Evidence. Oxford: Clarendon Press.

Morgan, L. 1935. Drevnee obshchestvo. Leningrad: Institut narodov Severa.

Moshkova, M.G. 1989. Srednesarmatskaya kul'tura, in A.I. Melukova (ed) Arheologiya SSSR. Stepi evropeyskoy chasti SSSR v skifo-sarmatskoe vremya: 177–191. Moskva: Nauka.

Nosov, E.N. 1999. Sovremennye arheologicheskie dannye po varyazhskoy probleme na fone tradiciy russkoy istoriografii, in Rannesrednevekovye drevnosti Severnoy Rusi i ee sosedey: 151–163. Sankt-Peterburg: Institut istorii materialnoy kultury RAN.

Piaskowski, J. 1974. Untersuchungen der Fruh-Mittelalterlichen Eisen- und Stahltechnologie der Slaven in der Gebieten zwischen Weichsel und der Oder, Archeologia Polona XV: 67–96.

Pleiner, R. 1967. Die Technologie des Schmiedes in der Gross marischen Kultur, Slovenska archeologia XV-1: 77–188.

Pleiner, R. 1969. Ironworking in Ancient Greece. Praha: National Technical Museum.

Pleiner R., 2000. Iron in Archaeology. The European Bloomery Smelters. Praha: Archeologický Ústav AVČR. 400 p.

Radzievs'ka, V.Є., Shramko, B.A., 1980. Novi arheologichni pam'yatki na Har'kivshchini. Arheologiya 33: 100–108.

Rozanova, L.S., 1994. K voprosu o tekhnologicheskih priyomah izgotovleniya zheleznyh izdeliy iz Staroy Ladogi v doknyazheskiy period. Novgorodskie chteniya: 175–179. Novgorod.

Rozanova et al. 2008. Rozanova, L.S., Terekhova, N.N., Ryabinin, E.A., Shcheglova, O.A. Metallograficheskoe issledovanie zheleznyh izdeliy Lyubshanskogo gorodishcha in A.N. Kirpichnikov (ed). Ladoga i Ladozhskaya zemlya v epohu srednevekov'ya 2: 13–48. Sankt-Peterburg: Nestor-Istoriya.

Shramko, I.B. and Buynov, Yu.V. 2012: Perehod ot bronzyi k zhelezu v Dnepro-Donetskoy lesostepi, Rossiyskiy arkheologicheskiy ezhegodnik 2: 309–332.

Shramko et al. 1977. Shramko, B.A. Fomin, L.D. Solntsev, L.A. Nachalnyiy etap obrabotki zheleza v Vostochnoy Evrope (doskifskiy period) Sovetskaya arkheologiya 1: 57–74.

Smirnov, K.F. 1964. Savromaty. Moskva: Nauka.

Snodgrass, A.M. 1980. Iron and early metallurgy in the Mediterranean, in T.A. Wertime (ed) The Coming of the Age of Iron: 335—374. New Haven, London: Yale University Press.

Tavadze et al., 1977. Tavadze, F.N., Sakvarelidze, T.N., Abesadze, C.N., Dvali, T.A. K istorii zheleznogo proizvodstva v drevney Gruzii Restavraciya, konservaciya, tekhnologiya muzeynyh eksponatov 2: 5–61. Tbilisi.

Terekhova, N.N. 2002: Tehnologicheskie traditsii v obrabotke chyornogo metalla iz mogilnika Serzhen-Yurt, in V.I. Kozenkova. U istokov gorskogo mentaliteta. Mogilnik epohi pozdney bronzyi – rannego zheleza u aula Serzhen-Yurt, Chechnya: 151–154. Moskva: Pamyatniki istoricheskoy myisli.

Terekhova, N.N. 2015. Zheleznye izdeliya iz Ul'skih kurganov v kontekste kuznech-nogo remesla skifskoy epohi in A.I. Ivanchik, A.M. Leskov (eds). Ul'skie kur-gany. Kul'tovo-pogrebal'nyy kompleks skifskogo vremeni na Severnom Kavkaze: 77–86. Moskva-Berlin-Bordo: Paleograf

Terekhova, N.N. and Zavyalov, V.I. 2018. Kavkazskie tekhnologicheskie tradicii v proizvodstve zheleznogo inventarya iz pamyatnikov Stepnoy Skifii XXX «Krupnovskie chteniya»: 266–268. Karachaevsk: Karachaevo-Cherkesskiy gosudarstvennyy universitet.

Terekhova, N.N. and Erlikh, V.R. 2002. K probleme perehoda k rannemu zheleznomu veku na Severnom Kavkaze. Dve kulturno-istoricheskie traditsii. Materialnaya kultura Vostoka 3: 134–152.

Tylecote, R.F. 1976. A History of Metallurgy. London: Maney Publishing.

Voznesenskaya, G.A. 1975. Tehnologiya proizvodstva zheleznykh predmetov Tliyskogo mogilnika, in B.A. Kolchin (ed.) Ocherki tehnologii drevneyshih proizvodstv: 76–116. Moskva: Nauka.

Voznesenskaya, G.A. 1979. Tekhnika kuznechnogo proizvodstva u vostochnykh slavan v 7th–10th vv. Sovetskaya arkheologiya 2: 70–77.

Waldbaum J.C., 1978. From bronze to iron. Göteborg: Paul Åströms förlag. 106 p.

Waldbaum, J.C. 1980. The First Archaeological Appearance of Iron and the Transition to the Iron Age // The Coming of the Age of Iron. New Haven and London: Yale University Press. P. 69–98.

Wang Q., Crew P., 2013. Three ores, three irons and three knives // The World of Iron. London: Archetype. P. 393-401.

Yalçin, Ü. 1999. Early Iron metallurgy in Anatolia, Anatolian Studies V, 49: 177—187.

Zavyalov, V.I. and Terekhova, N.N. 2016. K probleme perekhoda ot epohi bronzy k epohe zheleza (tekhnologicheskiy aspekt). Kratkie soobshcheniya Instituta arkheologii 242: 199–211.

Zavyalov, V.I. and Terekhova, N.N. 2017. Stanovlenie kuznechnogo remesla v stepnoy Skifii (na primere Kamenskogo gorodishcha). Kratkie soobshcheniya Instituta arkheologii 248: 317–331.

Zavyalov, V.I. and Terekhova, N.N., 2018. Tekhnologicheskie harakteristiki sarmatskogo oruzhiya. XXI Ural'skoe arheologicheskoe soveshchanie. Samara: Samarskiy gosudarstvennyy social'no-pedagogicheskiy universitet. 206–208.

Zavyalov, V.I. and Terekhova, N.N., 2018. Two iron technology diffusion routes in Eastern Europe, Archeologické rozhledy LXX–2018: 328–334.

Zavyalov, V.I. and Terekhova, N.N., 2019. Tekhnologicheskie transformacii v proizvodstve klinkovogo oruzhiya sarmatov, Stratum plus 4: 313–320

Falling from the sky. Aerial photogrammetry and LiDAR applied to the Archaeology of Architecture and Landscape: two fortifications from the Alpujarra (Granada, Spain)

Jorge Rouco Collazo (*MEMOLab – Laboratory of Biocultural Archaeology, University of Granada*), José Antonio Benavides López (*Department of Architectural Graphic Expression and Engineering, University of Granada*), José María Martín Civantos (*MEMOLab – Laboratory of Biocultural Archaeology, University of Granada*)

Abstract

The introduction of new technologies in recent decades has opened new methodological avenues and theoretical approaches that are of great interest to archaeological research and conservation of historical heritage. This study delves into two of these, Structure from Motion photogrammetry by drone and LiDAR, and describes their advantages and disadvantages in the framework of Architecture and Landscape analyses. Case studies of each type were carried out on two medieval fortresses, Órgiva and Poqueira (and their surroundings) perched on steep slopes of Sierra Nevada (Granada, Spain). Each of the studies took into account questions of graphic quality, geometric precision, coverage and handling costs and offer a method allowing integration of the microspatial scale of Archaeology of Architecture into the macrospatial scale of Landscape Archaeology. These new remote sensing technologies are of great use in obtaining quality and precise records that enable offering new data and perspectives to old historical and archaeological problems.

Keywords

LiDAR, photogrammetry, UAV, fortification, Middle Ages

1. Introduction[9]

The aim of this study is to carry out a comparative analysis of the new remote sensing systems and graphic techniques serving to record archaeological features based on SfM multi-image photogrammetry (*Structure from Motion*) and LiDAR (*Light Detection and Ranging or Laser Imaging Detection and Ranging*). The study also offers a series of methodological novelties based on different aspects gleaned from the analyses of two medieval fortresses of the Alpujarra, a region along the southern face of the Sierra Nevada in the Province of Granada (Spain).

These new technologies form the basis of a complex research project seeking to bring together all the means to identify the evolution of the medieval fortifications and their relationship with the respective landscapes by applying the methods of Archaeology of Architecture and Landscape Archaeology as well as a review of old written sources (Figure 1).[10]

Archaeology has traditionally reverted to objective graphic techniques to collect as much information as possible to geolocate and contextualise features. These are fundamental tools serving to analyse, understand and explore archaeological features (Martínez Rubio, Fernández Martín and San José Alonso 2018). In certain cases, they are also valuable tools to disseminate artistic or cultural values (Martín Talaverano 2014). What remains unclear today is which recording technique is the most effective for each case and what are the requirements demanded of new representations for them to offer better results. Factors such as surface extension, type of intervention, speed, precision, budget, operator training, deadline and the characteristics intrinsic to each site play a role as to which equipment and method to put to use (Benavides López et al. 2016).

[9] This work was supported by the FPU15/03012 grant of the Ministry of Universities of Spain's Government, the project TerraSAgE: Terraces as Sustainable Agricultural Environments, funded by the UK Arts and Humanities Research Council (AHRC) and the project R+D "PREFORTI. Sustainable methodology for the preservation and conservation of earthen medieval fortifications of the Southeast of Iberian Peninsula. Diagnosis and prevention ahead of natural and anthropic risks" (BIA2015 69938-R) funded by the Spanish State Research Agency and European Regional Development Fund (ERDF).

[10] All figures in text are available at full resolution in http://hdl.handle.net/10481/62100.

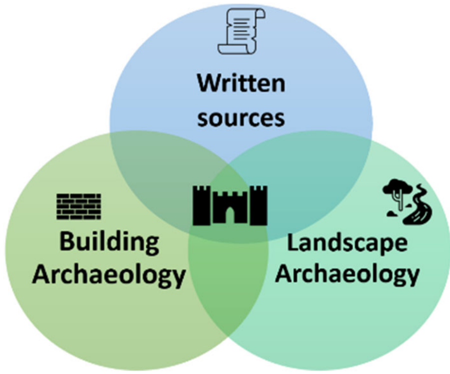

Figure 1: Scheme of the methods put to use to analyse the rural medieval fortifications of Poqueira and Órgiva (Alpujarra, Granada, Spain).

The techniques serving to create graphic records of archaeological and architectural heritage have led to great advances in efficiency and accuracy. Although the traditional method par excellence of cultural heritage representation has been ground, elevation and section line drawings, other techniques such as photogrammetry or mass point capture (ground-based laser scanners or LiDAR) have recently emerged yielding complex three-dimensional representations. In any case, they pursue the same goal as the line drawings, that is, to offer the most complete image of an object.

These new procedures make it possible to identify the differences between technological and analytical representations while simultaneously share the goal of recording and document the cultural features. The technological representations are based on a digital reproduction resorting to laser scanners, photogrammetry, LiDAR and three-dimensional digital modelling. The analytical representations, in turn, are founded on the interpretation of the material reality, that is, expressing the information obtained after a critical analysis of a historical feature.

The representations, more precisely, the technological reproductions are carried out quasi-automatically following a method that depends on the technique chosen to assure reliable data. The analytical representation process, on the contrary, requires a historical-constructive and therefore interpretative analysis which depends on the knowledge of the individual carrying out the task (Martín Talaverano 2014).

The chronological analysis requires access to highly detailed graphic records to identify the different historical features as well as their interrelationships. Orthophotos not only allow registering the different Stratigraphic Units (SU), but to reinterpret the features and potentially add other more modest elements which may be key to identifying a feature's historical nature.

The impact of the new, more efficient and accurate technologies, fundamentally LiDAR scanner and SfM multi-image photogrammetry, is transforming the paradigms of the methods of archaeological recording and analysis of information. The development of digital photography has led to automations that yield rapid and highly accurate virtual models (Romero Pellitero and Martín Civantos 2017; Rouco Collazo, Martín Civantos and Benavides López 2018, 2020).

Although it is certain that sketches and photographs assisted by direct measurements taken with tape measures, laser distance meters or total stations are still valid recording techniques, the data they yield no longer compensate the effort. It is in most cases easier and more useful to generate three-dimensional models of features that preserve both their complex original geometry and texture. Moreover, direct drawing by hand, that is, transforming complex three-dimensional shapes into two-dimensional planes, is not only a slow and tedious process, but is prone to error and subjectivity. In this sense, the new digital LiDAR and automated photogrammetry techniques offer ample options and inexpensive graphic documents of high metric and visual quality.

In any case, the intention of this study is to identify the initial criteria required to choose the most appropriate tools and methods to apply to historical features. This allows to lay down the protocols to adopt in function of the type of record (3D model, orthophotography, 2D line drawing), as well as the type of format that will serve as a means of communication and exchange.

2. Methodology

The objectives of this analysis are therefore to evaluate the virtues and drawbacks of applying LiDAR and SfM photogrammetry to the sites of Órgiva and Poqueira, two medieval fortresses in the Province of Granada.

2.1. Aerial photogrammetry for Landscape and Architecture

The International Society for Photogrammetry and Remote Sensing (ISPRS) defines photogrammetry as an art, science and technology for obtaining reliable measurements of physical objects and their environment, through recording, measurement and interpretation of images and patterns of radiant electromagnetic energy. This highly generic definition requires clarification based on the objectives and methods put to use. In any case, the principle of photogrammetry is to define the three-dimensional coordinates of any point from two or more photos shot from different positions or, in other words, reconstruct a three-dimensional model of a feature from two-dimensional images.

This science which emerged in the 18th century and established throughout 19th and 20th centuries has evolved radically from the digital capture of images and its subsequent computer processing to artificial intelligence applications. It is currently used extensively by professionals of many different disciplines. Moreover, new recording software and devices have in recent years become inexpensive and simple to use leading to an exponential increase of their application to archaeology. Resorting to multiple image-based modelling has become one of the most significant alternatives for recording and documenting archaeological features (Benavides López et al. 2016; Benavides López, Martín Civantos and Rouco Collazo 2020; Howland, Kuester and Levy 2014; Nex and Remondino 2014; Prins, Adams, Homsher and Ashley 2014; Quartermaine, Olson and Howland 2013; Remondino, Barazzeti, Scaioni and Sarazzi 2011; Rodríguez Navarro 2012; Roosevelt, Cobb, Moss, Olson and Ünlüsoy 2015; Romero Pellitero and Martín Civantos 2017).

The method is improving different aspects of archaeology mainly at the level of precision and efficiency. Less investment in time to record archaeological features is key as it reduces the expenses of fieldwork and alleviates the financial burden of commercial archaeology (Aranda Jiménez 2011). The possibility of obtaining precise, high-quality representations is nonetheless its most significant innovation (Benavides López et al. 2016). Furthermore, these digital tools also facilitate exchange and interoperability, enhancing real time collaboration between archaeologists by means of the cloud (Levy et al. 2012).

The analyses of the medieval fortifications of Órgiva and Poqueira centre on the 3D digital representations (point clouds and meshes) so as to then obtain other elaborate graphics such as digital elevation models (DEM), contour maps, sections, as well as orthophotos for floor plans and elevations serving for subsequent analyses.

A correct recording of archaeological heritage through multi-image photogrammetry requires simultaneous application of different tools and methods. These steps are identified below (Benavides López 2017).

2.1.1. Fieldwork

2.1.1.1. Planification

A complete registration of a feature of heritage by SfM photogrammetry requires a pre-planning process that optimises image capture and avoids the areas without coverage. A flight plan must be organised taking into account the following criteria: level of detail (Ground Sample Distance range), image overlap, flight altitude, speed, lighting, environmental conditions and judicial constraints.

Planning the capture of images requires a control over a series of specific aspects. These include the type of equipment available, characteristics of the area (accessibility, space to carry out the capture, obstacles, movement of people or vehicles, etc) as well as other organisational and legislative issues.

2.1.1.1. Site georeferencing

A step prior to the SfM photogrammetry with an Unmanned Aerial Vehicle (UAV) is to deploy on and around the features a network of control points (targets) measured by the Global Navigation Satellite System (GNSS). Geolocating the points throughout the different fortresses of the Ravine of Poqueira and the Plain of Órgiva was carried out with the universal reference system (UTM-ETRS89) by means of a global positioning equipment with real-time correction capability (Figure 2). The precision of these devices ranges from 1 to 4 cm depending on the number and geometry of the satellites at the moment of capture, and the distance from the GNSS receiver to the reference antennas.

Figure 2: Aerial view with the position of the georeference points serving to orient and scale the photogrammetric model of the site of Órgiva.

The geolocation differences of the images due to the positioning error of the UAV's internal GNSS (which can attain up to several metres) requires correction by means of the ground-based control or reference points (De Castro Ferreira, Yodono García and Cândido de Oliveira 2019; Gabrilik, la Cour-Harbo, Kalvodova, Zalud and Janta 2018; Galván Rangel, Rito Gonçalves and Pérez 2018). These points take on the form of targets placed on the ground and structures that are visible on the images taken with the UAV's camera (Oniga, Breaban and Statescu 2018) (Figure 3).

Figure 3: UAV view with the target serving as a ground point.

2.1.1.2. Image capture

Multi-image photogrammetry allows combining images captured manually from the ground with aerial images captured by drones.

UAV image capture takes advantage of the high resolution offered by the proximity of the object and avoids the occlusions typical of ground photogrammetry. But this deferred system of image capture requires programming the parameters to attain a high radiometric quality with an adequate overlap. Applications such as DJI Ground Station Pro, Pix4D capture, Mission Planner, Litchi or Map Pilot installed on a Smartphone or Tablet, which can be programmed rapidly in the field, generate almost automatically an optimal UAV route that guarantees the best and most complete coverage (Figure 4). The applications calculate the number of passes and the appropriate speed of the aircraft based on a series of parameters such as the size of the area, flight height, GSD length (measurement of the distance between adjacent pixels), image type (JPG or RAW), overlap, etc.

Figure 4: Programme of the route of the UAV photogrammetric flight carried out with the IOS MAP-PILOT app in the site of Órgiva. The regular capture of the images (red dots) leads to longitudinal and transversal overlaps of 85% and 60%.

In this sense, the Ground Sampling Distance (GSD) (Figure 5) determines the resolution or level of detail and conditions of the remaining flight parameters. That is, the final resolution or the GSD will fix, depending on the type of camera, the necessary height, which in turn determines the drone's speed and interval between shots so as to guarantee an adequate image overlap.

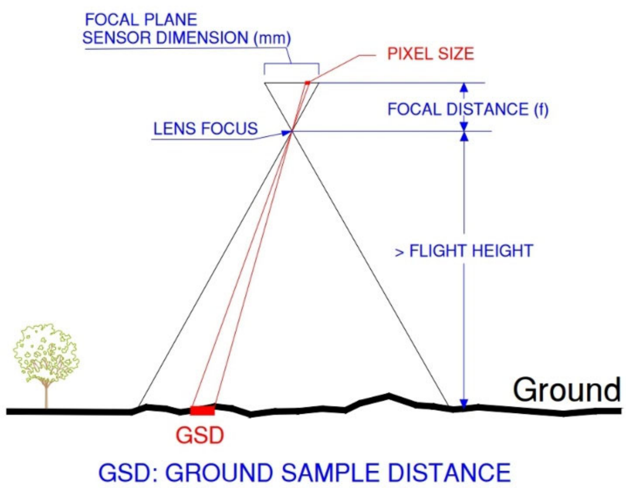

Figure 5: Scheme of the GSD in function of the factors of flight height, focal length and geometric resolution of the sensor.

The formula serving to calculate the GSD in cm/pixel is the following:

GSD=(WS*H*100)/(dF*nPixel)

WS = width of the sensor (mm);

H = height of the flight or distance to the feature (m):

dF = Focal distance (mm)

nPixel = number of pixels at the width of the sensor

This theoretical approach is nonetheless complicated to carry out in the field based due to other variables such as structure height or lighting conditions. Very low flight heights yield better GSD resolution but also require, due to the terrain, a more extensive UAV flight and therefore a greater shift of the pixels in the image or the lack of overlap of the higher features of the structures (Figure 6). The ambient lighting likewise conditions the speed of the camera and must therefore be regulated simultaneously in function of the speed of the UAV's equipment to avoid blurring due to excessive speed. The ideal is a combination of the highest possible camera speed with the lowest possible aircraft speed.

Another factor is lens focal length. Cameras with a wide angle of view (< focal length) lead to deformations that hinder a correct construction and application of texture. Although they can be calculated and corrected by photogrammetric programs, they require greater adjustment errors. As a general rule, cameras with a smaller field of view (> focal length) allow flights at higher altitudes and suffer less deformation, which leads to higher quality 3D models.

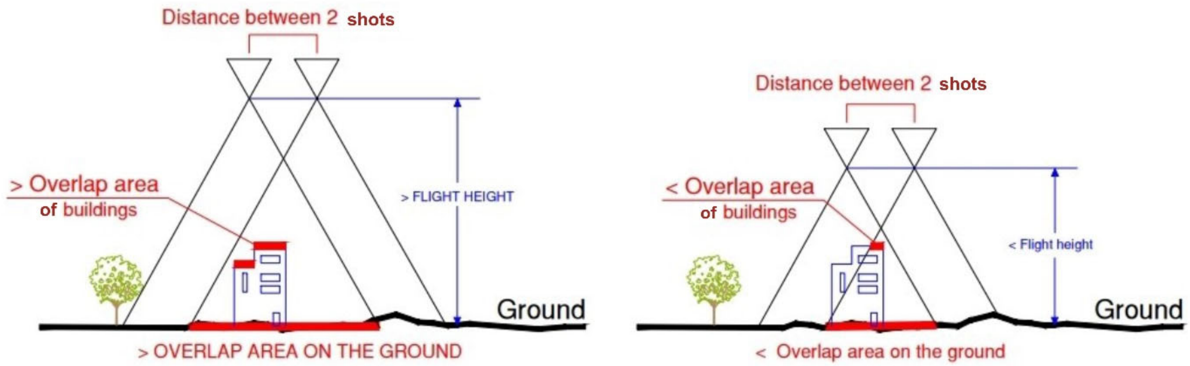

Figure 6: Scheme indicating the overlap and relative displacement of pixels in function of flight height. Lower heights lead to less overlap and impede registration of the feature's higher areas.

2.1.2. Laboratory tasks

2.1.2.1. SfM photogrammetric processing

The precision and resolution of a 3D model depend on several factors linked to photographs. The geometric and radiometric variables of the images must be controlled and corrected to guarantee their quality (Kersten and Lindstaedt 2012; Westoby, Brasington, Glasser, Hambrey and Reynolds 2012).

For this it is necessary to carry out two orientations or transformations. The first is intrinsic to the image (internal orientation), whereas the second associates the images with a reality (external orientation). Internal orientation consists, in essence, of determining a system of bi-dimensional coordinates of each of the images based on the internal parameters of the camera (focal length, centre of projection, distortions, etc.) (Figure 7). External orientation, in turn, determines the position and spatial orientation of the coordinate system of each camera with respect to the object's global coordinate system. This processing must follow the steps described below (Benavides López et al. 2016; Schönberger and Frahm 2016).

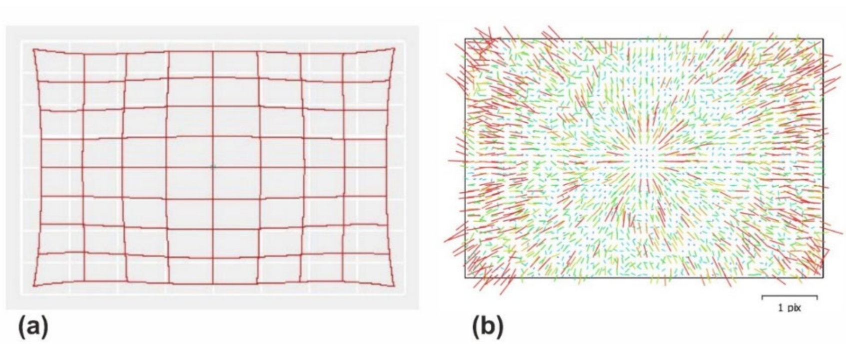

Figure 7: (a) Scheme of the different deformations of the image provoked by the lens. Ideal value (white). Image before correction (red). (b) Pattern of calibration of the lens indicating the radial and tangential deformations.

2.1.2.1.1. Image adjustment and orientation

Images are the source for the reconstruction of the 3D model and therefore, before processing, must be selected and filtered so as to eliminate those of inferior quality. Placing and orienting images in their original position is and continues to be an issue fundamental to photogrammetry. The process called relative orientation is carried out by algorithms related to the field of Computer Vision. Resorting to Scale Invariable Feature Transform (SIFT) algorithms (Lowe 1999) allows detecting and linking thousands of single points (Figure 8). These homologous points form the basis to determine the position and relative orientation of each of the cameras with respect to the others using Bundle-type beam adjustment algorithms (Cefalu, Haala and Fritsch 2017) (Figures 9 and 10).

Figure 8: Position of the SIFT points at the site of Órgiva. Their correlation allows locating and orienting image pairs by means of the Bundler adjustment algorithm.

It is necessary to clarify that models generated automatically by SfM processing exclusively using images do not meet archaeological requirements as they do not bear sufficient levels of dimension, orientation and precision. Therefore, it is essential to incorporate and adjust the control points measured in the field so as to apply a scale and an orientation according to the coordinate system of choice. The control points (targets) also serve to correct the projection errors inherent to camera lenses. This process called absolute orientation is carried out by assigning real coordinates (field measurements) to the control points on the images.

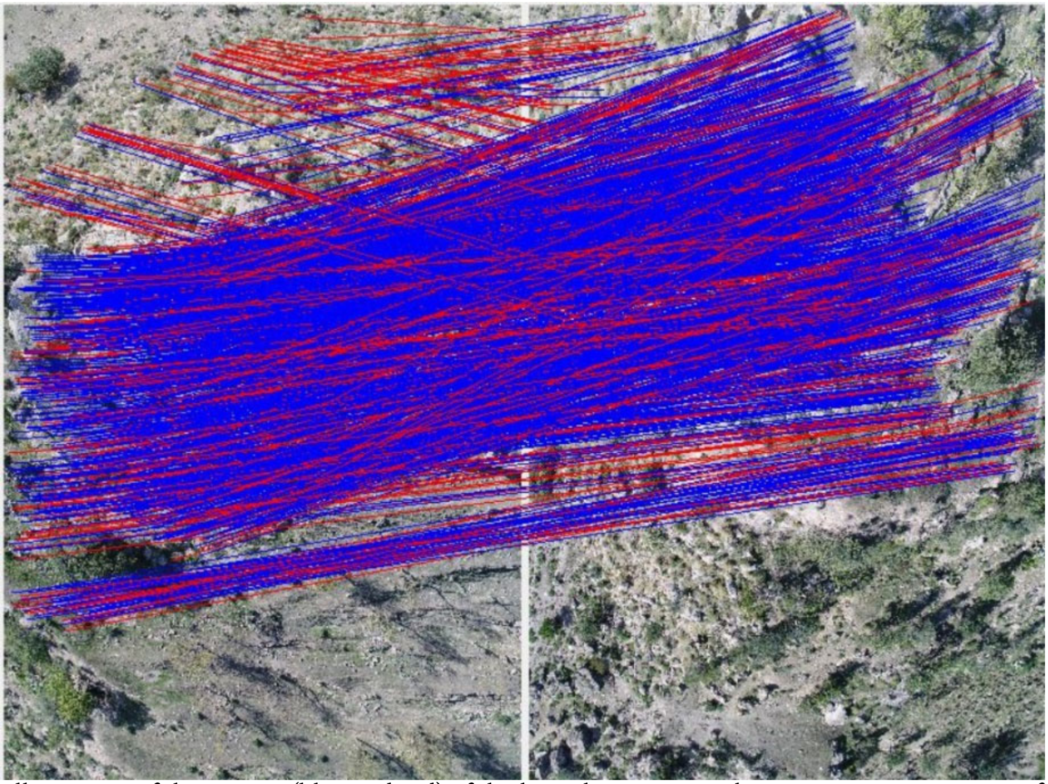

Figure 9: Illustration of the pairing (blue and red) of the homologous points between two UAV images of the site of Órgiva.

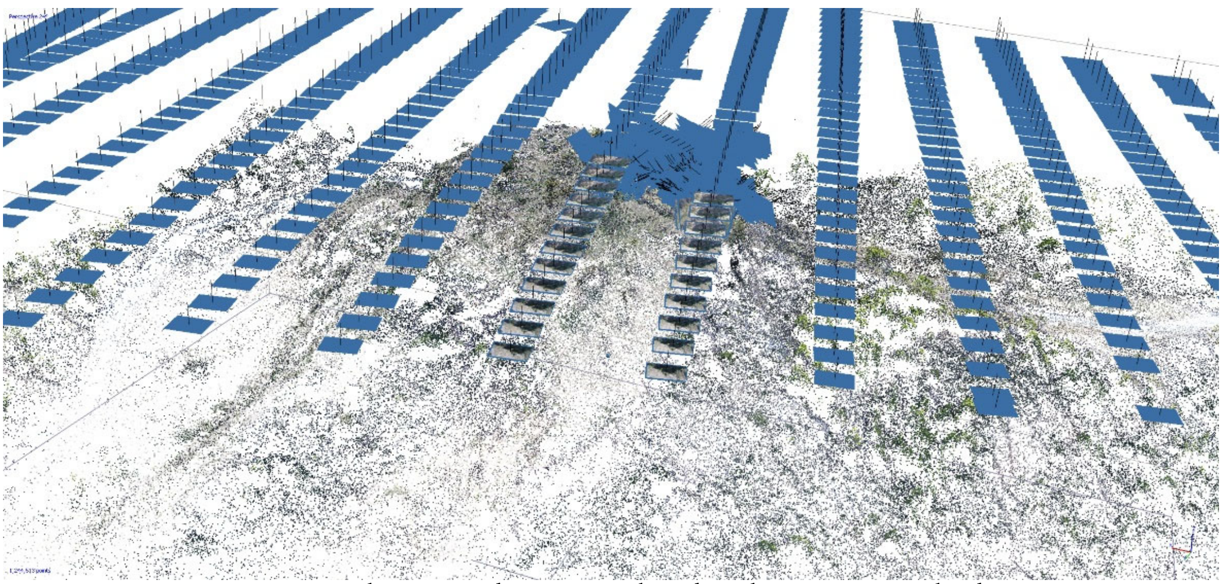

Figure 10: Image location and orientation based on the sparse point cloud.

2.1.2.1.2 Generating a dense point cloud

After calculating the exact position and orientation of the cameras and calibrating the internal geometry of the lens, begins the process, through the intersection of multiple beams, of generating a dense point cloud comprising millions of 3D points that correspond faithfully to the real model (Figure 11).

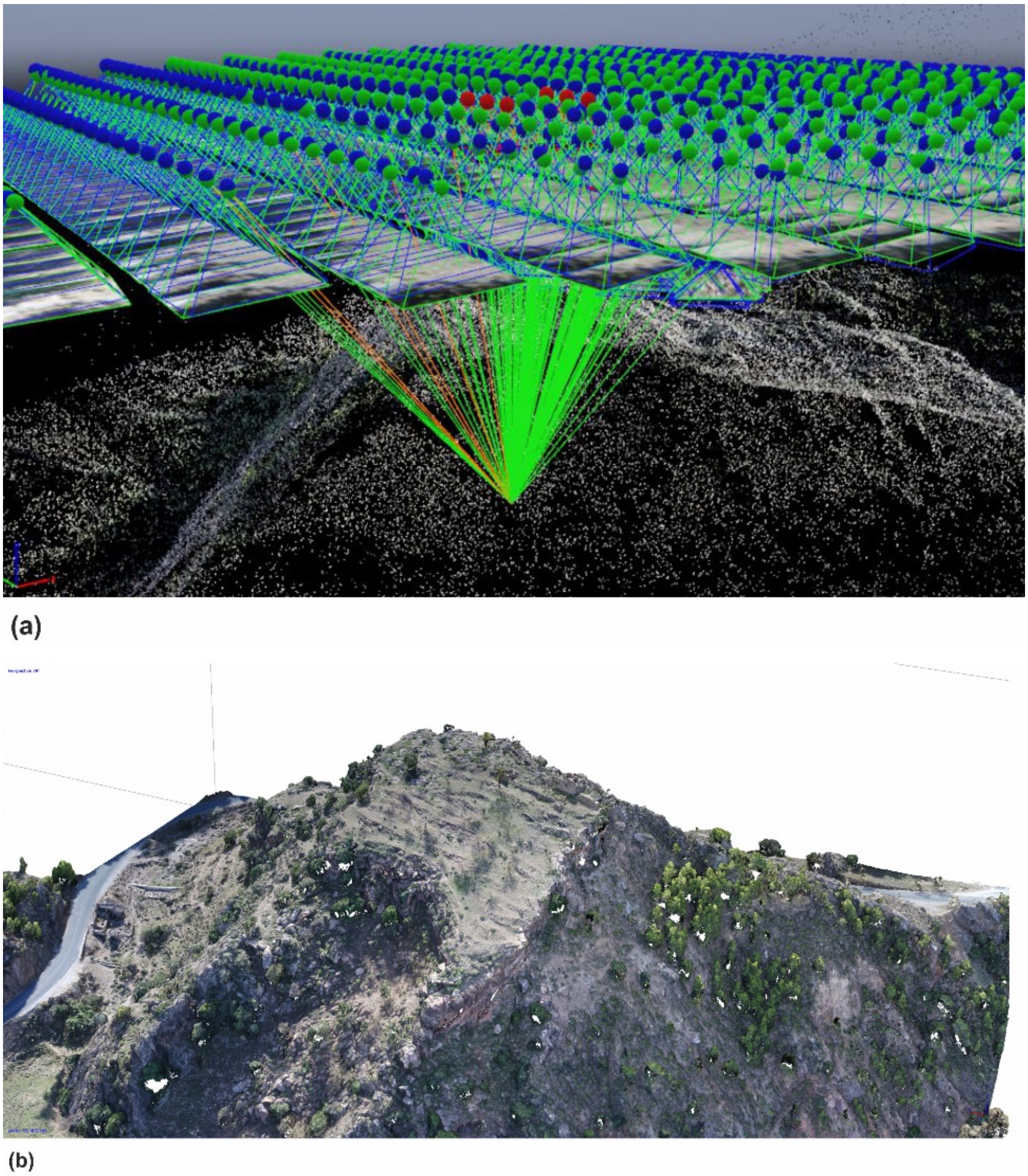

Figure 11: (a) 3D Dense point cloud generated by multiple beam intersection from localised, oriented and calibrated 2D images of the site of Órgiva. (b) Dense coloured point cloud of the site of Órgiva.

Setting the resolution is decisive when generating point clouds and 3D meshes. It is generally determined by the needs of the study and the size of the GSD. Very precise models require more processing time and yield larger files that can at times hinder their handling.

2.1.2.1.3 Generating digital surface models (DSM) and digital elevation models (DEM)

The lack of definition of shapes generated by clouds of points raises the need for a much more realistic and effective digital surface model (DSM). This process consists of applying different triangulation, decimation and smoothing algorithms. The accuracy of the Triangular Irregular Network (TIN) mesh depends on the initial resolution of the point cloud (Peucker, Fowler and Little 1978).

These surface models constitute an ideal base to obtain graphic documents serving to capture the results of analyses of cultural heritage features. High-definition digital elevation models, microtopography or orthophotos can be used or transferred to other specific software applications for a better extraction of information (Figures 12-14).

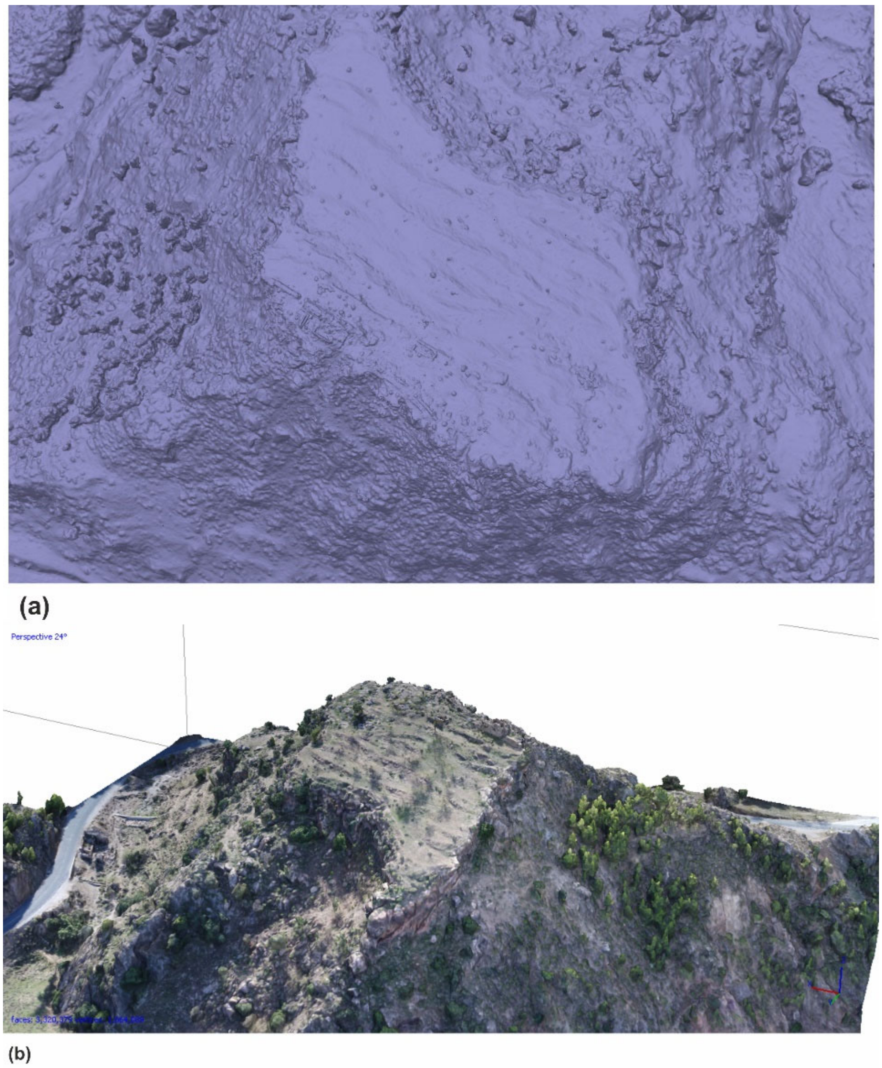

Figure 12: (a) Digital model of the surface generated by means of triangulating the points of the dense cloud. (b) Applying the texture gleaned from the images superimposed on a MDS offers great realism and helps interpret features.

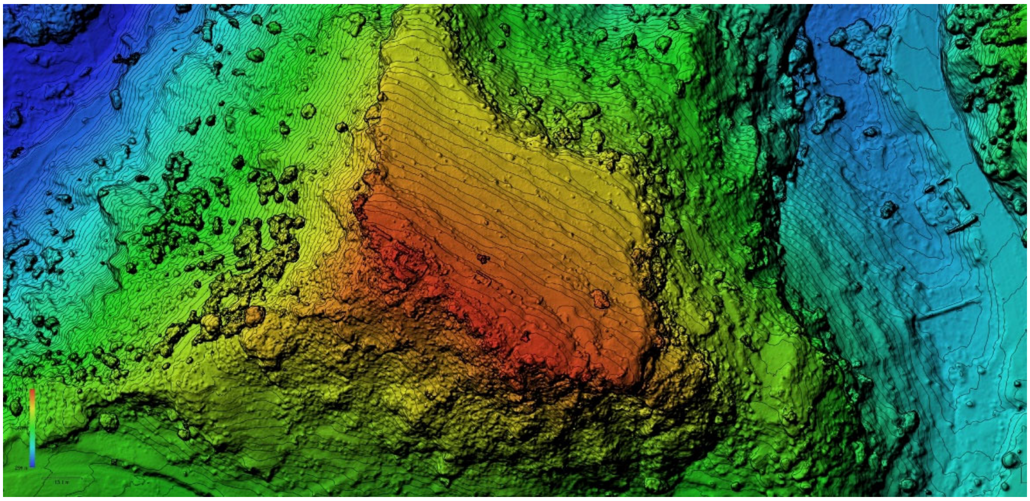

Figure 13: Digital Surface Model (DSM) of the site of Poqueira.

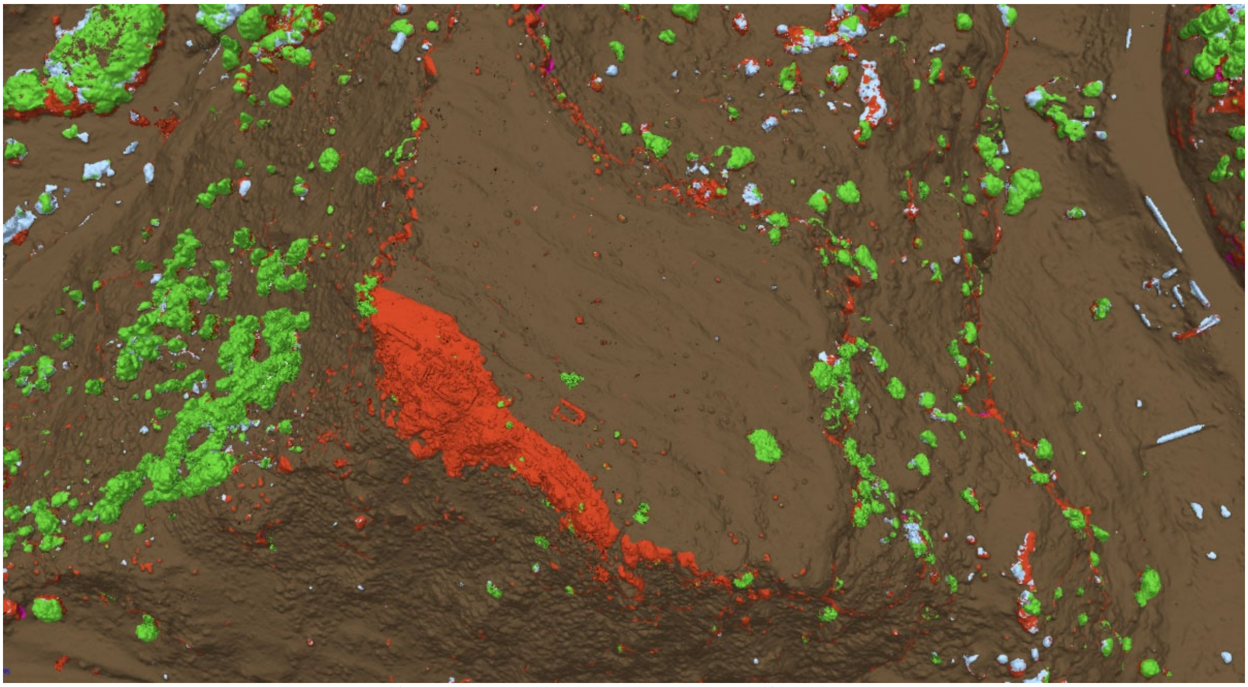

Figure 14: Classification of the points (terrain, vegetation, buildings, etc.) carried out with the Agisoft Metashape v1.6 program of the site of Órgiva.

2.1.2.2. Technological graphic documents

Technological representations are the product of managing three-dimensional virtual models. Orthophotography stand out as the fundamental tool for a more advanced and complete recording of features of heritage as they facilitate the drawing and serve to justify the analysis and its subsequent reinterpretation.

The structural or historical complexity of a feature is impossible to define by a single drawing (Figure 15). It is therefore necessary, to assure a complete vision of the structure, to produce as many orthoimages and sections as necessary.

Figure 15: High resolution orthophotographic representation (1.2 cm/pixel) of the fortress of Órgiva.

2.1.2.3. Analytical graphic documents

Archaeological graphic records collected in the field are based on orthophotographs generated from 3D digital models. The graphic quality of the image and the different characteristics of the feature's materials (typology, state of preservation, phases, etc.) serve this purpose. These representations most often resort to graphic resources such as line drawings and coloured patterns (Figure 16).

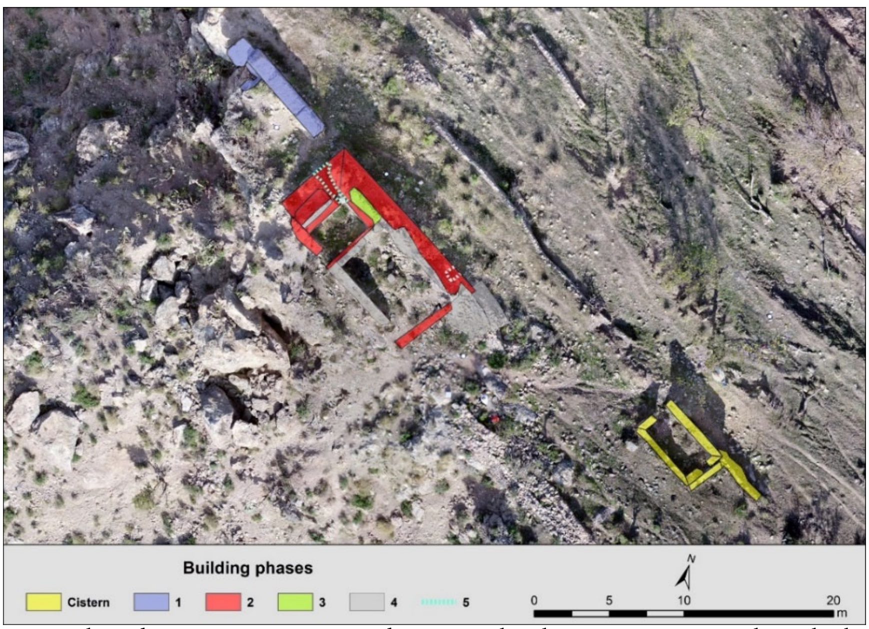

Figure 16: Planimetric line drawings superimposed on an orthophoto serving to analyse the building phases of the fortress of Órgiva.

Digital drawing must follow certain infographic criteria serving for a rigorous understanding of elements of cultural heritage. The true aim of graphic documentation should be a proper recording of data (geometry, construction elements, pathologies, archaeological contexts, etc.) so that they serve as a means of analysis and communication of the cultural values we attempt to preserve (Martín Talaverano, Cámara Muñoz and Murillo Fragero 2018).

The analyses of the two sites of this article were approached from the Archaeology of Architecture perspective, a discipline focusing on the stratigraphical classification of historical constructions. Stratigraphy can be broken down into functional, structural and material changes that yield vital information as to the societies that raised and used the features (Brogiolo and Cagnana 2012; Parenti 1988a). This study resorted to the following three hierarchical levels for the stratigraphical analyses:

- Structural Complex (SC): group of Structures that make up a physical space with a given function.
- Structure (S): grouping of Stratigraphic Units that meet the same structural function.
- Stratigraphic Unit (SU): minor elements that can be stratigraphically individualised according to their composition and construction technique (Rouco Collazo, Martín Civantos and Benavides López 2018, 2020).

These three elements can be individualised and drawn directly in the field. The characteristics of these units are recorded in forms that basically take into account their individual features: surface, contour and relief, topographic position, stratigraphic position and absolute chronology.

The main object of study is the antero-posteriority and contemporaneity of the three levels of analysis (Parenti 1996: 77-83) so as to obtain an evolutionary sequence of each structure (S) based on the relationships of each stratigraphic unit (SU) reflected through a Harris matrix (1989). After establishing the sequences of all the structures, the study moves on to interpret of the constructive evolution of the fortresses' different structural complexes (SC).

Once the orthophotos were obtained through photogrammetry, they were entered into a Geographic Information System which georeferences all the data so it can be transferred into a database with absolute coordinates. Thus, the data as to each SU are linked and their limits drawn. This method is especially useful for hard-to-reach points in the field and for the review of stratigraphic relationships in the laboratory whenever necessary thanks to the quality of the three-dimensional models. However, a 3D rendering through GIS poses numerous difficulties in regard to the Z axis or dimension. This is a problem in the field of archaeology that has been the subject of debate for several years that has yet led to an application rendering it possible to realistically treat planimetries directly in three dimensions with geospatial data (Lanjouw 2016; Van Leusen and Van Gessel 2016). Therefore, we chose to horizontally unfold the orthophotos of each structure at their point of elevation. Hence, despite that the absolute coordinates of the Z axis are distorted, it is possible to analyse the planimetries with real measurements directly linked to alphanumeric information.

2.2. The LiDAR method

LiDAR (Light Detection and Ranging) is a large-scale active remote sensing technique serving to record vast areas of territory. It is carried out by a laser scanner mounted on an aircraft, usually a helicopter or light airplane, that emits hundreds of pulses per second, measuring the time it takes for the pulse to bounce back. A GNSS and an inertial measurement system serve to coordinate the pulses (Figure 17). Measurements of the time and type of rebound generate highly accurate georeferenced three-dimensional point clouds that can be classified by different algorithms depending on the type of surfaces they strike (vegetation, buildings, terrain, etc.). Raw LiDAR data consist therefore of a set of measurements of the times and intensities of the returns of the laser pulses which are normally stored in binary LAS or LAZ format (Mlekuž 2013: 115-116; Samberg 2007).

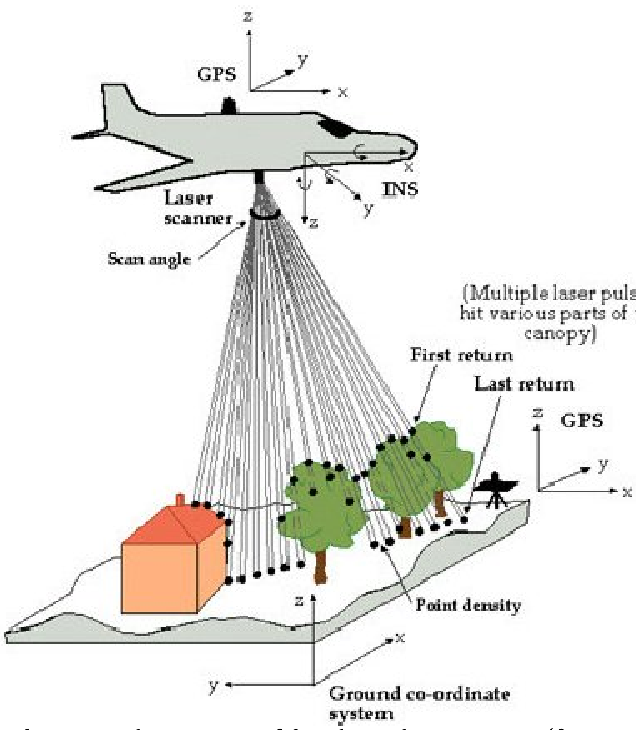

Figure 17: Scheme depicting the capture of data by airborne LiDAR (from Dowman 2004).

The recent introduction of the LiDAR technique by different state agencies and its open publication has led to its application to archaeology (Brogiolo and Sarabia-Bautista 2017; Citter and Patacchini 2017; Crutchley 2010, 2015; Historical England 2018). This is due to its greater precision compared to other traditional topographic survey methods and its much wider radius of action, rendering it extremely useful to Landscape Archaeology. LiDAR also has the advantage that it indiscriminately records on a large scale, without being limited by the desires of researcher. It therefore avoids undertaking landscape analyses with a bias as it treats an entire sector equally. It in fact analyses the features it highlights, whether human or natural, as a sorts of historical palimpsests of a cultural landscape (Mlekuž 2018).

The current study used LiDAR data generated by the National Geographic Institute (IGN). The IGN data of the specific study area, the Province of Granada, correspond to an initial coverage with a density of 0.5 points per m2, that is, one point for every 2 meters. It must be noted that the IGN is currently undertaking a second coverage with a greater precision (1 to 2 points per m2). The data for Andalusia, however, is not expected to be available until 2021.[11] This type of coverage can be obtained by contracting private flights of more or less extensive areas or, in the case of smaller sectors, resorting to a UAV with a built-in LiDAR sensor. These alternatives are nonetheless still too costly for most archaeological projects.

After securing the raw data it is necessary to process and filter them before creating the Digital Surface Models (DSM) and Digital Elevation Models (DEM), LiDAR's most common applications for archaeology. This processing can be carried out by different programs available on the market such as FUSION (McGaughey 2020), LAStools (Isenburg 2020) or tools integrated into the different Geographic Information Systems. The DEM and DSM models for this specific study were achieved by means of automatic filtering of the different classes to eliminate the vegetation. At times it was also necessary to carry out a manual classification of specific areas. The resolution generated for these digital surfaces is 2 x 2 m per pixel, the maximum allowed due to the raw resolution of the original IGN LiDAR data. This led to a 0.5 m pixel mesh by neighbour imputation where a higher resolution is required to visualise it correctly. The last option, however, may lead to slight deviations, although not significant, with respect to the real terrain.

Generating DEM and DSM models opens the door to two options. The first is their direct use as a base for spatial analysis. In this case, a visual basin and intervisibility analysis was carried out to shed light

[11] https://pnoa.ign.es/estado-del-proyecto-LiDAR/segunda-cobertura

on the relationship of the two fortifications with their respective territories. This type of analysis, long applied to archaeology (Canosa-Betés 2016; Dytchowskyj, Aagesen and Costopoulos 2005; Kantner and Hobgood 2016; Murphy, Gittings and Crow 2018), depends greatly on the quality, results and precision of the DEM stemming from the algorithm integrated by the ESRI GIS software (Geographic Information System) ArcGIS 10.2. This geographic base also allows carrying out a series of analyses such as cost areas, drainage basins, insolation, etc. which are not described in the current study due to limitations of space (Conolly and Lake 2006).

The second way is to improve the visualisation is to facilitate the recognition and interpretation of traces in the landscape, in particular anthropic structures. Many algorithms have been developed over the last few years to enhance DEM relief (Romero Pellitero, Delgado Anés and Martín Civantos, 2020; Van der Zee and Zuidhoff 2012). The present study resorted mainly to Local Relief Model (LRM), also known as Local Dominance or Trend Removal (Hesse 2012), Multiple Hillshading, Principal Component Analysis (PCA) and Sky View Factor. This LRM technique consists of cancelling the height variation of large shapes of the relief so as to highlight the areas with modest traces. Multiple Hillshading requires direct illumination from multiple light sources with different azimuths that accentuate different elevated terrain features. PCA, in turn, is a statistical analysis of the first three hillshade components generating an interpretive RGB map. Finally, Sky View Factor represents an illumination from the portion of the sky visible from a certain point of the terrain (Mlekuž 2013: 117-118). These analyses can be carried out with the Relief Visualization Toolbox v. 2.2.1 developed by the Slovenian Academy of Arts and Sciences (Kokalj and Somrak 2019; Zakšek, Oštir and Kokalj 2011). Other similar applications are of open access.

2.2.1. Classifying the LiDAR points

LiDAR data, as mentioned above, can be classified into a series of categories according to the types of obstacles. The American Society for Photogrammetry and Remote Sensing (ASPRS) defined a series of categories currently in version 1.4 (ASPRS 2011) although flights along the lines of previous versions still exist. This is the case of those carried out by the first IGN coverage applying the ASPRS point classes 1.2, format 3 (Table 1).

ASPRS LiDAR Point Classes 1.2	
0	Created, never classified
1	Unclassified
2	Ground
3	Low Vegetation
4	Medium Vegetation
5	High Vegetation
6	Building
7	Noise
8	Model Key-Point
9	Water
10	Reserved for ASPRS Definition
11	Reserved for ASPRS Definition
12	Overlap
13-31	Reserved for ASPRS Definition

Table 1: LiDAR point classification system (v. 1.2, ASPRS).

The LiDAR data most often are automatically classified based on different algorithms by the institutions that carried out the fieldwork. There are also various other tools serving to reclassify them so as to obtain reliable point clouds applicable to archaeology. These are carried out through DEM and DSM from different parameters such as the intensity of the returns, the angle, and the relative height with respect to the surrounding points. A good filtering of the points requires a profound knowledge of remote sensing and LiDAR tools, skills that are normally beyond the reach of archaeologists. It is therefore necessary to proceed with caution and carry out preliminary tests as to the quality of the point cloud classification.

It is therefore advisable, when possible, to resort to a photointerpretation to manually verify the quality of the classification, in particular to differentiate features of terrain and vegetation, key to interpreting archaeological structures. This is nonetheless a fairly expensive method. Carrying out a point-to-point review of these types of files is tedious as a grid of 4 km2 can easily comprise between 3 and 8 million points. Therefore, landscape studies at a macro scale when facing vast quantities of data require automatic classification algorithms whose margin of error are negligible.

Manual classifications are worth carrying out when the interest focuses on determining the microtopography of a modest area such as an archaeological site. This is the case of the fortresses of Órgiva and Poqueira where it is possible to distinguish the differences between automatic and manual classifications. Thus the vast rocky outcrop of the upper enclosure of Poqueira, as in the case of Órgiva, was initially interpreted in the category of High Vegetation instead of Ground. Here the majority of the surface of its terraces is also interpreted as High Vegetation. It is also noteworthy that none of the few pulses impacting on the medieval masonry and rammed earth features yielded returns that can be automatically interpreted as anthropic constructions. This is probably due to the type of materials rendering difficult their visibility, especially in the cases when they are erroneously classified as High Vegetation. Therefore, a manual classification is a necessity as there are considerable differences between automatic and manual classifications (Table 2, Figures 18-22).[12]

LiDAR Órgiva					
		Automatic classification		**Manual classification**	
		Point count	Percentage (%)	Point count	Percentage
Classification	2 Ground	22,299	24.06	25,155	99.14

[12] Manually classified LAS archives of Poqueira's and Órgiva's fortresses are available at http://hdl.handle.net/10481/62100.

	3 Low Vegetation	1419	1.53	0	0
	4 Medium Vegetation	7918	8.54	0	0
	5 High Vegetation	8510	9.18	12	0.05
	6 Building	25	0.03	205	0.81
	7 Noise	1392	1.5	0	0
	12 Overlap	51,133	55.16	0	0
LiDAR Poqueira					
		Automatic classification		**Manual classification**	
		Point count	Percentage (%)	Point count	Percentage
Classification	2 Ground	26,506	63.3	14,245	86.9
	3 Low Vegetation	179	0.43	84	0.51
	4 Medium Vegetation	5584	13.33	1490	9.09
	5 High Vegetation	2277	5.44	548	3.34
	6 Building	0	0	20	0.12
	7 Noise	138	0.33	5	0.03
	12 Overlap	7191	17.17	0	0

Table 2: Comparison of the LiDAR automatic point classification and the manual reclassification based on the observations at the sites of Poqueira and Órgiva.

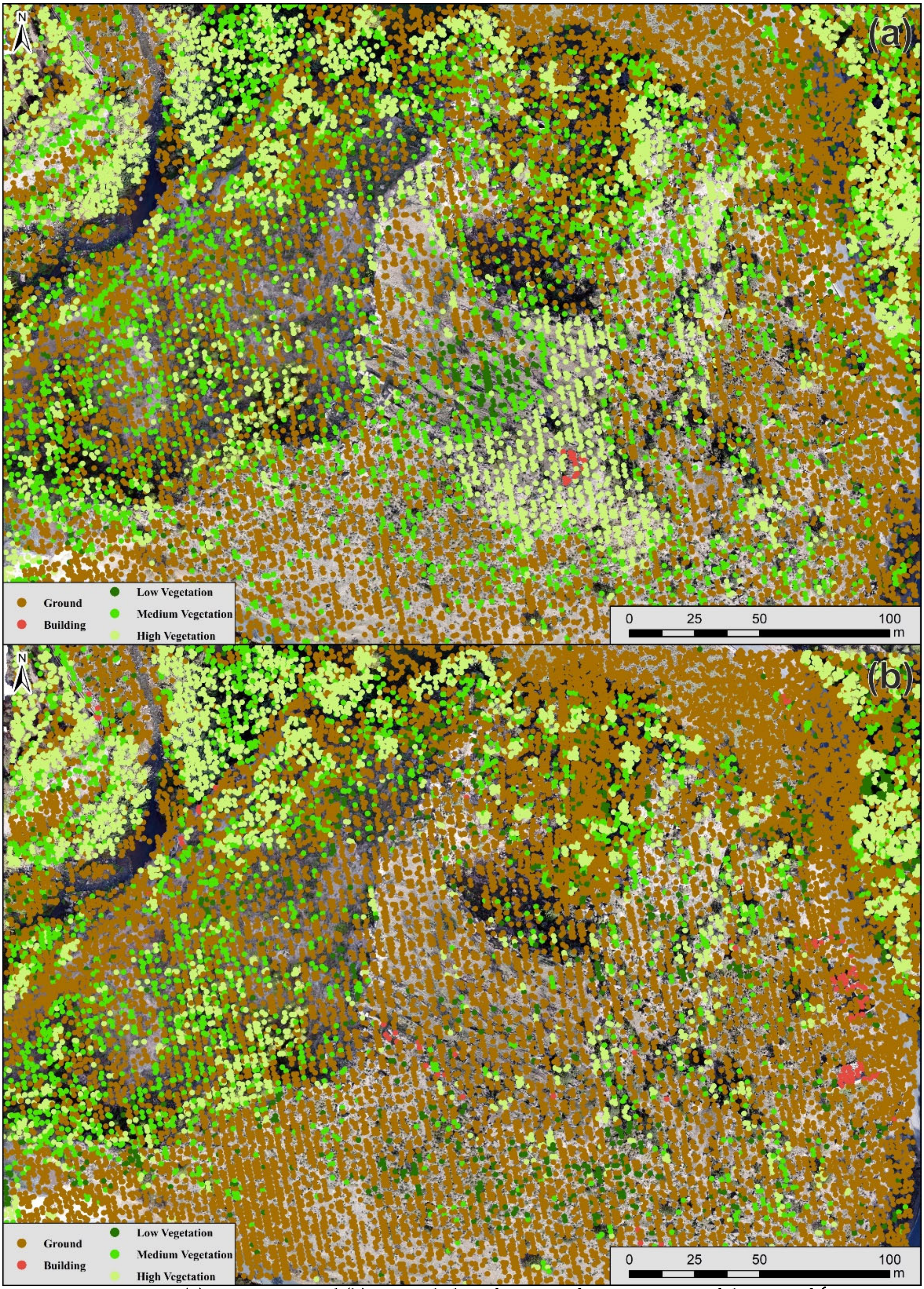

Figure 18: (a) Automatic and (b) manual classification of LiDAR points of the site of Órgiva.

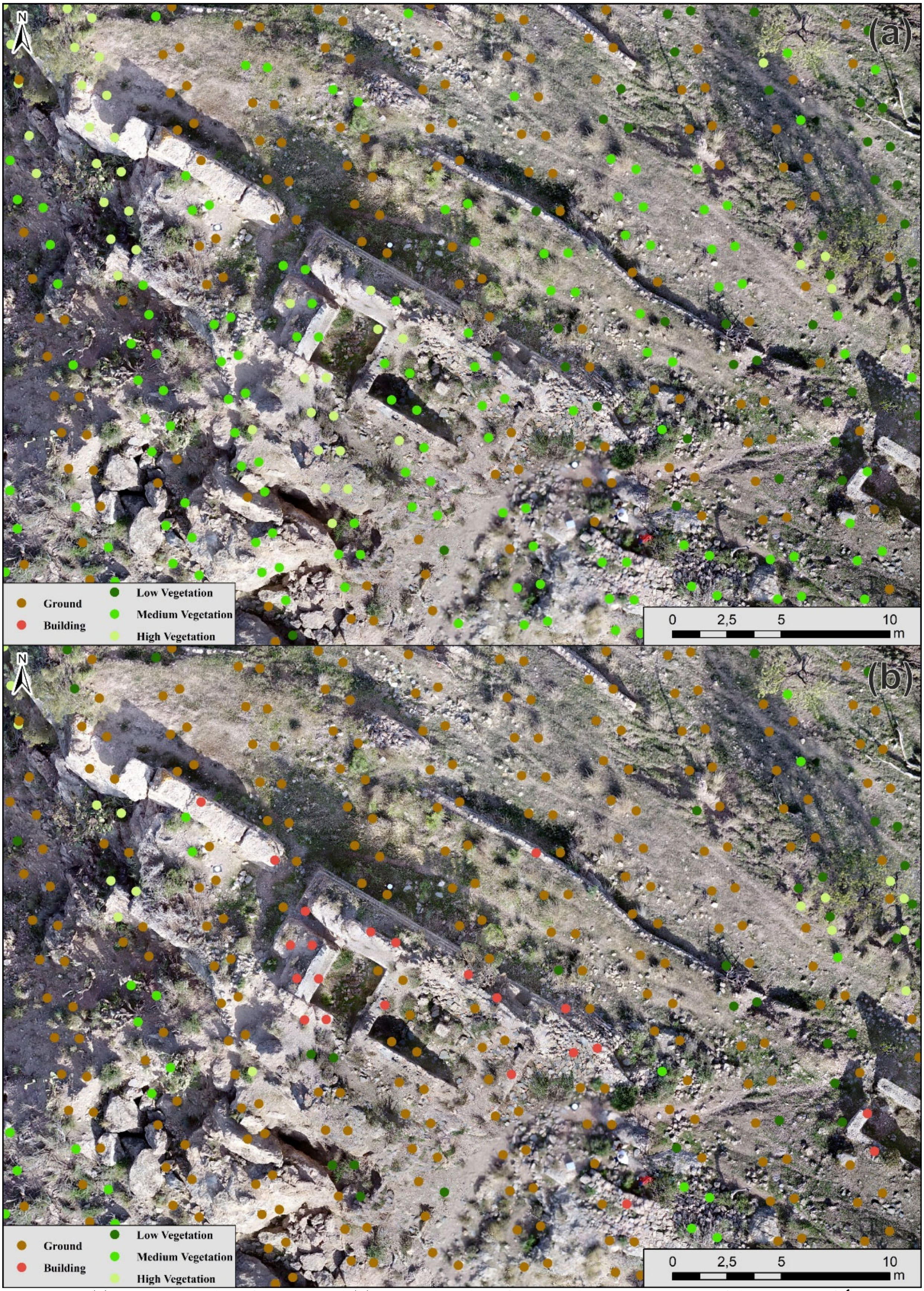

Figure 19: (a) Automatic classification and (b) manual reclassification the LiDAR points of the Tower of Órgiva.

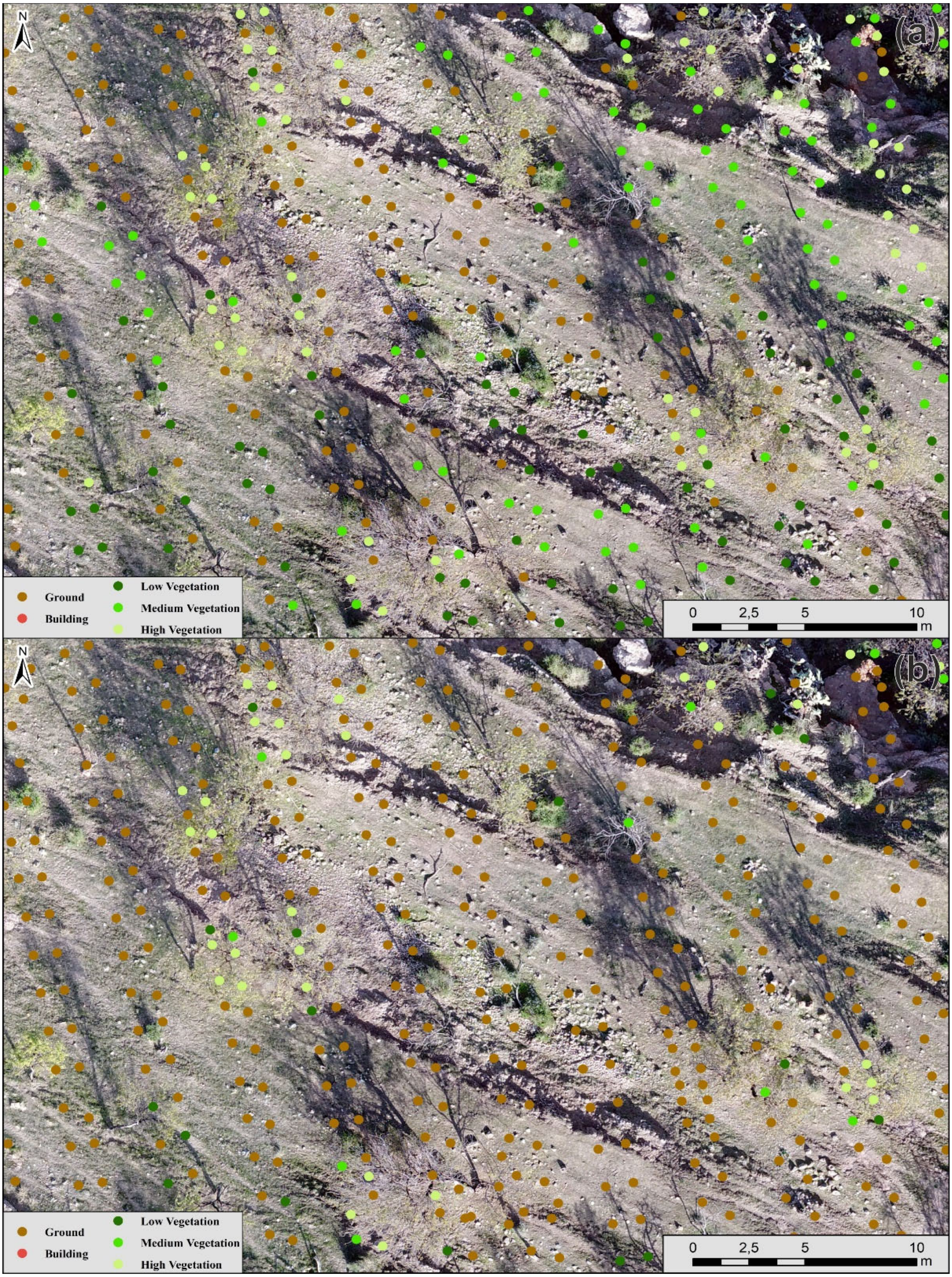

Figure 20: (a) Automatic classification and (b) manual reclassification of the LiDAR points of agricultural terraces of the fortress of Órgiva.

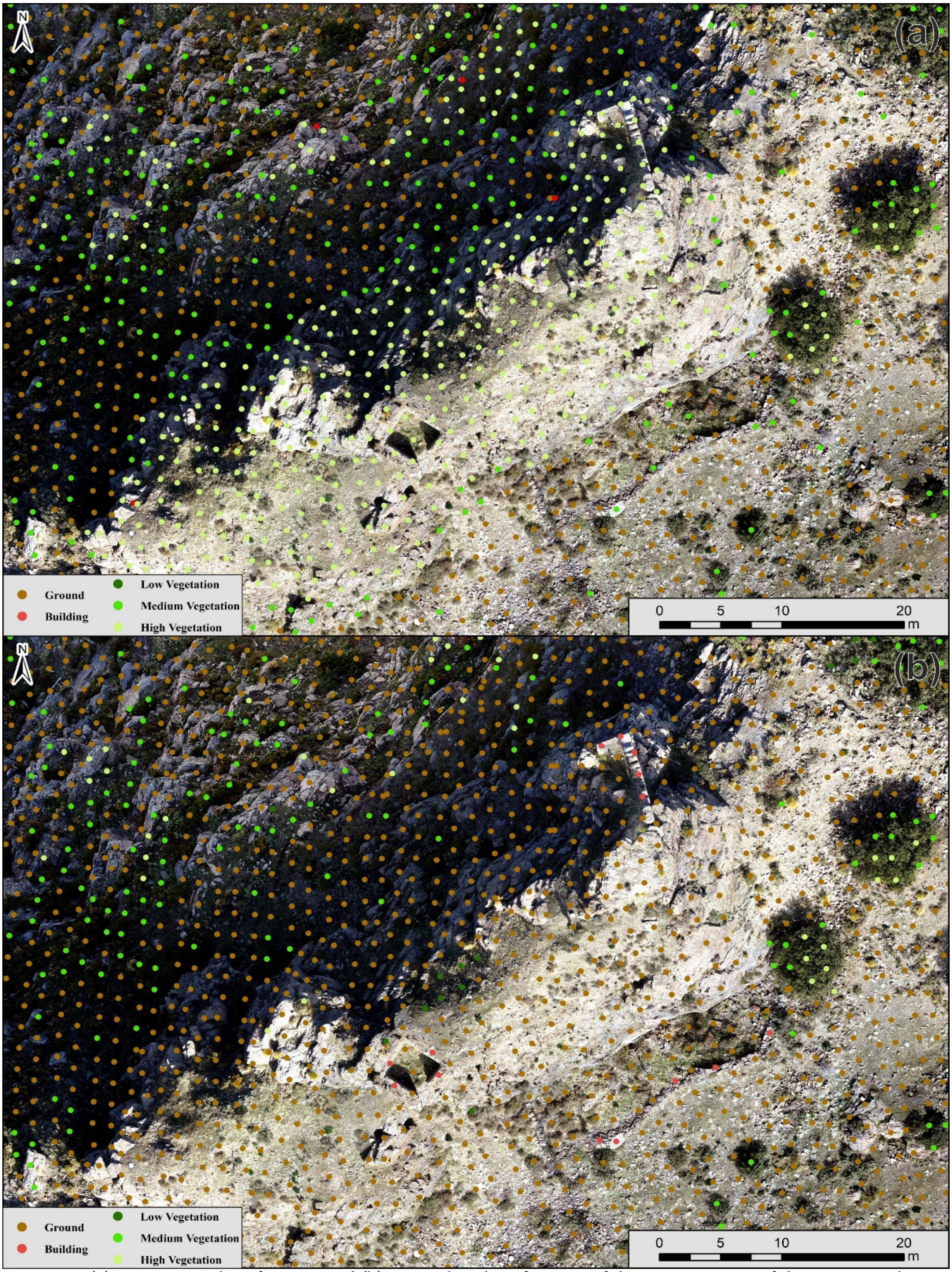

Figure 21: (a) Automatic classification and (b) manual reclassification of the LiDAR points of the upper enclosure of Poqueira.

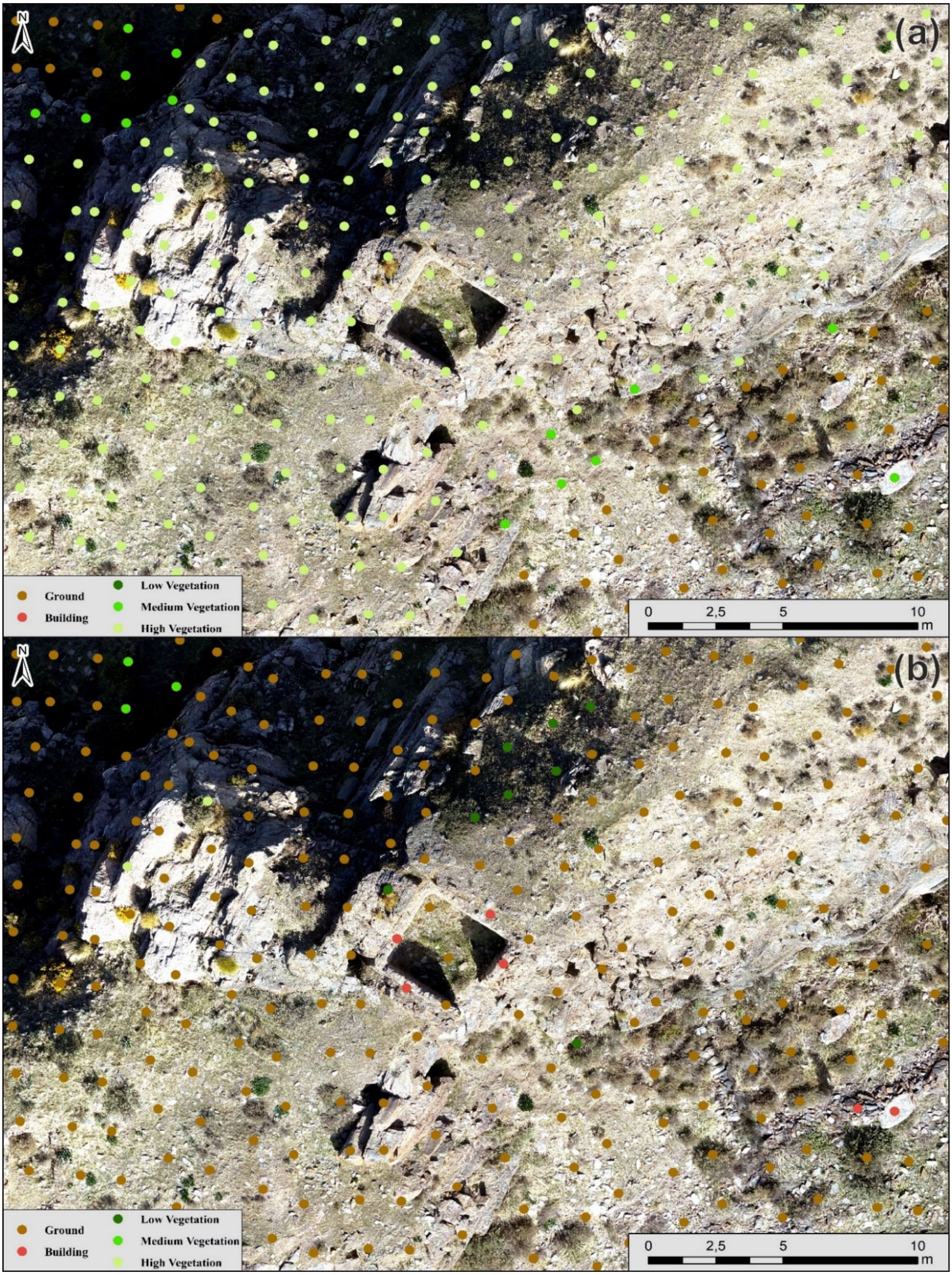

Figure 22: (a) Automatic classification and (b) manual reclassification of the LiDAR points of cistern of the fortress of Poqueira.

2. 3. Applying LiDAR and photogrammetry. The outset of a vast workflow

The ramifications of photogrammetry and LiDAR surveys in recent years have been of great utility to archaeological research (Mlekuž 2013, 2018; Opitz 2013). Photogrammetry, especially when carried out with UAVs, yields high quality graphic coverage of either vast areas of land or to study of features that are of difficult access, as in the cases of the fortifications of Órgiva and Poqueira. Thus, applying remote sensing through both photogrammetry and LiDAR represent the first step of a workflow that offers a large number of potential analyses as well as products that can serve to disseminate the results (Figure 23).

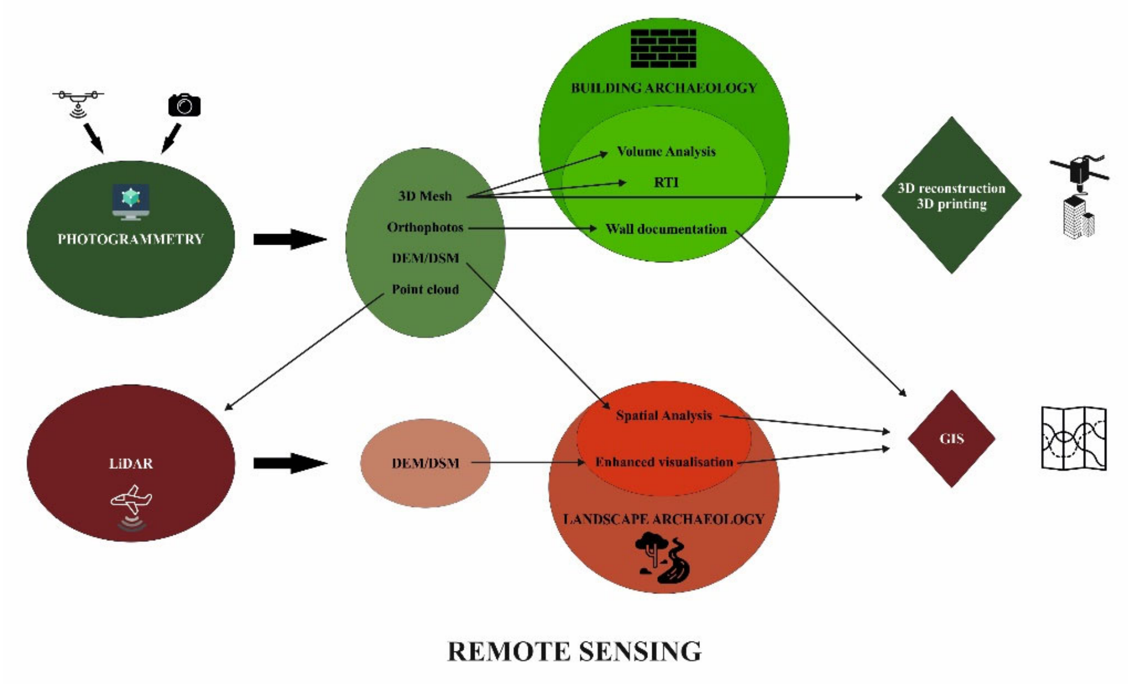

Figure 23: Scheme depicting the remote sensing workflow.

Photogrammetric surveys backed by precision topography offer a large array of products fundamental to the current project. Orthophotos gleaned from mesh and three-dimensional textures are the graphic foundation of paramental analyses as they yield useful visual and metric quality, especially when it comes to features where traditional methods cannot be applied. It is for this reason that these new technologies are increasingly applied to record old constructions (Lejeune 2019). Furthermore, since they are georeferenced, they are easy to integrate and manage through GIS as an archaeological database with absolute coordinates.

The 3D model itself can serve as a base to a host of analyses due to its accuracy when calculating dimensions and volumes. It can likewise serve to estimate costs and construction times based on the quantity of materials required, an aspect increasingly common to Archaeology of Architecture (Brogiolo, Cavada, Camporeale, Bernard and Parisi 2017; Giacomello, Parisi and Schivo 2017; Maldonado Ruiz and Fernández García, in press; Vitelli, 2017a). It can likewise serve as a basis for computerised visualisation techniques such as Reflectance Transformation Imaging (RTI), also known originally as Polynomial Texture Mapping (PTM) (Malzbender, Gelb and Wolters 2001). It is a technique that when applied traditionally either with *highlight* or *dome* variants seeks to digitise the effect on a feature of different types of light with different angles, generating a digital re-lighting model. This makes it easier for the researcher to test the different angles and types of light to observe features of the construction that cannot be seen by the human eye. This explains why this technique was applied to a large number of archaeological items from different periods including Roman coins, Egyptian papyri, and medium and large-sized rock art (Carrero-Pazos, Vázquez-Martínez and Vilas-Estévez 2016; Dedík and Minaroviech 2017; Dellepiane, Corsini and Callieri 2006; Earl, Beale, Martínez and Pagi 2010; Earl, Martínez and Malzbender 2010; Horn, Pitman and Potter 2019; Kotoula and Kyranoudi 2013; Miles, Pitts, Pagi and Earl 2015; Mudge, Malzbender, Schroer and Lum 2006; Mudge, Voutaz, Schroer and Lum 2005; Piquette 2011; Vázquez Martínez, Vilas Estévez and Carrero Pazos 2015). It has even served in the field of Archaeology of Architecture to detect tool marks to identify construction techniques (Vitelli 2017b).

However, one of the main handicaps of applying this system is its rigidity. A camera with a fixed tripod is necessary throughout the entire process while varying the rate of light with an artificial source. It is therefore very complicated to apply to sites of difficult access and to large features. It is in these cases where it is better to resort to a photogrammetric model as the basis for the backlight model generated in a virtual environment known as virtual RTI. Application of 3D modelling software leading to realistic light simulation such as the Blender (Blender Foundation 2017), available as an open source, allows recreating a virtual stage with the 3D model of the object and apply different illuminations to create a RTI model (Maldonado Fernández and Rouco Collazo, in press; Maldonado Ruiz, 2020: 139-170). This can be done with the free RTI Builder software and viewed with the RTI Viewer (Cultural Heritage Imaging 2013a, 2013b). This eliminates the problems of the scale of the object and access with the necessary equipment. This method served in an experiment related to the external wall of the Órgiva cistern whose results are displayed below.

In addition, the 3D model is an optimal base through which to carry out archaeological reconstructions that depict working hypotheses subsequent to the paramental analysis. The three-dimensional reconstruction is therefore useful for research since the process itself raises new questions as to the interpretation of the remains. But it is above all a very useful and simple means of dissemination information through digital methods, increasing the number of platforms serving to spread content

(Previtali and Valente 2019; Scopigno, Callieri, Dellepiane, Ponchiov Potenziani 2017; Statham 2019). For this reason, it is gaining in popularity among scientific disciplines (García Carpintero López de Mota and Gallego Valle 2018; Maldonado Ruiz 2020: 225-233).

Another application of 3D modelling, digitally reconstructed or raw, is 3D printing. This technique represents a great stride forward due to the liberalisation of patents and the introduction of affordable printers that can reproduce small and medium-sized objects with an error equal or less to 0.1 mm. Fundamental to this process was Boyer's (2004) RepRap project (Replicating Rapid-prototyper) intended to develop self-replicating 3D printers free of patent using Fused Filament Fabrication (FFF or FDM) technology to print small components and prototypes (Jones et al. 2011). Several prototypes proceeded from this project with the Prusa produced in 2010 in different versions by J. Prusa as the most common. This printer is equipped with a motor for each of the three axes (X, Y, Z) that allows the filament to be deposited precisely following the form of the object (Brus and Barvíř 2015).

Today there are different printing techniques (such as the FFF cited above) which generate models from layers of filaments of different materials or from photopolymer-based materials using Digital Light Processing (DLP) or Stereolithography (SLA) techniques (Brus and Barvíř 2015: 46-48). The technology therefore yields highly accurate affordable models and reconstructions which can serve to disseminate historical information. Physical reproductions are in fact more accessible to the general public and, above all, bring heritage closer to groups with reduced mobility or through other functional diversity such as hypovision, as they are easily adaptable to typhlological frameworks (Maldonado Ruiz 2020: 213-225; Marqués, Velázquez Pascual, Bonmatí Lledó and Marcos González 2018; Meschini and Sicuranza 2016; Montuori 2018; Schwarzbach, Sarjakoski, Oksanen, Sarjakosi and Weckman 2011). It is also very useful for didactic activities of different age groups as the exact replicas of archaeological items eliminate the risk of damage to the originals. For this reason it has seen an increase in use in archaeology as part of informative projects and even to generate scaled models of sites (Esclapés Jover, Molina Vidal, Muñoz Ojeda, Fabregat Bolufer and Tejerina Antón 2017; Montuori 2018; Zennaro 2013).

The current study resorted to an Ender 3 Pro (FDM Prusa i3 type) 3D printer manufactured by Creality. The polymer serving for the prints was polylactic acid (PLA) which melts at 180º C. In order for the photogrammetric model to be printed, it must be laminated with specific software, in this case Ultimaker Cura (Ultimaker 2019). This converts the models with the parameters indicated for the printer to G-Code thus establishing the Cartesian coordinates that serve for the printing. As it is open source software, it also is an ideal platform to share information and render its models available to anyone.

To close the section on products serving for remote sensing we turn to the theme of DEMs generated from both photogrammetry and LiDAR data, modellings that are essential to carrying out a broad spatial analysis within the framework of Landscape Archaeology (Mlekuž 2013). SfM photographs carried out with a drone combined with correct topographic data generate a highly accurate DEM that is extremely useful to reproduce a site's microtopography. The same can be said of the LiDAR clouds. The disadvantage of the lower number of points per meter of most of the LiDAR surveys accessible to archaeologists carried out by the state organisations is compensated by the advantage that their coverage is much wider than that attained and processed by UAV photogrammetry. In addition, the automated filtering methods are more developed among the different programs designed to handle this type of data, yielding precise DEMs devoid of vegetation and structures. These filtering methods can also be applied to the point clouds of the photogrammetry.

The DEMs, either generated by photogrammetry or LAS data, can also serve as a foundation of spatial analyses (visibility, intervisibility, catchment areas ...) that can be improved by applying visualisation algorithms to interpret structures that can subsequently be verified by field work.

3. The study area: The Poqueira Ravine and the Órgiva Plain

The two sites selected for this study are in the western Alpujarra Alta Mountains (Granada) and correspond respectively to the Poqueira Ravine and the fertile Plain of Órgiva along the Guadalfeo River (Figure 24). The study area forming the basis of this Landscape Archaeology analysis comprises a total surface of 320 km2 extending from the peaks of the Sierra de la Contraviesa to those of the Sierra Nevada. The sector includes some of the highest peaks on the Iberian Peninsula, notably the Mulhacén at 3482 m and the Veleta at 3392 m a.s.l.. The area's geology comprises two superimposed complexes, the Nevado-Filábride and the Alpujárride. The first is mainly characterised by graphite shales alternating with quartzites generated by metamorphic processes affecting rocks of marine and magmatic origin. The Alpujárride, which outcrops in the middle and low mountains, is basically made up of black schists, limestones, dolomites and marbles (Villalobos Megía and Pérez Muñoz 2006: 115-135).

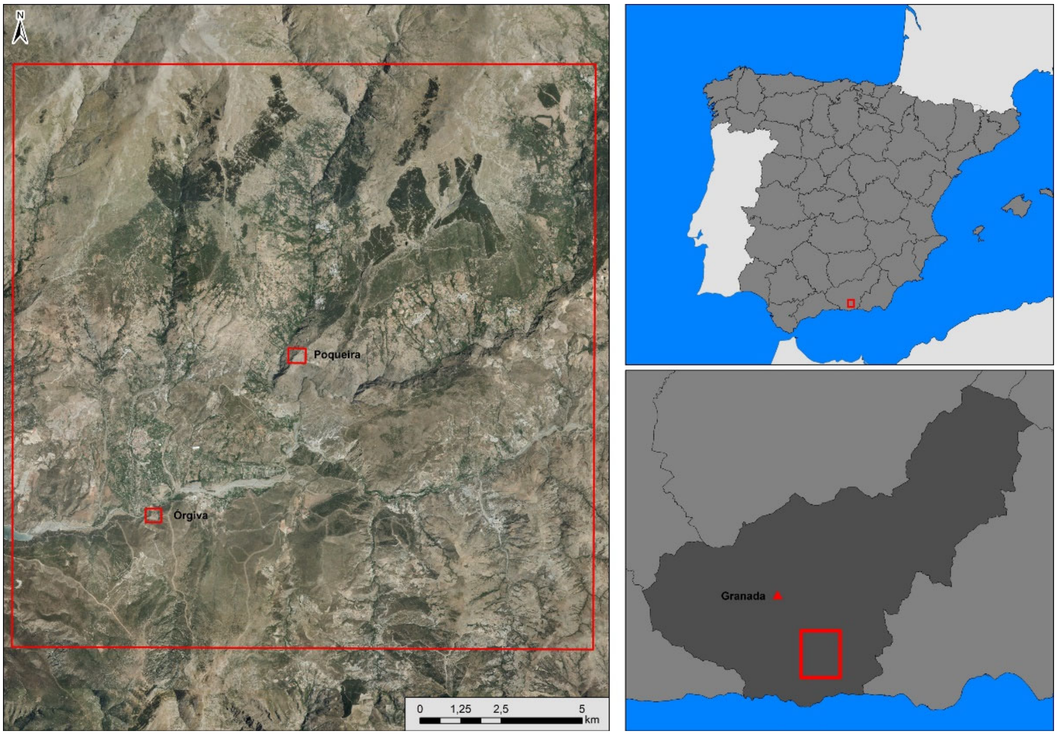

Figure 24: Maps of the Iberian Peninsula and the Province of Granada with the rectangle indicating the study area and aerial view indicating the position of Órgiva and Poqueira.

The area currently comprises eight municipalities. Five are linked to the Órgiva Plain (Órgiva, Bayacas, Cáñar, Soportújar and Carataunas) while three are in the Poqueira Ravine (Capileira, Bubión and Pampaneira). There is also evidence from written records immediately following the Castilian conquest that several hamlets and villages (*alquerías*) had been depopulated in medieval times, notably Alguástar and Beni Odmán in Poqueira, and five absorbed by Órgiva (Sortes, Benizalte, Pago, Benisiete and Tíjola). Two others in the surroundings of Cañar (El Fex and Barjas), and one in Bayacas (Haratalachín) were also abandoned (Figure 25). The features examined in this microspatial study in the wider Archaeology of Architecture framework correspond to the two site's fortifications and their immediate surroundings.

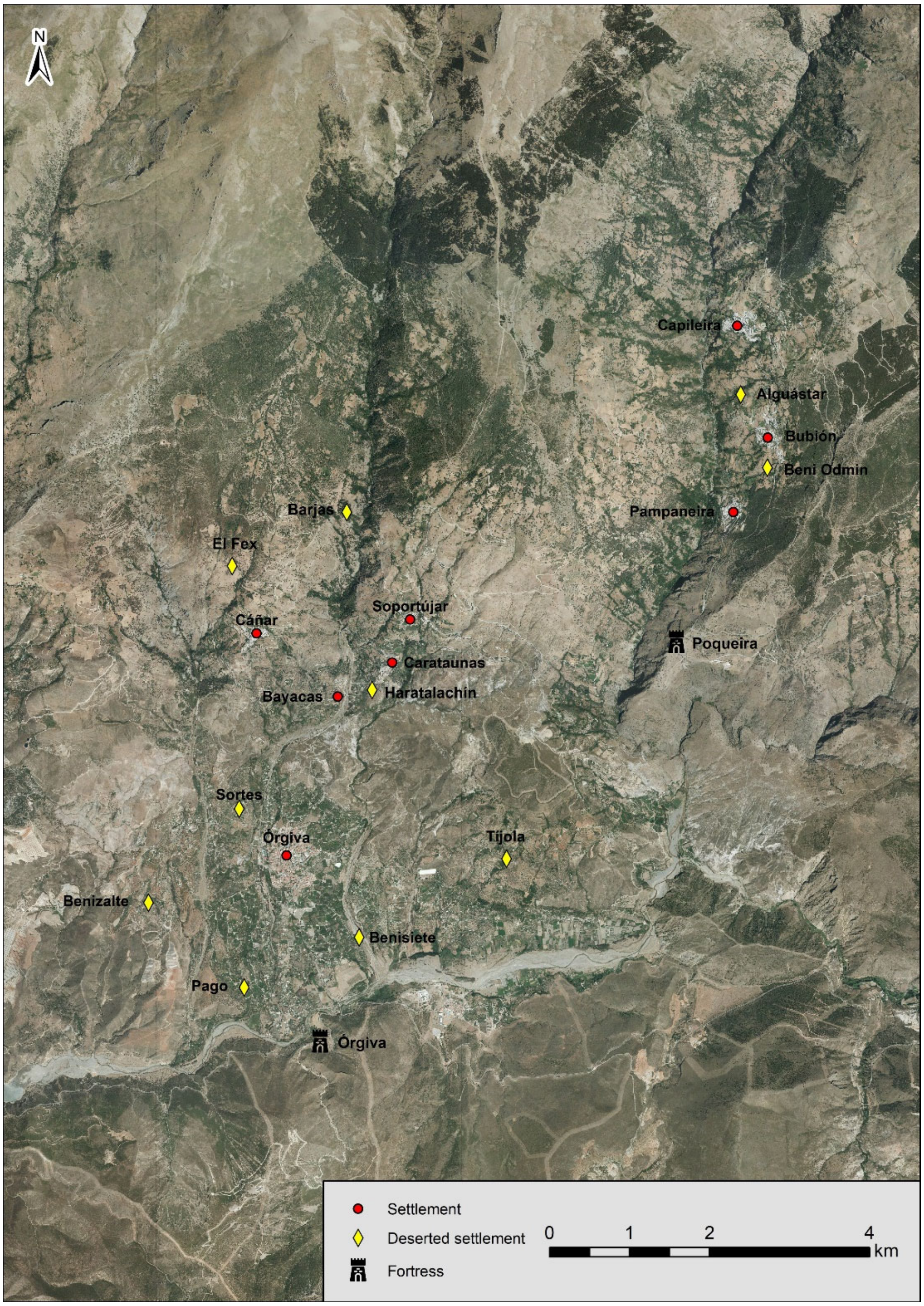

Figure 25: Aerial view with the position of the fortifications, towns and farmhouses cited in the text.

3.1. The Fortress of Poqueira

The Poqueira Fortress is perched on a promontory on the left bank of the Poqueira Ravine south of the towns of Bubión, Pampaneira and Capileira (Martín García, Bleda Portero and Martín Civantos 1999). This isolated hill dominates its surroundings and forms the spur of a higher range of mountains that descend from the summits of Sierra Nevada (Figure 26). The 11th-century Andalusi author Al-'Udri in his geography mentions the *djuz* of *Buqayra* probably based on information from the previous century (Sánchez Martínez 1976). P. Cressier's research on the Alpujarra in the 1980s places the fortification at least as far back as the 10th century (Cressier 1983, 1984, 1992). It would have served as the head of the *djuz* (*adjza* in its plural form), a small administrative district of the Caliphate of Cordoba (10th-11th centuries) whose specific characteristics are still the subject of heated debate (Jiménez Mata 1985-1986; Jiménez Puertas 2002; Martín Civantos 2013; Trillo San José 1991: 119-127). It is nonetheless possible to define it as a territory dependent on a fortification (*hisn*) controlled by the central power. The *djuz* (district) of Poqueira would have retained the same name when it became a *ta'a* (district) during the administrative reforms initiated under the Nasrid rule (14th-15th century) (Cressier 1984, 1992).

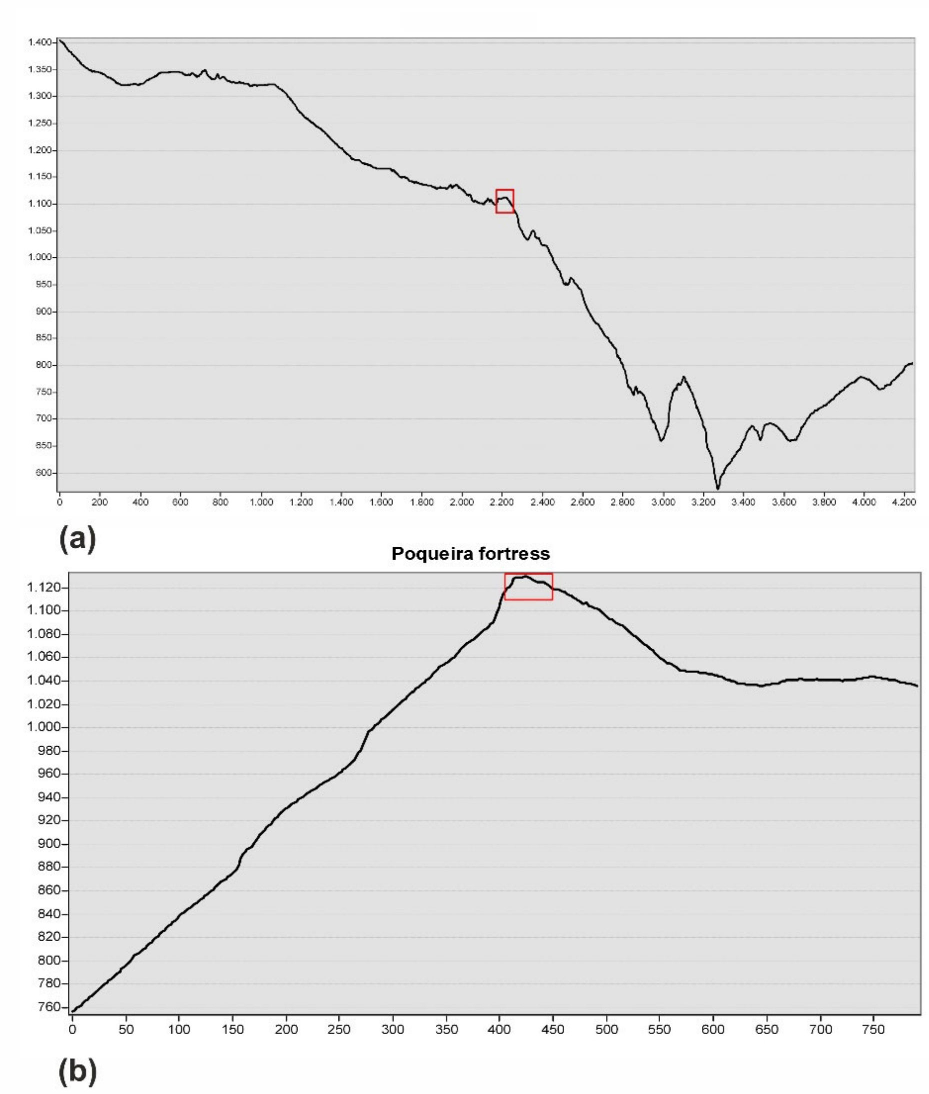

Figure 26: Topographic profiles of the positon of the site of Poqueira (a) NE-SW (b) NW-SE.

The fortification's remaining features indicate it was articulated by two different enclosures (Figure 27). Its interior extends over a steep rocky promontory oriented NE-SW. Remnants of a lime mortar masonry enclosure founded directly on the bedrock are preserved to the NE, E and SW. Its NE sector retains the remains of a rectangular rammed earth tower. It preserves its eastern (5.44 m in length; 0.9 m in width) and part of its (2.8 x 0.9 m) northern façades forming a right angle. To the south is another E-W rammed earth wall today measuring 1.1 by 0.7 m. This feature, spotted with circular transversal putlogs, was built with a whitish, highly packed lime mortar concrete packed in formwork boxes. At the angle of each of the structures are circular negatives of wooden fittings toward the middle of the box serving to reinforce the corner. Certain larger stones inside the boxes give the wall a *calicanto* (Rouco Collazo, Martín Civantos and Benavides López 2020) appearance, especially at the point of contact with the bedrock in the southern sector of the tower. Both structures are raised on a masonry foundation of local limestone slabs bonded with a whitish lime mortar. This foundation served to level the base from which to raise the rammed earthed feature.

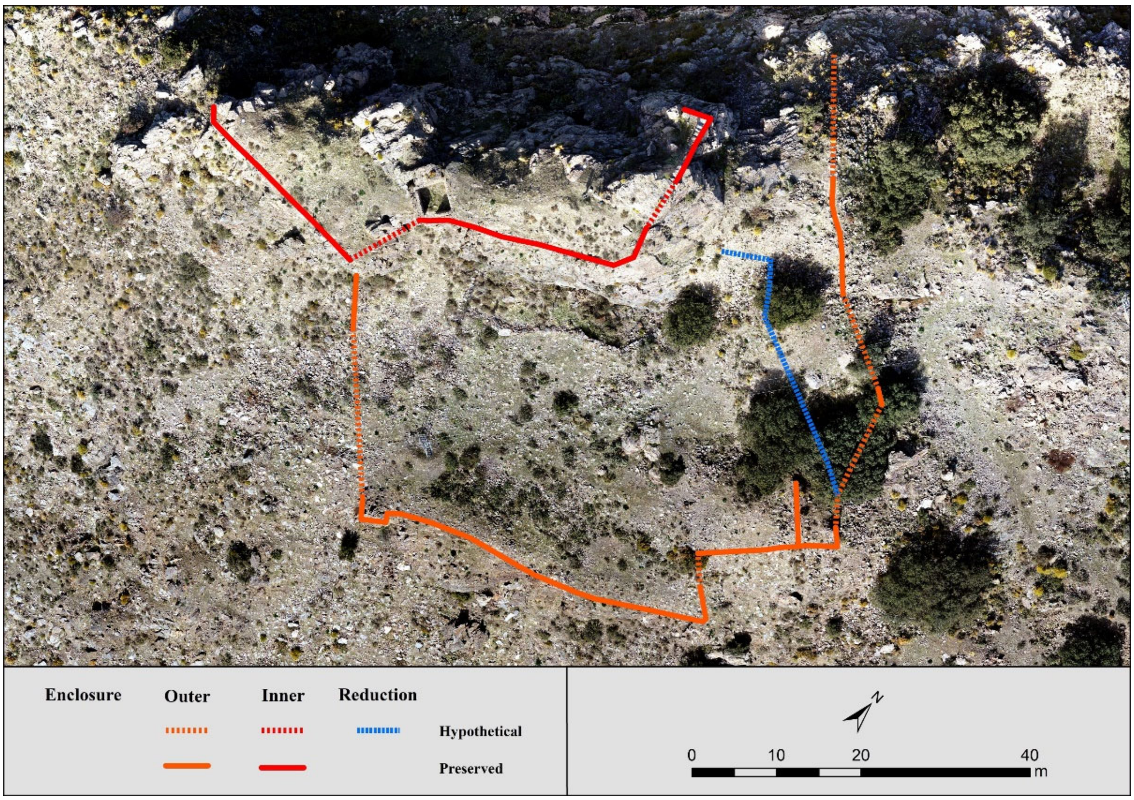

Figure 27: Poqueira. Limits of the different enclosures.

The other notable structure of the upper enclosure is a large central cistern. It was also raised with rammed earth concrete, although its proportion of sand and gravel differ from that of the tower. This could either indicate that they are not contemporary or that the different technique is linked to the cistern's function. Its plan is almost quadrangular (4.3 x 3.9 m) with walls 0.3 m thick. It leans against the remains of the masonry wall of the upper perimeter. Elsewhere small walls can be observed at certain points corresponding to internal structures whose interpretation is complicated by their slight elevation (Figure 28).

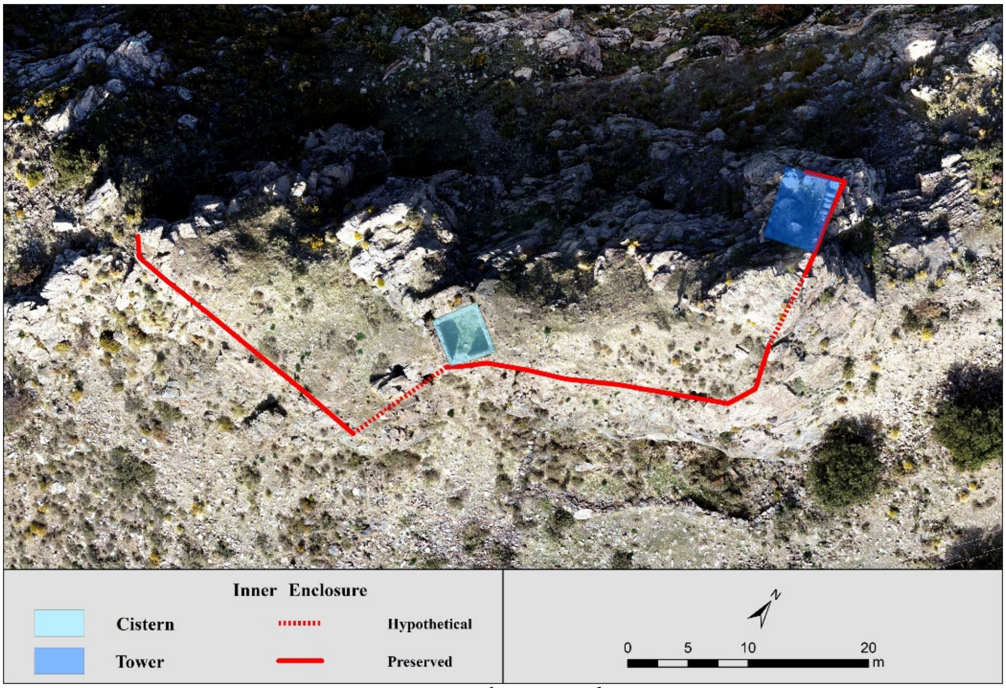

Figure 28: Poqueira. Upper enclosure and its main structures.

The second enclosure surrounds the upper enclosure to the NE and E. It is also made of limestone masonry interlocked with lime mortar, as in the case of the interior wall. At certain points such as the western wall, where it leans (oriented NS) against the outer enclosure, it has a maximum width of 1.2 m. To the south its maximum preserved height is 3.5 m. It cannot be ruled out that these masonry walls are not simply large foundations of rammed earth, as is the case of other Andalusi fortresses such as the Qaba de Aldeire and Fuerte de Lanteira on Sierra Nevada's northern slope (Jiménez Puertas, García-Contreras Ruiz and Mattei 2010; Martín Civantos 2002). There are no interior structures that can be dated to medieval times, only dry wall features reused later probably to pen livestock. The outer wall of the eastern façade lines a cut in the bedrock. The only feature of masonry possibly corresponding to a tower is in the enclosure's NE corner.

The Poqueira Fortress according to P. Cressier (1983) dates to at least the outset of the Caliphal period. The few very fragmented surface potsherds collected during an extensive survey point nonetheless to an occupation roughly between the 10th and 12th centuries. They are mostly fragments of straight-rimmed cooking and storage ware covered with either caliphal brown and dark green glaze or white paint with incisions (Fuertes Santos 1995; Koffler Urbano 2010; Melero García 2009). This ware is in line with Al-‘Udri's references. The tower of the upper enclosure, also raised with concrete, likewise resembles from the architectural standpoint other features raised in the 12th century (Gurriarán Daza and Sáez Rodríguez 2002: 603-615; Martín Civantos 2002; Rouco Collazo et al. 2020: 9-10). The finds include a single Type I pot with a notched rim dating from the 13th or outset of the 14th century suggesting that occupations from the Almohad and Nasrid periods were sporadic (Navarro Palazón 1991). Thus it is not possible to assure that the fortress was fully operational as such at this late medieval phase due to the scarcity of material and the absence of characteristic construction techniques and mural stratigraphy. It is also worth noting that certain façades collapsed toward the interior, contrary to the natural slope. This suggests an intentional destruction of part of these structures at an undetermined moment when they were no longer useful as the damage does not appear to be linked to violence.

3.1.1. Photogrammetric survey of the Poqueira Fortress

The photogrammetric UAV survey carried out of the Poqueira Fortress has proven to be a total, rapid and quality means of acquiring geospatial data. The drone was a DJI *Phantom 4 professional* equipped with a DJI-FC6310 camera. 62 m was the altitude chosen for the flight due both the height of Poqueira's defensive features and the unevenness of the surroundings. This yielded a thorough GSD of 1.27 cm/pixel in the feature's upper area (takeoff sector), 1 cm/pixel for the higher structures, and 3.2 cm/pixel for the lower ones.

The DJI-FC6310 camera mounted on the UAV features a 84° FOV with a focal equivalent to 24 mm. It also has a 1-inch (8.8 x 24 mm) CMOS sensor and a resolution of 5472 x 3648 pixels. Given the site's good atmospheric and lighting conditions, the speed of the UAV was set at 1.5 m/s which at certain heights leads to a displacement of pixels of an order of 4 mm in the field. The parameters of image capture correspond to an aperture of f/5.6 at ISO 100 with an automatic exposure time varying between 1/400s and 1/800s.

The design of the UAV flight allowed the best registration of the structures, improving their geometry and decreasing the total number of images (546) which translates into a significant gain of the time of processing (Figure 29).

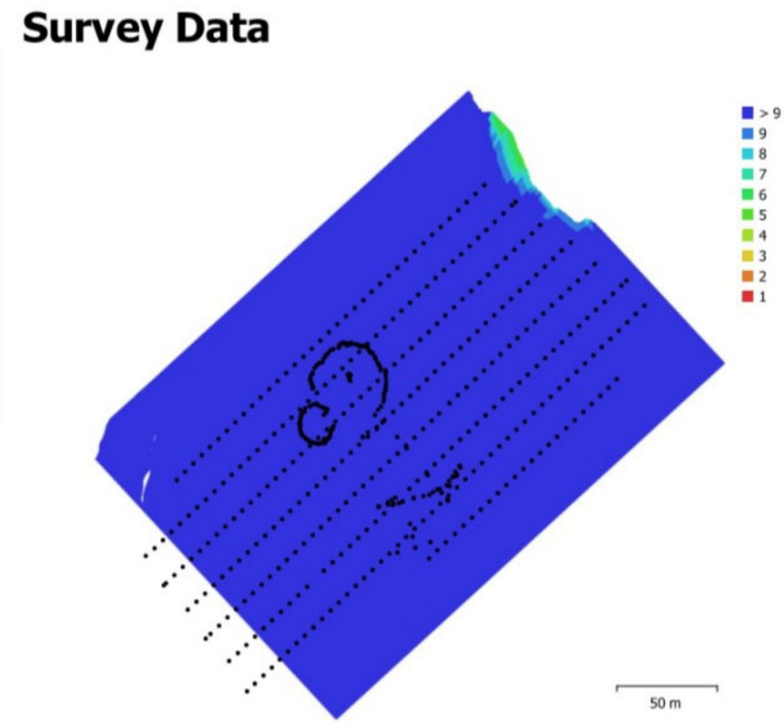

Fig. 1. Camera locations and image overlap.

Number of images:	546	Camera stations:	546
Flying altitude:	61.2 m	Tie points:	24,107
Ground resolution:	1.27 cm/pix	Projections:	307,220
Coverage area:	0.0488 km²	Reprojection error:	1.04 pix

Figure 29: Plan of the UAV flight over the Poqueira fortress indicating data as to the image capture and overlap.

It was necessary to carry out a fine adjustment of the position and orientation of the cameras, as well as a calibration of the lens, prior to generating the dense point cloud (Figure 30). A series of control targets were therefore placed throughout the area so as to georeference their coordinates with GNSS equipment connected to the national GPRS network. The estimated error after adjusting the control points (Table 3) validates the reliability of the digital model.[13]

[13] The processing report of the photogrammetric survey of Poqueira's fortress is available in http://hdl.handle.net/10481/62100.

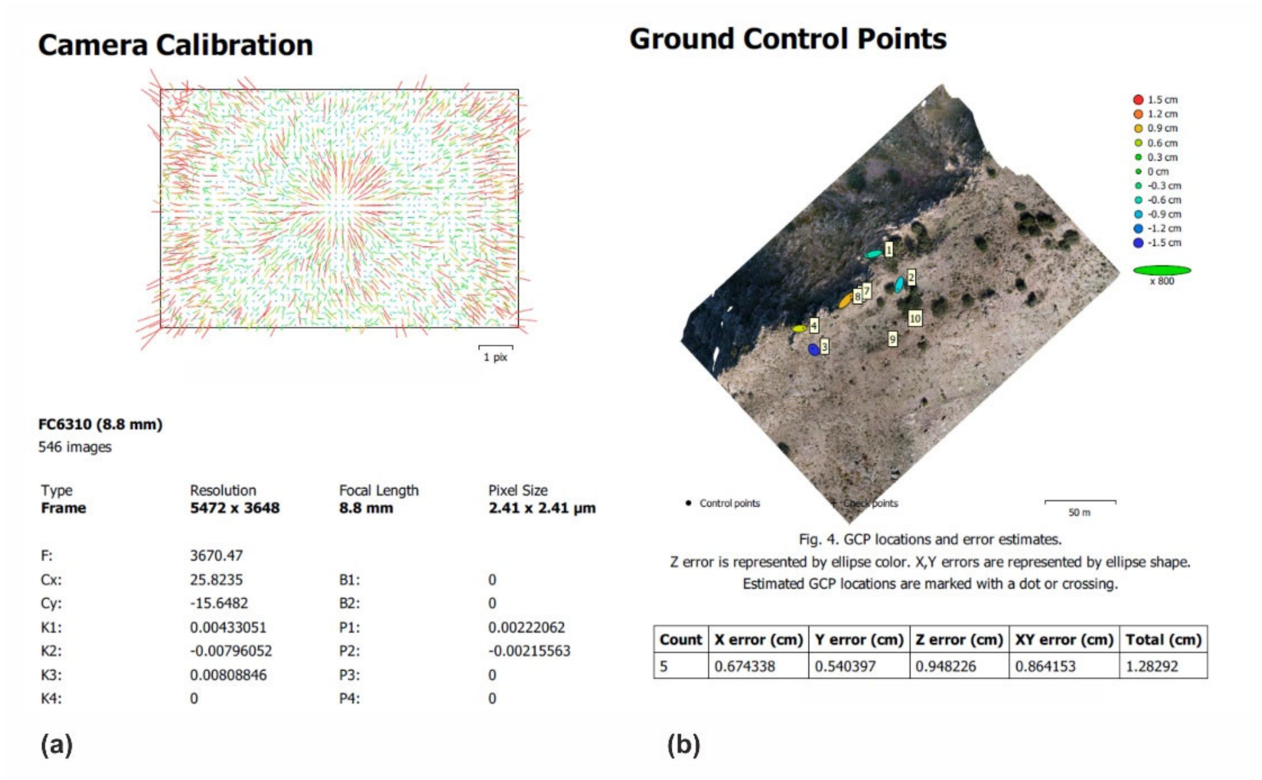

Figure 30: (a) Camera calibration based on the Poqueira survey control points. (b) Location and error estimates of the ground control points.

Label	X error (cm)	Y error (cm)	Z error (cm)	Total (cm)	Image (pix)
3	-0.180	0.234	-1.478	1.507	0.449
4	0.691	0.072	0.701	0.987	0.448
2	-0.257	-0.807	-0.787	1.156	0.404
1	-1.038	-0.278	-0.551	1.208	0.374
5	0.788	0.820	0.946	1.479	0.294
Total	**0.674**	**0.540**	**0.948**	**1.283**	**0.420**

Table 3: Poqueira. Estimation of the errors after adjustments based on the control points.

The high precision and quality of the photogrammetric method led to very precise recording of the site's structures and walls, essential to a paramental analysis in an Archaeology of Architecture framework (Figure 31). Furthermore, the highly accurate DEM model was very useful not only to analyse the site but its relationship with its surrounding landscape.

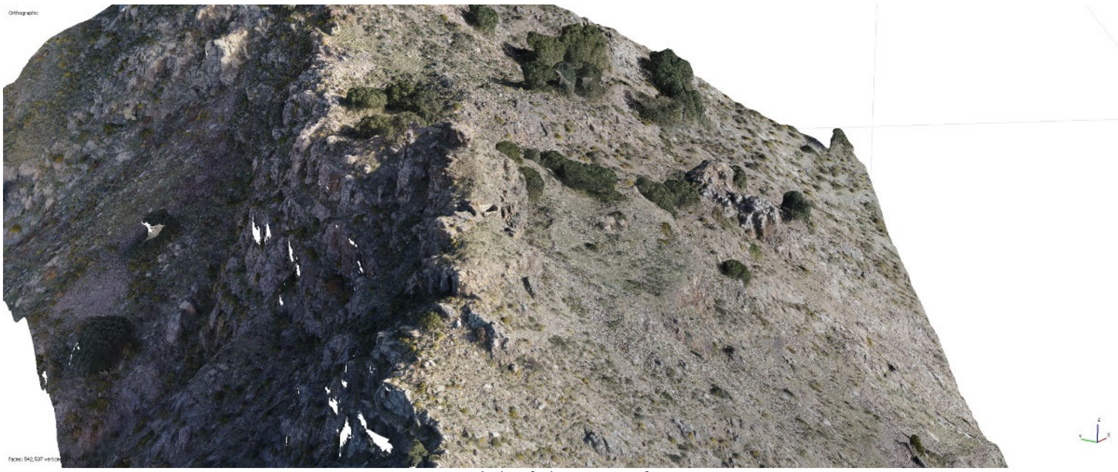

Figure 31: 3D model of the site of Poqueira.

Generating a model with a very rich geometry (7700 million faces) and a photorealistic texture allows obtaining orthophotos of high geometric and visual quality that also serve to identify the site's stratigraphic units and structures. They are likewise fundamental to carry out measurements to characterise and quantify the construction materials (Figure 32).

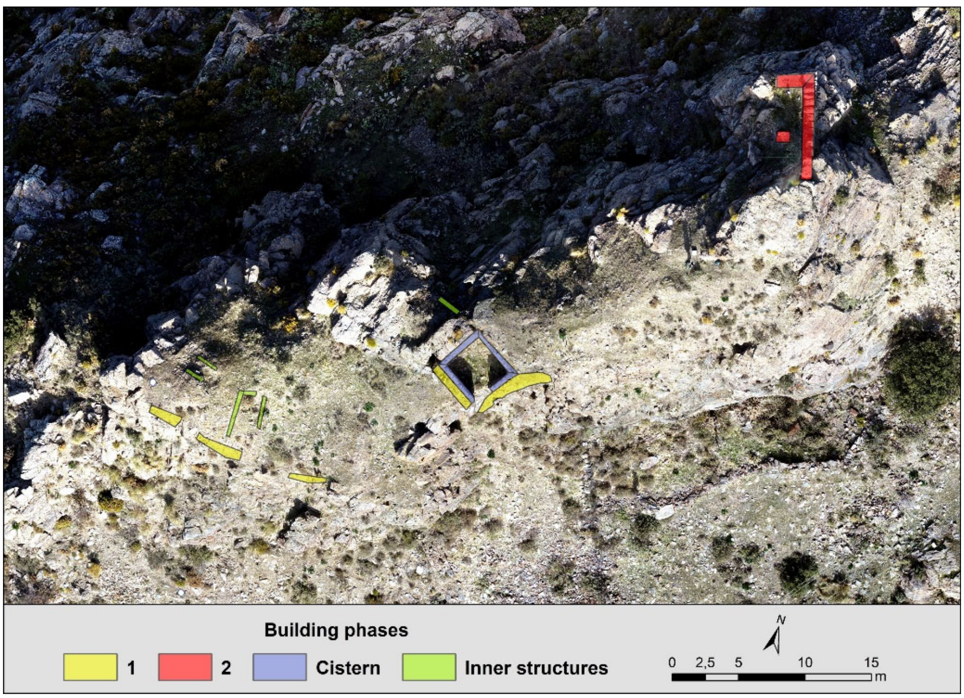

Figure 32: Graphic record of the structures of the Poqueira fortification superimposed on a flat orthophoto generated by MDS with a resolution of 1.27 cm/pixel.

In addition, the possibility to combine the SfM UAV photogrammetry with photos taken during fieldwork allows to enhance the quality in particular of features inaccessible due to Poqueira's rugged orography. This applies in particular to the tower of the upper enclosure standing above the great ravine to the NW of the promontory. Recording its upper structures, in fact, would have been very arduous with traditional archaeological drawing methods. The method was very rapidly, a factor critical to reduce the fieldwork of features difficult to access due to their distance and/or orography (Figures 33-34).

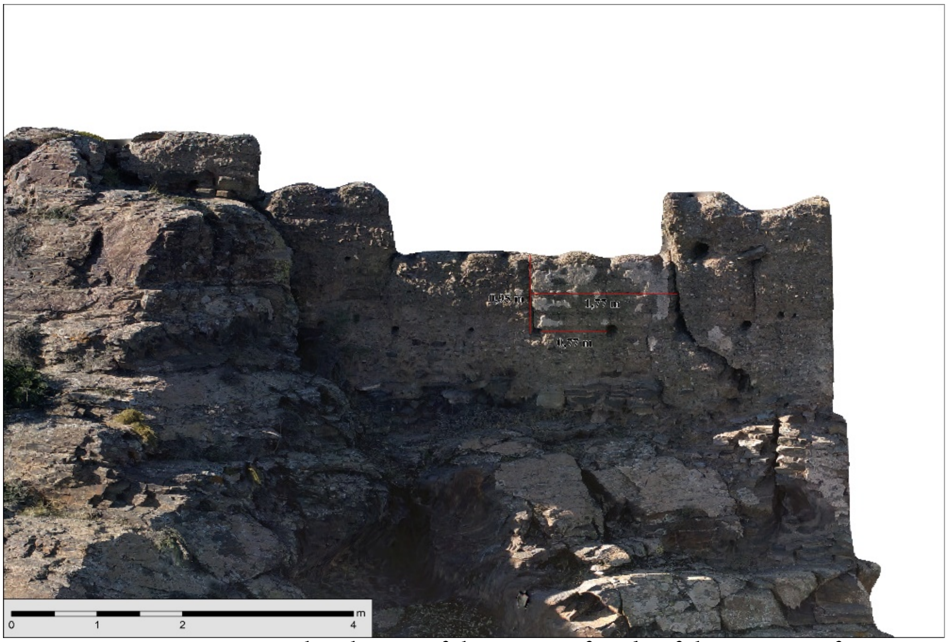

Figura 33: Stratigraphical units of the eastern façade of the Poqueira fortress.

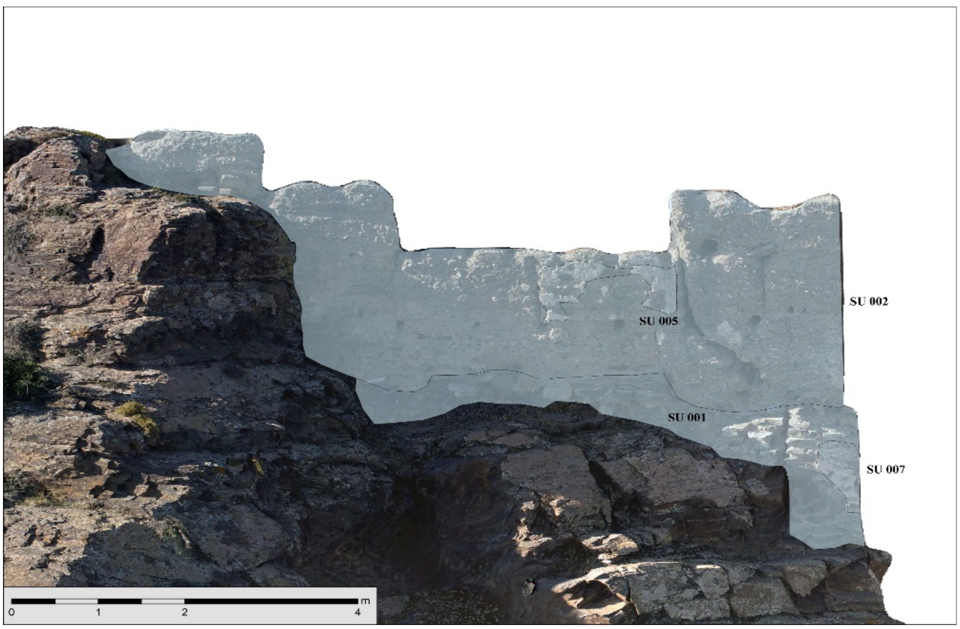

Figure 34: Measurements of the formwork wall of the Poqueira tower.

A high pixel metric quality was obtained for the DEM of the Poqueira Fortress. The resolution of 0.04 m per pixel was more than enough for this task. In addition, it was possible to eliminate the higher vegetation and attain a bare terrain. Although the Agisoft Metashape 1.6 software serving to process the photogrammetric data includes automatic point cloud classification tools, the software is founded on the height relative to the nearest neighbour leading it to an incorrect filtering of this abrupt terrain. A manual classification of the points therefore had to be carried out to eliminate the high vegetation and obtain a DEM of a quality suited for the microspatial study (Figures 35 and 36).

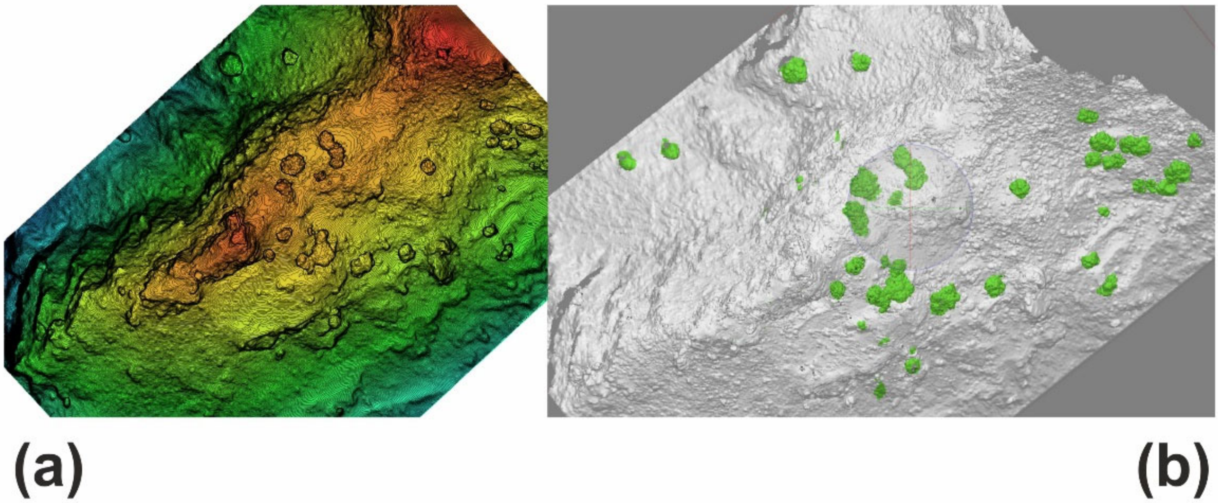

Figure 35: (a) Digital Surface Model with 1 m contour lines which allows classification of the points (terrain, vegetation, structures, etc.) and elimination of unwanted points. (b) Dense cloud with classified high and medium vegetation.

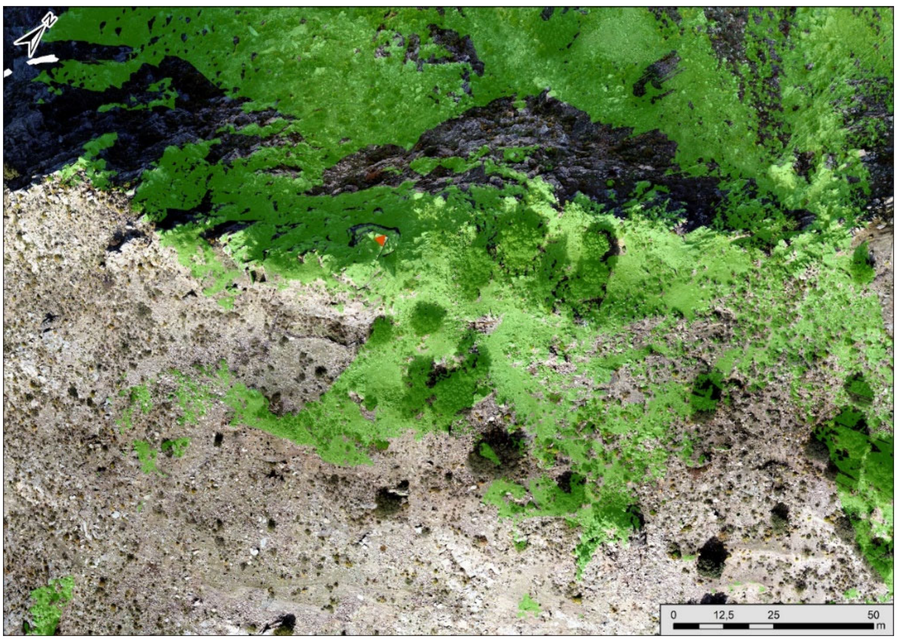

Figure 36: Visibility (green) from the tower of the Poqueira fortress.

3.1.2. The LiDAR survey of Poqueira

The data extracted from the LiDAR for Poqueira corresponds to the same surface covered by the drone. The *dataset* comprises a total of 16,392 points classified manually into different categories (Ground, High, Medium and Low Vegetation, Building...).[14] A file was then generated from this classification by means of LiDAR filtering tools based uniquely on the Ground and Building categories for a DEM with a cell size of 0.5 m. Although this requires interpolating certain calculations taking into account the density of 0.5 points per m2, it is nonetheless a resolution that is much higher when applying the different procedures of improved visualisation than a mesh pitch of 2 m, the maximum without having to resort to interpolations.

The DEM designed with a 0.5 m/pixel base was then subjected to a series of enhancement algorithms to verify up to what point it is possible to recognise the structures observed in the field. This allowed perceiving the SE flank of the lower enclosure and the upper enclosure's vast rocky platform. This level of precision was nonetheless not enough to identify the different structures. It is for this reason that we decided to apply a DEM visualisation devoid of high vegetation generated by the photogrammetric model. The results in this case are clear as all the structures are easily recognised. The topographic contours and the changes of levels likewise are clear. This facilitated drawing their edges, a task that is more difficult to carry out from the nadiral orthophotos extracted from photogrammetry. Even a series of small internal structures to the NW of the upper enclosure, in spite of being practically completely filled, can be observed through specific methods of visualisation such as Multiple Hillshading, PCA and Sky View Factor (Figures 37-39).

[14] Avalaible in http://hdl.handle.net/10481/62100.

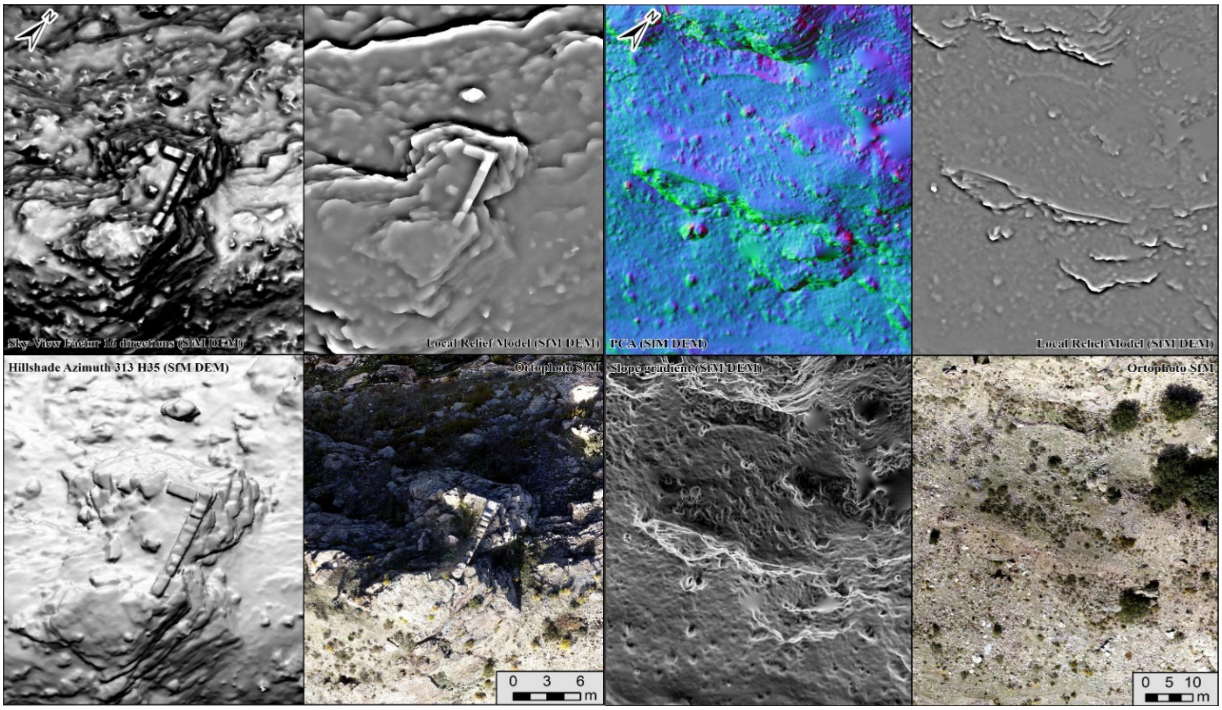

Figure 37-38: LiDAR views of the Tower of the Poqueira fortress. LiDAR views of section S of Poqueira's outer wall.

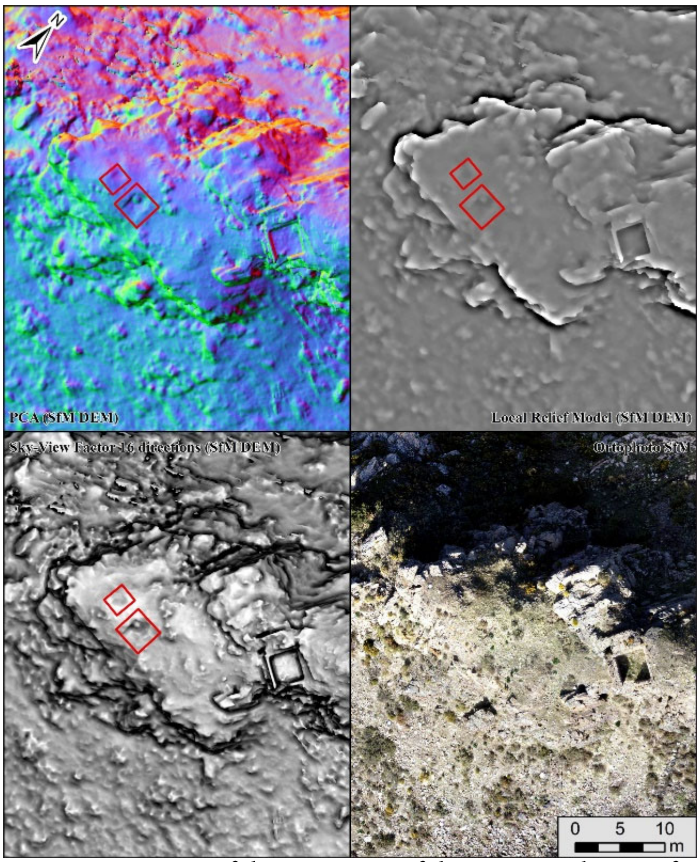

Figure 39: LiDAR views of the structures of the upper enclosure of Poqueira.

3.2. The Fortress of Órgiva

The Fortress of Órgiva is on a promontory along the left bank of the Guadalfeo River, opposite the town and the plain (Martín García et al. 1999) set apart from the foothills of the coastal Contraviesa Mountain range. As in the case of Poqueira, its elevation is inferior to that of the surrounding hills (Figure 40). It is identified by the medieval writer Al-‘Udri, as in the case of Poqueira, as the *hisn* of *Ardjuba* (Sánchez Martínez 1976), a *djuz* that endured as *ta’a* during the Nasrid period (Trillo San José 1990).

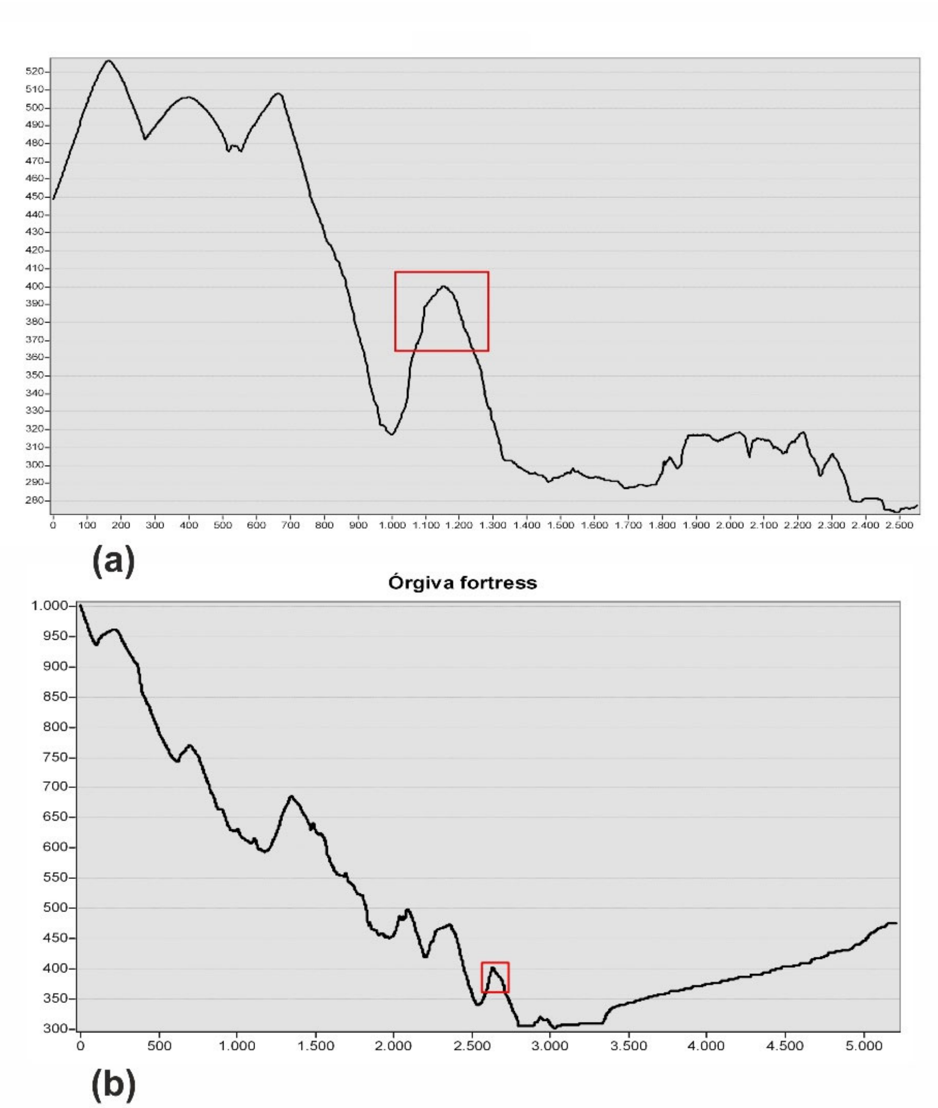

Figure 40: Órgiva. Topographic profiles of the promontory and its surroundings (a) E-W (b) N-S.

The fortress is on the upper platform of the promontory marked by a steep northward slope. The area was greatly altered by the construction of agricultural terraces almond orchards. This explains why the only remaining constructions are preserved in the upper sector to the south. Although polyorcetic logic dictates that the entire perimeter was walled, erosion and agricultural activities have left only two small walls in the lower sector (Figure 41).

The site's SW corner features a rectangular *calicostrado* tower or bulwark (12.8 x 6.3 m) enclosing a rectangular cistern (3.1 x 2.8 m) to the west. The northern wall has a maximum thickness of 2.5 m while the western wall is 2.7 m thick. The *calicostrado* rammed earth wall to the north reveals two footings of this material intended to support the structure's elevation which must have been considerable considering the thickness of the foundation and its walls. This structure saw a masonry and plaster addition in modern times of an eastern sector transforming it into farmhouse.

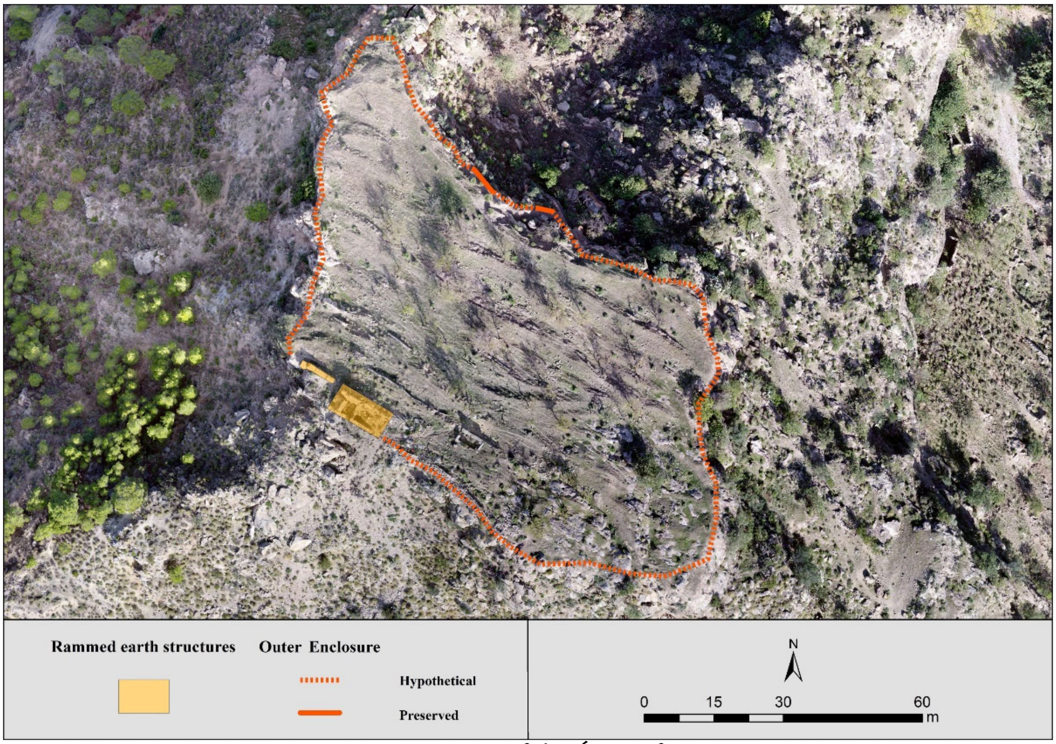

Figure 41: Structures of the Órgiva fortress.

To the west of the structure is another rammed earth *calicanto* feature preserved in the form of a wall 8.4 m long and 1.2 m wide along the cliffside. Its eastern extension is disturbed by the later *calicostrado* tower. Its poor state of preservation prevents interpreting whether it was part of an earlier enclosure or tower. The external face of a partially excavated lime concrete cistern located to the east of these structures is founded on a masonry base. The medieval structures of the promontory's upper sector were completed with what is now another poorly preserved wall raised with earth mortar under a contemporary terrace slightly to the north of the tower.

To complete the description of the structures of Órgiva is a defensive feature dating from the Spanish Civil War (1936-1939) made up of two parallel drystone walls, a parapet facing the town of Órgiva and a parados, a sort of rear parapet. This elevated "trench", occupied by the Loyalists in February 1937, assumed a key role after the fall of Málaga to Franco's Rebel forces as it became part of the front running through the Sierra Nevada that endured throughout the war (Alcalde Rodríguez, Ayala Carbonero, Cañadas Jiménez, Pérez Salguero and Ramos Lafuenta 2019: 49-96). Given the exposed bedrock, the structure was raised instead of excavated rendering it perfectly visible to the enemy. Its practically rectilinear layout marked only by a slight curve adapted to the form of the promontory also violated the basic fortification manuals of the time as it was bereft of a zigzag layout to absorb the detonation of a projectile. The dry stone technique using remains of tapial for this feature is indicative of the lack of means to fortify the promontory. The chips of stone produced by projectile impacts on the walls, devoid of mortar, also would have been a danger to the defenders. The *calicostrado* rammed earth tower also reveals an embrasure dug from side to side, from the wall of the cistern to the external face, a space that surely served as a machine gun nest. Traces of impacts on the N wall and the find of a Mauser .45 caliber casing suggest the site saw battle. In any case, the different elements point to a hasty occupation of the defensive position.

The occupation of Órgiva in medieval times, as in the case of Poqueira, is evidenced by Al-'Udri's geographical description (Cressier 1983; Sánchez Martínez 1976). The many potsherd finds, notably a piece of Late African Terra Sigillata, a fragment of Hayes 61 dating to the 5th century (Hayes 1972), suggest an extensive occupation from at least Late Antiquity (Trillo San José 1990) to Nasrid times (14th-15th centuries). The most important moment in the occupation, based on the percentage of potsherd fragments (in particular table ware) appears to range between the 12th and 15th centuries (Chisvert Jiménez and Amores Carredano 1993; Domínguez Bedmar et al. 1991; García Porras 1995, 2007; Melero García 2009; Navarro Palazón 1991). The wide variety of forms (storage, kitchen, table service), as well as a vast quantity of tiles and especially bricks, suggest the existence of a relatively stable settlement (Malpica Cuello 1996: 295-306). This hypothesis is further reinforced by the many fragments from this timeframe compared to the number collected in Poqueira.

3.2.1. The photogrammetric survey of the Fortress of Órgiva

The photogrammetric process applied to the site of Órgiva was identical to that of Poqueira, resorting to orthophotos of the walls extracted from the 3D model (9 million points) as the basis for an Archaeology of Architecture analysis. The high quality of both the morphological and textural elements of a photogrammetric model that can be currently attained is very useful even when interpreting and reinterpreting the stratigraphic relationships (relative chronology between the different SUs) (Harris 1989; Parenti 1988b, 1996).

The UAV flight at Órgiva was carried out with the same drone as that of Poqueira at a height of 50 m to assure the coverage. A GSD of 1.10 cm/pixel was applied to the upper sector (take-off) and 2.1 cm/pixel to the lower areas of the terrain. The speed of the UAV was set at 1.5 m/s. The aperture of the camera diaphragm was fixed at f/5.6 with an ISO 100 and an exposure time automatically fluctuating between 1/350s and 1/800s. This velocity is more than enough to assure that the displacements in the images are not significant (equivalent to 3 mm in terrain units). The total zenithal and oblique views (to record the lateral features of the structures) was 1120, a number requiring more processing time (Figure 42).

Survey Data

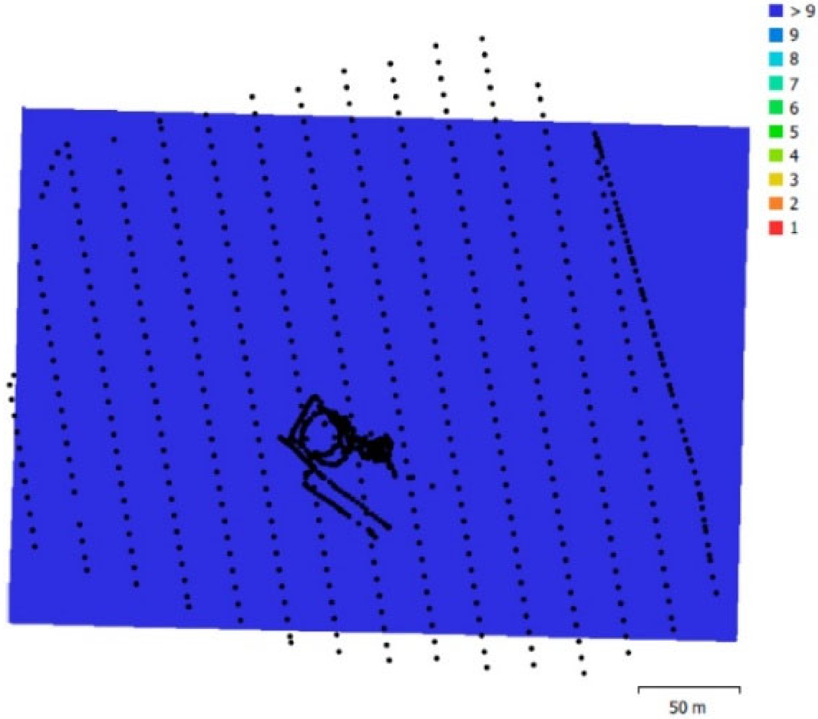

Fig. 1. Camera locations and image overlap.

Number of images:	1,120	Camera stations:	1,119
Flying altitude:	57.4 m	Tie points:	1,244,513
Ground resolution:	1.42 cm/pix	Projections:	6,214,654
Coverage area:	0.0908 km²	Reprojection error:	1.16 pix

Figure 42: Plan of the UAV flight over the Órgiva fortress indicating data as to the image capture and overlap.

As already noted, the calibration of the lens and the precise adjustment of the position and orientation of the cameras requires the correlation of the control points measured in the field with the targeted points registered on the images. An estimation of the error after adjusting the control points (Figure 43, Table 4) allows determining digital model's quality.[15]

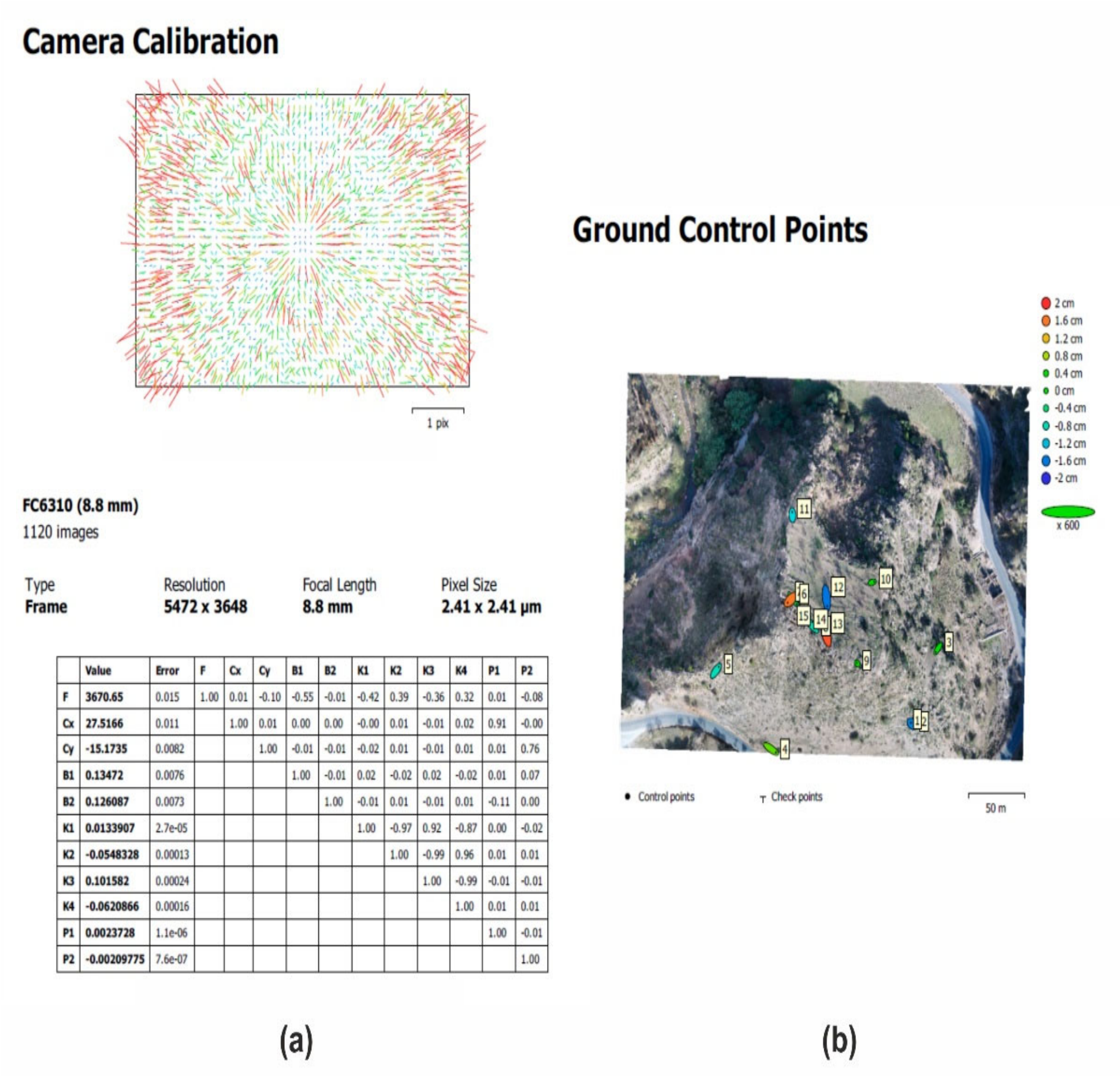

	Value	Error	F	Cx	Cy	B1	B2	K1	K2	K3	K4	P1	P2
F	3670.65	0.015	1.00	0.01	-0.10	-0.55	-0.01	-0.42	0.39	-0.36	0.32	0.01	-0.08
Cx	27.5166	0.011		1.00	0.01	0.00	0.00	-0.00	0.01	-0.01	0.02	0.91	-0.00
Cy	-15.1735	0.0082			1.00	-0.01	-0.01	-0.02	0.01	-0.01	0.01	0.01	0.76
B1	0.13472	0.0076				1.00	-0.01	0.02	-0.02	0.02	-0.02	0.01	0.07
B2	0.126087	0.0073					1.00	-0.01	0.01	-0.01	0.01	-0.11	0.00
K1	0.0133907	2.7e-05						1.00	-0.97	0.92	-0.87	0.00	-0.02
K2	-0.0548328	0.00013							1.00	-0.99	0.96	0.01	0.01
K3	0.101582	0.00024								1.00	-0.99	-0.01	-0.01
K4	-0.0620866	0.00016									1.00	0.01	0.01
P1	0.0023728	1.1e-06										1.00	-0.01
P2	-0.00209775	7.6e-07											1.00

Figure 43: Órgiva. (a) Calibration of the camera from the control points. (b) Location and estimated error of the control points.

[15] The processing report of the photogrammetric survey of Órgiva's fortress is available in http://hdl.handle.net/10481/62100.

Label	X error (cm)	Y error (cm)	Z error (cm)	Total (cm)	Image
2	-0.394	0.238	-1.528	1.595	0.149
3	-0.677	-0.795	0.081	1.047	0.140
5	0.864	0.901	-0.789	1.477	0.126
10	0.587	0.152	0.064	0.609	0.121
12	0.255	-1.816	-1.613	2.442	0.213
11	-0.054	0.694	-1.041	1.252	0.100
7	1.011	-1.027	-0.251	1.462	0.256
13	-0.584	1.719	1.786	2.547	0.171
4	1.490	-0.792	0.548	1.774	0.105
9	-0.146	0.132	0.225	0.299	0.073
6	-0.870	-0.659	1.596	1.934	0.256
8	-1.461	1.260	-0.737	2.065	0.213
Total	**0.830038**	**0.99916**	**1.05467**	**1.6732**	**0.166**

Table 4: Órgiva. Estimation of the errors after adjustments based on the control points.

The high graphic quality of the documents obtained at Órgiva has served for the paramental analysis of its structures, as well as for the study of the site itself and its relationship with its surrounding landscape. The use of orthophotos to record cultural heritage avoids the subjectivity of analyses and drawings of researchers. The images can also be reviewed or reused by other researchers to collate, discuss and even add new findings (Figures 44-45).

Figure 44: Analytical plan of the site of Órgiva superimposed on an orthophoto.

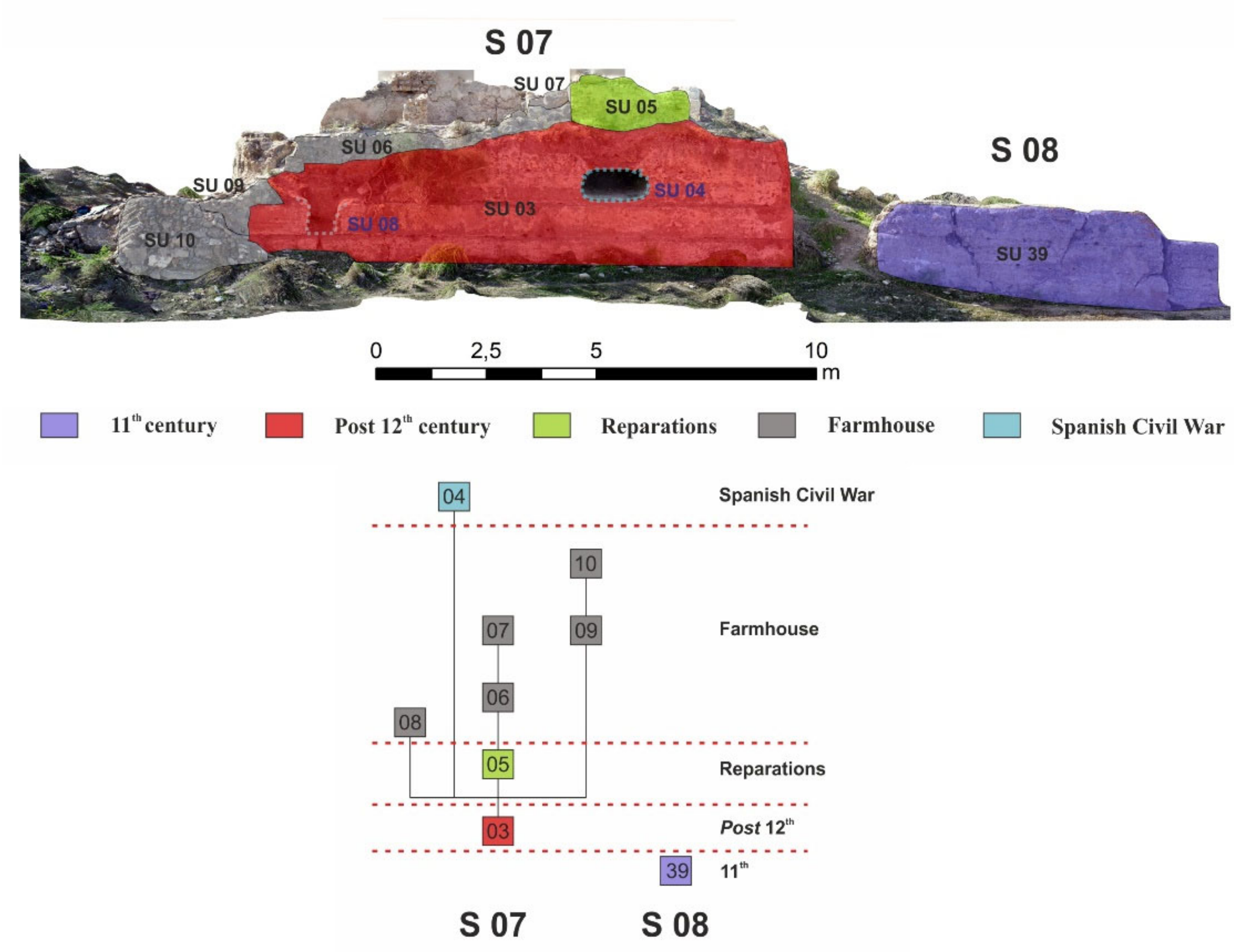

Figure 45: (a) Stratigraphic Units and (b) Harris matrix of the tower of Órgiva.

The decision from the outset was to carry out a DSM from photogrammetric data with a resolution of 0.05 m due to the high vegetation at the site consisting mainly of isolated almond trees throughout the different terraces that conceiled no structures. This also yielded a resolution higher than that obtained by LiDAR.

3.2.2. The LiDAR survey of Órgiva

As in the case of Poqueira, the LiDAR data for Órgiva was garnered from the IGN. The sweep totalled 25,372 points as this site's surface (0.086 km2) is slightly greater than that of Poqueira (0.047 km2). The procedure, also identical to that of Poqueira, consisted of reviewing all the points and classifying them manually in the event of error so as to subsequently create a DEM based exclusively on the Ground and Building classes.

Two different pixel resolutions (2 m and 0.5 m) were also applied serving as the base for the different visualisation techniques. The results were similar to that of Poqueira as the resolution of neither was sufficient to clearly observe any structure. This led to resorting to a DSM generated from photogrammetry. This method accompanied by an optimal resolution, by contrast, allowed observing the different structures.

The parapet and the parados from the Spanish Civil War are now much more visible as this technique makes it easier to identify the sections where these walls retain their full thickness, a task that is difficult in the field due to the many collapses. The different cultivation terraces and medieval structures are also much evident, in spite the considerable elevation of the few that remain (Figures 46-47).

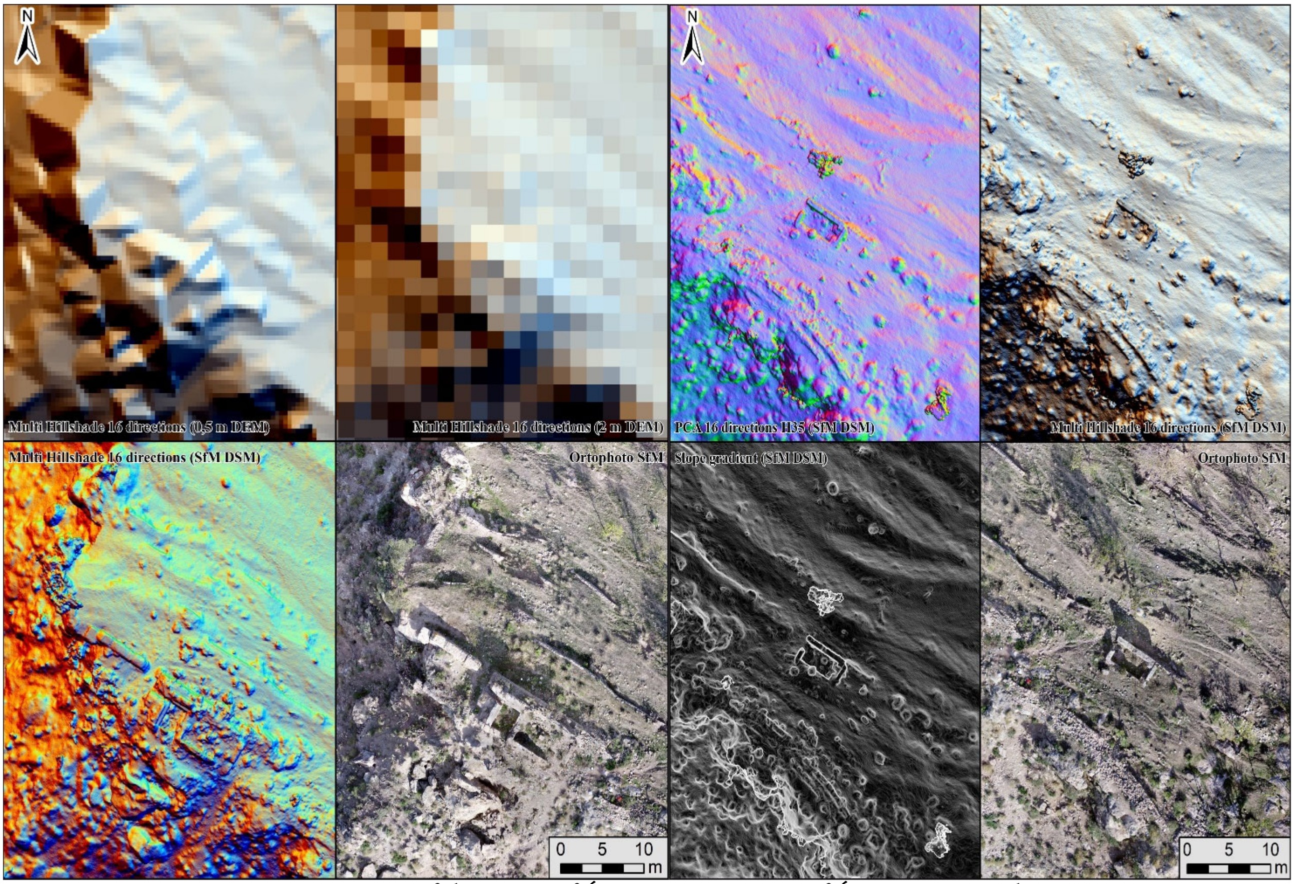

Figure 46-47: LiDAR views of the tower of Órgiva. LiDAR views of Órgiva's external cistern.

3.2.3. Reflectance Transformation Imaging (RTI)

The different digital methods were also applied to improve visualisation of a poorly preserved typical Andalusi incised herringbone decor on the plaster of the exterior of the northern wall of the cistern. As we were already in possession of the high resolution photogrammetric model combining views taken with the drone and photographs taken with a reflex camera, we applied virtual RTI to this feature, a procedure explained above (Maldonado Fernández and Rouco Collazo, in press; Maldonado Ruiz 2020: 139-170).

The feature was therefore extracted from the 3D model for a digital treatment with Blender with the different lighting points necessary to produce a RTI model. This yielded 106 renderings with different points of light on which a .ptm model was generated with the RTIBuilder software.[16] At this point the different interactive display modes of RTIViewer allowed a clear viewing of a incised motif common at the time comprising horizontal bands and parallel zigzag incisions (Márquez Bueno 2018) (Figures 48-50).

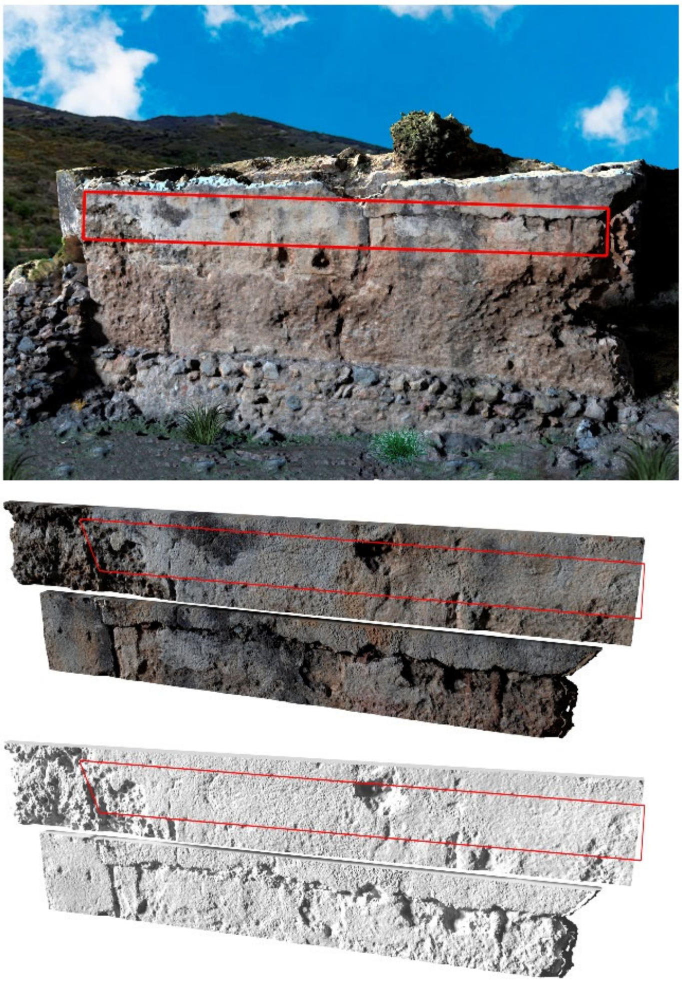

Figure 48: Órgiva cistern. Detail of the model and extract of the zone with the decor for Reflectance Transformation Imaging (RTI) processing.

[16] The RTI model of the cistern of Órgiva's fortress is available in (Maldonado Ruiz & Rouco Collazo, 2020) http://hdl.handle.net/10481/59188.

Figure 49: Digital view of the model with two metal balls serving for RTI hillshade processing.

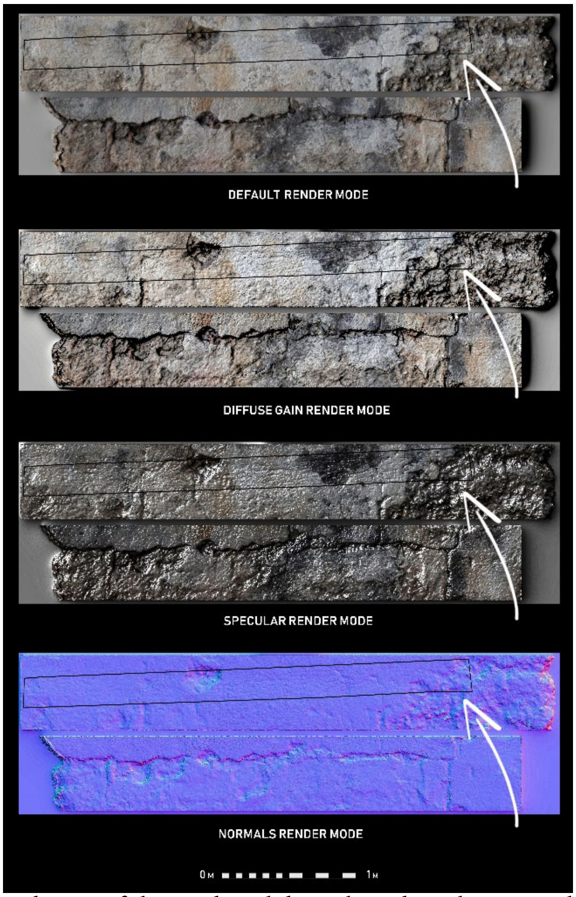

Figure 50: Rendering of the medieval decor based on the RTI technique.

3.2.4. 3D printing

A 3D printing was also carried out of the site of Órgiva based on the photogrammetric data. The intention was to verify the quality of the print and its suitability for the study of architectural heritage. The outer cistern and the *calicostrado* tower, the two features still standing, were selected for the printing.

The areas of each of these structures were extracted from the site's general model and their geometries determined with Blender as 3D printing only can be carried out with completely closed models. Cura lamination software was then used to determine the printing parameters and convert the model into a G-Code.[17] Printing was carried out with a layer resolution of 0.1 m. Although this resolution, the maximum accepted by the Ender 3 Pro PLA printer, lengthens the printing time, it maximises the quality (Figure 51).

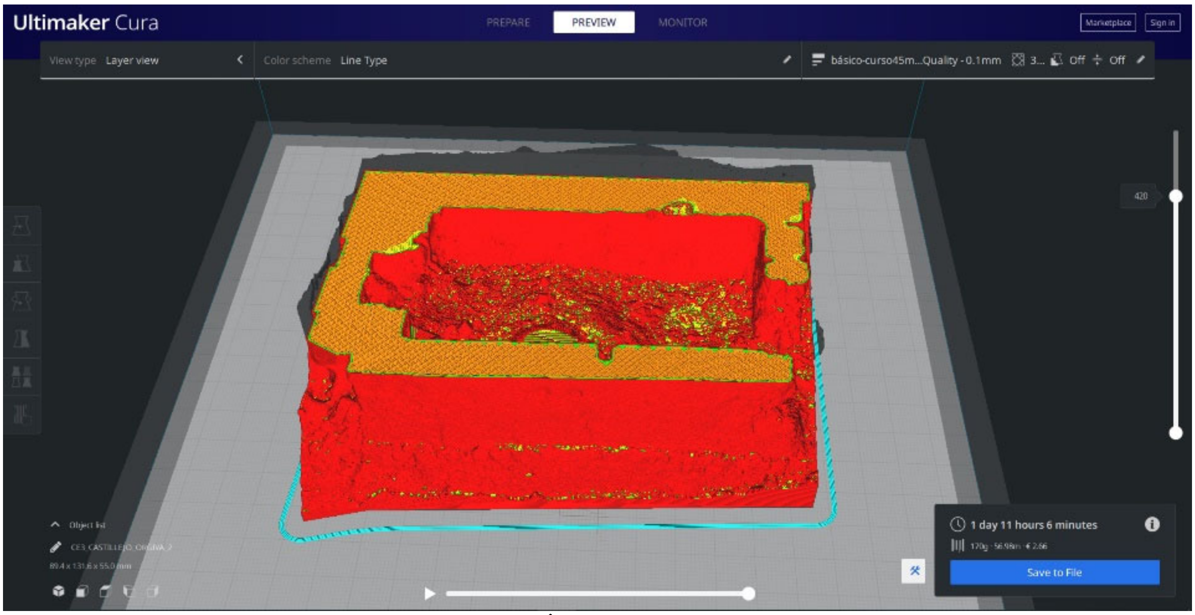

Figure 51: Lamination of the model of the Órgiva cistern for printing with Cura software.

In any case, the 3D printings of the tower and the cistern were more than satisfactory. All of their features in the larger-scaled print were perfectly visible and reveal all the details of their original geometry. 3D printings can therefore be of great utility both to disseminate information as they are faithful representations of features that can otherwise be very difficult to access. They are also valid for research as they offer a physical reproduction serving to contrast the observations in the field (Table 5, Figure 52).

[17] G-Codes of the two examples are available for download in http://hdl.handle.net/10481/62100.

	Órgiva cistern	**Órgiva tower**
Layer height	0.1 mm	0.15 mm
Initial layer height	0.2 mm	0.2 mm
Wall thickness	0. 8 mm	0. 8 mm
Top thickness	0.8	0. 8 mm
Bottom thickness	0. 8 mm	0. 8 mm
Layer nº	542	293
Infill density	30%	40%
Infill patern	zigzag	triangles
Printing temperature	205 ºC	205 ºC
Build Plate Temperature	60 ºC	60 ºC
Retraction distance	6 mm	5 mm
Retraction speed	40 mm/s	40 mm/s
Print Speed	45 mm/s	50 mm/s
Travel Speed	100 mm/s	110 mm/s
PLA used	170 g / 56.85 m	68 g / 22.8 m
Printing hours	35 h 6 min	6 h 59 min

Table 5: Parameters for the 3D printing (PLA) of the cistern and tower of Órgiva.

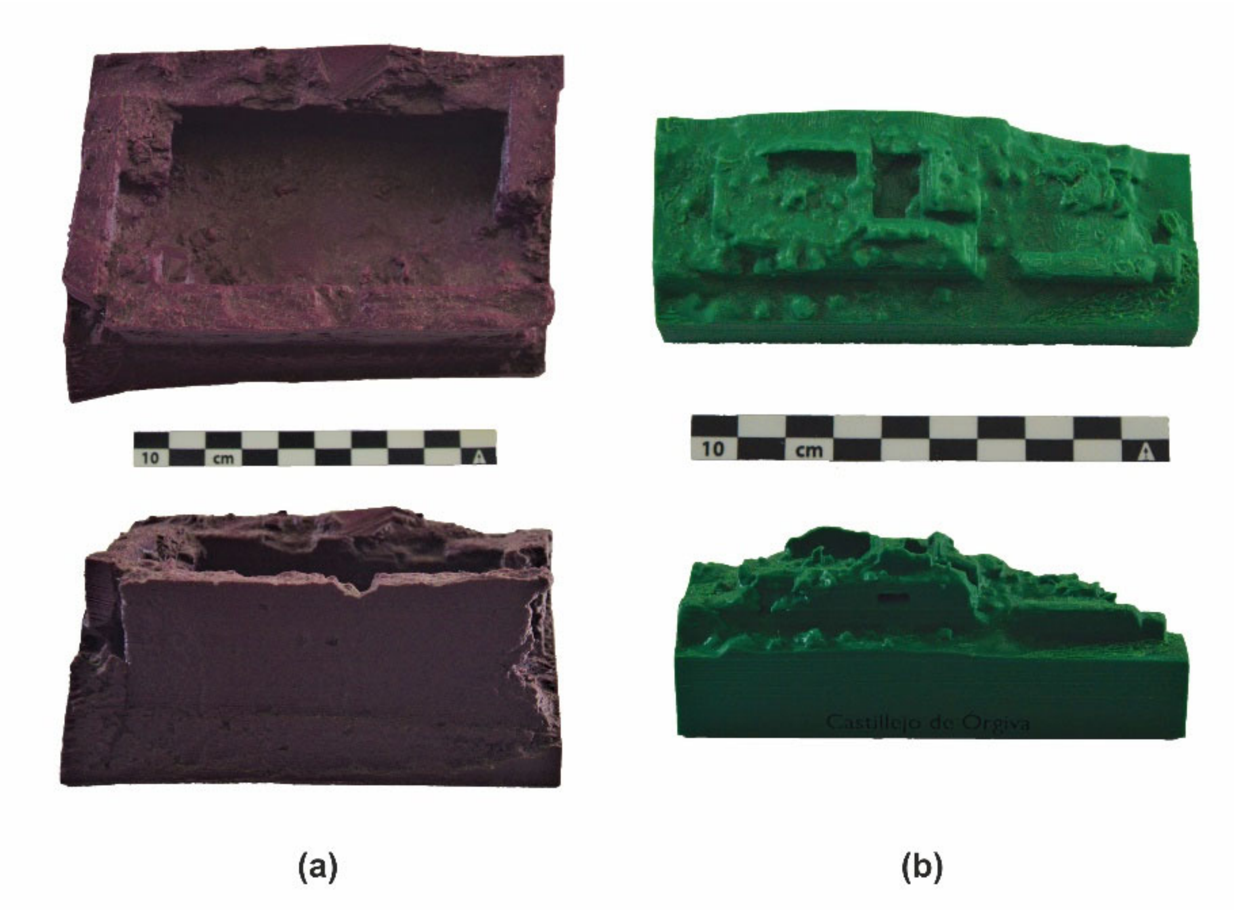

Figure 52: Views of the PLA 3D prints of (a) Órgiva's external cistern and (b) tower.

3.3. The territory

The research following the recording of the features of the two fortresses was geared toward a territorial analysis so as to truly delve into the question of the function and role of each site in its territory. This led to a series of spatial analyses within the framework of the methodology of Landscape Archaeology, a discipline that has progressively grown in recent years incorporating new technologies (Brogiolo, Angelucci, Colecchia and Remondino 2012). Although we have already noted that the discipline includes numerous applications, the current research focuses on visual analyses of both the site's surrounding basins and the question of intervisibility of the fortresses.

The first step necessary to carry out this analysis was to create a MDT for a territory corresponding to a surface of 320 km2 stretching from the Sierra de la Contraviesa to the peaks of Sierra Nevada. With the aim of establishing a comparison between the two methods, a DEM05 was generated by IGN with a precision of 5 meters per pixel. As in the case of the LiDAR flights, this is the maximum precision available for southern Spain although there already exist MDTs of certain regions with a precision of 2 m. Also, LiDAR from IGN data served this study to create the more accurate DEM02. This was done by automatically filtering the points and retaining exclusively those of the Ground class due to the vast extension of the study area which was not possible to review manually. A MDT for the entire territory surrounding the fortresses was then generated after a filtering with an accuracy of 2 m, more than enough to calculate the visibility of an area of this size.

After creating the territorial base, the study then turned to calculating the visibility basins of each fortification by means of the DEMs 02 and 05 m obtained from the LiDAR and the IGN. The heights of their respective towers served for this calculation. The value adopted for the height, based on studies of better preserved Andalusi towers, was 12 m (Malpica Cuello 1996: 80; Martín García 2000; Pedregosa Megías 2011). This value yields a view corresponding to a maximum distance of 30 km taking into account the refractive index of 0.13 for the curvature of the earth (Figure 53).

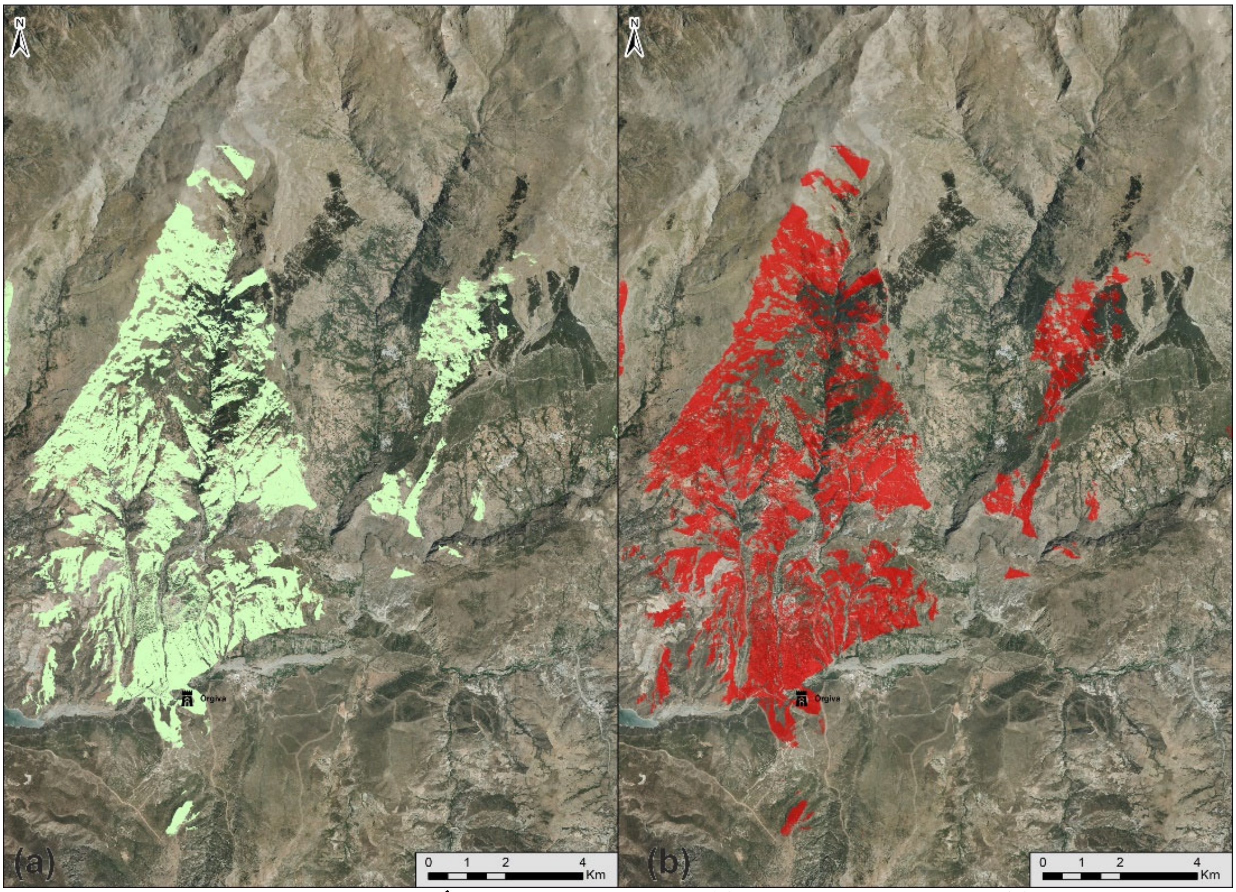

Figure 53: Visual basins of the Órgiva fortress based on (a) a MDT 05 from IGN and (b) a LiDAR.

The differences between the results of the two at first glance appear to be minimal. A computation of the percentage of agreement between the two results indicates that the visibility of Poqueira from the LiDAR and that generated from the MDT05 concur at 91.46% with a divergence of almost 10%. The difference is greater for Órgiva (84.81%). This indicates that LiDAR data for these macro scales yield a significantly higher resolution.

Taking into account that the fortifications were surely contemporary (10th-12th centuries, and possibly until the outset of the 14th century) this study embarked on an intervisibility analysis of each of the fortresses which resulted to be negative (Figures 54-55). Due to their lack of visual communication, the study then shifted optics toward calculating a joint visual basin to determine the points of the territory visible from each of fortresses (Figure 56). This is compelling because if the two formed part of a coordinated defence, one would expect to identify a watchtower or beacon serving to communicate between them at the intersection of their lines of visibility.

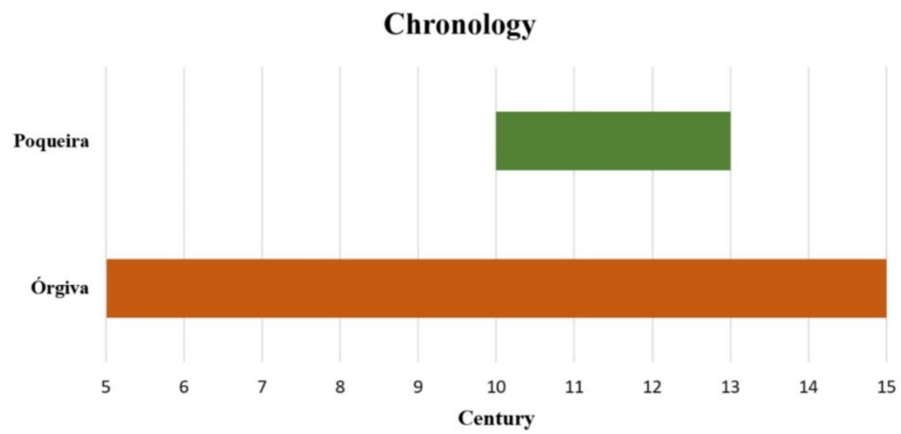

Figure 54: Chronology of the fortresses of Órgiva and Poqueira.

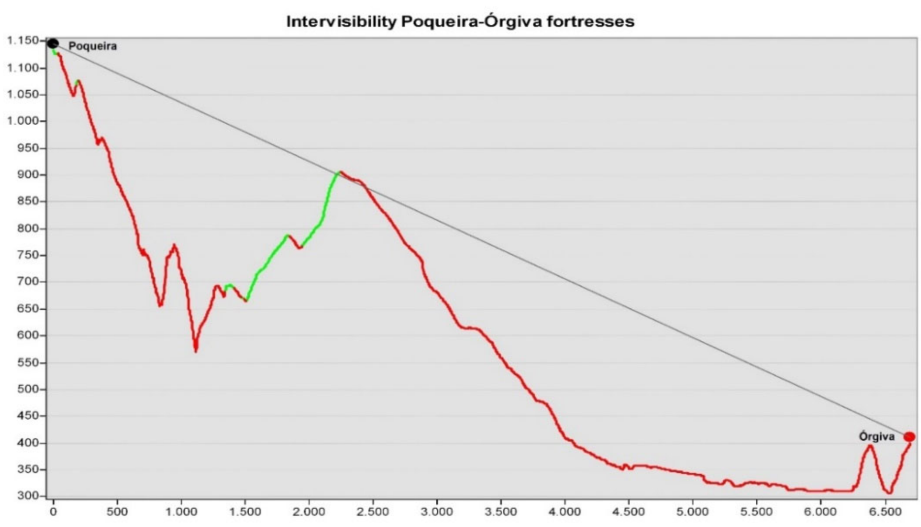

Figure 55: Graph indicating the intervisibility of the fortresses of Órgiva and Poqueira.

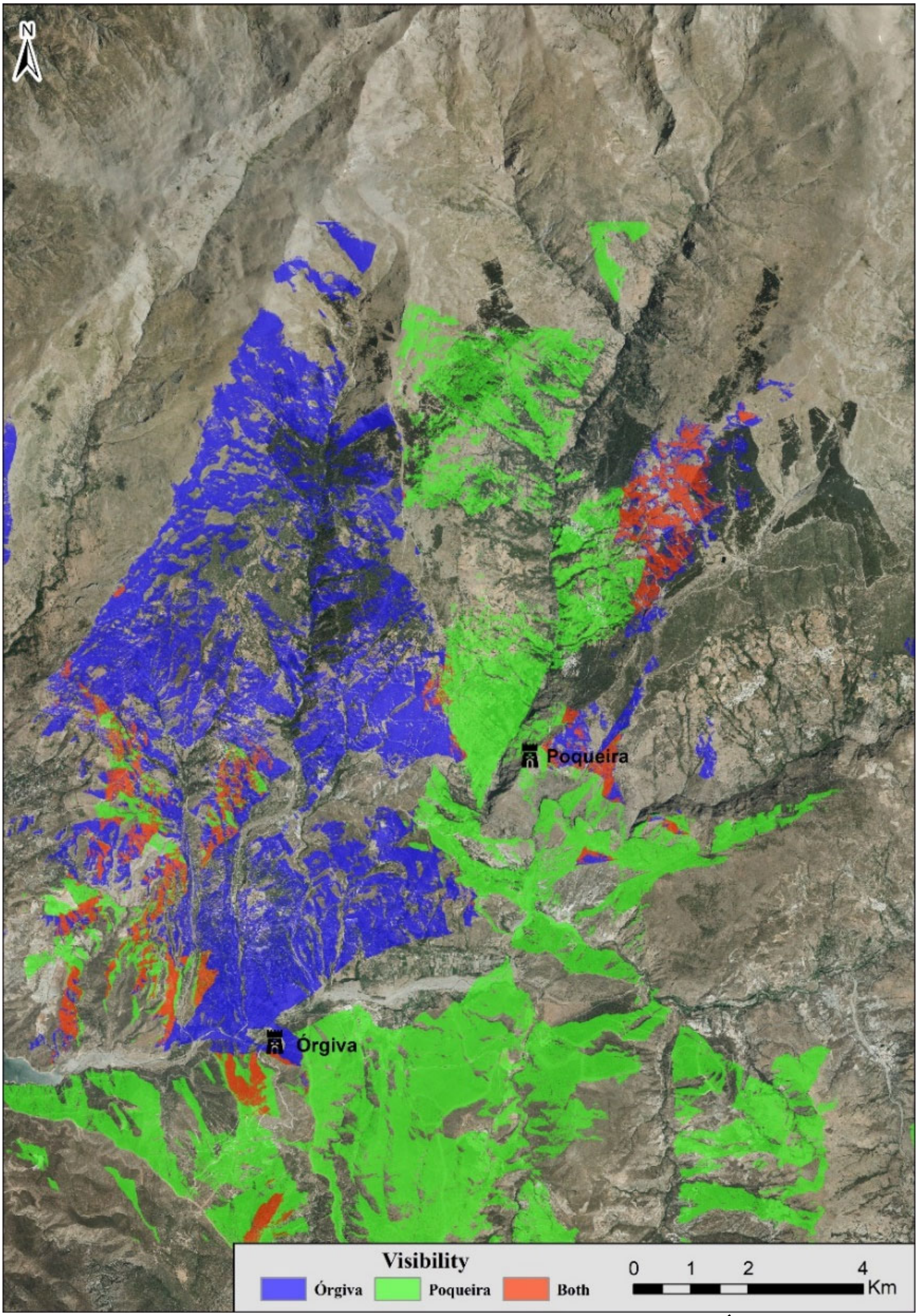

Figure 56: Plan indicating the cumulative visual basins of the fortresses of Órgiva and Poqueira.

This analysis identified two points of interest (Figure 57). The first is Cerro Negro, northeast of the Municipality of Órgiva near an old hamlet called Tíjola, that impedes a direct view between the two fortresses. The second is the Cerro de la Atalaya de Soportújar to the north of Órgiva and to the west of Poqueira. It is set on the opposite side of the homonymous ravine and is of great interest due to its toponym. An inspection carried out of each of the two points based on LiDAR tools to identify the remains of a structure serving as watchtower or beacon was nonetheless negative. The only anthropic features identified at Cerro Negro are a few forest paths, whereas at the Atalaya de Soportújar (a place name associated with a watchtower) the only structures are a Buddhist monastery and a facility linked to agriculture. Nor did the fieldwork yield positive results (Sánchez García 2018) (Figures 58-59). However, given the "Atalaya" toponym, it cannot be ruled out that the second hill could have served as an observation point in times of danger, without the need to raise a permanent structure such as a watchtower.

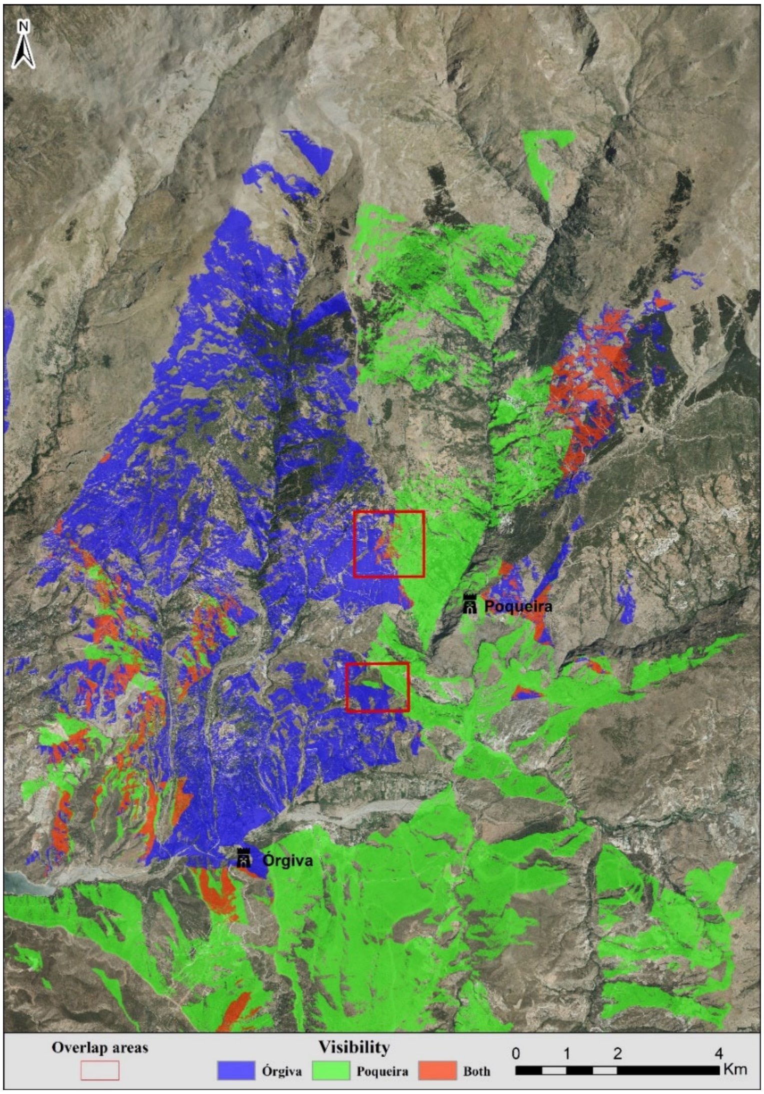

Figure 57: Plan indicating the areas of intervisibility of the visual basins of the fortresses of Órgiva and Poqueira.

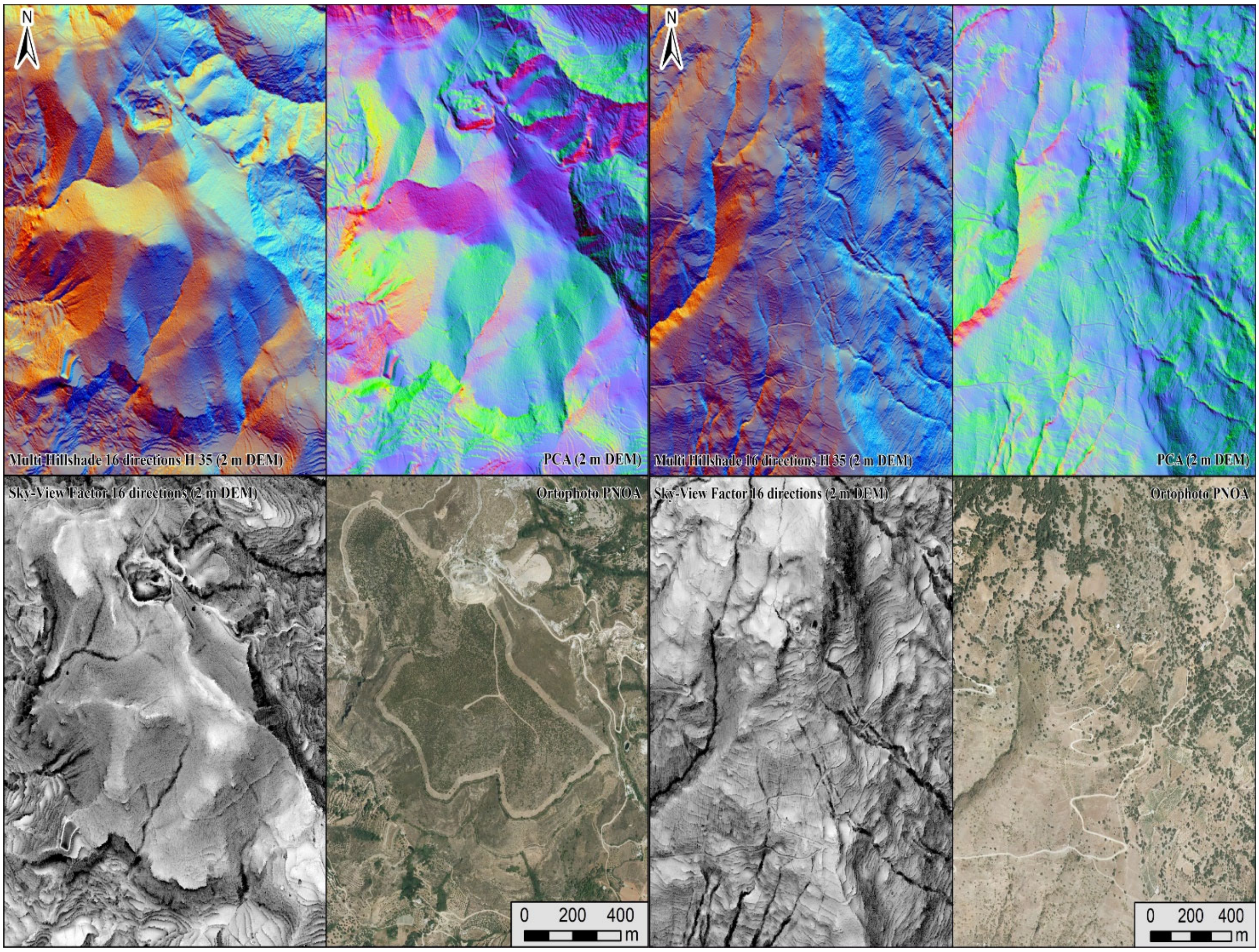

Figure 58-59: LiDAR views of the site of Cerro Negro. LiDAR views of the site of Cerro de la Atalaya.

The results of the visibility analysis are nonetheless conclusive. Each fortification was in a position to maintain a visual control over its district (first *djuz*, then *ta'a*), which corresponds for the most part to a specific geographic space (Figure 60). Thus, the feature of Órgiva had a visual contact of the population and the plain, including most of the villages as well as those along the foothills of the Sierra Nevada. Poqueira likewise has a direct view of both the villages in the valley (Capileira, Bubión and Pampaneira), as well as those that have since disappeared (Alguástar, Beni Odmin) (Trillo San José 1991; Sánchez García 2018). This has interesting implications as to the role of these fortifications in the territory, with respect to the State itself and their peasant communities, strategies and relationships. Yet these notions are beyond the scope of this study.

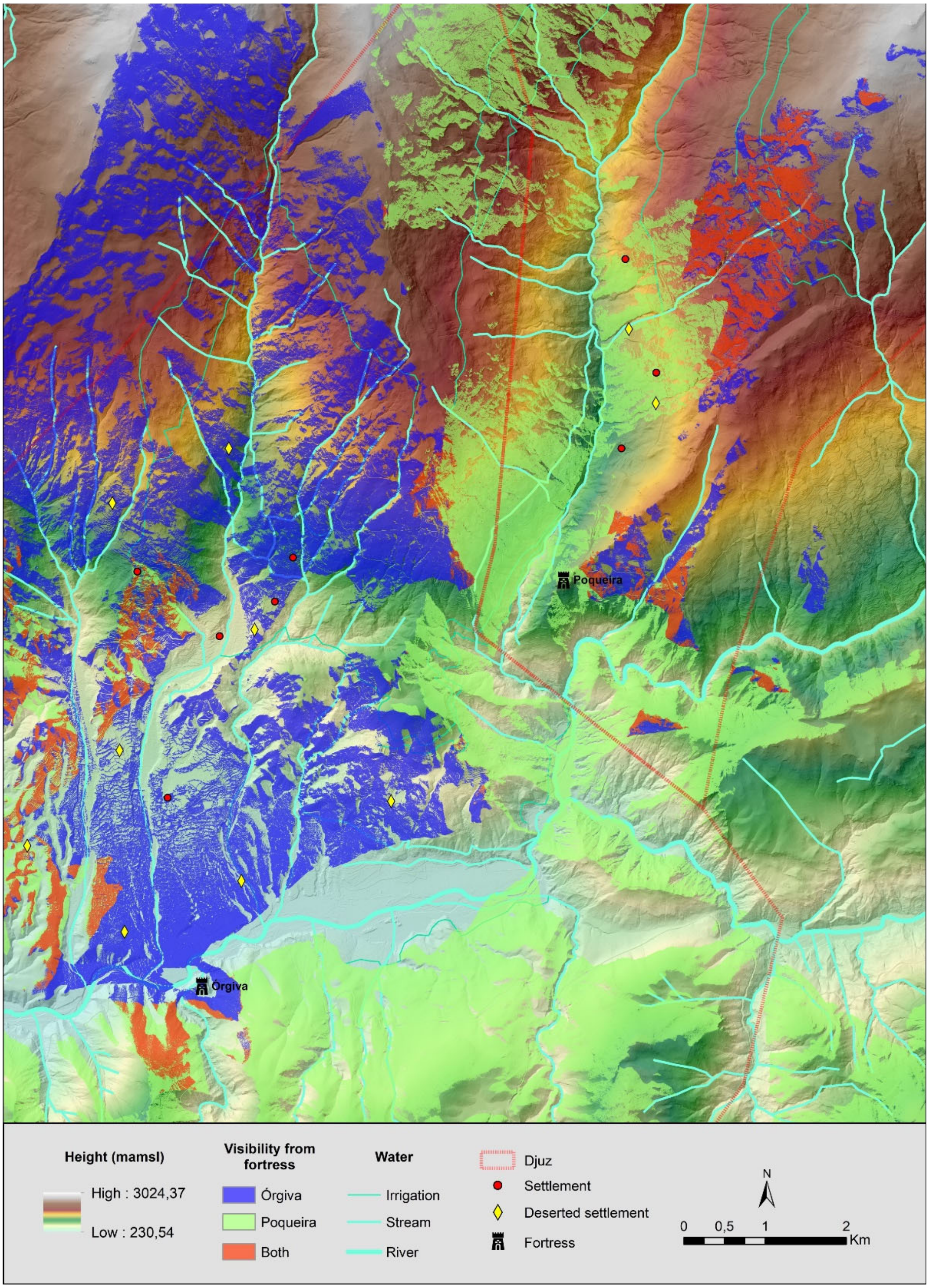

Figure 60: Plan of the visual basins of the fortifications of Órgiva and Poqueira and the theoretical limit (red line) between their respective *adjza* (districts).

LiDAR does not only allow generating a DEM serving as the base for observations. As in these specific cases of Órgiva and Poqueira, the DEM with a resolution of 2 m served to apply the algorithms for visualisation. In this case, as the scale is much larger, the precision is sufficient to identify structures. It is nonetheless useful to identify the terraces that with the systems of irrigation of Andalusi origin formed the base of the traditional agricultural economy in the Alpujarra Mountains. These features, in fact, represent the greatest anthropic transformation of the high mountain landscape of the Sierra Nevada (Martín Civantos 2012, 2015; Martos-Rosillo et al. 2019). These algorithms allow a much more precise view of the sector, especially compared to aerial photographs where each plot, often having more than one terrace, must usually be interpreted according to the types of crops and seasonal rhythms. This difference can be clearly observed both in the flat terrains such as the Plain of Órgiva, and in the steep Poqueira ravine (Figures 61-62).

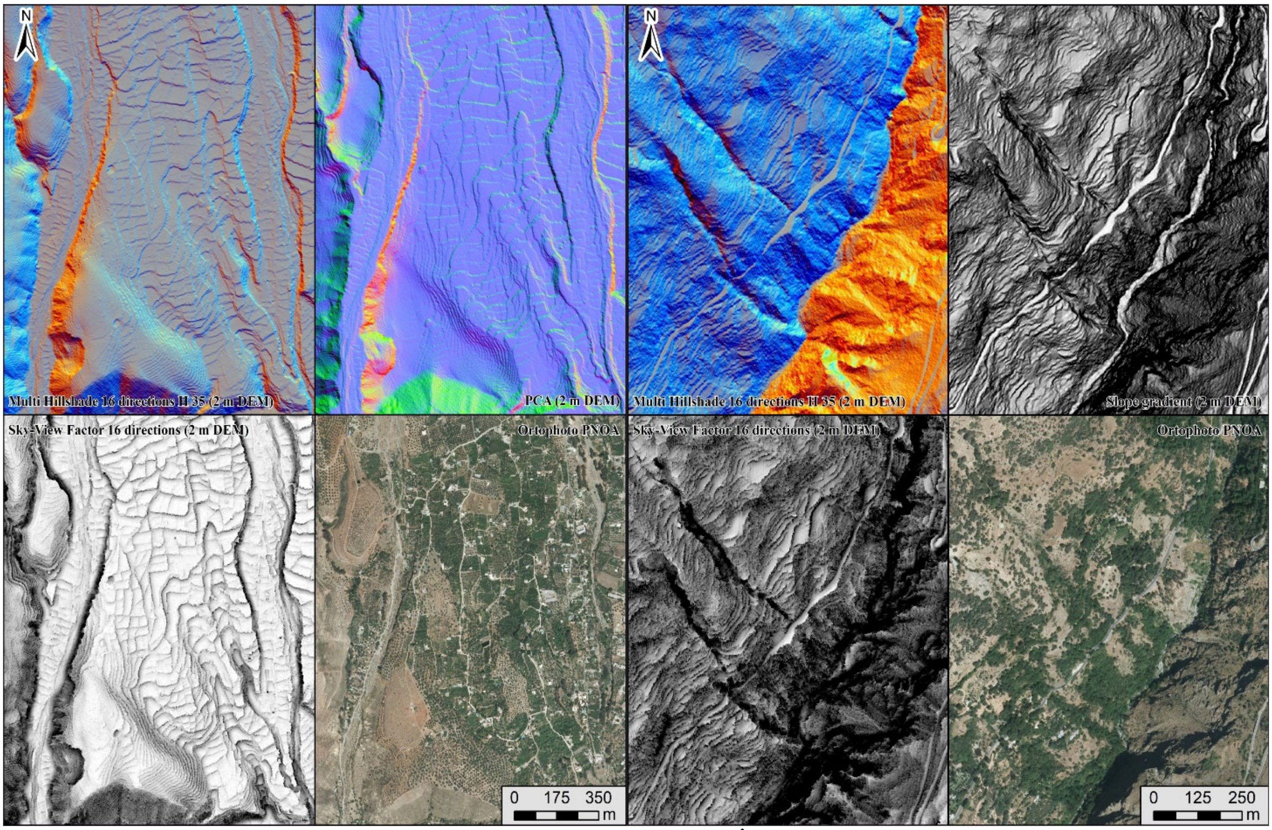

Figure 61-62: LiDAR views of the cultivated terraces of the Plain of Órgiva. LiDAR views of the cultivated terraces of the Poqueira Ravine.

4. Discussion

Manual drawing until recently has been the main method to record archaeological remains. The introduction of new technologies, nonetheless, has improved data collection and their subsequent representation. The traditional method of recording archaeological features by floor plans, elevations and sections without a physical or digital support that guarantees the goodness of information means that these documents often must, at least, be questioned. Traditional drawings not only contain measurement errors but can suffer from subjectivity and oversights. New drawing technologies are not affected by these problems and are more reliable as they always leave a record of the intervention apart from the depiction, description and measurement of the different variables (size, shape, volumes, distance, etc.).

Active remote sensing (LiDAR) and passive methods (photogrammetry) are clear improvements to the discipline of Architecture and Landscape Archaeology. They also lead to being able to work with more complex and global views combining scales and integrating architecture into its territorial context and vice versa. It is possible, subsequent to their application to the case studies of the fortresses of Órgiva and its fertile plain and Poqueira and its ravine, to observe differences in their use and relevance along three fundamental lines: spatial precision, coverage and cost.

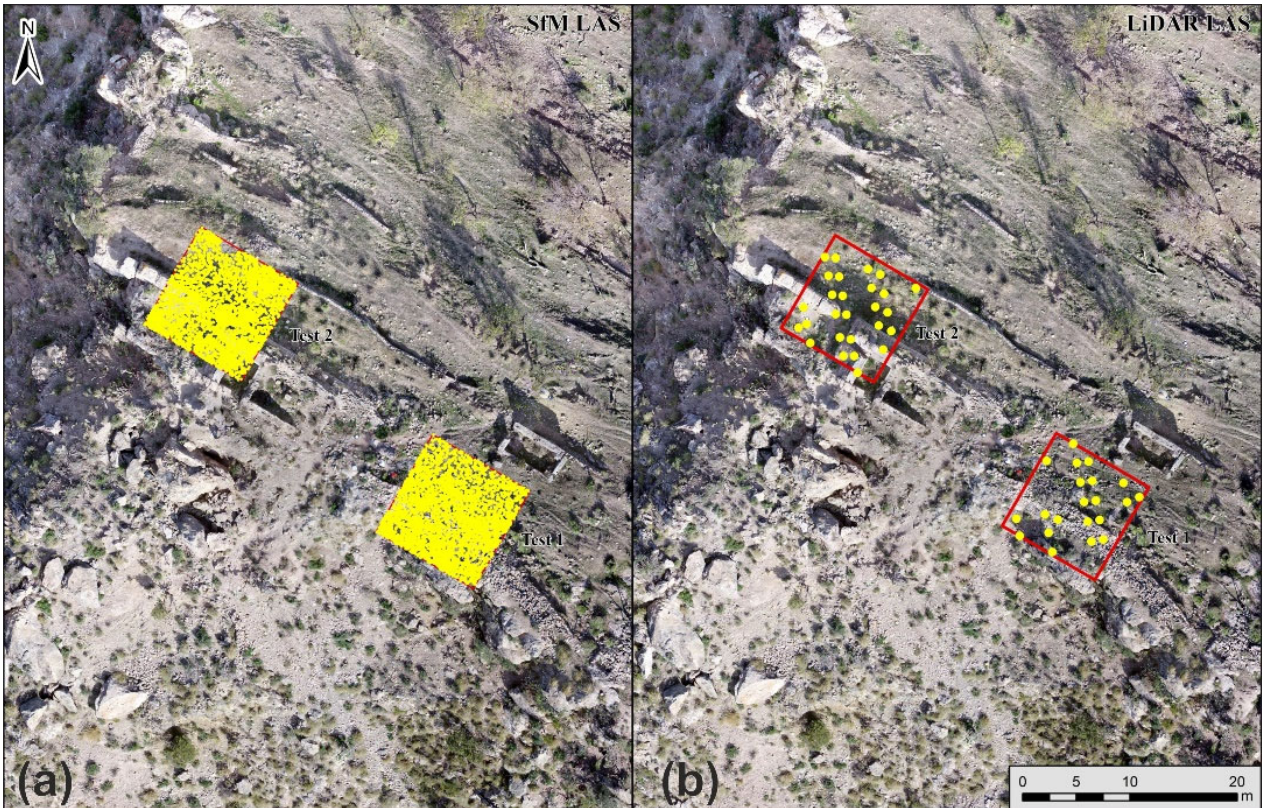

Figure 63: Órgiva. Tests of the (a) point cloud of the photogrammetric model and (b) of the LiDAR point cloud.

Applying one scale or another can lead to fundamental differences since the precision between techniques varies when carrying out a recording for a microspatial analysis. Thus, the difference between a point cloud extracted from photogrammetry and that from LiDAR is considerable as the precision of the LiDAR available for the region of the fortresses is only an average of 0.5 points per m2. To measure these differences, we selected two quadrangular test areas (10 by 10 m) from each site that include both structures and abrupt and flat areas. The findings point to a considerable difference between the coverage extracted from the SfM photogrammetric model point cloud with that from the LiDAR (Figures 63-64, Table 6). Thus, the SfM clouds generated with only a medium quality have a range of 2000 to 3000 times more points than LiDAR. This translates into a much greater spatial precision for the photogrammetry with a 0.03 to 0.05 m distance between points compared to a minimum distance of 2.1 m of better LiDAR test. This difference in density explains the disparate resolutions obtained when generating DEMs and DSMs from point clouds. The DEM gleaned from LiDAR for Órgiva, with two different resolutions of pixel size (2 m and 0.5 m), contrary to that obtained from photogrammetry, does not clearly depict the features at a microspatial scale.

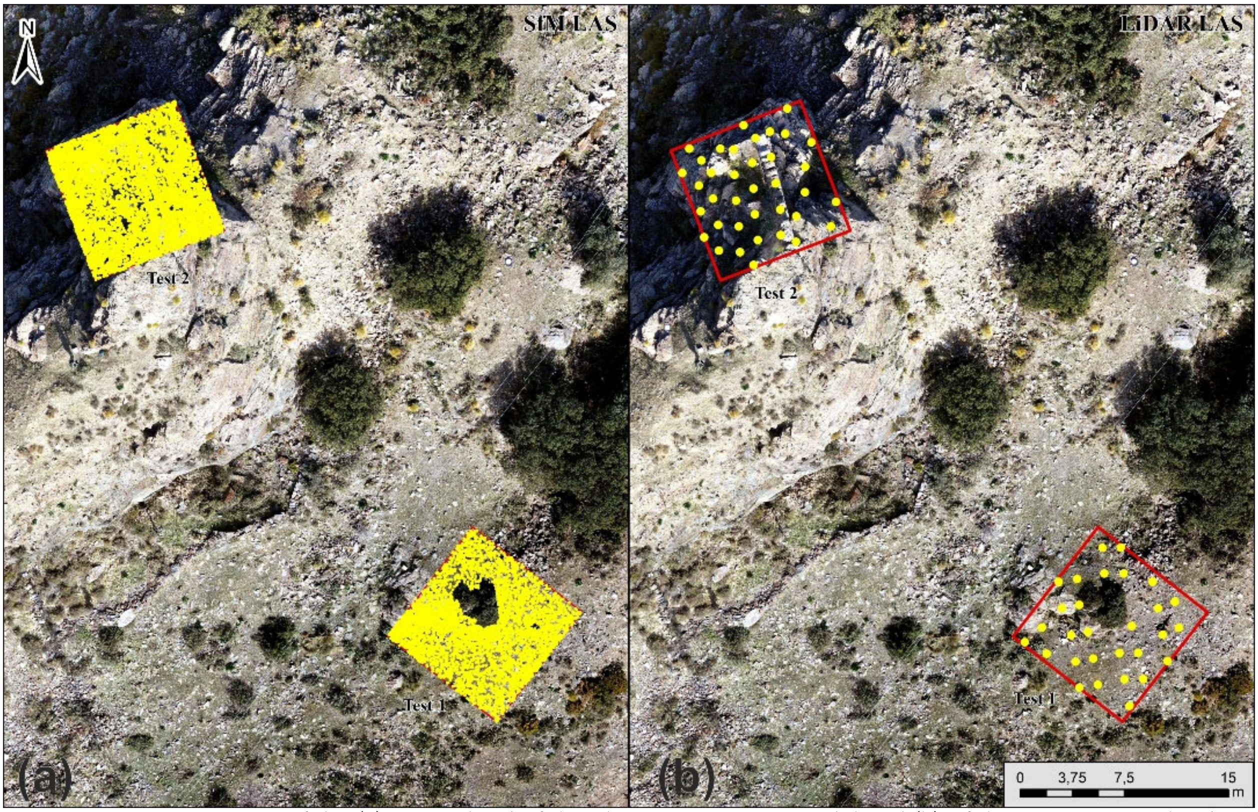

Figure 64: Poqueira. Tests of the (a) point cloud of the photogrammetric model and (b) of the LiDAR point cloud.

			SfM LAS		Lidar LAS	
		Area (m^2)	Point Count	Point Spacing (m)	Point Count	Point Spacing (m)
Poqueira	Test_1	100	138013	0,035	37	2,168
	Test_2	100	59368	0,056	29	2,384
Órgiva	Test_1	100	59150	0,056	21	2,619
	Test_2	100	64338	0,054	27	2,489

Table 6: Poqueira and Órgiva. Comparison of the values of the SfM photogrammetry and LiDAR point clouds from four 100 m^2 test areas (two from each site).

Apart from the horizontal resolution of both sets of data, this study also compared the height above sea level of the three DEMs. The first was generated from photogrammetry while the second was created with a resolution of 2 m from a manually classified LiDAR survey. The third was based on a 5 m DEM gleaned from the IGN. The verification of the heights of different points of each fortress (Figures 65-66 and Table 7) reveals that the precision of the DEM obtained from photogrammetry and LiDAR is much higher, with a difference of up to 2 metres, than that gleaned from the 5 m DEM. The margin between the photogrammetry and LiDAR tests is narrower, for the most part less than 1 m, which is a more acceptable margin of error in archaeology. It is interesting to observe, however, that the difference is greater among the points of structures (Point 1 of Órgiva, 7 of Poqueira), increasing to more than 1 m. Therefore, as observed when commenting on the automatic classification of LiDAR points, in both cases it appears that the precision of the LiDAR is not high enough to clearly detect the structures, at least those with rammed earth walls. But it is possible to conclude that both have a higher level of precision than the DEM 05 gleaned from the IGN.

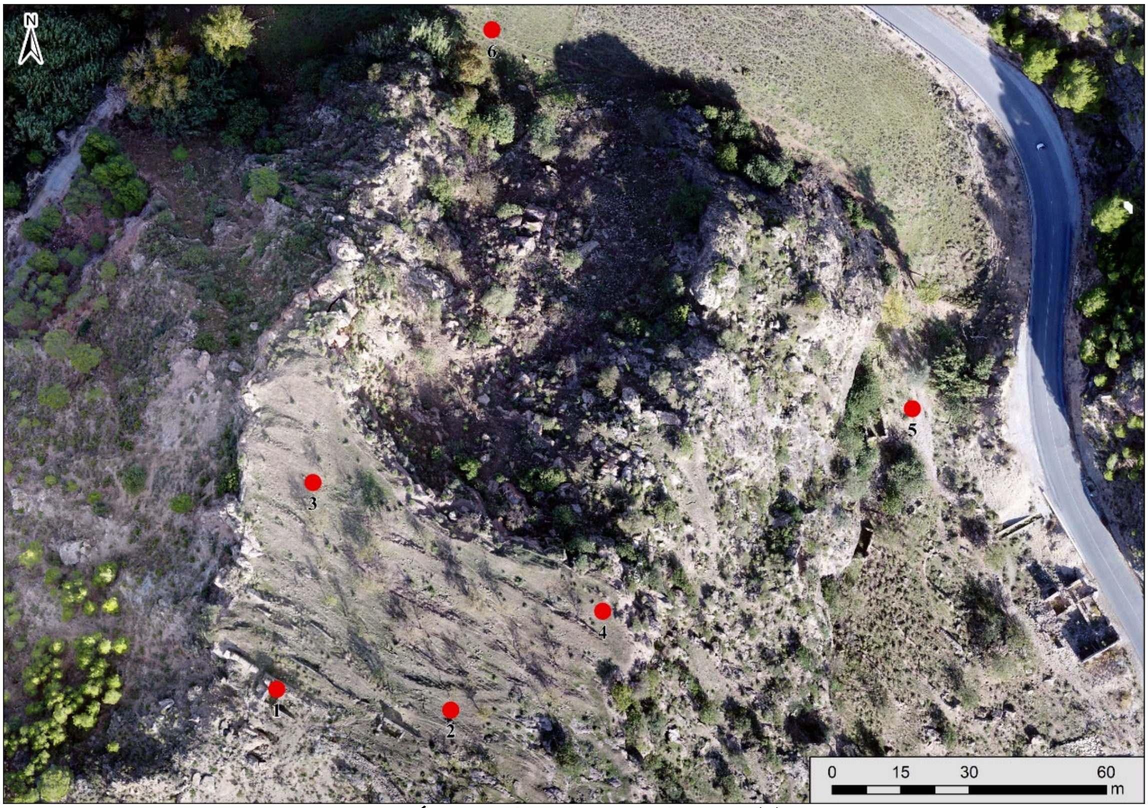

Figure 65: Órgiva. Altitude control points (Z).

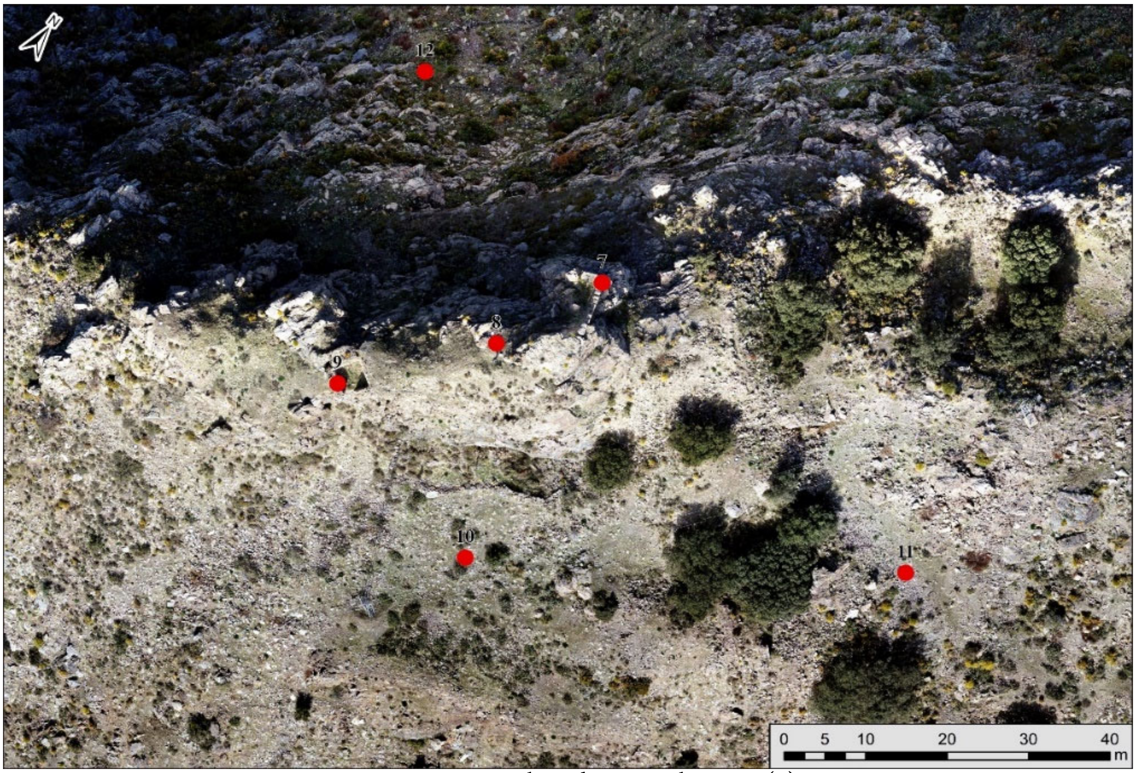

Figure 66: Poqueira. Altitude control points (Z).

Órgiva (z in m)			
Point	DEM SfM (0,05 m)	DEM LiDAR (2 m)	DEM IGN (5 m)
1	403,36706543	401,563018799	401
2	392,979522705	392,736022949	394
3	380,960754395	380,327026367	382
4	379,587554932	379,445007324	378
5	308,429931641	308,480010986	309
6	305,03604126	305,492004395	306
Poqueira (z in m)			
7	1135,9876709	1134,10107422	1129
8	1133,72668457	1133,51806641	1134
9	1127,09387207	1126,36206055	1125
10	1112,68457031	1112,4910887	1112
11	1114,77758789	1115,125	1115
12	1083,44677734	1082,93408203	1082

Table 7: Comparison of altitudes above sea level of the sites of Órgiva and Poqueira from the SfM model, the DEM extracted from LiDAR and the DEM 05 provided by the IGN.

The advantage of the LiDAR point cloud over that of photogrammetry is that it is already classified by the institution that created it. However, as noted, automatic classification at the microscale is often erroneous and does not lead to detecting all the structures. This requires it to be classified or photointerpreted manually although this is only really reliable when using the nadiral orthophotos of a photogrammetric flight due to the lack of resolution of the orthophotos supplied by the IGN (Figures 67-69). For its part, the SfM dense point cloud can also be classified, as noted, to eliminate the vegetation either automatically or by algorithm filters. They can also be classified manually, although the large number of points complicates the process. Furthermore, as verified in the examples with larger scales at the territory level, the LiDAR data are in fact useful in detecting anomalies and larger anthropogenic structures. It must also be borne in mind, however, that despite the greater precision of this technique, it is essential to verify the results by fieldwork (Horn III and Ford 2019; Romero Pellitero, Delgado Anés and Martín Civantos 2020).

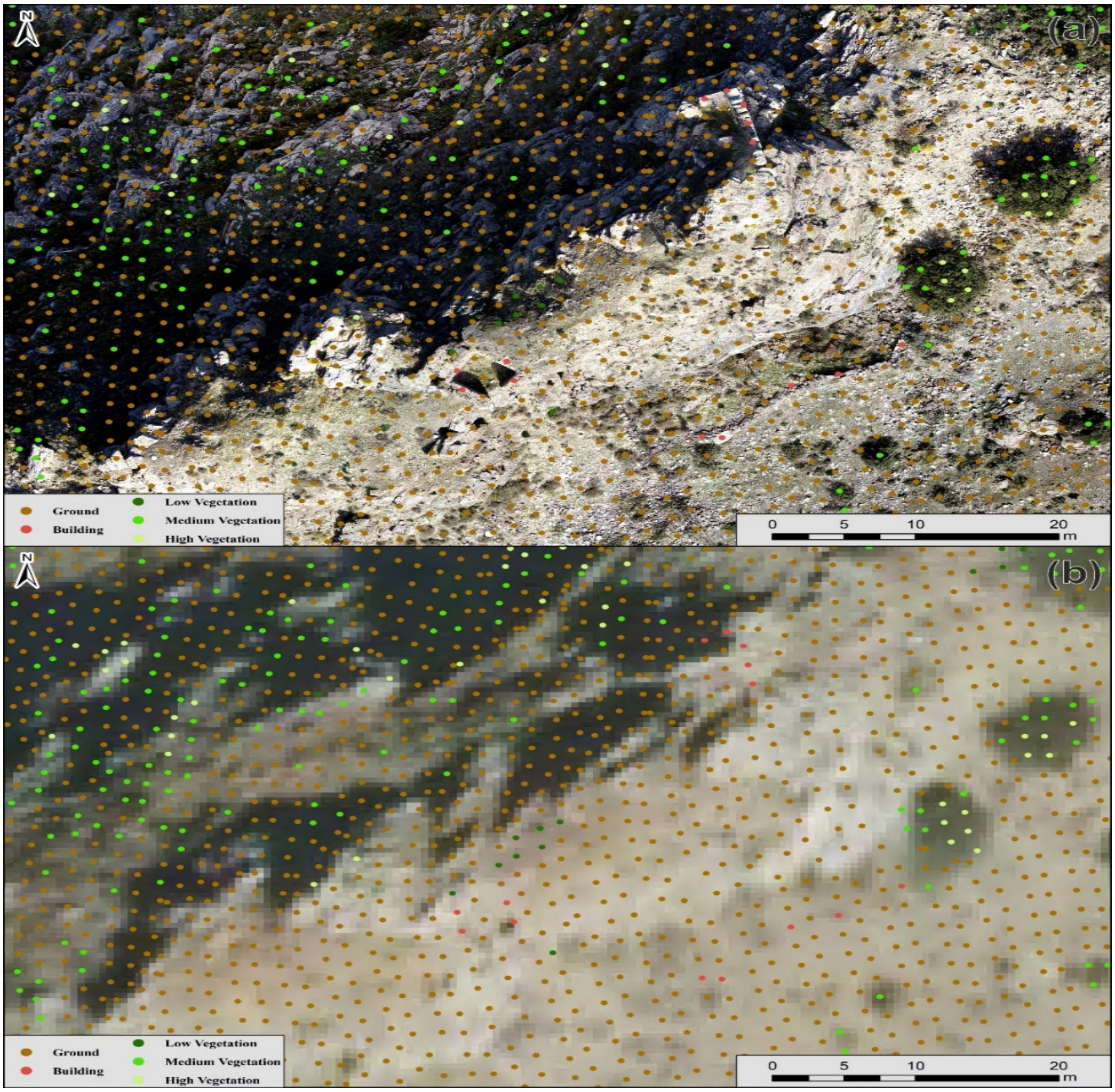

Figure 67: Upper enclosure of Poqueira. (a) LiDAR points superimposed on an orthophoto of the SfM model (b) LiDAR points superimposed on a PNOA orthophoto (IGN).

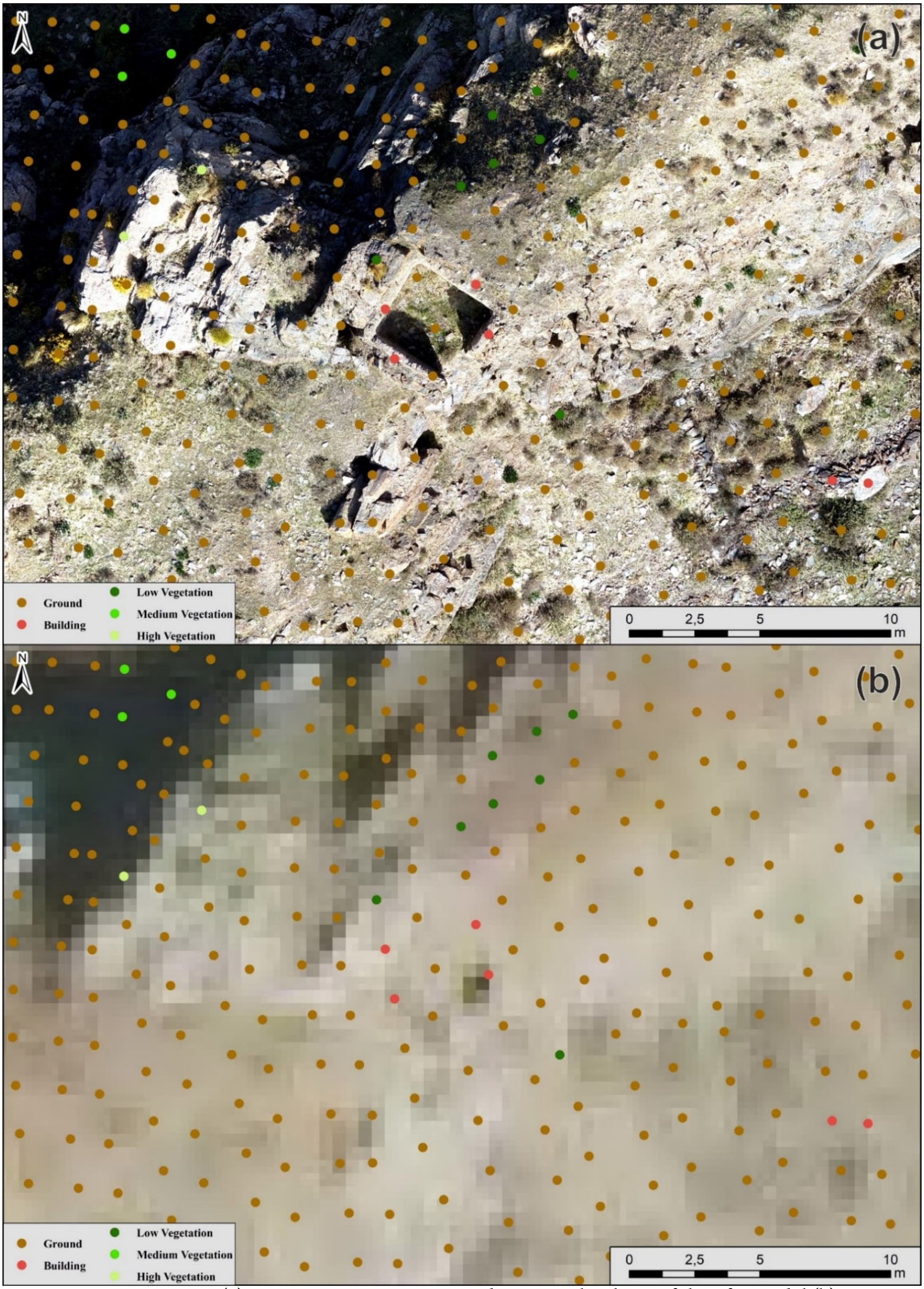

Figure 68: Poqueira cistern. (a) LiDAR points superimposed on an orthophoto of the SfM model (b) LiDAR points superimposed on a PNOA orthophoto (IGN).

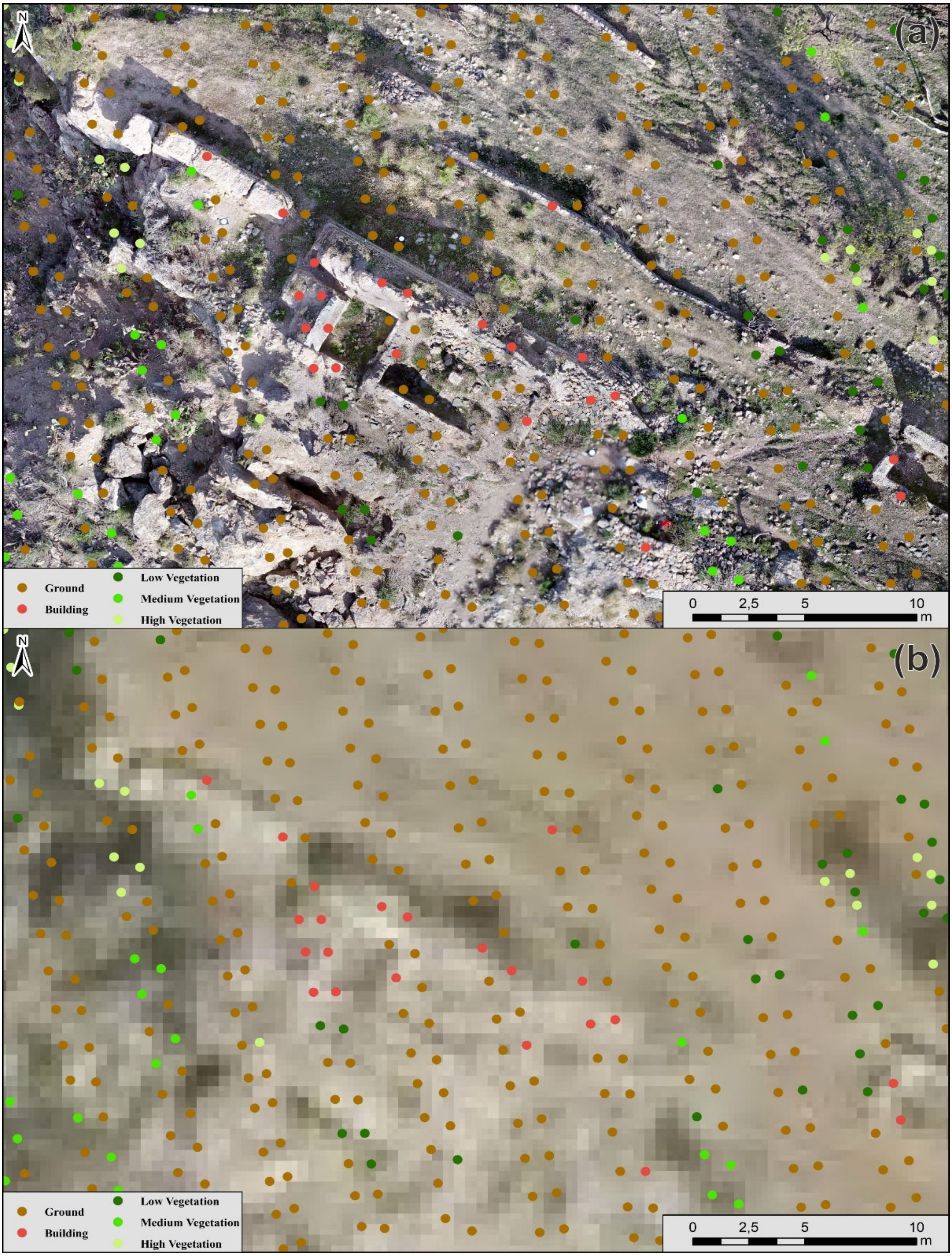

Figure 69: Órgiva tower. (a) LiDAR points superimposed on an orthophoto of the SfM model (b) LiDAR superimposed on a PNOA orthophoto (IGN).

There is also a considerable difference as to the range of coverage of each of the techniques. Most of the drones currently serving for photogrammetry in archaeology are electric powered quadcopters with a reduced autonomy (about 30 minutes for each battery). This timeframe, although allowing a coverage that is greater than that of terrestrial photogrammetry, remains limited to medium and small sites. This restriction also obliges the operator to carry out a field survey prior to the UAV flight to assure coverage of the total extension of the site's features. In spite of its limitations, this technique enables a precise and rapid recording of large sites such as rural Andalusi fortresses in very complex topographical contexts. These types of surveys following traditional methods or photogrammetry carried out manually by attaching cameras to poles imply a great investment in time and do not guarantee the quality of coverage of a UAV.

LiDAR is usually carried out by helicopter or light aircraft as these crafts offer a much greater range. In the case of Spain it covers the entire country. Therefore, its radius of action renders it very useful for macro-spatial analyses and fundamental for Landscape Archaeology. The successive overlapping passes of the aircraft offer a homogeneous and objective survey of a territory (Mlekuž 2018).

Finally, the costs of the techniques also vary. UAV photogrammetric surveying is increasingly accessible to archaeologist given that drones mounted with quality cameras are affordable. The ground topographic support necessary for georeferencing accurately is likewise more accessible either through the purchase or renting GPS devices. The main limitation of this method continues to be the massive quantity of images needed to record large tracts of land to generate the models and their storage requiring very powerful hardware (processor and RAM). This, along with the lack of flight autonomy of commercial drones, is the main impediment to applying photogrammetry as a method to record large surfaces.

The use of LiDAR in archaeology has also grown due to the increase of state agencies carrying out this type of coverage and offering the data to the public and companies. However, most of the current available LiDAR coverage is characterised by low point density. LiDAR flights carried out specifically for archaeological projects are still too expensive in spite of the fact that the price of higher precision sensors mounted on drones is descending offering hope for future use. Moreover, the data yielded by LiDAR, in addition to being available in classified form, are lighter and require less sophisticated computer equipment.

The advantages and disadvantages of each technique can be largely compensated by applying a joint methodology, as noted in the case studies of the fortresses. Thus, the photogrammetric model can be very useful as a base of a manual review of a LiDAR classification. And the photogrammetric point cloud can be filtered by classes applying LiDAR and the DEM techniques. These can be generated and treated with the same improved display algorithms. Even the micro-scale DEMs generated by photogrammetry can be integrated into macro-scaled DEMs from LiDAR to increase the precision of the specific points of interest to the researcher.

LiDAR and photogrammetry are basic tools serving Landscape and Architecture Archaeology that yield a workflow ranging from stratigraphic and spatial analyses through GIS to 3D model printing with PLA. These techniques offer new perspectives in interpreting and understanding complex architectural features and cultural heritage.

5. Conclusions

The development of new technologies has led to a revolution in the means of recording archaeological features. The high quality achieved both in geometry and in realism is a great improvement over the traditional scaled floor plans and elevations which largely depend on the subjective interpretation of the researcher and often suffer from geometric errors (Giacomello et al. 2017).

Application of UAV photogrammetry to this field has also led to a gain in time of fieldwork and the recording with the same equipment of features of difficult access due to steep terrain and/or great height that would normally require ladders or scaffolding. LiDAR, in turn, is an extremely useful and precise tool to survey vast areas of a territory.

The use of new technologies under constant development and improvement is therefore fundamental to applying the Archaeology of Architecture and Archaeology of Landscape to the fortifications of the Alpujarra of Granada. They are applicable to all of the phases of research, from the initial recording, to the spatial analyses, to the dissemination of the results.

This high-quality documentary base allows applying new methods and approaches that offer valuable information to interpret both rural medieval fortifications and the ancient Andalusi landscape. Its utility, therefore, goes far beyond an aesthetic and spectacular graphic representation. Its potential in the field of Archaeology has yet to be developed and there are still broad sectors that, recognising its aesthetic value, and even its potential for diffusion, are unable to identify the significance of the changes that are currently underway. An apparently simple and classic example is the finding that the fortresses of Órgiva and Poqueira did not benefit from direct visual communication, a factor necessary to coordinate the defence of the territory. Each of the fortresses focused most of its visual domain on the territory it headed as it was visible from most of the hamlets or small villages as well as a large part of the irrigated areas that even today are of great economic importance. Moreover, the fact that each fortress was located to the south of its respective irrigated areas indicates that their position was conditioned by where this type of agriculture took place. It is therefore also necessary not only to take into account the relationship of the fortifications with the settlements, but their link to the productive spaces of the community essential to sustenance and to the main thoroughfares. Integrating the landscape analyses with that of the fortifications yields new interpretations as to their function and the relationship between the authorities and the peasant groups, a classic topic of debate even today in Al-Andalus archaeology.

These technical methods, therefore, generate complex workflows marked by massive data that open up vast fields of interpretation that are worth exploring to attain a greater understanding of historical and archaeological heritage. This supposes a change and an advance at both methodological and epistemological levels in archaeology and in landscape analyses that offer compelling results even if the techniques are still in their infancy. The possibility of combining and changing the resolution, precision and scale is fundamental not only to render our conception of Archaeology and its methodology more complex and integrated, but to promote a better interdisciplinary and transdisciplinary integration. The three-dimensional conception (and four-dimensional conception due to diachronicity) of the aim of this study and the way of analysing it represents not only aesthetic or visual alterations, but also conceptual and epistemological changes that opens new avenues of reflection and research that are currently under development. The representations carried out by the new digital technologies have already reached an enormous degree of reliability yielding visual and geometrical records without suffering from the subjectivity of the researcher. The multiplication of channels and platforms to disseminate high-quality three-dimensional models opens the door to different researchers to carry out their interpretations based on an objective record. The increase of use of these technologies in archaeology will, therefore, lead to obtaining an empirical foundation forming the basis of a progressively more complex discussion by integrating into one different scales of work.

6. References

Alcalde Rodríguez, F., J. J. Ayala Carbonero, M. Cañadas Jiménez, A. J. Pérez Salguero and A. J. Ramos Lafuenta 2019. *La Guerra en las Alpujarras*. Motril: Ayuntamiento de Motril.

Aranda Jiménez, G. 2011. El presente y futuro de la arqueología en Andalucía, in J. Almansa Sánchez (ed.) *El futuro de la Arqueología en España*: 13-20. Madrid: JAS Arqueología.

Benavides López, J. A. 2017. *Nuevas tecnologías aplicadas a la documentación gráfica del patrimonio. La alcazaba de Guadix y el castillo de Píñar.* PhD dissertation: Universidad de Granada, Granada.

Benavides López, J. A., G. Aranda Jiménez, M. Sánchez Romero, E. Alarcón García, S. Fernández Martín, Á. Lozano Medina, Á. and J. A. Esquivel Guerrero 2016. 3D modelling in archaeology: the application of Structure from Motion methods to the study of the megalithic necropolis of Panoria (Granada, Spain). *Journal of Archaeological Science: Reports,* 10: 495-506. doi: https://doi.org/10.1016/j.jasrep.2016.11.022

Benavides López, J. A., J. M. Martín Civantos and J. Rouco Collazo 2020. Levantamiento arquitectónico y análisis arqueológico del castillo de Píñar como punto de partida para su conservación. *Virtual Archaeology Review* 11 (22): 95-115.

Brogiolo, G. P., D.E. Angelucci, A. Colecchia and F. Remondino 2012. *APSAT 1. Teoria e metodi della ricerca sui paesaggi d'altura*. Mantova: SAP.

Brogiolo, G. P., and A. Cagnana 2012. *Archeologia dell'architettura. Metodi e interpretazioni*. Firenze: All'Insegna del Giglio.

Brogiolo, G. P., E. Cavada, S. Camporeale, E. Bernard and F. Parisi 2017. Per un approcio quantitativo e sistemico allo studio delle architetture e dei procedimenti costruttivi medievali. Il caso della Pieve di Lomaso (Trentino sudoccidentale). *Archeologia dell'Architettura* 22: 85-99.

Brogiolo, G. P., and J. Sarabia-Bautista 2017. Land, rivers and marshes: changing landscapes along the Adige River and the Euganean Hills (Padua, Italy). *Post-Classical Archaeologies* 7: 149-171.

Brus, J. and R. Barvíř 2015, Coping with Integrating Low-Cost 3D Printing and Surface Models: A Case Study on Prusa i3, in K. Růžičková and T. Inspektor (eds) *Surface Models for Geosciences. Lecture Notes in Geoinformation and Cartography*: 45-59. Cham: Springer.

Canosa-Betés, J. 2016. Border surveillance: testing the territorial control of Andalusian defense network in center-south Iberia through GIS. *Journal of Archaeological Science: Reports* 9: 416-426.

Carrero-Pazos, M., A. Vázquez-Martínez and B. Vilas-Estévez 2016. AsTrend: Towards a new method for the study of ancient carvings. *Journal of Archaeological Science: Reports* 9: 105-119. doi: https://doi.org/10.1016/j.jasrep.2016.06.044

Cefalu, A., N. Haala, and D. Fritsch (2017). Hierarchical Structure from Motion combining global image orientation and structreless bundle adjustment. *International Archives of Photogrammetry, Remote Sensing and Spatial Informations System,* XLII(1/W1): 535-542.

Citter, C. and A. Patacchini 2017. Il territorio della città di Este attraverso lo studio dil palinsesto dei catasti storici, in G. P. Brogiolo (ed.) *Este, l'Adige e i Colli Euganei. Storie di paesaggi, .* Mantova: SAP.

Conolly, J., and M. Lake 2006. *Geographical Information Systems in Archaeology*. Cambridge: Cambridge University Press.

Cressier, P. 1983. L'Alpujarra médiévale: une aproche archéologique. *Mélanges de la Casa de Velázquez,* 19 : 89-124.

Cressier, P. 1984. Le château et la division territoriale dan l'Alpujarra médievale: du hisn à la ta'a. *Mélanges de la Casa de Velázquez,* 20: 115-144.

Cressier, P. 1992. El castillo y la división medieval de la Alpujarra: del hisn a la ta'a, in P. Cressier (ed.) *Estudios de arqueología medieval en Almería*: 7-48. Almería: Instituto de Estudios Almeriense.

Crutchley, S. 2010. The light fantastic: using airborne Lidar in Archaeological Survey, in W. Wagner and B. Székely (eds) *International Archives of Photogrammetry and Remote Sensing*: Vol. 38, 7B, 160-164. Vienna: International Society of Photogrammetry and Remote Sensing.

Crutchley, S. 2015. Using airborne LiDAR for interpreting archaeological landscapes, in A. Chavarría Arnau and A. Reynolds (eds) *Detecting and Understanding Historic Landscapes*: 67-86. Mantova: SAP.

Cultural Heritage Imaging 2013a. RTIBuilder (Version 2.0.2).

Cultural Heritage Imaging 2013b. RTIViewer (Version 1.1.0).

Chisvert Jiménez, N. and F. Amores Carredano 1993. Tipología de la cerámica bajomedieval y moderna sevillana (s. XV-XVIII): I, la loza quebrada de relleno de bóvedas. *Spal* 2: 269-328.

De Castro Ferreira, A. A., M. V. Yodono García and H. Cândido de Oliveira 2019. Avaliação da qualidade altimétrica de modelos digitais de terreno derivados de levantamento topográfico com VANT, in *Anais do XIX Simpósio Brasileiro de Sensoriamento Remoto.* Santos: INPE.

Dedík, L., and J. Minaroviech 2017. Project of the Digital Monuments Funds: Digitization of the Cultural Heritage of Slovakia. *Studies in Digital Heritage,* 1: 590-606. doi: 10.14434/sdh.v1i2.23286

Dellepiane, M., M. Corsini and M. Callieri 2006. High Quality PTM Acquisition: Reflection Transformation Imaging for Large Objects, in M. Ioannides, D. Arnold, F. Niccolucci and K. Mania (eds) *The 7th International Symposium on VAST International Symposium on Virtual Reality, Archaeology and Cultural Heritage*: 179-186. Eurographics Association.

Domínguez Bedmar, M., I. Flores Escobosa, A. Malpica Cuello, P. Cressier, M.M. Riera Frau and G. Rosselló-Bordoy 1991. La cerámica tardo almohade y los orígenes de la cerámica nasri, in L. A. da Silva and R. Mateus (eds) *A cerâmica medieval no Mediterrâneo ocidental*: 215-246. Mértola: Campo Arqueológico de Mértola.

Dowman, I. 2004. Integration of LiDAR and IFSAR for Mapping. *International Archives of Photogrammetry and Remote Sensing* 35: 90-100.

Dytchowskyj, D., S. Aagesen and A. Costopoulos 2005. The use of Thiessen polygons and viewshed analysis to create hypotheses about prehistoric territories and political systems. *Archaeological Computing Newsletter,* 62: 1-6.

Earl, G., G. Beale, K. Martínez and H. Pagi 2010. Polynomial Texture Mapping And Related Imaging Technologies For The Recording, Analysis And Presentation Of Archaeological Materials, in J. P. Mills, D. M. Barber, P. E. Miller and I. Newton (eds) *Proceedings of the ISPRS Commission V Mid-Term Symposium 'Close Range Image Measurement Techniques' 21-24 June 2010 Newcastle upon Tyne, United Kingdom*: 218-223. Newcastle (UK): ISPRS.

Earl, G., K. Martínez and T. Malzbender 2010. Archaeological applications of polynomial texture mapping: analysis, conservation and representation. *Journal of Archaeological Science* 37: 2040-2050. doi: https://doi.org/10.1016/j.jas.2010.03.009

Historical England 2018. *Using Airborne Lidar in Archaeological Survey. The Light Fantastic*. Swindon: Historic England.

Esclapés Jover, F. J., J. Molina Vidal, J. Muñoz Ojeda, L. Fabregat Bolufer and D. Tejerina Antón 2017. La restauración virtual. Aplicaciones a la conservación del patrimonio arqueológico, in M. Bueso (ed.) *La Ciencia y el Arte VI Ciencias experimentales y conservación del patrimonio*: 152-164. Madrid: Secretaría General Técnica. Subdirección General de Documentación y Publicaciones.

Blender Foundation 2017. Blender 2.79: Blender Foundation.

Fuertes Santos, M. d. C. 1995. Un conjunto cerámico post-califal procedente del yacimiento de Cercadilla, Córdoba. *Anales de Arqueología* Cordobesa 6: 265-291.

Gabrilik, P., A. la Cour-Harbo, P. Kalvodova, L. Zalud and P. Janta. Calibration and accuracy assessment in a direct georeferencing system for UAS photogrammetry. *International Journal of Remote Sensing* 39 (15-16): 4931-4959. doi: 10.1080/01431161.2018.1434331

Galván Rangel, J. M., G. Rito Gonçalves and J.A. Pérez, J. A. 2018. The impact of number and spatial distribution of GCPs on the positional accuracy of geospatial products derived from low-cost UASs. *International Journal of Remote Sensing* 39 (21): 7154-7171.

García Carpintero López de Mota, J. and D. Gallego Valle 2018. La arqueología de las órdenes militares en Castilla-La Mancha y la reconstrucción virtual de su patrimonio. *Virtual Archaeology Review* 9 (19): 76-88.

García Porras, A. 1995. Cerámica nazarí tardía y cristiana de "El Castillejo"(Los Guájares, Granada). *Arqueología y Territorio Medieval* 2: 243-257.

García Porras, A. 2007. La distribución de productos cerámicos entre la época Almohade y la Nazarí: el caso de El Castillejo (Los Guájares). *Arqueoweb: Revistra sobre Arqueología en Internet* 9 (1): 1-26.

Giacomello, F., F. Parisi and S. Schivo 2017. Una proposta di metodo per l'interpretazion del reimpiego del mattone romano tramite analisis GIS. *Archaeologia de la Architetture* 22: 133-145.

Gurriarán Daza, P., and Á.J. Sáez Rodríguez 2002. Tapial o fábricas encofradas en recintos urbanos andalusíes, in *Actas del II Congreso Internacional "La ciudad en al-Andalus y el Magreb" (Algeciras, noviembre 1999)*: 561-625. Granada: El Legado Andalusí.

Harris, E. C. 1989. *Principles of archaeological stratigraphy*. London: Academic Press.

Hayes, J. W. 1972. *Late Roman Pottery*. Roma: British School at Rome.

Hesse, R. 2012. Using lidar-derived Local Relief Models (lrm) as a new tool for archaeologicalprospection, in S. J. Kluiving and E. B. Guttmann-Bond (eds) *Landscape Archaeology between Art and Science*: 369-378. Amsterdam: Amsterdam University Press.

Horn, C., D. Pitman and R. Potter 2019. An evaluation of the visualisation and interpretive potential of applying GIS data processing techniques to 3D rock art data. *Journal of Archaeological Science: Reports* 27: 1-13.

Horn III, S. W., and A. Ford 2019. Beyond the magic wand: methodological developments and results from integrated Lidar survey at the ancient Maya Center El Pilar. *STAR: Science & Technology of Archaeological Research*: 1-14. doi: 10.1080/20548923.2019.1700452

Howland, M. D., F. Kuester and T.E. Levy 2014. Structure from Motion: twenty-first century field recording with 3D technology. *Near Eastern Archaelogy* 77 (3): 187-191.

Isenburg, M. 2020. LAStools.

Jiménez Mata, M. C. 1985-1986. Datos para una reflexión sobre la división geográfico-administrativa de la Granada islámica. *Estudios de Historia y Arqueología Medievales* V-VI: 33-41.

Jiménez Puertas, M. 2002. *El poblamiento del territorio de Loja en la Edad Media*. Granada: Editorial Universidad de Granada.

Jiménez Puertas, M., G. García-Contreras Ruiz and L. Mattei 2010. El Fuerte de Lanteira (Granada). Análisis de una fortificación de alquería de época nazarí. *Arqueología de la Arquitectura* 7: 191-211.

Jones, R., P. Haufe, E. Sells, P. Iravani, V. Olliver, C. Palmer and A. Bowyer 2011. RepRap – the replicating rapid prototyper. *Robotica* 29: 177-191.

Kantner, J., and R. Hobgood 2016. A GIS-based viewshed analysis of Chacoan tower kivas in the US Southwest: Were they for seeing or to be seen? *Antiquity* 90: 1302-1317.

Kersten, T. P., and M. Lindstaedt 2012. Automatic 3D Object reconstruction from multiple images for architectural, cultural heritage and archaeological applications using open-source software and web services. *Photogrammetrie - Fernerkundung – Geoinformation* 2012 (6): 727-740.

Koffler Urbano, T. 2010. La cerámica de Castell de Ferro. De la Baja Edad Media a la Edad Moderna, in M. Crespo Díez and R. Martín Peñín (eds), *Metodología de análisis aplicada a los estudios de la cerámica tardoantigua y medieval de la Península Ibérica*: 121-132. León: Lobo Sapiens.

Kokalj, Ž., and M. Somrak 2019. Why not a single image? Combining visualizations to facilitate fieldwork and on-screen mapping. *Remote Sensing* 11 (7): 747.

Kotoula, E., and M. Kyranoudi 2013. Study of coins using Reflectance Transformation Imaging. *e-conservation* 25: 74-88.

Lanjouw, T. 2016. Discussing the obvious or defending the contested: why are we still discussing the "scientific value" of 3D applications in archaeology?, in H. Kamermans, W. de Neef, C. Piccoli, A. G. Posluschny and R. Scopigno (eds) *The three dimensions of archaeology. Proceedings of the XVII UISPP World Congress (1-7 September 2014, Burgos, Spain)*: vol 7,1-11. Oxford: Archaeopress Archaeology.

Lejeune, M. 2019. Étudier une architecture difficile d'accès grâce aux techniques numériques : l'exemple de la flèche de la cathédrale de Senlis (Oise), in *La recherche sur le patrimoine et les outils numériques à l'épreuve de l'expérimentation, Journé d'étude de la SFR*. Lille.

Levy, T. E., N. G. Smith, M. Najjar, T. A. DeFanti, F. Kuester and A. Y.-M. Lin (2012). *Cyber-Archaeology in the Holy Land.* San Diego: California Institute for Telecommunications and Information Technology.

Lowe, D. 1999. Object recognition from local scale-invariant features, in *The Proceedings of the Seventh IEEE International Conference on Computer Vision*: vol 2, 1150-1157). Washington: IEEE Computer Society.

Maldonado Fernández, A. and J. Rouco Collazo in press. El uso combinado de Reflectance Transformation Imaging (RTI) y fotogrametría SfM para la mejora de la visualización y el estudio de elementos patrimoniales deteriorados y de difícil acceso. *Virtual Archaeology Review*.

Maldonado Ruiz, A. 2020. *La Aplicación de la Fotogrametría (SFM) y las Nuevas Tecnologías para la Mejora de la Documentación, Difusión y Divulgación del Patrimonio Arqueológico de Pequeño y Mediano Tamaño.* Unpublished PhD dissertation, University of Granada.

Maldonado Ruiz, A., and M. I. Fernández García in press. Técnicas de digitalización, reconstrucción y visualización 3D aplicadas a los moldes de terra sigillata del yacimiento romano de Los Villares de Andújar (Municipio Isturgitano). Las posibilidades en la difusión, estudio y conservación del patrimonio arqueológico. *Pyrenae*: 52.

Maldonado Ruiz, A., and J. Rouco Collazo 2020. *Material complementario para: El uso combinado de Reflectance Transformation Imaging (RTI) y fotogrametría SfM para la mejora de la visualización y el estudio de elementos patrimoniales deteriorados y de difícil acceso*. http://hdl.handle.net/10481/59188

Malpica Cuello, A. 1996. *Poblamiento y castillos en Granada*. Barcelona: El Legado Andalusí.

Malzbender, T., D. Gelb and H. Wolters 2001. Polynomial Texture Maps, in *Proceedings of the 28th Annual Conference on Computer Graphics and Interactive Techniques*. New York, NY, USA: ACM.

Marqués, N. F., M. J. Velázquez Pascual, C. Bonmatí Lledó and A. Marcos González 2018. Virtualización e impresión 3D aplicadas a la accesibilidad del patrimonio cultural. De la planificación a los acabados y los contenidos accesibles, in *Actas 5è Congrés d'Educació i Accesibilitat a museus i patrimoni*: 251-264. Barcelona: Institut de Cultura de Barcelona, Institut Municipal de Persones amb Discapacitat i Museu Marítim de Barcelona.

Márquez Bueno, S. 2018. La tecnología constructiva andalusí: obra encofrada y revistimiento en la arquitectura militar (ss. XI-XIII). El ejemplo de las torres. *Arqueología de la Arquitectura* 15: e076.

Martín Civantos, J. M. 2002. Ensayo de análisis comparativo de técnicas, materiales y tipos constructivos en las fortificaciones medievales del Zenete (Granada). *Miscelánea Medieval Murciana,* XXV-XXVI: 183-220.

Martín Civantos, J. M. 2012. Hydraulic Archaeology in South-east Spain Mountainous Landscapes, in G. P. Brogiolo, D. E. Angelucci, A. Colecchia and F. Remondino (eds) *APSAT 1. Teoria e metodi della ricerca sui paesaggi d'altura*: 51-73. Mantova: SAP.

Martín Civantos, J. M. 2013. Del distrito castral a la alquería: las fortificaciones andalusíes en el Sureste de la Península Ibérica (Granada-Almería), in I. C. Ferreira Fernandes (ed.) *Fortificações e territorio na Península Ibérica e no Magreb (séculos VI a XVI)*: vol 1, 133-140). Lisboa: Ediçoes Colibrí.

Martín Civantos, J. M. 2015. Landscape Archaeology and Rural Communities: ethnoecology and social involvement, in A. Chavarría Arnau and A. Reynolds (eds) *Detecting and understanding historical landscapes*: 335-358. Mantova: SAP.

Martín García, M. 2000. Torres de alquería de la provincia de Granada, in A. Graciani, S. Huerta, E. Rabasa and M. A. Tabales (eds) *Actas del Tercer Congreso Nacional de Historia de la Construcción (Sevilla, 26-28 octubre 2000)*: 651-664. Sevilla: Instituto Juan de Herrera.

Martín García, M., J. Bleda Portero and J. M. Martín Civantos 1999. *Inventario de arquitectura militar en la provincia de Granada*. Granada: Diputación Provincial de Granada.

Martín Talaverano, R. 2014. Documentación gráfica de edificios históricos: principios, aplicaciones y perspectivas. *Arqueología de la Arquitectura* 11: e011.

Martín Talaverano, R., L. Cámara Muñoz and J. I. Murillo Fragero 2018. Análisis integrado de construcciones históricas: secuencia estratigráfica y diagnóstico patológico. Aplicación en la iglesia de Santa Clara (Córdoba). *Arqueología de la Arquitectura* 15: e067.

Martínez Rubio, J., J. J. Fernández Martín and J. I. San José Alonso 2018. Implementación de escáner 3D y fotogrametría digital para la documentación de la iglesia de La Merced de Panamá. *Expresión Gráfica Arquitectónica* 32: 208-219.

Martos-Rosillo, S., A. Ruiz-Constán, A. González-Ramón, R. Mediavilla, J. M. Martín Civantos, F. J. Martínez-Moreno, J. Jódar, C. Marín-Lechado, A. Medialdea, J. Galindo-Zaldívar, A. Pedrera and J. J. Durán 2019. The oldest managed aquifer recharge system in Europe: New insights from the Espino recharge channel (Sierra Nevada, southern Spain). *Journal of Hydrology* 578.

McGaughey, R. J. 2020. FUSION (Version 3.8): Forest Service of the Department of Agriculture of the United States.

Melero García, F. 2009. El vertedero medieval de Cártama, Málaga: las cerámicas de los pozos de época emiral y califal. *Arqueología y Territorio Medieval* 16: 33-52.

Meschini, A., and F. Sicuranza 2016. Per una rappresentazione "sensibile": la comunicazione della forma per una percezione aptic, in S. Bertocci and M. Bini (eds) *Atti del 38° Convegno internazionale dei docenti delle discipline della rappresentazione*: 1515-1522. Firenze: Gangemi Editore.

Miles, J., M. Pitts, H. Pagi, and G. Earl 2015. Photogrammetry and RTI Survey of Hoa Hakananai'a Easter Island Statue, in A. Traviglia (ed.) *Across Space and Time. Papers from the 41st Conference on Computer Applications and Quantitative Methods in Archaeology. Perth, 25-28 March 2013*: 144-164.

Mlekuž, D. 2013. Skin Deep: LiDAR and Good Practice of Landscape Archaeology, in C. Corsi, B. Slapšak & F. Vermeulen (eds), *Good Practice in Archaeological Diagnostics. Non-invasive Survey of Complex Archaeological Sitres*: 113-129. London: Springer.

Mlekuž, D. 2018. Airborne Laser Scanning and Landscape Archaeology. *Opvscula Archaeologica* 39-40: 85-95.

Montuori, R. 2018. Modelado e impresión 3D de vestigios arqueológicos: el caso de la acrópolis de La Blanca, in L. Agudo Pérez, C. Duarte, A. García Escárzaga, J. M. Geiling, A. Higuero Pliego, S. Núñez de la Fuente, F. J. Rodríguez Santos and R. Suárez Revilla (eds), *Actas de las IX Jornadas de Jóvenes en Investigación Arqueológica*: 71-79. Santander: Instituto Internacional de Investigaciones Prehistóricas de Cantabria.

Mudge, M., T. Malzbender, C. Schroer and M. Lum. 2006. New Reflection Transformation Imaging Methods for Rock Art and Multiple-Viewpoint Display, in *The 7th International Symposium on Virtual Reality Archaeology and Cultural Heritage VAST2006*: 195-202.

Mudge, M., J.-P. Voutaz, C. Schroer and M. Lum 2005. Reflection Transformation Imaging and Virtual Representations of Coins from the Hospice of the Grand St. Bernard, in W. H. Dieter, W. Fellner, Werner Purgathofer and François Sillion (ed.) *The 6th International Symposium on Virtual Reality, Archaeology and Intelligent Cultural Heritage*: 29-40. Pisa: Eurographics Association.

Murphy, K. M., B. Gittings and J. Crow. 2018. Visibility analysis of the Roman communication network in southern Scotland. *Journal of Archaeological Science: Reports* 17: 111-124.

Navarro Palazón, J. 1991. *Una casa islámica en Murcia: estudio de su ajuar, siglo XIII*. Murcia: Centro de Estudios Árabes y Arqueológicos Ibn Arabi.

Nex, F., and F. Remondino. 2014. UAV for 3D mapping applications: a review. *Applied geomatics* 6 (1): 1-15.

Oniga, V.-E., A.-I. Breaban and F. Statescu. 2018. Determining the Optimum Number of Ground Control Points for Obtaining High Precision Results Based on UAS Images. *Proceedings* 2 (7): 352.

Opitz, R. S. 2013. An overview of airborne and terrestrial laser scanning in archaeology, in R. S. Opitz and D. C. Cowley (eds) *Interpreting archaeological topography: airborne laser scanning, 3D data and ground observation:* 13-31. Oxford: Oxbow.

Parenti, R. 1988a. Le tecniche di documentazione per una lettura stratigrafica dell'elevato, in R. Francovich and R. Parenti (eds) *Archeologia e restauro dei monumenti*: 249-279. Florencia: All'Insegna del Giglio.

Parenti, R. 1988b. Sulle possibilità di datazione e di classificazione delle murature, in R. Francovich and R. Parenti (eds) *Archeologia e restauro dei monumenti*. Firenze: All'Insegna del Giglio.

Parenti, R. 1996. Individualización de las unidades estratigráficas murarias, in L. Caballero Zoreda and C. Escribano Velasco (eds) *Arqueología de la arquitectura: el método arqueológico aplicado al proceso de estudio y de intervención en edificios históricos*: 75-85. Salamanca: Junta de Castilla y León.

Pedregosa Megías, R. J. 2011. La Torre de Márgena o Marchena, Dúrcal (Granada): una torre de alquería y su albacar. *ANTIQVITAS* 23: 293-302.

Peucker, T. K., R. J. Fowler and J. J. M. Little. 1978. The triangulated irregular network *Proceedings of the Digital Terrain Models (DTM) Symposium*. Falls Church: American Society of Photogrammetry.

Piquette, K. E. 2011. Reflectance Transformation Imaging (RTI) and Ancient Egyptian Culture. *Damqatum; The CEHAO Newsletter-El boletín de noticias del CEHAO* 7: 16-20.

Previtali, M., and R. Valente. 2019. Archaeological documentation and data sharing: digital surveying and open data approach applied to archaeological fieldworks. *Virtual Archaeology Review,* 10 (20): 17-27.

Prins, A. B., M. J. Adams, R. S. Homsher and M. Ashley. 2014. Digital archaeological fieldwork and the Jezreel Valley regional project, Israel. *Near Eastern Archaelogy* 77 (3): 192-197.

Quartermaine, J., B. R. Olson and M. Howland. 2013. Using photogrammetry and geographic information systems (GIS) to draft accurate plans of Qazion. *Journal of Eastern Mediterranean Archaeology and Heritage Studies 1*: 169-174.

Remondino, F., L. Barazzeti, F. Nex, M Scaioni and D. Sarazzi. 2011. UAV Photogrammetry for mapping and 3D Modeling. Current status and future perspectives. *International Archives of the Photogrammetry, Remote Sensing and Spatial Information Sciences* XXXVIII-1/C22: 25-31.

Rodríguez Navarro, P. 2012. Fotogrametría digital automatizada (SfM) con apoyo aéreo de proximidad, in *XI Congreso Internacional de Expresión Gráfica aplicada a la Edificación*: 783-789. Valencia: Universidad Politécnica de Valencia.

Romero Pellitero, P., L. Delgado Anés and J. M. Martín Civantos. 2019. Comunidades locales y paisaje cultural en Sierra Nevada. Desde la Teledetección a la Arqueología comunitaria, in L. A. Polo Romero and K. Trápaga Monchet (eds) *Arqueología, Historia y Medio Ambiente: Visiones Cruzadas*: 149-174. Madrid: Dykinson.

Roosevelt, C. H., P. Cobb, E. Moss, B. R. Olson and S. Ünlüsoy. 2015. Excavation is digitazion: advances in archaeological practice. *Journal of Field Archaeology* 40 (3): 325-346.

Rouco Collazo, J., J. M. Martín Civantos and J. A. Benavides López. 2018. Análisis arqueológico de la torre-puerta de la alcazaba de Guadix (Granada). *Arqueología de la Arquitectura* 15: e072.

Rouco Collazo, J., J. M. Martín Civantos and J. A. Benavides López. 2020. Building Archaeology of the Alcazaba of Guadix (Granada, Spain): An Example of Implanting Power in the Urban Centres of Al-Andalus. *International Journal of Architectural Heritage*. doi: 10.1080/15583058.2020.1719231

Samberg, A. 2007. An implementation of the ASPRS LAS Standard. *The Analyst* 36: 363-372.

Sánchez García, A. 2018. *Estudio histórico y arqueológico del Barranco del Poqueira (Granada).* MA dissertation, University of Granada.

Sánchez Martínez, M. 1976. La cora de Ilbira (Granada y Almería) en los siglos X y XI, según Al-'Udri (1003-1085). *Cuadernos de Historia del Islam* 7: 5-82.

Scopigno, R., M. Callieri, M. Dellepiane, F. Ponchio and M. Potenziani. 2017. Delivering and using 3D models on the web: are we ready?. *Virtual Archaeology Review,* 8 (17): 1-9. doi: 10.4995/var.2017.6405

Schönberger, J. L., and J. M. Frahm. 2016. Structure-from-motion revisited, in *Proceedings of the IEEE Conference on Computer Vision and Pattern Recognition*: 4104-4113.

Schwarzbach, F., T. Sarjakoski, J, Oksanen, L. T. Sarjakosi and S. Weckman. 2011. Physical 3D models from LIDAR data as tactile maps for visually impaired persons, in M. Buchroithner (ed.) *True-3D in Cartography. Autosterescopic and Solid Visualisation of Geodata*: 169-183. Berlin: Springer.

American Society for Photogrammetry and Remote Sensing 2011. LAS specification 1.4 - R6. Bethesda.

Statham, N. 2019. Scientific rigour of online platforms for 3D visualisation of heritage. *Virtual Archaeology Review* 10 (20): 1-16. doi: 10.4995/var.2019.9715

Trillo San José, C. 1990. La ta'a de Órgiva: un señorío en la Alpujarra al final de la Edad Media. *Revista del Centro de Estudios Históricos de Granada y su Reino* 4: 49-70.

Trillo San José, C. 1991. *La Alpujarra al final de la Edad Media.* PhD dissertation, Universidad de Granada, Granada.

Ultimaker. 2019. Ultimaker Cura (Version 4.4).

van der Zee, R., and F. Zuidhoff. 2012. New methods to analyse lidar-based elevation models for historical landscape studies with five time slices, in S. J. Kluiving and E. B. Guttmann-Bond (eds) *Landscape Archaeology between Art and Science* (pp. 443-457). Amsterdam: Amsterdam University Press.

Van Leusen, M., and S. Van Gessel. 2016. Towards 3D GIS. Notes from the 2012 CAA-NL/DE chapter session 'from 2.5 to 3 spatial dimensions', in H. Kamermans, W. de Neef, C. Piccoli, A. G. Posluschny and R. Scopigno (eds) *The three dimensions of archaeology. Proceedings of the XVII UISPP World Congress (1-7 September 2014, Burgos, Spain*: vol. 7, 33-37. Oxford: Archaeopress Archaeology.

Vázquez Martínez, A., B. Vilas Estévez and M. Carrero Pazos. 2015. Sobre as técnicas de reprodución dos gravados rupestres galaicos ao aire libre. *Férvedes: Revista de Investigación* 8: 17-24.

Villalobos Megía, M., and A. B. Pérez Muñoz. 2006. *Geodiversidad y Patrimonio Geológico de Andalucía. Itinerario Geológico por Andalucía, guía prática de campo.* Sevilla: Junta de Andalucía.

Vitelli, D. 2017a. Applicazioni di 'GIS verticale' per la quantificazione delle opere architettoniche in muratura e i loro tempi di realizzazione: il caso del castello di Drena. *Archeologia dell'Architettura* 22: 101-111.

Vitelli, D. 2017b. Tempi di lavorazione e analisi quantitative in GIS, in G. P. Brogiolo (ed.) *Toscolano e Maderno. Paesaggi, comunità, imprenditori tra medioevo ed età moderna*: 81-109. Mantova: SAP.

Westoby, M. J., J. Brasington, N. F. Glasser, M. J. Hambrey and J. M. Reynolds. 2012. 'Structure-from-Motion' photogrammetry: A low-cost, effective tool for geoscience applications. *Geomorphology* 179: 300-314.

Zakšek, K., K. Oštir and Ž. Kokalj. 2011. Sky-View Factor as a Relief Visualization Technique. *Remote Sensing* 3 (2): 398-415.

Zennaro, M. 2013. The Role of Open Source Software and Hardware in the 3D Printing Revolution, in E. Canessa, C. Fonda and M. Zennaro (eds) *Low-Cost 3D Printing for Science, Education and Sustainable Development*: 61-66. Trieste: The Abdus Salam International Centre for Theoretical Physics.

Early Roman Iron Age Jewellery in the Northern Barbaricum: Between Stylistic and Technological Simplicity and Luxury

Audronė Bliujienė (*Klaipėda University, Institute of Baltic Region History and Archaeology*), Gediminas Petrauskas(*Klaipėda University, Institute of Baltic Region History and Archaeology & National Museum of Lithuania, Department of Archaeology*), Jurga Bagdzevičienė (*Klaipėda University, Institute of Baltic Region History and Archaeology & The Lithuanian National Museum of Art, Pranas Gudynas Centre for Restoration*), Sergej Suzdalev (*Klaipėda University, Institute of Baltic Region History and Archaeology & Klaipėda University, Marine Research Institute*), Evaldas Babenskas (*Klaipėda University, Institute of Baltic Region History and Archaeology*)

Abstract

The article examines two interregional types of early Roman Iron Age jewellery, the so-called eye fibulae and neck-rings with hollow trumpet-shaped terminals. These ornaments in the 1st and 2nd centuries were widespread in the vast areas of the Central European *Barbaricum* and in the territory of the Baltic people living between the Pasłęka and Daugava (Western Dvina) rivers. These fibulae and neck-rings are also known from the territories populated by the Finno-Ugrians, extending up to the Gulf of Finland. Eye fibulae were born on the periphery between the antique and barbarian worlds – in the northern provinces of the Roman Empire, most likely as an amalgamation of the antique and barbarian cultural traditions. However, because of the relatively simple production and ornamentation, they became mass products across the *Barbaricum*. Unlike eye fibulae, neck-rings with hollow trumpet-shaped terminals required more complex technological skills for their production. Prototypes of these neck-rings came from the La Tène and Roman cultural legacy and were later absorbed by the Germanic people. In the lands of the Balts the idea of such neck-rings was adopted from similar Scandinavian golden neck-rings. These neck-rings are ornate jewellery items, custom-made of copper alloys using complex technologies that required highly-skilled jewellers. These technically elaborate neck-rings in terms of territorial distribution and social significance stand in contrast to the contemporaneous eye fibulae that were widespread throughout the *Barbaricum*. The present article reviews the composition of the alloys of 51 fibulae and 4 neck-rings analysed by means of X-ray fluorescence (XRF) and describes their manufacturing technique. The technological and XRF analyses revealed that the eye fibulae and neck-rings with hollow trumpet-shaped terminals found in Lithuania, much like this type of jewellery

found in other barbarian countries, were made of brass, brass/gunmetal, gunmetal/bronze or bronze using the same (eye fibulae) or simpler (neck-rings) manufacturing technologies.

Keywords

Early Roman Iron Age, Northern *Barbaricum*, the Balts, eye fibulae, neck-rings with hollow trumpet-shaped terminals, XRF analysis, technological analysis

1. Introduction

The article examines two types of jewellery common in the Early Roman Age (middle of 1st century-end of 2nd century AD) in the Eastern Baltic Sea region: the so-called eye fibulae and neck-rings with hollow trumpet-shaped terminals. Although both these jewellery items were made of copper alloys, there are significant differences in their manufacturing techniques and stylistic features. Eye fibulae are known from available archaeological material on the settlements and frontier forts in the northern provinces of the Roman Empire bordering on the river Rhine (beginning of 1st century-third quarter of 1st century AD) (Riha 1979; Voß 2008). However, the study of the origin and development of eye fibulae conducted as early as 19 century lead to an essential question – whether these fibulae were the type of jewellery shaped by Roman traditions, which later spread among the Germanic tribes, or whether they were rooted in the Germanic tradition itself.

The name 'eye fibulae' (Ger. *Augenfibeln*) originates from a characteristic ornament of the fibulae – pairs of circle and dot decorations (eyes) arranged on the foot or, sometimes, on the bow. The complexity of the origin context of eye fibulae (whether Roman or Germanic) is illustrated by the set of over 200 so-called Prussian series eye fibulae found on the territory of the workshop in the Roman military camp *Augusta Vindelicorum* (province of *Raetia*, currently Augsburg). The Prussian series eye fibulae were termed so because of one of the biggest collections of jewellery from the territory of Prussia lying between the lower Vistula (**Wisła**) river (Germanic Wielbark Culture) and the Sambian peninsula (Baltic Sambian-Natangian Culture area)[18]. Part of the eye fibulae discovered in *Augusta Vindelicorum* camp were finished products while another part were semi-manufactured articles. Therefore, it is likely that the eye fibulae found in *Augusta Vindelicorum* camp were made on purpose, i.e. to be exchanged with the Germanic people. This assumption is indirectly confirmed by the very intensive exchange between Romans and Barbarians along the so-called Amber Route taking place since the second half of 1st

[18] In literature this cultural area is referred to as Dollkeim (Kovrovo) Culture (Nowakowski 1996).

century AD, which was briefly interrupted by the Marcomannic wars (cf. Bliujienė 2011; Lund Hansen 1987).

The massive spread of eye fibulae within the *Barbaricum* suggests that these fibulae were not merely an imported article. Early from the middle of 1st century AD these mostly one-piece, easily manufactured, identically ornamented fibulae spread north of the Roman Empire border and through to Southern Finland to include other countries of the Baltic Sea region (Andrzejowski and Cieśliński 2007; Kivikoski 1973; Khavrin *et al.* 2011; Michelbertas 1986; Moora 1938; Voß 2008). The cemeteries of the Sambian-Natangian Culture (East Prussia, currently Kaliningrad Oblast) located in the Balts cultural area between the Pasłęka and Daugava rivers yielded the greatest number of eye fibulae (Chilińska-Früboes 2017, 2018). About 200 eye fibulae were found in Northern Latvia and North-Eastern Estonia in *tarand* type cemeteries (Roxburgh and Olli 2019). Thus, eye fibulae are the first Early Roman Age fibulae widespread in the lands of the Baltic and Finno-Ugric people. During the La Tène period, in the Eastern Baltic Sea region only few imported iron fibulae were known (Grigalavičienė 1995; Roxburgh and Olli 2019).

Contrary to eye fibulae, the contemporaneous neck-rings with hollow trumpet-shaped terminals were an exclusive type of jewellery. In the middle of the 1st century AD, people of the Sambian-Natangian Culture, living in the Sambian peninsula, began making copper-alloy copies of these neck-rings by following the Scandinavian golden neck-ring Havor-type[19] design (Khomiakova 2011; Rzeszotarska-Nowakiewicz 2010; Skvortsov 2018). The Havor type neck-rings were designed by adopting and integrating the Celtic and antique cultural heritage as well as the manufacturing technologies of the early La Tène period. There is good evidence to believe that diverse cultural contacts, migration processes and transfer of technologies made it possible for the North Germanic people, as early as in the 1st century AD, to begin making various gold jewellery objects (Andersson 1995; Nylén 1996; Nylén *et al.* 2005).

Simplified versions of these neck-rings made of copper alloys in the middle-second half of 1st century AD spread to Lithuania, the Finno-Ugric *tarand* area in Northern Latvia and some time later to North-Eastern Estonia as well as South-Western coast of Finland. The neck-rings with hollow trumpet-shaped terminals have become one of the earliest jewellery items created by the Baltic jewellers that spread to the Eastern Baltic region and South-Western Finland (*Hackman* 1905; Lang 2007; Michelbertas 1986, 1989; Moora 1938; Oras 2015; Rzeszotarska-Nowakiewicz 2010). For the Baltic jewellers the neck-rings

[19] The name ‘Havor’ originates from the rich hoard found in a ring fort in the village of Havor in Gotland (Hablingbo parish) in 1961. The Havor hoard consisted of a golden neck-ring (257 mm in diameter and weighing close to 800 grams), which was enclosed in a *situla* along with Roman wine-serving utensils and a pair of bronze bells (Nylén *et al.* 2005).

with hollow trumpet-shaped terminals have become the prototype for creation of a simpler version of this exquisite piece of jewellery, i.e. neck-rings with hollow trumpet-shaped terminals cast in a single mould, which in Lithuania were especially popular in the second half of 2nd century-beginning of 3rd century AD (Michelbertas 1986).

In recent years, spectrometric analysis methods have been largely employed for the definition of elemental composition of copper alloys in artefacts and identification of the metallurgical alloy groups (Bayley *et al.* 2008; Pollard *et al.* 2018). The analysis of these main archaeometallurgical problems provides solutions to other important issues relating to the sourcing of raw materials, directions of distribution of raw materials or jewellery articles, diversity of manufacturing techniques and differences between the production of jewellery workshops. The answers to the issues raised above can, at least partially, be obtained by means of spectrometric analysis of the elemental composition of copper alloys in the eye fibulae that were mass produced in large quantities and spread beyond the borders of the Roman Empire to the vast areas of the *Barbaricum* as well as the study of the manufacturing technology of these jewellery items. The study of the then rare contemporaneous jewellery items involving complex manufacturing technology, i.e. neck-rings with hollow trumpet-shaped terminals, which were common throughout the Eastern Baltic Sea region, allows solving these issues at both regional and interregional (raw metal in the region, jewellers workshops, spread of jewellery articles and cultural influence) as well as trans-European level (exchange of raw materials, dissemination of cultural ideas and technologies within the *Barbaricum*).

The article presents data from the analysis of the composition of copper alloys in eye fibulae and neck-rings with hollow trumpet-shaped terminals by means of X-ray fluorescence (XRF) method as well as data obtained from the analysis of their manufacturing technology. 51 eye fibulae (out of 205 known in Lithuania) and 4 neck-rings (out of 16 known) have been analysed using XRF method. The finds are dated to the second half of the 1st century-2nd century AD. Based on the analyses, the examined objects were divided into metallurgical groups, commonly acknowledged in archaeometallurgical research. The analyses performed make it possible to interpret the eye fibulae equally as being imported or manufactured locally or regionally. At that time, the neck-rings with hollow trumpet-shaped terminals were most certainly manufactured in the settlements located in the Sambian peninsula and the region of the lower Nemunas (Memel, Neman) river. The XRF analysis of the composition of copper alloys of eye fibulae and neck-rings shows that there were ways of sourcing copper alloys or the raw materials required for the manufacture of jewellery or other articles that were identical to the ones used at the time throughout the Roman Empire and the *Barbaricum*. The results of the analyses of copper alloys in eye fibulae and neck-rings obtained by the authors may be compared with the published data, which allows having a better knowledge of the directions of distribution of the jewellery articles, as interregional goods, within the *Barbaricum* and the Eastern Baltic Sea region.

2.Archaeological background

The issues related to the typology, chronology, distribution and, partly, the alloy composition of these jewellery items, common in the *Barbaricum* of Central Europe, were widely studied (cf. Almgren 1923; Andrzejowski 1998; Andrzejowski and Cieśliński 2007; Gan 2015; Kunow 1998; Roxburgh and Olli 2019; Voß 2008). In Lithuania, however, only the distribution, typology and chronology of these fibulae have been reviewed (cf. Michelbertas 1986, 1997). Eye fibulae became common in Lithuania in the middle-second half of 1st century AD and disappeared in the second half or as late as the end of 2nd century AD, once the possibilities of the development of their design, manufacturing techniques and ornament had been exhausted. Moreover, at that time, new and more diverse jewellery designs, relevant to that period, emerged. According to the recent studies, 205 eye fibulae are known in Lithuania from 59 sites (Fig. 1).

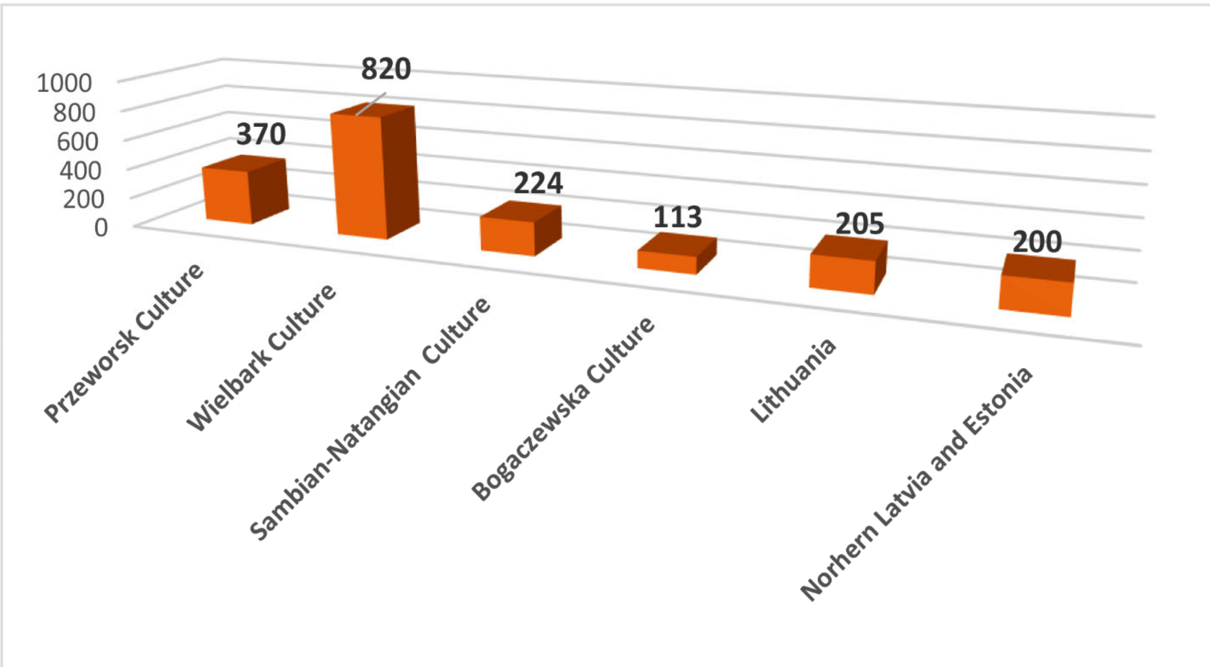

Figure 1. The number of the eye fibulae found in the Eastern Baltic region. After Andrzejowski and Cieśliński 2007; Michelbertas 1997; Roxburgh and Olli 2019 and authors of this paper. Diagram by Audronė Bliujienė.

The fibulae were discovered in all cultural areas of Lithuania of the Early Roman Age. However, the distribution of eye fibulae in Lithuania is uneven. Most of them were found in the western part of the Samogitian and Northern Lithuanian Barrow Culture area (Fig. 2; Appendix 1). Although a total of 76 fibulae are known to be from that area, nearly half of them were discovered in Paragaudis barrow cemetery (Michelbertas 1997). In the area of the Central Lithuanian Grave Fields Culture the largest number of eye fibulae was found in Sargėnai cemetery (43 fibulae). A relatively small number of eye fibulae is known to have come from the West Lithuanian Stone Circle Graves Culture area, with Lazdininkai (Kalnalaukis) cemetery being the most prolific site.

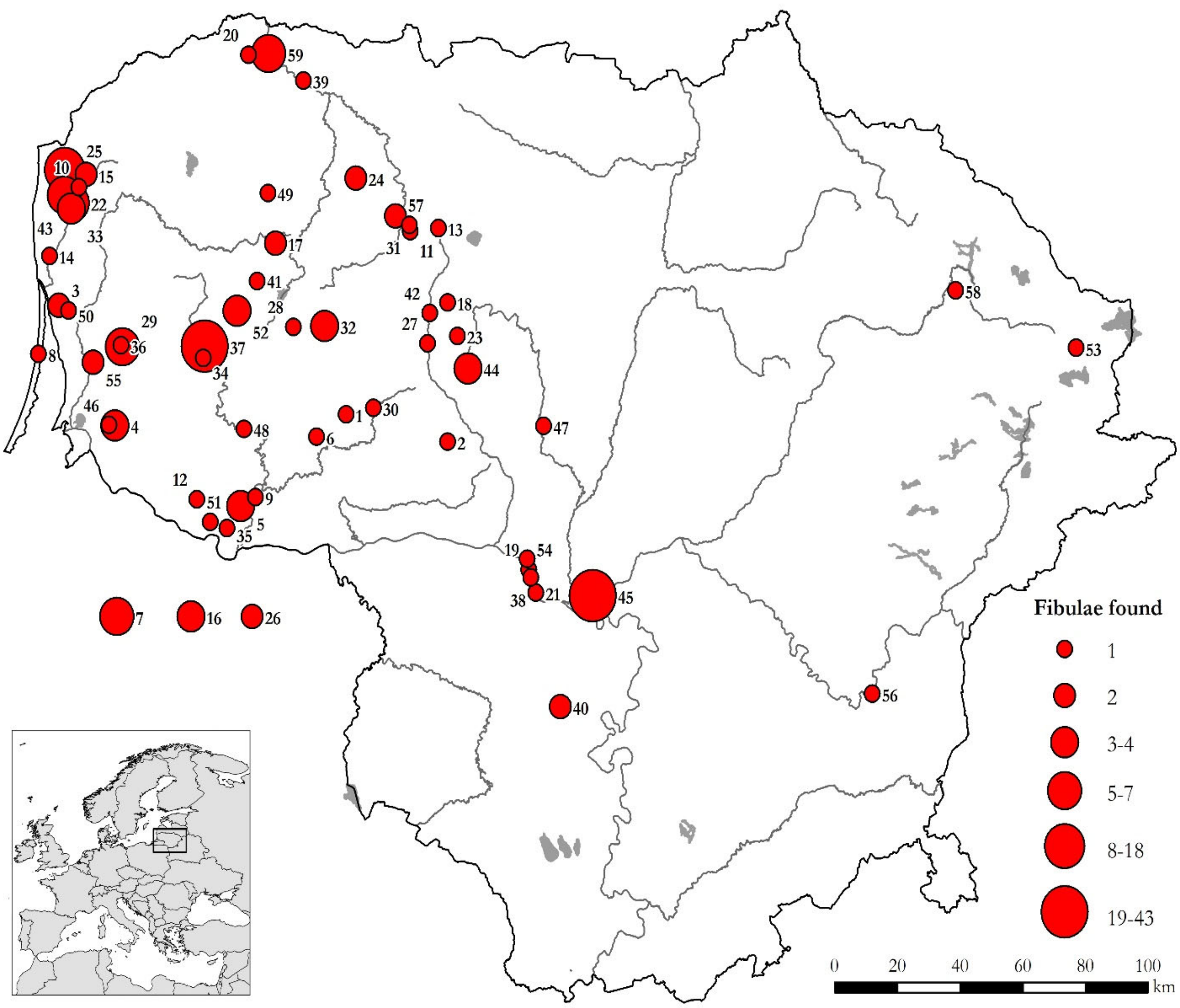

Figure 2. Find spots of the eye fibulae in Lithuania (see Appendix 1). After Michelbertas 1997 and authors of this paper. Drawing by Gediminas Petrauskas.

In the Early Roman Age, eye fibulae were quite common. For example, in Paragaudis barrow cemetery 61% of the graves contained eye fibulae, while in Sargėnai cemetery this type of fibulae was found in just over 12% of the graves. In Lithuania a larger number of eye fibulae were found in male graves (56) and a lesser number – in female (26) and children's (4) graves. However, due to lack of grave goods or indeterminate composition of grave inventories and other reasons related to destruction of graves or uncertain circumstances of discovery and the failure to carry out anthropological investigations, it is impossible to differentiate most of the graves containing eye fibulae according to gender or age of the deceased person. Commonly, one eye fibula was put into the grave of the dead person. The majority of eye fibulae were found together with other grave goods, jewellery items, dating to the second half of 1st century AD (including neck-rings with hollow trumpet-shaped terminals) as well as work tools and weapons (Michelbertas 1989, 1997; Svetikas 2019).

The typology and chronology of eye fibulae is defined on the basis of the universally accepted Oscar Almgren's (1923) classification. According to this classification, eye fibulae are attributed to Group III. In Almgren's typology fibulae of types A52-53 are classified as eye fibulae of the main series (to which also belong types A45-51, rarely found in the *Barbaricum*), while types A57-61 fall under the so-called Prussian series (Almgren 1923). However, it was not possible to identify the type of some of eye fibulae found in Lithuania either due to their poorly preserved state or because they were not retained in museum collections. In terms of fibula typology, the prevailing eye fibulae in the Baltic cultural areas are the Prussian series eye fibulae of types A60 and A61. There are few known main series eye fibulae of types A52 and A53 (Fig. 3, 4).

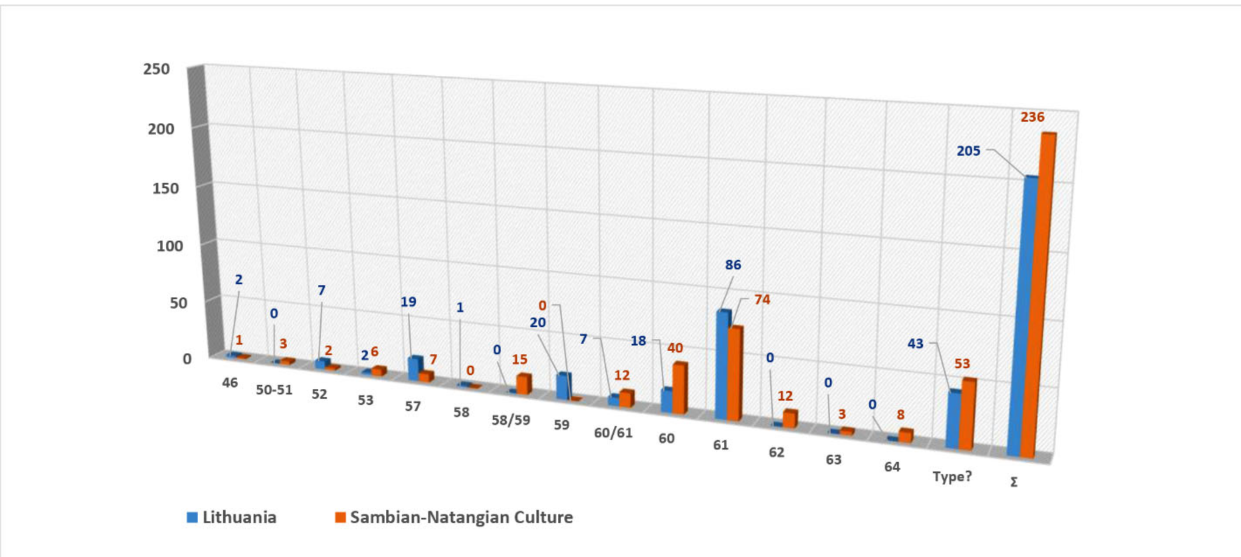

Figure 3. Typological distribution of the eye fibulae. After Chilińska-Früboes 2017, 2018 and authors of this paper. Diagram by Audronė Bliujienė.

Figure 4. Eye fibulae found in Lithuania: 1 – type A52 (Paragaudis, barrow 26, burial 3; LNM AR 721: 139); 2 – type A60 (Sandrausiškė barrow 2, burial 6; VDKM AR 1588: 18); 3 – type A57 (Gilvyčiai, stray find; VDKM AR 668: 7); 4, 5 – types A59 and A60 (former Kaunas Governorate, the exact place of discovery is unknown; LNM AR 58: 6; VDKM AR 672: 1). Photo by Audronė Bliujienė.

Eye fibulae of the main series close to type A46 are not large, they are 5-7 cm long and weigh about 10-15 grams. The early fibulae discovered in the northern provinces of the Roman Empire have similar dimensions and weight (Riha 1979: 68). The type A52 fibulae found in Lithuania are larger (approx. 7-9 cm long) and heavier (weigh 28-36 g). Eye fibulae of the Prussian series (of types A59-61) are the largest of all fibulae (mostly 6.8-7.8 cm in length), the better preserved ones weighing 15-26 grams.

In the Sambian-Natangian Culture and in Lithuania the neck-rings with hollow trumpet-shaped terminals became widespread in the middle-second half of 1st century AD (i.e. at a similar time as the eye fibulae); they disappeared in the beginning of 2nd century AD or as late as the last quarter of 2nd century AD (Michelbertas 1989, 1997; Rzeszotarska-Nowakiewicz 2010). Based on the design of these neck-rings, less technically intricate cast neck-rings with trumpet-shaped terminals were created, the first versions of which appeared as early as the end of 2nd century AD (Moora 1938; Michelbertas 1986). In other words, these ornate neck-rings were coexisting for some time with their simpler versions.

The largest number of neck-rings with hollow trumpet-shaped terminals was discovered in the place of their origin, i.e. in the Sambian-Natangian Culture area (Fig. 5; Appendix 2). It was there that the elaborate copper alloy neck-rings were created according to the Havor-type golden neck-rings. However, despite the attempt to replicate the techniques and sophisticated fastening which holds together the hollow terminals, the neck-rings crafted by the Baltic jewellers were simpler. According to latest available data, 16 neck-rings with hollow trumpet-shaped terminals were found from a total of 14 Lithuanian burial grounds and sites. The majority of such neck-rings is known to have come from the Samogitian, North Lithuanian and South Latvian Barrow Culture area. As many as three neck-rings and, most likely, fragments of bows of two more neck-rings were discovered while investigating Paragaudis barrow cemetery (Michelbertas 1997). To date, these are the only neck-rings with hollow trumpet-shaped terminals found in graves. The circumstances of discovery of other neck-rings found in Lithuania are unknown or uncertain, therefore, they may have originated from either destroyed graves or hoards.

The neck-rings with hollow trumpet-shaped terminals found in Paragaudis barrow cemetery with a diameter of 16-20 cm and weight of 140-213 g are one of the lightest in this type of jewellery. However, the neck-rings discovered in unclear circumstances in Vilkų Kampas, Adakavas and Paventė sites are 20-22 cm in diameter and weigh between 244-313 grams. In terms of size, the neck-rings from Glaušiai (25.5 cm in diameter) and Linkuva (24-26 cm and 24.9-33.2 cm in diameter) stand out, but regrettably, the circumstances of their discovery are uncertain (Bitner-Wróblewska and Sobczak 2009; Jaskanis *et al.* 1992). In fact, the size of these neck-rings equals that of the Scandinavian examples made of gold (cf. Nylén 1996; Nylén *et al.* 2005).

With regard to the manufacturing technique, the neck-rings with hollow trumpet-shaped terminals are the most technically sophisticated, largest and heaviest Early Roman Age jewellery items found in Lithuania. Though in Estonia and Finland fewer neck-rings with hollow trumpet-shaped terminals were found than in the lands of the Balts, nearly all of them belong to the unique types characteristic of the

Finno-Ugric context. However, not all these neck-rings have hollow terminals. The bodies of some neck-rings discovered in Estonia and Finland are widened and their trumpet-shaped terminals are enlarged. Such neck-rings were cast in one mould (Hackman 1905; Kivikoski 1973; Lang 2007; Oras 2015). In Estonia, these neck-rings are found in wealth deposits which contain artefacts common to the Balts, or they are found in *tarand* type graves. Each of the neck-rings weighs as much as about 1.9 kg (Lang 2007; Oras 2015).

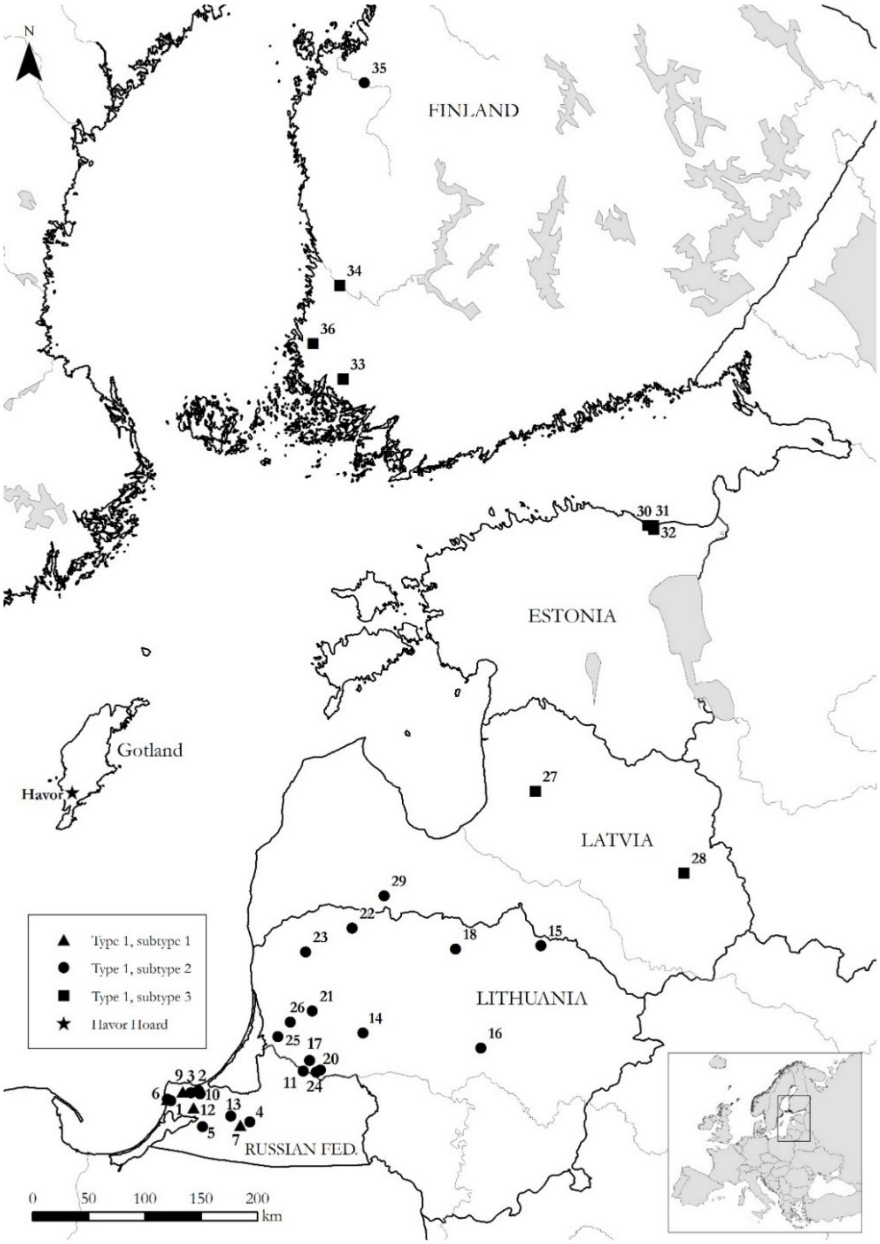

Figure 5. Find spots of the neck-rings with hollow trumpet-shaped terminals in the Eastern Baltic region and Finland (see Appendix 2). After Khomiakova 2011; Michelbertas 1989; Rzeszotarska-Nowakiewicz 2010; Skvortsov 2018 and authors of this article. Drawing by Gediminas Petrauskas.

The neck-rings with hollow trumpet-shaped terminals attracted researchers' attention as early as the beginning of 20th century (Bezzenberger 1904; Hackman 1905). Much attention was given to the typology and chronology of the neck-rings, though these issues have not been fully resolved yet.[20] Neck-rings of subtype 1.1 were found in the burial sites of the Sambian-Natangian Culture; the bow of these neck-rings is made from 6-11 twisted wires. The neck-rings are closed with a fastening element fixed to the ends of the hollow trumpet-shaped terminals, some of the neck-rings have profiled trumpet-shaped terminals, while others – sheet metal terminals (Fig. 6). In both Scandinavian and antique[21] prototypes as well as in the Baltic versions the ends of the neck-ring's bow terminate in a truncated cone-shaped 'box'. However, unlike their prototypes, the sides of the trumpets of neck-rings designed by the Baltic jewellers are not ornamented, if made of metal sheet.

The technique used in subtype 1.2 neck-rings with hollow trumpet-shaped terminals is less sophisticated. The bows of the neck-rings are cast and smooth, their terminals are hollow. Besides, the ends of the neck-rings are not hooked and are left open. Trumpets of some neck-rings are made of metal sheet (subtype 1.2a), while hollow trumpet-shaped terminals of other neck-rings are cast (subtype 1.2b). It is likely that subtype 1.2b neck-rings influenced the appearance of the Finno-Ugric neck-rings with massive terminals. Some unique neck-rings with trumpet-shaped terminals have been discovered on the Lithuanian territory in Glaušiai and Linkuva sites. Though terminals of these neck-rings are hollow, they are cylinder-shaped and have two or three flat discs around them (subtype 1.2c) (Bitner-Wróblewska and Sobczak 2009; Jaskanis *et al.* 1992; Kulikauskienė and Rimantienė 1958). In their construction the neck-rings with hollow trumpet-shaped terminals from Glaušiai and Linkuva resemble one type of the Celtic gold *torcs* (Eluère 1987). However, there is a large chronological gap between subtype 1.2c neck-rings found in Lithuania and the La Tène Celtic specimens.

[20] The present article uses, as a reference point, the typological scheme of neck-rings with hollow trumpet-shaped terminals proposed by Aleksandra Rzeszotarska-Nowakiewicz (2010) as well as revised chronology. This typological scheme has been revised according to neck-ring specimens found in Lithuania by introducing two additional a-c subtypes of type 1.

[21] Here reference is made to Olbia, a Greek colony on the shore of the Southern Bug estuary (today Parutine, Mykolaiv Oblast, Ukraine), and their gold neck-rings with trumpet-shaped terminals from the 1st century AD. Again, similar gold neck-rings were found at Zalevki near Smela (Cherkasy Oblast, Ukraine (Nylén 1996; Rzeszotarska-Nowakiewicz 2010).

Figure 6. Neck-rings with hollow trumpet-shaped terminals: 1 – Regehnen/Kalinovo, stray find, reconstruction (Skvortsov 2018); 2 – Koddien/Velikolukskoe, finding circumstances unknown (SB MVF PM IV 10.5233); 3 – Adakavas, finding circumstances unknown (LNM AR 429: 13); 4 – Warengen/Kotelnikovo (SB MVF PM III 1621021); 5 – Plateliai (Dvarlaukis), finding circumstances unknown (LNM AR 26: 1); 6 – Paragaudis barrow 32 (LNM AR 721: 149); 7 – Paragaudis barrow 38, burial 2 (LNM AR 721: 70); 8 – Vilkų kampas, finding circumstances unknown (VDKM AR 1585: 1); 9 – Paventė, finding circumstances unknown (VDKM AR 823); 10 – Grebieten/Okunevo, finding circumstances unknown (SB MVF PM V.184.8017); 11 – Paragaudis barrow 2, burial 1 (LNM AR 721: 5). 1, 2, 4 – subtype 1.1; 3, 9, 11 – subtype 1.2b; 5–8, 10 – subtype 1.2a; 1 – Copper alloy, silver, enamel; for the composition of other neck-rings see Table 1. Photo by Audronė Bliujienė.

3. Methods

3.1. X-ray fluorescence (XRF)

X-ray fluorescence (XRF) analysis was conducted of the composition of copper alloys used to make eye fibulae and neck-rings with hollow trumpet-shaped terminals to identify the main alloying elements of the copper alloys, establish the composition of the alloys, classify the alloys into groups and compare them with those found in the *Barbaricum*. The artefacts analysed were conserved and coated with corrosion deposits (patina layer), which possibly contains remains from the archaeological context. Corroded metal is one of the most problematic materials to investigate with XRF because the outer corrosion has an altered composition relative to its original (uncorroded) state. The analysis of the finds was carried out by means of a portable XRF spectrometer Niton XL3t (power 2 W, voltage – 50kV, detector area ~ 50 mm^2, producer Thermo Fisher calibration mode 'General Metals'). Each find was irradiated (for 30 s) in at least two (in the case of eye fibulae) and 3-5 (in the case of neck-rings) spots. The measuring spot has been selected according to the geometry of the artefact and its separate parts, which could be made of a different alloy.

3.2. Technological Analysis

The manufacturing techniques of eye fibulae and neck-rings with hollow trumpet-shaped terminals were defined through a visual examination of the artefacts in museums and by photographing with a digital microscope (Q-scope 9.0 MP - 200x) the specific manufacturing features and repairs, as well as surface treatment techniques and methods of ornamentation. Also, several eye fibulae and neck-rings were examined in order to assess their condition, i.e. degree of corrosion, construction and design subtleties using portable diagnostic X-ray device *Econet meX +100*. Considering the differences in the thickness of metals, their degree of corrosion and technological characteristics, two X-ray imaging modes were used – I (voltage - 80kV, exposure - 2.0 mAs) and III (voltage - 80kV, exposure - 2.0 mAs).

4. Results

The results of XFR analysis of eye fibulae and neck-rings are given in Table 1. The found values were averaged and used as data (given in %) for further analysis. Chemical elements are listed in the order of decreasing average alloy values. The chemical elements were established and presented without eliminating the low values found for elements, such as antimony, bismuth, silver, nickel and etc., which are significant in the analysis of recycling and reuse of metal objects. However, in this case, we have confined ourselves to classification by the amount of each alloying element present (zinc, tin and lead), displayed as a ternary diagram (plotting only the normalised values of these three elements). Classification of alloys was conducted according to J. Bayley and S. Butcher (2004). The following ternary diagram visualises the alloy ratios of all 51 analysed eye fibulae (Fig. 7). The effects of corrosion on the alloying elements tin, lead and zinc, when plotted as a ratio in ternary diagrams, did not prevent the measurements from falling into broad compositional groups (Roxburgh *et al.* 2019). This visualisation method is particularly useful as it allows clusters of results to be compared to one another. Compositional analysis of the alloys yielding intermediate/marginal results, such as brass/gunmetal, must take into account the possible effect of corrosion on copper alloys, which may lead to the reduction of the amount of zinc in copper alloys. Indeed, radiographic images of some eye fibulae reveal not only their construction and manufacture defects (the jeweller failed to place the fastening of the fibula exactly in the middle of the foot), but also the poorly preserved condition of the alloy as a result of corrosion (Fig. 8). However, zinc decline in copper alloys is related to the shift in the composition of copper alloys that was taking place since 1st century AD in the Roman Empire and provinces, resulting in a steady decline in zinc level (cf. Caley 1964; Dungworth 1997; Pollard *et al.* 2015). Another reason for zinc decline is attributable to recycling of copper alloys, which gained momentum already in the Early Roman Age, thereby gunmetal with different percentages of Zn, Pb and Sn was becoming more common (Bayley and Butcher 2004; Pollard *et al.* 2015; Roxburgh *et al.* 2016). The trend of change in copper alloy composition as well as that of alloy recycling is also observed for the alloys discussed in this article.

Arte-fact/ type	Dis-trict	ID	Cu	Zn	Sn	Pb	Fe	Sb	Ag	Bi	Ni	Mn	Cr	Mo	Nb	Pd	Se	Ti	V	W	Zr	Alloy type
Eye fibula, A52	Šiauliai	Kyb: 496-3	**93.68**	**5.07**	**0.17**	**0.23**	**0.65**	**0.07**	< 0.1	< 0.01	< 0.01	< 0.01	< 0.92	**0.042**	**0.026**	< 0.01	< 0.01	< 0.06	< 0.07	< 0.13	< 0.004	Brass
A52	Šiauliai	Kyb: 496-5	**8.42**	**10.58**	**3.2**	**1.3**	**0.61**	**0.19**	**0.13**	< 0.01	< 0.01	< 0.01	< 0.92	**0.051**	**0.031**	< 0.01	< 0.01	< 0.06	< 0.07	**1.45**	< 0.006	Brass/ gunmetal
Eye fibula, A57	Telšiai	Keg: 1678-1	**85.34**	**7.6**	**4.39**	**1.87**	**0.59**	**0.13**	< 0.10	**0.02**	< 0.01	< 0.01	< 0.92	< 0.003	< 0.003	< 0.01	< 0.01	< 0.07	< 0.07	< 0.13	< 0.004	Gunmetal
A57	Šiauliai	Gil: 668-7	**86.47**	**8.98**	**3.01**	**0.91**	**0.51**	**0.1**	< 0.10	**0.02**	< 0.01	< 0.01	< 0.92	< 0.003	< 0.002	< 0.01	< 0.01	< 0.06	< 0.07	< 0.13	< 0.004	Gunmetal
A57	Šiauliai	Jon: 645-14	**90.49**	**6.68**	**1.32**	**0.73**	**0.66**	**0.07**	< 0.10	**0.02**	< 0.01	< 0.01	< 0.92	< 0.012	**0.01**	< 0.01	< 0.01	< 0.06	< 0.07	< 0.13	< 0.004	Brass
A57	Kaunas	Sar: 1616-141	**74.78**	**22.65**	**0.38**	**0.42**	**0.86**	**0.04**	< 0.10	< 0.01	< 0.01	< 0.01	< 0.92	< 0.003	**0.01**	< 0.01	< 0.01	< 0.06	< 0.07	**0.86**	< 0.004	Brass
A57	Kaunas	Sar: 1616-224	**81.93**	**11.99**	**2.39**	**0.46**	**0.24**	**0.05**	< 0.10	< 0.01	< 0.02	< 0.01	< 0.92	< 0.003	< 0.003	< 0.01	< 0.01	< 0.06	< 0.07	**0.24**	< 0.004	Brass
A57	Kaunas	Sar: 1616-80	**85.98**	**11.78**	**1.52**	**0.35**	**0.21**	**0.1**	< 0.10	< 0.01	< 0.01	< 0.01	< 0.92	< 0.003	< 0.003	< 0.01	< 0.01	< 0.06	< 0.07	< 0.14	< 0.004	Brass
A57	Kaunas	Sar: 1229-45	**76.57**	**13.91**	**7.83**	**0.64**	**0.69**	**0.11**	< 0.10	< 0.01	< 0.01	< 0.01	< 0.92	< 0.003	< 0.003	< 0.01	< 0.01	**0.10**	< 0.07	**0.19**	< 0.004	Gunmetal
A57	Kaunas	Sar: 1616-187	**76.4**	**7.9**	**11.73**	**2.61**	**1.07**	**0.08**	< 0.10	**0.04**	< 0.01	< 0.01	< 0.92	< 0.003	< 0.003	< 0.01	< 0.01	**0.161**	< 0.07	< 0.13	< 0.004	Gunmetal

Eye fibula, A60	Raseiniai	San: 1588-19	**84.24**	**3.46**	**9.6**	**0.99**	**1.15**	**0.2**	**0.21**	**0.02**	< 0.01	< 0.01	< 0.92	< 0.003	< 0.003	< 0.01	**0.042**	< 0.08	< 0.07	< 0.13	< 0.004	Gunmetal
A60	Kaunas	Sar: 1616-64	**85.73**	**12.46**	**1.07**	**0.36**	**0.29**	**0.07**	< 0.10	< 0.01	< 0.01	< 0.01	< 0.92	< 0.003	< 0.003	< 0.01	< 0.01	< 0.06	< 0.07	< 0.13	< 0.004	Brass
A60	Kaunas	Sar: 1616-63	**84.26**	**9.58**	**4.47**	**0.94**	**0.62**	**0.12**	< 0.10	< 0.01	< 0.01	< 0.01	< 0.92	< 0.003	< 0.003	< 0.01	< 0.01	< 0.06	< 0.07	< 0.13	< 0.004	Brass/gunmetal
A60	Kaunas	Sar: 1616-151	**86.05**	**8.67**	**3.72**	**0.67**	**0.75**	**0.13**	< 0.10	< 0.01	< 0.01	< 0.01	< 0.92	< 0.003	< 0.003	< 0.01	< 0.01	< 0.06	< 0.07	< 0.13	< 0.004	Brass/gunmetal
Eye fibula, A61	Kelmė	Paa: 304	**88.36**	**5.75**	**5**	**0.52**	**0.22**	**0.15**	< 0.10	< 0.01	< 0.01	< 0.01	< 0.92	< 0.003	< 0.003	< 0.01	< 0.01	< 0.06	< 0.07	< 0.13	< 0.004	Brass/gunmetal
A61	Kelmė	Paa: 301	**95.6**	**3.97**	**0.04**	**0.15**	**0.2**	**0.058**	< 0.10	< 0.01	< 0.01	< 0.01	< 0.92	< 0.003	< 0.003	< 0.01	< 0.02	< 0.06	< 0.07	< 0.13	< 0.004	Brass
A61	Kelmė	Paa: 128	**71.9**	**4.17**	**20.39**	**1.198**	**1.88**	**0.21**	< 0.10	< 0.01	< 0.01	< 0.01	< 0.92	< 0.003	< 0.003	< 0.01	< 0.01	**0.23**	< 0.07	< 0.13	< 0.004	Bronze
A61	Kelmė	Paa: 621	**86.03**	**8.18**	**4.19**	**0.83**	**0.61**	**0.15**	< 0.10	< 0.01	< 0.01	< 0.01	< 0.92	< 0.003	< 0.003	< 0.01	< 0.01	**0.06**	< 0.07	< 0.13	< 0.004	Brass/gunmetal
A61	Kelmė	Mai: 460-1	**73.05**	**22.65**	**0.64**	**0.73**	**0.31**	**0.14**	< 0.10	< 0.01	< 0.02	< 0.01	< 0.92	< 0.003	< 0.003	< 0.01	< 0.01	**0.33**	< 0.07	**2.17**	< 0.004	Brass
A61	Kretinga	Kur: 1-63	**86.04**	**4.14**	**8.33**	**0.75**	**0.59**	**0.14**	< 0.10	< 0.01	< 0.01	< 0.01	< 0.92	< 0.003	< 0.003	< 0.01	< 0.01	< 0.06	< 0.07	< 0.13	< 0.004	Gunmetal/bronze
A61	Kretinga	Kur: 1-64	**60.53**	**23.59**	**11.15**	**2.01**	**1.95**	**0.31**	< 0.10	< 0.01	< 0.02	< 0.01	< 0.92	< 0.003	< 0.003	< 0.01	< 0.01	**0.10**	< 0.07	**0.37**	< 0.004	Brass/gunmetal

A61	Kretinga	Kur: 1-118	**79.1**	**4.39**	**9.84**	**5.58**	**0.77**	**0.25**	<0.10	<0.01	<0.01	<0.01	<0.92	<0.003	<0.003	<0.01	<0.01	<0.08	<0.07	<0.13	<0.004	Bronze/leaded
A61	Kretinga	Kur: 1-126	**88.2**	**5.45**	**4.42**	**1.05**	**0.69**	**0.14**	<0.10	<0.01	<0.01	<0.01	<0.92	<0.003	<0.003	<0.01	<0.01	<0.06	<0.07	<0.13	<0.004	Gunmetal/bronze
A61	Kretinga	Kur: 1-129	**81.86**	**5.57**	**4.42**	**1.13**	**6.78**	**0.23**	<0.10	<0.01	<0.01	<0.01	<0.92	<0.003	<0.003	<0.01	<0.01	<0.06	<0.07	<0.13	<0.004	Gunmetal/bronze
A61	Kretinga	Kur: 1-156	**79.46**	**14.7**	**4.42**	**0.52**	**0.47**	**0.14**	<0.10	<0.01	<0.02	<0.01	<0.92	<0.003	<0.003	<0.01	<0.01	<0.06	<0.07	**0.36**	<0.004	Brass/gunmetal
A61	Raseiniai	San: 1588-24	**79.94**	**5.68**	**11.79**	**1.015**	**1.31**	**0.169**	<0.10	<0.01	<0.01	<0.01	<0.92	<0.003	<0.003	<0.01	<0.01	<0.07	<0.07	<0.13	<0.004	Gunmetal/bronze
A61	Šilalė	Paj: 572-9	**82.43**	**8.66**	**3.1**	**3.51**	**0.56**	**0.12**	<0.10	<0.01	<0.01	<0.01	**1.59**	<0.021	<0.003	<0.01	<0.01	<0.06	<0.07	<0.13	<0.004	Gunmetal/leaded
A61	Utena	Vos: 75-16	**89.1**	**7.15**	**1.47**	**0.42**	**1.05**	**0.13**	<0.10	<0.01	<0.01	**0.7**	<0.92	<0.003	<0.003	<0.01	<0.01	<0.06	<0.07	<0.13	<0.004	Brass
A61	Kaunas	Vil: 787-13	**89.48**	**5.06**	**3.96**	**0.55**	**0.76**	**0.15**	<0.10	<0.01	<0.02	<0.01	<0.92	<0.003	<0.003	<0.01	<0.01	<0.06	<0.07	<0.13	<0.004	Brass/gunmetal
A61	Kaunas	Pas: 6571-1	**80.45**	**13.86**	**4.53**	**0.3**	**0.35**	**0.14**	<0.10	<0.01	<0.02	<0.01	<0.92	<0.003	<0.003	<0.01	<0.01	<0.06	<0.07	**0.37**	<0.004	Brass/gunmetal
A61	Kaunas	Sar: 1229-49	**84.31**	**10.73**	**3.83**	**0.53**	**0.46**	**0.14**	<0.10	<0.01	<0.01	<0.01	<0.92	<0.003	<0.003	<0.01	<0.01	<0.06	<0.07	<0.13	<0.004	Brass/gunmetal
A61	Kaunas	Sar: 1229-60	**81.46**	**1.14**	**15.83**	**0.96**	**0.35**	**0.12**	<0.10	<0.01	0.025	<0.01	<0.92	<0.003	<0.003	<0.01	<0.01	**0.1**	<0.07	<0.13	<0.004	Bronze

A61	Kaunas	Sar: 1229-68	**84.58**	**10.43**	**3.7**	**0.74**	**0.4**	**0.14**	< 0.10	< 0.01	< 0.01	< 0.01	< 0.92	< 0.003	< 0.003	< 0.01	< 0.01	< 0.06	< 0.07	< 0.13	< 0.004	Brass/gunmetal
A61	Kaunas	Sar: 1616-61	**76.18**	**18.52**	**4.32**	**0.33**	**0.27**	**0.12**	< 0.10	< 0.01	< 0.01	< 0.01	< 0.92	< 0.003	**0.005**	< 0.01	< 0.01	< 0.06	< 0.07	**0.26**	< 0.004	Brass/gunmetal
A61	Kaunas	Sar: 1616-69	**80.49**	**15.41**	**3.6**	**0.2**	**0.11**	**0.1**	< 0.10	< 0.01	< 0.02	< 0.01	< 0.92	< 0.003	**0.005**	< 0.01	< 0.01	< 0.06	< 0.07	**0.15**	< 0.004	Brass/gunmetal
A61	Kaunas	Sar: 1616-68	**80.6**	**16.75**	**2.17**	**0.28**	**0.09**	**0.09**	< 0.10	< 0.01	< 0.01	< 0.01	< 0.92	< 0.003	< 0.004	< 0.01	< 0.01	< 0.06	< 0.07	< 0.13	< 0.004	Brass/gunmetal
A61	Kaunas	Sar: 1616-90	**81.37**	**16.24**	**1.51**	**0.26**	**0.27**	**0.07**	< 0.10	< 0.01	< 0.02	< 0.01	< 0.92	< 0.003	**0.005**	< 0.01	< 0.01	< 0.06	< 0.07	**0.29**	< 0.004	Brass/gunmetal
A61	Kaunas	Sar: 1616-97	**84.93**	**11.86**	**2.16**	**0.59**	**0.34**	**0.09**	< 0.10	< 0.01	< 0.01	< 0.01	< 0.92	< 0.003	< 0.003	< 0.01	< 0.01	< 0.06	< 0.07	< 0.13	< 0.004	Brass/gunmetal
A61	Kaunas	Sar: 1616-103	**80.82**	**14.58**	**3.46**	**0.56**	**0.42**	**0.13**	< 0.10	< 0.01	< 0.02	< 0.01	< 0.92	< 0.003	< 0.003	< 0.01	< 0.01	< 0.06	< 0.07	< 0.13	< 0.004	Brass/gunmetal
A61	Kaunas	Sar: 1616-102	**72.41**	**23.15**	**3.11**	**0.64**	**0.14**	**0.16**	< 0.10	< 0.01	< 0.01	< 0.01	< 0.92	< 0.003	**0.006**	< 0.01	< 0.01	< 0.06	< 0.07	**0.38**	< 0.004	Brass
A61	Kaunas	Sar: 1616-129	**87.31**	**8.26**	**3.58**	**0.56**	**0.18**	**0.1**	< 0.10	< 0.01	< 0.01	< 0.01	< 0.92	< 0.003	< 0.003	< 0.01	< 0.01	< 0.06	< 0.07	< 0.13	< 0.004	Brass/gunmetal
A61	Kaunas	Sar: 1780-10	**84.79**	9	**4.48**	**0.57**	**0.98**	**0.13**	< 0.10	< 0.01	< 0.01	< 0.01	< 0.92	< 0.003	< 0.003	< 0.01	< 0.01	< 0.06	< 0.07	< 0.13	< 0.004	Brass/gunmetal
A61	Kaunas	Sar: 1616-138	**75.42**	**20.55**	**2.86**	**0.15**	**0.2**	**0.11**	< 0.10	< 0.01	< 0.01	< 0.01	< 0.92	< 0.003	< 0.004	< 0.01	< 0.01	< 0.06	< 0.07	< 0.13	< 0.004	Brass

A61	Kaunas	Sar: 1616-179	**72.23**	**19.05**	**5.47**	**1.57**	**1.07**	**0.13**	<0.10	<0.01	<0.02	<0.01	<0.92	<0.003	**0.005**	<0.01	<0.01	<0.06	<0.07	**0.52**	<0.004	Brass/gunmetal
A61	Kaunas	Sar: 1817-75	**75.655**	**13.94**	**8.98**	**0.67**	**0.55**	**0.14**	<0.10	<0.01	<0.02	<0.01	<0.92	<0.003	<0.003	<0.01	<0.01	<0.06	<0.07	<0.13	<0.004	Brass/gunmetal
A61	ND	Kau: 58-7	**69.28**	**26.81**	**2.85**	**0.45**	**0.17**	**0.1**	<0.10	<0.01	<0.01	<0.01	<0.92	<0.003	<0.003	<0.01	<0.01	<0.06	<0.07	**0.3395**	<0.004	Brass
A61	ND	Kau: 58-8	**73.78**	**19.08**	**4.53**	**0.27**	**0.65**	**0.17**	<0.10	<0.01	<0.02	<0.01	<0.92	<0.003	<0.003	<0.01	<0.01	<0.06	<0.07	**1.51**	<0.004	Brass/gunmetal
A61	Kretinga	Kur: 1-119	**80.14**	**13.13**	**4.08**	**0.33**	**0.5**	**0.35**	<0.10	<0.01	<0.01	<0.01	<0.92	<0.003	<0.003	<0.01	<0.01	<0.06	<0.07	**1.53**	<0.004	Brass/gunmetal
A61	Telšiai	Keg: 917	**81.56**	**4.6**	**11.26**	**0.83**	**1.34**	**0.24**	<0.10	**0.02**	<0.01	<0.01	<0.92	<0.003	<0.003	<0.01	<0.01	**0.12**	<0.07	<0.13	<0.004	Gunmetal/bronze
Artefact	**Region**	**ID**	Cu	Zn	Sn	Pb	Fe	Sb	Ag	Bi	Ni	Mn	Cr	Mo	Nb	Pd	Se	Ti	V	W	Zr	**Alloy type**
Neck-ring	Tauragė	ADA 429_13_5	73.69	2.82	7.91	14.83	0.39	0.22	<0.10	<0.01	<0.01	<0.01	<0.92	<0.003	<0.003	<0.01	<0.01	**0.10**	<0.07	<0.13	<0.005	Leaded bronze
	Plungė	PLA 26_1_5	84.48	7.23	5.9	0.93	0.91	0.18	**0.20**	**0.02**	<0.01	<0.01	<0.92	<0.003	<0.003	<0.01	<0.01	**0.22**	**0.13**	<0.13	<0.004	Gunmetal
	Šilutė	Vilk 1585 1 1	83.86	12.26	1.19	0.86	1	0.09	<0.10	<0.01	<0.01	<0.01	<0.92	<0.003	<0.003	<0.01	<0.01	<0.06	<0.07	<0.13	<0.004	Brass
	Mažeikiai	Pav 823 1 4	90.43	7.63	0.15	0.54	0.64	0.04	<0.10	<0.01	<0.01	<0.01	<0.92	<0.01	**0.021**	<0.01	<0.01	<0.06	<0.07	<0.13	<0.014	Brass

Table 1. Elemental composition (wt%) of the eye fibulae and neck-rings with hollow trumpet-shaped terminals from Lithuania based on XRF analysis. Classification of the alloy types after Bayley and Butcher 2004.

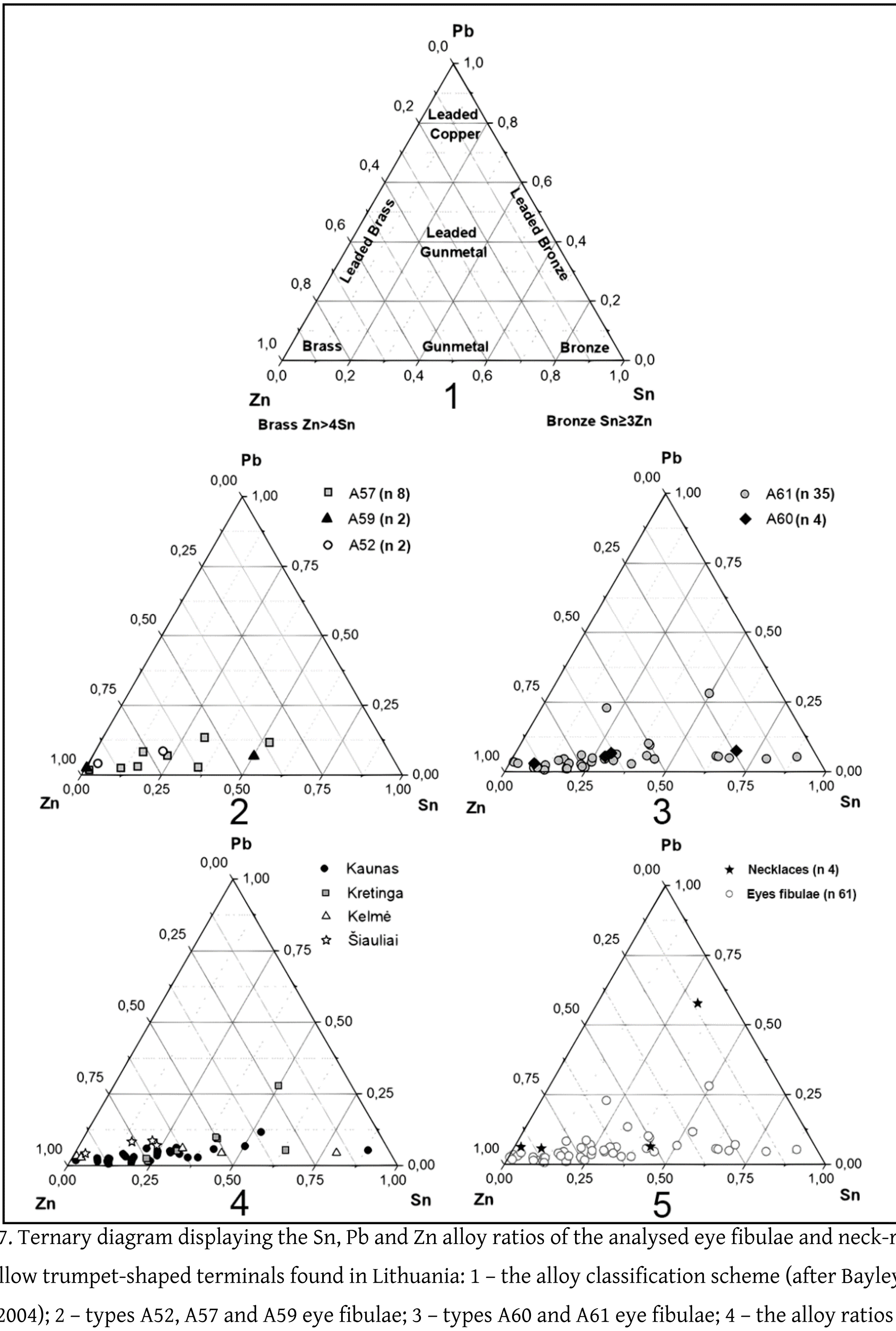

Figure 7. Ternary diagram displaying the Sn, Pb and Zn alloy ratios of the analysed eye fibulae and neck-rings with hollow trumpet-shaped terminals found in Lithuania: 1 – the alloy classification scheme (after Bayley and Butcher 2004); 2 – types A52, A57 and A59 eye fibulae; 3 – types A60 and A61 eye fibulae; 4 – the alloy ratios of the analysed eye fibulae from Kaunas city, Kretinga, Kelmė and Šiauliai districts; 5 – the alloys of the neck-rings (stars) compared to the alloys of all types of eye fibulae (circles). Diagram by Jurga Bagdzevičienė.

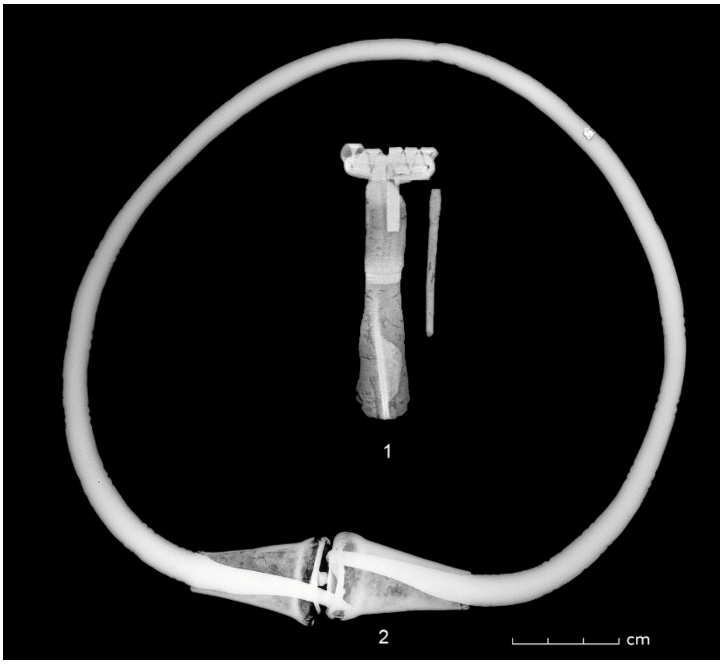

Figure 8. Radiograph of the A60 type eye fibula from Barzūnai burial 3 (LNM GRD 108822) (1) and the neck-ring with hollow trumpet-shaped terminals from Paragaudis barrow 2, burial 1 (LNM AR721: 5). **R**adiograph by Rapolas Vedrickas.

5. Discussion

The findings of XRF analysis of eye fibulae indicate that the type A52 eye fibulae of the main series were made of brass. Classification of the alloys in the eye fibulae of the Prussian series of types A57, A59 and A60 suggests that they were manufactured of brass, gunmetal and bronze. However, a number of alloys falling under intermediate/marginal groups, have been detected, i.e. brass/gunmetal or gunmetal/bronze. Therefore, the assessment of the composition of such artefacts must take into account the possible effect of copper alloy corrosion, along with the overall process of zinc decline as well as zinc loss through recycling and mixing of different alloys (metal scrap). The intermediate/marginal results obtained for copper alloys due to their recycling may be traced by analysing trace elements in the copper objects based on the presence or absence of four key trace elements in the copper itself – arsenic, antimony, silver and nickel (Bray and Pollard 2012; Pollard and Bray 2014). However, the present analysis was confined to identification of the main alloying elements of copper alloys and classification of alloys into metallurgical groups, since identification of alloy impurities requires a larger dataset. In the case of gunmetal, the analysis was based on the increase in the amount of Sn, which is detected by XRF analysis of the surface of the objects – tin comes to the surface due to corrosion process.

The sites in Lithuania like those of the Sambian-Natangian Culture mostly yield type A61 eye fibulae. The analysed fibulae of this type were made of more varied copper alloys; though fibulae made of brass and brass/gunmetal prevail, fibulae made of gunmetal/bronze and bronze have also been found.

Considering the elemental composition of copper alloys of eye fibulae from Wielbark and Przeworsk cultures, which were the southern neighbours of the Balts, and fibulae of this type found in the northern provinces of the Roman Empire, we can assume that most of the jewellery was made of brass and brass/gunmetal (Andrzejowski 1998; Gan 2015; Pietrzak 1997; Roxburgh et al. 2016, 2019) (Fig. 9). However, the zinc content of the alloy of the main series eye fibulae found in the territories of Przeworsk and Wielbark cultures is higher than that of the Prussian series fibulae alloy (Andrzejowski 1998; Pietrzak 1997).

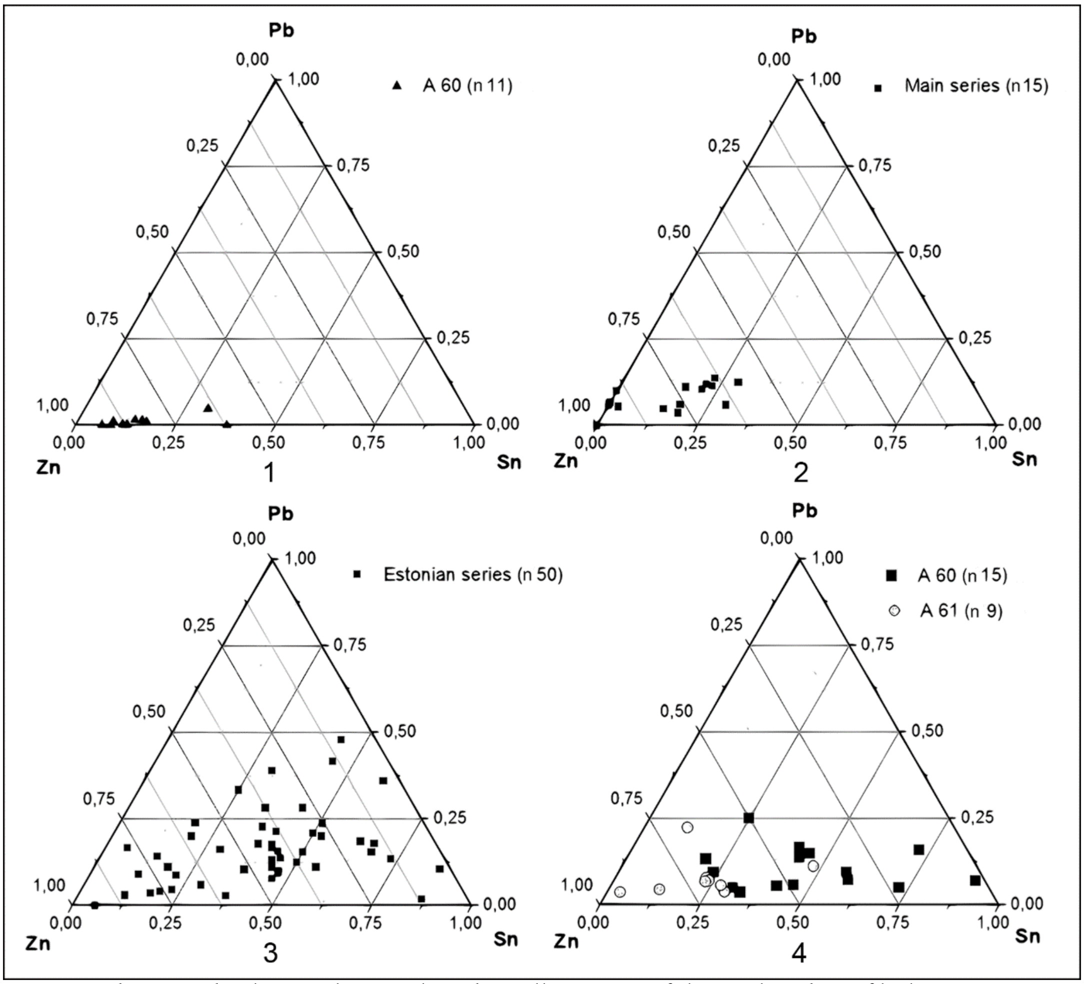

Figure 9. Ternary diagram displaying the Sn, Pb and Zn alloy ratios of the analysed eye fibulae: 1 – type A60 fibulae from the Wielbark *Culture cemetery at Czarnówka 5 in Poland*; 2 – the main series eye fibulae from the North Eastern Latvia and North Eastern Estonia; 3 – the Estonian series eye fibulae from the North Eastern Latvia and North Eastern Estonia. 4 – the Prussian series eye fibulae from the North Eastern Latvia and North Eastern Estonia. After Gan 2015; Roxburgh and Olli 2019. Diagram by Jurga Bagdzevičienė.

Eye fibulae of the main series belonging to the northern neighbours of the Balts, Finno-Ugrians, who lived in Northern Latvia and North Eastern Estonia, were made of brass, as was the case in Lithuania (Fig. 9). At the same time, the distinctive eye fibulae of the Estonian series were made of a wider range of copper alloys, including brass, gunmetal, leaded bronze and bronze (Roxburgh and Olli 2019). The copper alloys of fibulae of types A60 and A61 of the Prussian series found in Northern Latvia and North Eastern Estonia are similar to those of the fibulae of the same type discovered in Lithuania. XRF analyses of the eye fibulae confirm that, already in the Early Roman Age, there was a mechanism of dissemination of goods and cultural ideas between the Balts and Finno-Ugrians (cf. Banytė-Rowell and Bitner-Wróblewska 2005; Bliujienė 2005; Olli and Roxburgh 2018; Roxburgh and Olli 2019). Composition of the copper alloys of the main series eye fibulae and their spread in the Eastern Baltic region shows that the fibulae could have found their way to Northern Latvia and North Eastern Estonia through Baltic intermediaries living on the territory of Lithuania. At the same time, the eye fibulae of the Prussian series or raw metal used in their manufacture may have been brought to these northern territories from or through Western Lithuania.

Comparison of the copper alloys of eye fibulae found in Lithuania's neighbouring regions and the *Barbaricum* makes it possible to conclude that, already in the Early Roman Age, the fibulae were manufactured from similar copper alloys, among which brass and gunmetal prevail. The larger part of the eye fibulae found in the northern provinces of the Roman Empire are mostly made of brass (cf. Bayley and Butcher 2004; Roxburgh et al. 2016). Therefore, at least two assumptions can be made with regard to the appearance of eye fibulae in the northern *Barbaricum*, including Lithuania, and their archaeometallurgical analysis. First, the fibulae could have been brought to the Northern *Barbaricum* as import; second, the manufacturing of eye fibulae types by utilizing simpler technologies and imitating the imported fibulae was undertaken by local craftsmen-jewellers. However, with the level of knowledge available, it is most likely that eye fibulae of the main series and part of the fibulae of the Prussian series were imported during the whole period of their use, the other part being a local product. Certainly, in order to ensure local production, it would be necessary to have a continuous flow of raw materials as well as craftsmen-jewellers who would be capable to make eye fibulae and other items.

Eye fibulae reached the Eastern Baltic region, including the territory of modern Lithuania, as import from the places of their manufacture in the northern provinces of the Roman Empire through a number of intermediaries. Such assumption could be justified by the fact that eye fibulae of type A46, dated to the first half of 1st century AD, are very seldom found outside the borders of the Roman Empire. Single specimens of type A46 eye fibulae have been discovered in the burial sites of Przeworsk and Wielbark cultures (Kunow 1998; Mączyńska 2004). Only one fibula that is close to type A46 is known from grave

13 of the Sambian-Natangian Culture Gurjevsk Novy (formerly Trausitten) cemetery. It is believed that the fibula was introduced to the Sambian peninsula in the second half of 1st century AD as import from the Wielbark Culture (Bezzenberger 1904; Chilińska-Früboes 2018). In Lithuania two eye fibulae, close to those of type A46, are known. One of them was discovered in Batakiai cemetery in the lower river Nemunas area, the other – in grave 1 of Toleikiai (formerly Thaleiken-Jacob) cemetery in the West Lithuanian Stone Circle Graves Culture area (Tamulynas 2002; Bliujienė *et al.* forthcoming). Both fibulae of this type are likely to have reached the Lithuanian sea-coast as import from the Roman Empire via the Sambian-Natangian Culture territory.

Type A52 eye fibulae were brought to Lithuania also as import. This assumption is, on the one hand, supported by the compositional analysis of the alloys of the eye fibulae of this type and, on the other hand, by a specific manufacturing technology. The bow and foot of type A52 two-component eye fibula found in Paragaudis cemetery is one structural part of the object, the spring being the other, independent part. A wire is passed through a hole drilled in the upper part of the bow, the wire is twisted into a spring, having one end riveted to the front side, the other end riveted to the rear side of the fibula. The rivet's head on the front side has become a decorative element of the fibula (Fig. 10:4). The manufacturing technology of the fibula is identical to that of several fibulae of the main series (of types A45, A47 and A50) found in cemeteries of Wielbark Culture on the lower Vistula (**Wisła**) river and Przeworsk culture in Mazovia (cf. Schuster 2014). Therefore, it may be possible that the above-mentioned fibulae were made in the same workshops of the northern Roman province where such manufacturing technology was used or the fibulae were repaired so as to hide their manufacturing defect, which did not prevent them to be traded to barbarians. The assumption regarding the import of fibulae of all types (including A60 and A61) is substantiated by the fibulae found in *Augusta Vindelicorum* workshops, which most likely were specifically made for the purpose of exchange with barbarians (Bakker 2003; Voß 2008).

The idea of local production of the eye fibulae would be supported by a large concentration of fibulae of types A60 and A61 in the central and western parts of Lithuania. These the most popular eye fibulae of the Prussian series were being crafted by the jewellers of the Wielbark, Sambian-Natangan and Bogaczew cultures (cf. Andrzejowski and Cieśliński 2007). Certainly, some of the fibulae may have reached Lithuania also via these cultural areas, as archaeological material provides evidence of quite close cross-cultural contacts and exchanges.

The manufacturing technique of eye fibulae was relatively simple. They were casted using the **lost-wax process**, most of them being one-component pieces, i.e. the foot and bow of the fibula were cast in a single mould. The body of the fibula transitions into a spiral, then the bow, the other part of the spiral and ends in a pin. At the end of the body of the fibula the metal is split in two parts, the lower of which is hammered into a square or circular profile. The hammered part is twisted into a spiral which continues into a pin-fastening with a square or circular section, while the upper part ends in a short loop, thereby the bow of the spiral is fixed tightly to the body of the fibulae (Fig. 10:2). The wire with a circular or square section was made by hammering. This manufacturing technique can be seen in the spirals of the analysed fibulae: the wire has been hammered unevenly, therefore, almost in all cases the shape and diameter of its section is different. The bow of the fibulae is often somewhat coarsely shaped, with stamping or polishing marks left on the inside (Fig. 10:3).

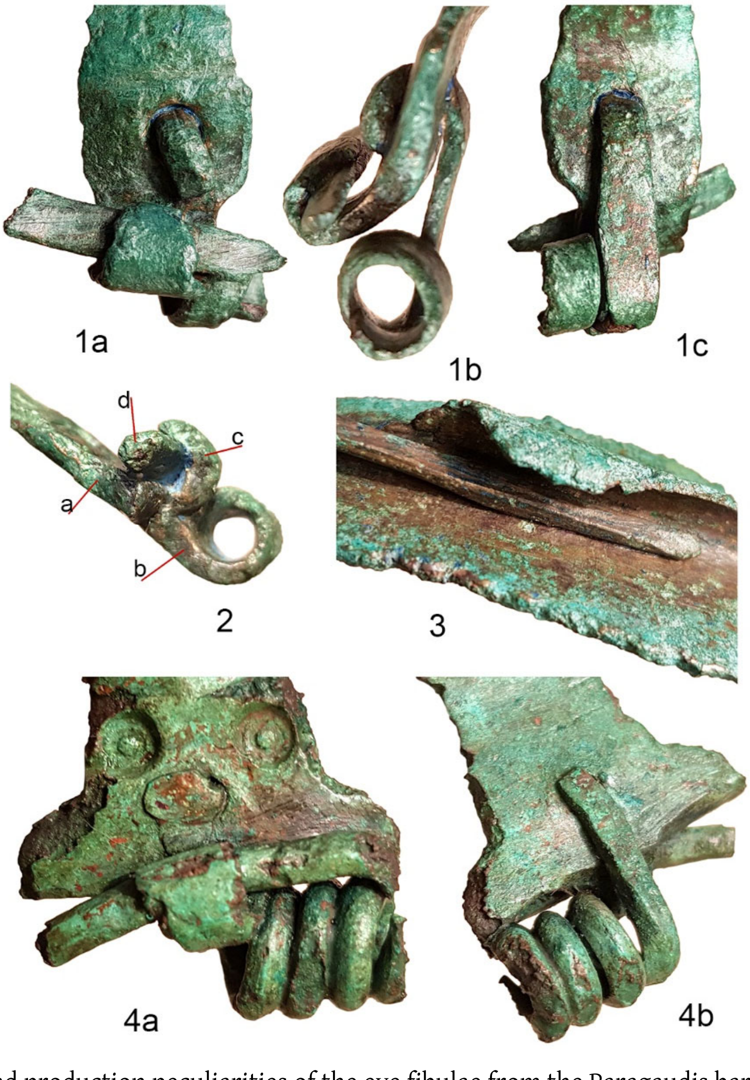

Figure 10. Repair and production peculiarities of the eye fibulae from the Paragaudis barrow cemetery: 1 – type A59 fibula (barrow 39, stray find; LNM AR 721: 90): 1a – front side, 1b – a spiral, 1c – back side; 2 – type A57 fibula

(barrow 22, burial 1; LNM AR 721: 109): 2a – upper part of the body, 2b – transition of the body to a spiral, 2c – part of a fastening spiral, 2d – fragment of a spiral; 3 – catch plate and tip of the fastening needle of type A61 fibula (barrow 13, burial 1; LNM AR 721: 39); 4 – fastening of type A52 fibula spiral to the body (barrow 26, burial 3; LNM AR 721: 139): 4a – front side, 4b – back side. Enlarged 50x. Photo by Evaldas Babenskas.

Nearly all of the most popular eye fibulae of types A60 and A 61 of the Prussian series have been coarsely made. Eye fibulae of the Prussian series found in Lithuania and in other Balts lands are longer, they are often wrought of a few millimetres thick metal sheet, their bows and feet have been widened and the feet are often triangular. Thus, their manufacturing technique seems to have deteriorated and they have become less ornate. There is no requisite symmetry or distance between the elements in the ornament, the ringed dots often overlap, and the decoration pattern on the bow is irregular, not resembling that of a notched wire. This would suggest 'a serial' manufacture of these eye fibulae. This assumption is indirectly substantiated by the emergence of eye fibulae lacking clearly distinct features defining their type. Moreover, the comparison of type A61 eye fibulae found in Sargėnai cemetery (Central Lithuania) and in Paragaudis barrow cemetery (Western part of Lithuania) indicates that there is little difference in the length of the fibulae obtained from these burial sites, however, the fibulae from Sargėnai cemetery are much heavier (Fig. 11). It is likely that the weight of the jewellery could have been determined by the easiness of acquisition of raw metals by the ancient communities and the skills of the jewellers. In the Early Roman Age, Central Lithuanian cemeteries (Sargėnai and other) were located at the confluence of the largest Lithuanian rivers – Nemunas and Neris, which served as the main arteries for the movement of people and goods. Since the most popular type A61 eye fibulae are large, their lighter weight might have been due to the smaller flows of raw materials which compelled the jewellers to save materials. On the other hand, most of the eye fibulae were made of alloys, relatively termed as intermediate, including brass/gunmetal, gunmetal or gunmetal/bronze, which are likely to have resulted from remelting of copper alloys of different composition. Gunmetal could have been obtained by melting brass and bronze scrap metal (cf. Pollard *et al.* 2015; Roxburgh and Olli 2019). This leads to questions regarding the ways of obtaining of raw metal and its composition, since, already in the Early Roman Age, jewellery items of local origin (e.g., bracelets with bud-shaped terminals) or those of regional origin (e.g., neck-rings with trumpet-shaped terminals) were manufactured in increasing numbers, which required large quantities of non-ferrous metals.

The main decoration of the eye fibula are ringed dots (eyes), arranged in three or two pairs in a mirror-like manner on the foot of the fibula, and sometimes also on the bow (one pair). Moreover, there are eye fibulae that are not decorated with the eye ornament. However, the 'eyes' of eye fibulae of the main and the Prussian series and especially those of types A60 and A61 look differently. Among the eye fibulae specimens of the main and Prussian series found in Lithuania there are fibulae with deep 'eyes', impressed using great force with one stamp (Fig. 10:4). The eye motif of most of eye fibulae of the Prussian series consists of two concentric circles with a raised eye-shaped spot in the middle of the circle of smaller dimension. However, within motifs the diameter of the circles, i.e. the distance between the concentric rings, as well as the proportions of the motif itself, varies. The concentric circles are generally regular, but some fibulae are decorated with rings impressed with a misaligned stamp, which recur in all elements of the fibula. Besides, sometimes a triangle-shaped pattern, composed of grooves is incorporated in the lower part of the foot. Another decorative feature of the fibulae is the vertical line in the middle of the bow. The bow is sometimes decorated with imprinted notches or a line of double dots decorated with a vertical double line.

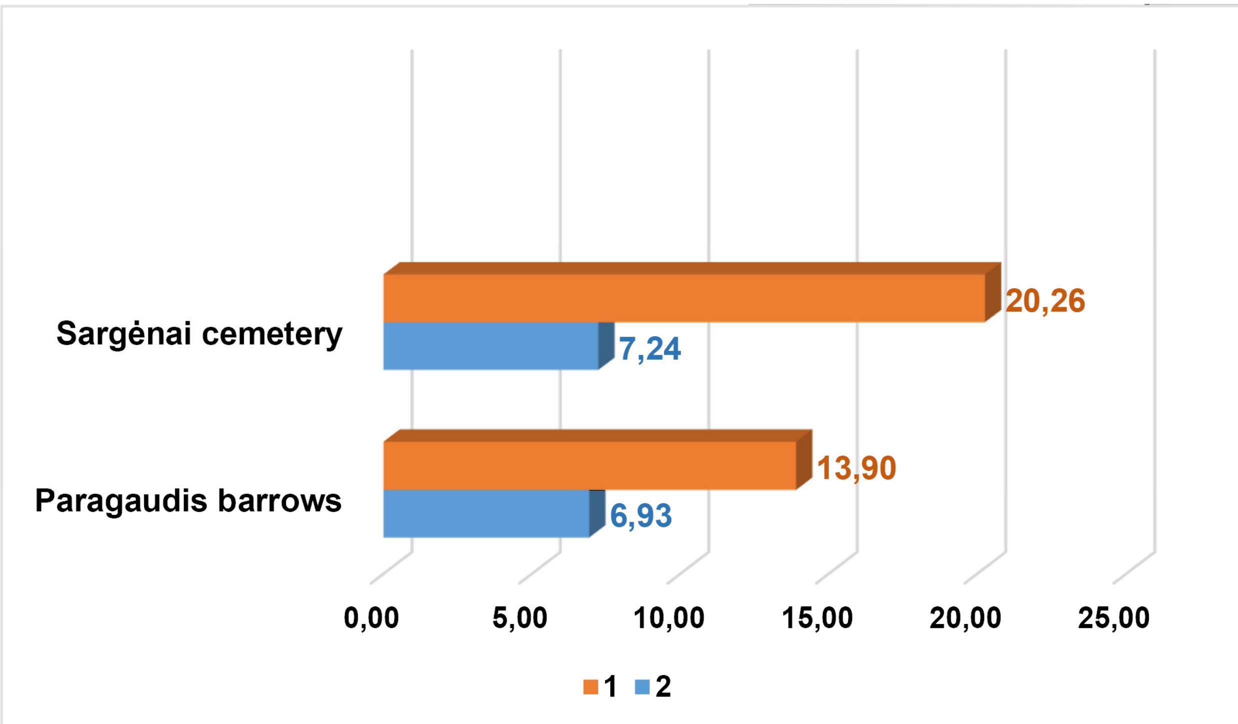

Figure 11. Type A61 eye fibulae from Sargėnai cemetery and Paragaudis barrow cemetery: 1 – weight; 2 – length. Diagram by Audronė Bliujienė.

The fibulae could be ornamented in two ways: by decorating the wax model of the fibula or by hammering into a cast piece. The ornament on most fibulae has been impressed in the wax model, as suggested by the smooth borders of the pattern's constituent motifs (Fig. 12). The decoration on the bow of some fibulae is embossed, which also points to the ornament being carved into the wax model prior to casting. These technological aspects involved in making eye fibulae (especially those of types A60 and A61), giving the impression of their hurried 'serial' manufacture, as well as the elemental composition of copper alloys, indicating the use of scrap metal for the fibulae, would appear to suggest that at least part of the eye fibulae may have been made by local craftsmen in the settlement located near the burial site. Yet, the only type A61 eye fibula known to-date from Lithuanian settlement sites is the brass eye fibula found in Vosgėliai hillfort. The fact of local production is additionally confirmed by a similar elemental composition of the copper alloys of the eye fibulae. It is likely that type A61 eye fibulae discovered in graves 22 and 42 of Sargėnai cemetery were made by one and the same jeweller. The composition of brass of both fibulae is identical, the stamp used to impress the eyes on the fibulae is similar, but the most important are the almost identical ornamentation features – there are no gaps between the eyes stamped on the lower part of the foot. This feature might indicate that some other type A61 eye fibulae found in Sargėnai cemetery (e.g., in graves 49, 151 and 226) were crafted by one and the same person.

Figure 12. Pairs of circles (eyes) of the eye fibulae: 1 – type A61 eye fibulae, eyes stamped asymmetrically in a wax model (Paalksniai barrow 6, burial 1; LNM GRD 68594); 2 – type A60 fibula, eyes stamped on the foot of the casted fibula (Sargėnai burial 76; VDKM AR 1616: 63); 3 – type A61 fibula, eyes stamped with different stamps (Sargėnai burial 139; VDKM AR 1780: 10); 4 – type A59 fibula, eyes stamped in a wax model with a misaligned stamp (Sargėnai burial 258; VDKM AR 1817: 77). Enlarged 50x. Photo by Evaldas Babenskas.

Crossbow-shaped eye fibulae were discovered in the burial sites of Przeworsk and Wielbark cultures, and also in the territories populated by the Balts (Andrzejowski and Cieśliński 2007). Crossbow-shaped eye fibulae are also known from the Lithuanian sites, e.g. Paragaudis barrow cemetery (barrow 20, grave 1) (Michelbertas 1997) or from the former Kaunas Governorate (the exact place of discovery is unknown). Among the items found there were eye fibulae, which, when being repaired, were remade into crossbow fibulae (e.g., Kurmaičiai, grave 41), and also eye fibulae which were repaired to fix a broken spring (Paragaudis, barrow 39). As can be seen in Fig. 10:1, one end of the spring on the front side of type A59 eye fibula is bent backwards, the other end is most likely riveted on the rear side.

The analysis of archaeological material indicates that in Western and Central Lithuania, where the largest number of eye fibulae was found, they were affordable to many members of the community, mostly men. Whereas the spread of the eye fibulae in the Balts lands can, as such, be viewed as a consequence of broad and multifaceted trans-European contacts and one of the signs of the 'Romanization' of the Northern *Barbaricum* manifested by the appearance of common jewellery, which in turn encouraged its local production from copper alloys with an elemental composition similar to that of the alloys used in the Roman Empire.

The analysed neck-rings with hollow trumpet-shaped terminals from Adakavas, Paventė, Plateliai (Dvarlaukis) and Vilkų Kampas sites were made from at least 6 different component parts (the bow, two hollow trumpets and the parts covering the trumpets). The neck-rings analysed by means of XRF were made of brass or gunmetal, excluding that from Adakavas – this splendid adornment was made of leaded bronze. The alloys of the neck-rings and eye fibulae found in Lithuania have similar elemental composition. The metal of which the neck-rings with hollow trumpet-shaped terminals of the Sambian-Natangian Culture were made has not been analysed.[22] In terms of manufacturing technique and ornamentation, the neck-ring with hollow trumpet-shaped terminals from Adakavas bears the closest resemblance to that found in Koddien (Velikolukskoe) site. Therefore, the neck-ring from Adakavas may have been made by the Sambian-Natangian jewellers or a travelling jeweller who was capable of casting complex-shaped items.

Regarding the manufacturing technique, the neck-rings with hollow trumpet-shaped terminals are the most complex jewellery items ever found in the territory inhabited by the Balts. The neck-rings of subtype 1.1 found in the Sambian-Natangian Culture were made using several manufacturing techniques. Their trumpet-shaped terminals have been cast in moulds, the wire, of which the neck-

[22] Except the elemental composition of the neck-ring from Warengen (Kotelnikovo) site (Cu 83.1%, Zn 14.2%, Sn 2.2%, Pb 0.2%, Fe 0.2%, Ni – traces), published by A. Bezzenberger (1904).

ring’s bow is made, has been hammered, the bow itself has been twisted from 6/9-11 wires, while the ends of the bow have been joined (soldered?) to the hollow trumpet-shaped terminals decorated with cross-hatching and other geometric ornaments. The cross-hatching motif’s grooves of the neck-ring from Regehnen/Kalinovo (stray find) are filled with red enamel, adorned with beaded silver wire and stamped with geometrical patterns (Skvortsov 2018) (Fig. 6:1). The neck-rings with hollow trumpet-shaped terminals of subtype 1.1 are fastened with a kind of ‘key-hole’ mechanism. The fastening mechanism is rather simple: there is a T-shaped slot on the flattened end of one trumpet-shaped terminal, and a pin matching in shape to the slot on the other trumpet.

Neck-rings of subtype 1.2 found in Lithuania and in cemeteries of the Sambian-Natangian Culture were made using a simpler technique merely because they cannot be fastened. The bodies of these neck-rings are cast, their ends are extended by hammering and thinned (the hammering marks are clearly visible). Such observation regarding construction of this type of neck-rings is supported by X-ray imaging analysis of the neck-ring with hollow trumpet-shaped terminals found in Paragaudis (barrow 2, grave 1), showing that the metal core of the neck-ring’s bow is solid, uniform, with slight corrosion marks. On the sides of the bow motifs of triple notches in relief, arranged in groups, are visible. The conical ends of the neck-ring are hollow, they are covered by a small four-spoked openwork wheel plate (‘lid’). The X-ray image clearly shows the ends of the neck-ring’s bow inserted into the trumpet-shaped terminals. One pointed end of the neck-ring’s bow is deliberately inserted into the wheel’s hole of the opposite trumpet, while the other most probably broken end might have been inserted into the hole of the other openwork wheel. The ends of the bow might have been joined in such a way as to fasten the neck-ring (Fig. 6:10). However, such fastening design could not be functional, thus suggesting that the neck-ring was ‘repaired’ specifically for the funeral.

The trumpet-shaped terminals of this type of neck-ring are either cast or wrought of metal sheet using repoussage metalworking technique, and, therefore, needed not to be joined by riveting, soldering or welding. Both cast and wrought trumpet-shaped terminals are attached to the neck-ring’s bow and their narrow part rests against the expanding part of the neck-ring. The wide part of the trumpet is covered with a plate (‘lid’), which has a hole in the middle; through that hole the thinner end of the neck-ring’s bow is pulled split into two parts. The split ends of the neck-ring’s bow are bent outwards, thus firmly attaching the trumpet to the neck-ring bow. It seems that the lid of the trumpet was rolled, i.e. pressed around the edge of the wide end of the hollow cylinder.

Trumpets of several neck-rings are covered with hollow four or five ‘spoke’ wheels and a hole in the centre (subtype 1.2b). On the one hand, this creates a composition that is not cantered, and on the other hand, the wheel through a hole in its middle is attached to the end of the neck-ring's bow. Also, the trumpet end is firmly joined to the neck-ring's bow. Ornamentation of the neck-rings with hollow trumpet-shaped terminals is geometric (composed of ringed dots, cross-hatched ornament, notched lines), the ornamental motif consists of symmetrically arranged stripes. The geometric ornament is carved into a wax model or the item's surface is decorated by engraving and stamping or using both techniques together. Furthermore, the geometric ornament of both neck-rings and eye fibulae imitates granule and filigree wire decoration.

The manufacturing techniques of the subtype 1.2 neck-rings with hollow trumpet-shaped terminals discovered in the Sambian-Natangian Culture are similar to those of the objects found in Lithuania. The above similarities suggest the existence of trade exchange, close multi-faceted cross-cultural contacts, including technology transfer, which encouraged the emergence of jewellery workshops of different skill levels capable to manufacture products for both local and regional markets; they also indicate the presence of travelling craftsmen-jewellers and the crafting of exquisite custom-made jewellery. Both the large number of the serial manufactured Romano-Germanic eye fibulae and the exquisite custom-produced jewellery, such as neck-rings with hollow trumpet-shaped terminals, used as social status insignia, point to stratification processes going on in the Baltic society in the Early Roman Age.

It is worth noting the importance of neck-rings, as an exclusive insignia of social rank, at least from the La Tène period, when the Celtic gold *torcs* were worn by the Celtic nobles and sorcerers. These neck-rings were primary divine attributes and sacrifice objects offered to gods (Eluère 1987; Görman 1996). The important role of *torc* is reflected in the Celtic iconography (god Cernunnos with *torc* on the cauldron of Gundestrup, goddess with *torc* on the cauldron of Rynkeby, Denmark) as well as in the written sources. The Greek historian Polybius (Lat. *Polýbios*; *c.* 208 – *c.* 125 BC) in his work *The Histories*, covering the period of 264–146 BC, describes the battle at Telamon in 225 BC, in which Romans completely defeated a large Celtic army. Battle flags and heavy golden *torcs*, representing status symbols, were taken from the defeated Celtic warlords as spoils of war (cf. Görman 1996). In the context of the later Romano-Celtic fights, the neck-rings (Lat. *Torquesque*) retain their importance as a social rank symbol, as in such context they are mentioned by antique authors, including Publius Cornelius Tacitus (56–120 AD) (Tacitus 1970, *Germania*, §15). In the Early Roman Age, the need of the Northern Germanic society to have exceptional insignia and sacrifice objects led to the appearance of golden neck-rings of a similar design with hollow trumpet-shaped terminals in Scandinavia (Andersson 1995; Nylén 1996; Nylén *et al.* 2005). Archaeological analysis of the material from the Baltic cultural areas indicates that a neck-ring was an important social status sign (Vaitkunskienė 1996). In Paragaudis barrow cemetery the neck-rings with hollow trumpet-shaped terminals were found only in two female graves, rich in grave goods, and in another destroyed, probably female, grave (Michelbertas 1997). Circumstances of discovery of other neck-rings reviewed in this article are unknown. The neck-rings found in Estonia are from rich jewellery hoards (Oras 2015). These rarely found elaborate pieces of jewellery were insignia of high social rank, some of them may have served an economic purpose or were finds from sacrifice hoards or offerings to gods.

6. Conclusions

The article has examined two types of jewellery, that is, eye fibulae and neck-rings with hollow trumpet-shaped terminals that were common in the Eastern Baltic Sea region during the Early Roman Age (middle of 1st century-end of 2nd century AD). Eye fibulae were born on the periphery between the antique and barbarian worlds – in the northern provinces of the Roman Empire, most likely as a result of the amalgamation of the antique and barbarian cultural traditions. As regards the neck-rings with hollow trumpet-shaped terminals, in the 1st century AD, people of the Sambian-Natangian Culture living in the Sambian peninsula, began making copper-alloy copies of these neck-rings by following the Scandinavian golden neck-ring Havor-type design. Although both the eye fibulae and neck-rings were made of copper alloys of similar composition, there are significant differences in their manufacturing techniques and stylistic features.

The XRF analysis of the eye fibulae indicates that type A52 eye fibulae of the main series were made of brass, whereas eye fibulae of the Prussian series of types A57, A59 and A60 were manufactured of brass, gunmetal and bronze. However, a number of alloys fall under intermediate/marginal groups, e.g., brass/gunmetal or gunmetal/bronze. Therefore, the assessment of the composition of such finds must take into account the possible effect of copper alloy corrosion, along with the overall process of zinc decline that was taking place in the Roman Empire as well as zinc loss through recycling of alloys and mixing of different alloys (metal scrap). The neck-rings analysed by means of XRF were made of brass or gunmetal, excluding a neck-ring from Adakavas – this splendid adornment was made of leaded bronze.

The technological examination and XRF analysis of the eye fibulae make it possible to equally interpret these fibulae as being imported or manufactured locally or regionally. At that time, the neck-rings with hollow trumpet-shaped terminals were most certainly manufactured in the settlements located in the Sambian peninsula and the region of the lower Nemunas river. The conducted analysis of the copper alloys suggests that the neck-rings were made of copper alloys with an elemental composition similar to that of the alloys used in the Roman Empire. Moreover, the pattern of switching from brass to gunmetal to leaded bronze and bronze is consistent with similar changes that were taking place in the Roman Empire and the *Barbaricum*, including its Northern periphery.

The spread of eye fibulae in the *Barbaricum* and the eastern Baltic region seems to indicate trade exchange, close multi-faceted cross-cultural contacts, including technology transfer, which encouraged the emergence of jewellery workshops of different skill levels capable to manufacture products for both local and regional markets; it also indicates the presence of travelling craftsmen-jewellers and the crafting of exquisite custom-made jewellery. At the same time, the spread of common jewellery can be viewed as broad and diverse manifestations of the 'Romanization' process in the Northern *Barbaricum*, evident through the appearance of common jewellery, which encouraged its local production. The presence in the region of both the large number of the Romano-Germanic eye fibulae of serial manufacture and the exquisite custom-produced jewellery, such as neck-rings with hollow trumpet-shaped terminals, used as social status insignia, point to the fact that, in the Early Roman Period, the Baltic society was not socially homogeneous.

7. Acknowledgements

This study was supported by the Research Council of Lithuania under grant number S-MIP-19-50. We are grateful to the National Museum of Lithuania and Vytautas the Great War Museum for the opportunity to study and publish the artefacts.

Audronė Bliujienė, Assoc. Prof., is Research Professor at the Institute of Baltic Region History and Archaeology at Klaipėda University. During the last decades, her work has concentrated on the development and technological process of the societies of the Roman and Migration periods in the Baltic region. She is the author and co-author of 5 monographs and more than 60 articles.

Contact: audrone.bliujiene@gmail.com

Gediminas Petrauskas, PhD, is Head of Department of Archaeology at the National Museum of Lithuania and a research fellow at the Institute of Baltic Region History and Archaeology at Klaipėda University. His research interests cover archaeology of Lithuanian Partisan War and cremation practices in medieval Lithuania. He is the author of about 15 publications and co-author of a research study titled *Partizanų bunkeris Daugėliškių miške: kompleksinių tyrimų studija ir šaltiniai* (in Lithuanian, *Partisan Bunker in Daugėliškiai Forest: Complex Research Study and Sources*, Raseiniai, 2017).

Contact: petrauskasgediminas@gmail.com

Jurga Bagdzevičienė, PhD, is a conservation scientist at Pranas Gudynas Centre for Restoration at the Lithuanian National Museum of Art (since 1995) and a research fellow at the Institute of Baltic Region History and Archaeology at Klaipėda University as well as lecturer at Vilnius Academy of Arts (since 2014). Her scientific activity focuses on the studies and conservation of cultural heritage objects (easel paintings, history textiles, graphic arts, ceramics, glass, archaeological finds etc.), identification of pigments, bindings, varnish, textile fibres, natural organic dyes and metals by microscopic, microchemical, FTIR, SEM/EDX, XRF and XRD methods, preparation of recommendations for conservation and restoration proceedings of Artwork. She is the author of about 20 publications.

Contact: jbagdzeviciene@gmail.com

Sergej Suzdalev, PhD, is a researcher at the Marine Research Institute at Klaipėda University and a member of the Aquatic biogeochemistry and ecosystem functioning research group. His scientific activity mainly focuses on the assessment of pollution processes and the analysis of maritime sector activities development as well as their impact on the marine environment. At the Marine Research Institute, he is responsible for the application of X-ray fluorescence spectrometry for needs of archaeological-geochemical investigation.

Contact: sergej.suzdalev@apc.ku.lt

Evaldas Babenskas, graduated Vilnius University in 2002. He has a master's degree in archaeology and during the last two decades has been actively working in experimental archaeology. He is researching the goldsmith techniques and working with reconstructions of ancient jewellery. Also, he is the author and co-author of several publications.

Contact: girvilka@gmail.com

8. Abbreviations

LNM – National Museum of Lithuania, Vilnius

MVF PM – Museum für Vor- und Frühgeschichte, Staatliche Museen zu Berlin (Museum of Pre- and Early History, The Berlin State Museums)

VDKM – Vytautas the Great War Museum, Kaunas

9. Bibliography

Almgren, O. 1923. *Studien über Nordeuropäische Fibelformen der ersten nachchristlichen Jahrhunderte, mit Berücksichtigung der provinzialrömischen und südrussischen Formen.* Leipzig: Curt Kabitzsch.

Andersson, K. 1995. *Romartida guldsmide i Norden* III. *Övriga smycken, teknisk analys och verkstadsgrupper.* Uppsala: Uppsala University.

Andrzejowski, J. 1998. *Nadkole 2. A Cemetery of the Przeworsk Culture in Eastern Poland* (Monumenta Archaeologica Barbarica V). Kraków: Secesja.

Andrzejowski, J. and A. Cieśliński 2007. Germanie i Bałtowie u schyłku starożytności. Przyjazne związki czy wrogie sąsiedztwo?, in A. Bitner-Wróblewska (ed.) *Kultura bogaczewska w 20 lat później.* Materiały z konferencji, Warszawa, 26–27 marca 2003 (Seminarium Bałtyjskie I): 279–319. Warszawa: Państwowe Muzeum Archeologiczne w Warszawie, Stowarzyszenie Naukowe Archeologów Polskich, Oddział w Warszawie.

Bakker, L. 2003. Zeugnisse des Handels. Neues aus der rätischen Hauptstadt AELIA AVGVSTA (Augsburg), in W. Menghin and D. Planck (eds) *Menschen - Zeiten - Räume. Archäologie in Deutschland* 3: 262–264. Stuttgart: Theiss.

Banytė-Rowell, R. and A. Bitner-Wróblewska 2005. From Aestii to Eesti. Connections between the Western Lithuanian group and the area of distribution of Tarand-graves, in V. Lang (ed.) *Culture and Material Culture.* Papers from the First Seminar of the Baltic Archaeologists (BASE) Held at the University of Tartu, Estonia, October 17th–19th, 2003 (Interarchaeologia 1): 105–120. Tartu, Riga and Vilnius: University of Tartu.

Bayley, J. and S. Butcher 2004. *Roman Brooches in Britain: A Technological and Typological Study based on the Richborough collection.* London: The Society of Antiquaries of London.

Bayley, J., D. Crossley and M. Ponting (eds) 2008. *Metals and Metalworking. A Research Framework for Archaeometallurgy* (HMS Occasional Publication 6). London: The Historical Metallurgy Society Ltd.

Bezzenberger, A. 1904. *Analysen vorgeschichtlicher Bronzen Ostpreussens*. Königsberg: Gräfe & Unzer.

Bitner-Wróblewska, A. and C. Sobczak 2009. Lithuanian Artifacts in the Collection of the Department of Balt Archaeology in State Archaeological Museum in Warsaw. *Archaeologia Lituana* 10: 84–114.

Bliujienė, A. 2005. Iš baltų amatininkystės istorijos: baltiški *Berlock* kabučiai. *Archaeologia Lituana* 6: 112–130.

Bliujienė, A. 2011. *Northern Gold. Amber in Lithuania (c. 100 to c. 1200)* (East Central and Eastern Europe in the Middle Ages, 450–1450 18). Leiden and Boston: Brill.

Bliujienė, A., A. Hofmann, H. Neumayer and G. Zabiela (forthcoming). Die Wiederentdeckung des wikingerzeitlichen Gräberfeldes von Batakiai ein Beispiel für landerubergreifende archäologische Forschung. *Blickpunkt Archäologie.*

Bray, P.J. and A.M. Pollard 2012. A New Interpretative Approach to the chemistry of Copper Alloy Objects: Source, Recycling and Technology. *Antiquity* 86: 853–867.

Caley, E.R. 1964. *Orichalcum and Related Ancient Alloys: Origin, Composition, and Manufacture, with Special Reference to the Coinage of the Roman Empire* (Numismatic Notes and Monographs 151). New York: American Numismatic Society.

Chilińska-Früboes, A. 2017. Zapinki oczkowate serii Prusskiej z terenu kultury Dollkeim-Kovrovo. *Wiadomości Archeologiczne* LXVIII: 45–106.

Chilińska-Früboes, A. 2018. Zapinki oczkowate serii głównej jako głos w dyskusji nad początkami kultury Dollkeim-Kovrovo, in S. Wadyl, M. Karczewski and M. Hoffmann (eds) *Materiały do archeologii Warmii i Mazur* 2: 15–41. Warszawa, Białystok and Olsztyn: Instytut Archeologii Uniwersytetu Warszawskiego, Wydział Historyczno-Socjologiczny Uniwersytetu w Białymstoku, Instytut Historii i Stosunków Międzynarodowych Uniwesytetu Warmińsko-Mazurskiego w Olsztynie.

Dungworth, D.B. 1997. Roman Copper Alloys: Analysis of Artefacts from Northern Britain. *Journal of Archaeological Science* 24: 901–910.

Eluère, Ch. 1987. Celtic Gold Torcs. *Gold Bulletin* 20: 22–37.

Gan, P. 2015. *Charakterystyka chemiczna zabytków z cmentarzyska* w *Czarnówku – analizy* wprowadzające, in J. Andrzejowski (ed) *Czarnówko, stan. 5. Cmentarzyska z późnej starożytności na Pomorzu 1 (Monumenta Archaeologica Barbarica, Series Gemina V): 175–214. Lębork and Warsawa:* Muzeum w Lęborku, Fundacja Monumenta Archaeologica Barbarica.

Görman, M. 1996. The Necklace as a Divine Symbol and as a Sign of Dignity in the Old Norse Conception. *Scripta Instituti Donneriani Aboensis* 16. *Dance, Music, Art, and Religion*: 111–*150.*

Grigalavičienė, E. 1995. *Žalvario ir ankstyvasis geležies amžius Lietuvoje.* Vilnius: Mokslo ir enciklopedijų leidykla.

Jaskanis, D., M. Kaczyński, W. Brzeziński, G. Iwanowska and A. Bitner-Wróblewska (eds.) 1992. *I Balti. Alle origini dei Prussiani, degli Iatvinghi, dei Lituani e dei Lettoni Dal V secolo a. C. al XIV secolo.* Firenze: Cantini.

Hackman, A. 1905. *Die ältere Eisenzeit* in *Finnland* 1. *Die Funde aus den fünf ersten Jahrhunderten n. Chr. Helsingfors: Finn Altertumsgesellschaft/Tilgmann.*

Khavrin S.V. *et al.* = Хаврин, С.В., М.А. Юшкова, В.С. Кулешов 2011. Метал эпохи Римских влияний на Ижорской возвышенности, in Д.А. Мачинский (ed.). *Европейская Сарматия.* Сборник, посвященный Марку Борисовичу Щукину: 208–224. Санкт-Петербург: Нестор-История.

Khomiakova O.A. = Хомякова, О.А. 2011. Гривны с конусовидными окончаниями («тип Хавор») самбийско-натангийской культуры: вопросы генезиса и хронологии, in О.В. Шаров (ed.) *Петербургский апокриф. Послание от Марка*: 295–313. Санкт-Петербург-Кишинёв: Высшая антропологическая школа.

Kivikoski, E. 1973. *Die Eisenzeit in Finnland. Bildwerk und Text. Helsinki: Weilin & Göös.*

Kulikauskienė, R. and R. Rimantienė 1958. *Lietuvių liaudies menas. Senovės lietuvių papuošalai* I. Vilnius: Valstybinė grožinės literatūros leidykla.

Kunow, J. 1998. Die Hauptserie der Augenfibeln: Gruppe III, Abb. 45–54, in J. Kunow (ed) *100 Jahre Fibelformen nach Oscar Almgren.* Internationale Arbeitstagung 25.–28. 05. 1997, Kleinmachnow, Land Brandenburg (Forschungen zur Archäologie im Land Brandenburg 5): 93–118. Wünsdorf: Brandenburgisches Landesmuseum für Ur- und Frühgeschichte.

Lang, V. 2007. *The Bronze Age and Early Iron Ages in Estonia* (Estonian Archaeology 3). Tartu: University of Tartu Press.

Lund Hansen, U. 1987. *Römischer Import im Norden. Warenaustausch zwischen dem römischen Reich und dem freien Germanien während der Kaiserzeit unter besonderer Berücksichtigung Nordeuropas* (Nordiske Fortidsminder. Series B 10). Copenhagen: Kongelige Nordiske Oldskriftselskab.

Mączyńska, M. 2004. Bemerkungen über einige Typen der Augenfibeln im Barbaricum, in H. Friesinger and A. Stuppner (eds) *Zentrum und Peripherie – gesellschaftliche Phänomene in der Frühgeschichte.*

Materialien des 13. Internationalen Symposiums Grundprobleme der frühgeschichtlichen Entwicklung im mittleren Donauraum, Zwettl, 4.–8. Dezember 2000 (Mitteilungen der Prähistorischen Kommission der Österreichischen Akademie der Wissenschaften 57): 211–240. Wien: Österreichische Akademie der Wissenschaften.

Michelbertas, M. 1986. *Senasis geležies amžius Lietuvoje. I–IV amžius*. Vilnius: Mokslas.

Michelbertas, M. 1989. Antkaklių trimitiniais galais (III gr.) chronologijos klausimu. *Lietuvos archeologija* 9: 127–132.

Michelbertas, M. 1997. Paragaudžio pilkapynas. Vilnius: Vilniaus universiteto leidykla.

Moora, H. 1938. *Die Eisenzeit in Lettland bis etwa 500 n. Chr. 2. Analyse*. Tartu: Õpetatud Eesti Selts.

Nylén, E. 1996. Sagan om ringarna. *Fornvännen* 91: 1–12.

Nylén, E., U. Lund Hansen and P. Manneke 2005. *The Havor Hoard: The Gold, the Bronzes, the Fort.* Stockholm: Royal Swedish Academy of Letters, History and Antiquities.

Nowakowski, W. 1996. *Das Samland in der römischen Kaiserzeit und seine Verbindungen mit dem römischen Reich und der barbarischen Welt* (Veröffentlichung des Vorgeschichtlichen Seminars Marburg 10). Marburg: Druk.

Olli, M. and M. Roxburgh 2018. Disc Brooches of the Roman Iron Age from the Tarand Cemeteries of Estonia and North Latvia. *Lietuvos archeologija* 44: 39–70.

Oras, E. 2015. *Practices of Wealth Depositing in the 1st-9th century AD Eastern Baltic.* Leiden: Sidestone Press.

Pietrzak, M. 1997. *Pruszcz Gdański. Fundstelle 10. Ein Gräberfeld der Oksywie- und Wielbark-Kultur in Ostpommern* (Monumenta Archaeologica Barbarica IV). Kraków: Secesja.

Pollard, A.M. and P.J. Bray 2014. The archaeological bazaar: Scientific methods for sale? Or 'putting the 'arch-' back into archaeometry, in A. Wylie and R. Chapman (eds.) *Material Evidence: Learning from Archaeological Practice.* Abingdon and New York: Routledge.

Pollard, A.M., P. Bray, A. Cuénod, P. Hommel, Y.-K. Hsu, R. Liu, L. Perucchetti, J. Pouncett and M. Saunders 2018. *Beyond Provenance: New Approaches to Interpreting the Chemistry of Archaeological Copper Alloys* (Studies in Archaeological Sciences 6). Leuven: Leuven University Press.

Pollard, A.M., P. Bray, Ch. Gosden, A. Wilson and H. Hamerow 2015. Characterising Copper-Based Metals in Britain in the First Millennium AD: A Preliminary Quantification of Metal Flow and Recycling. *Antiquity*, 89(345): 697–713.

Riha, E. 1979. *Die römischen Fibeln aus Augst und Kaiseraugst* (Forschungen in Augst 3). Augst: Amt für Museen und Archäologie des Kantons Basel-Landschaft.

Roxburgh, M., S. Heeren, H. Huisman, H. and B. Van Os 2016. Early Roman Copper-Alloy Brooch Production: A Compositional Analysis of 400 Brooches from *Germania Inferior*. *Journal of Roman Archaeology* 29: 411–421.

Roxburgh, M.A., S. Heeren, D.J. Huisman and B.J.H. Van Os 2019. *Non-Destructive Survey* of *Early Roman Copper-Alloy Brooches Using* Portable *X-ray Fluorescence Spectrometry. Archaeometry* 61(1): 55–69.

Roxburgh, M.A. and M. Olli 2019. Eyes to the North: A Multi-Element Analysis of Copper-Alloy Eye Brooches in the Eastern Baltic, Produced during the Roman Iron Age. *Germania*, 96: 209–233.

Rzeszotarska-Nowakiewicz, A. 2010. Neckrings with trumpet-shaped terminals (*mit Trompetenenden*) – some remarks on traces of contacts in the Baltic Basin during the early Roman period, in U. Lund Hansen and A. Bitner-Wróblewska (eds.) *Worlds Apart? Contacts across the Baltic Sea in the Iron Age* (Nordiske Fortidsminder C(7)): 315–336. København and Warszawa: Det Kongelige Nordiske Oldkriftselskab.

Tamulynas, L. 2002. Toleikių kapinyno spėjamos vietos (Toleikių kaime, Dovilių drn. Klaipėdos r.) archeologinių žvalgomųjų tyrinėjimų 2001 m. ataskaita. Unpublished report of the archaeological excavations, Vilnius.

Schuster, J. 2014. Kolejne elementy mozaiki – nieznane zabytki z cmentarzyska z później starożytności w Skowarczu (D. Schönwarling), in J. Andrzejowski (ed.) *In medio Poloniae barbaricae. Agnieszka Urbaniak in memoriam* (Monumenta Archaeologica Barbarica III): 197–209. Warszawa: Fundacja Monumenta Archaeologica Barbarica, Instytut Archeologii Uniwersytetu Warszawskiego.

Skvortsov K.N. = Скворцов, К.Н. 2018. Грунтовый могильник Калиново (Калининградская область, Нестеровский район), in А.В. Энговатова (ed) *Города, селища, могильники. Раскопки 2017* (Материалы спасательных археологических исследований 25): 340–345. Москва: Институт археологии РАН.

Svetikas, E. 2019. *Sargėnų kapinynas.* Vilnius: Diemedžio leidykla.

Tacitus 1970. *Germania. The Earliest Beginnings and the Land of the Germans* 1. Cambridge (MA): Harvard University Press.

Vaitkunskienė, L. 1996. Senovės lietuvių papuošalai: simbolinis aspektas. *Lituanistica* 2(26): 3–15.

Voß, H.-U. 2008. Fremd, nützlich, machbar. Römische Einflüsse im germanischen Feinschmiedehandwerk, in S. Brather (ed) *Zwischen Spätantike und Frühmittelalter. Archäologie des 4. bis 7. Jahrhunderts im Westen* (Ergänzungsbände zum Reallexikon der Germanischen Altertumskunde 57): 343–365. Berlin and New York: Walter de Gruyter.

10. Appendix 1

Find spots of the eye fibulae in Lithuania. The number of fibulae found in the site is indicated in brackets (see Figure 2) After Michelbertas 1997 and authors of this paper.

1. Adakavas, Tauragė Dist. (1)
2. Anulynas, Raseiniai Dist. (1)
3. Bandužiai, Klaipėda city (2)
4. Barzdūnai/Barsduhnen, Šilutė Dist. (3)
5. Barzūnai, Pagėgiai Mun. (3)
6. Batakiai, Tauragė Dist. (1)
7. [Central Lithuania] (6)
8. [Curonian Spit/Kurische Nehrung] (1)
9. Dauglaukis, Tauragė Dist. (1)
10. Genčai, Kretinga Dist. (1)
11. Gilvyčiai, Šiauliai Dist. (1)
12. Gudai/Gudden, Pagėgiai mun. (1)
13. Jonelaičiai, Šiauliai Dist. (1)
14. Kalnuvėnai, Kretinga Dist.(1)
15. Kašučiai (Dubašiai), Kretinga Dist. (2)
16. [Kaunas Governate] (4)
17. Kegai, Telšiai Dist. (2)
18. Kiaunoriai, Kelmė Dist. (1)
19. Kriemala, Kaunas Dist. (1)
20. Kukiai (Petreliai), Mažeikiai Dist. (1)
21. Kulautuva, Kaunas Dist. (1)

22. Kurmaičiai, Kretinga Dist. (7)
23. Kuršiai, Kelmė Dist. (1)
24. Kybartiškė, Šiauliai Dist. (2)
25. Lazdininkai (Kalnalaukis), Kretinga Dist. (18)
26. [Lithuania] (2)
27. Maironiai (Saudininkai), Kelmė Dist. (1)
28. Medvėgalis (Karūžiškė), Šilalė Dist. (1)
29. Mikužiai, Klaipėda Dist. (5)
30. Nemakščiai, Raseiniai Dist. (1)
31. Noliškiai, Šiauliai Dist. (1)
32. Paalksniai, Kelmė Dist. (4)
33. Padvariai, Kretinga Dist. (3)
34. Pajūralis, Šilalė Dist. (1)
35. Palumpiai/Polompen, Pagėgiai Mun. (1)
36. Papilys (Skomantai), Klaipėda Dist. (1)
37. Paragaudis, Šilalė Dist. (39)
38. Paštuva, Kaunas Dist. (1)
39. Paulianka, Mažeikiai Dist. (1)
40. Pažarstis, Prienai Dist. (2)
41. Pribitka, Plungė Dist. (1)
42. Pūsdvaris (Padubysis), Kelmė Dist. (1)
43. Rūdaičiai II, Kretinga Dist. (5)
44. Sandrausiškė, Raseiniai Dist. (3)
45. Sargėnai, Kaunas city (43)
46. Šilutė/Heydekrug, Šilutė Dist. (1)
47. Šulaičiai, Kėdainiai Dist. (1)
48. Tamošaičiai, Tauragė Dist. (1)
49. Telšiai, Telšiai Dist. (1)
50. Toleikiai/Thaleiken-Jacob, Klaipėda Dist. (1)
51. Trakininkai/Trakeningken, Pagėgiai Mun. (1)
52. Vienragiai, Rietavas mun. (4)
53. Vigodka (Dūkštas), Ignalina Dist. (1)
54. Vilkija, Kaunas Dist. (1)
55. Vilkyčiai/Wilkieten, Klaipėda Dist. (2)

56. [Vilnius Dist.] (1)
57. Visdergiai (Papelkiai), Šiauliai Dist. (2)
58. Vosgėliai, Zarasai Dist. (1)
59. Zastaučiai, Mažeikiai Dist. (6)

11. Appendix 2

Find spots of the neck-rings with hollow trumpet-shaped terminals in the Eastern Baltic region and Finland. The number of neck-rings found in the site and the type is indicated in brackets (see Figure 5). After Khomiakova 2011; Michelbertas 1989; Rzeszotarska-Nowakiewicz 2010; Skvortsov 2018 and authors of this paper.

Kaliningrad Oblast, Russian Federation

1. Corjeiten/Putilovo, Kr. Fischhausen/Zelenogradsk Dist. (1). Subtype 1.2.
2. Dollkeim/Kovrovo, Kr. Fischhausen/Zelenogradsk Dist. (3). Subtype 1.2.
3. Eisliethen/Gerojskoe, Kr. Fischhausen/Zelenogradsk Dist. (2). Subtype 1.2.
4. Friedrichsthal/Soldatovo, Kr. Wehlau/Gvardejsk Dist. (1). Subtype 1.2.
5. Fürstenwalde-Neidtkeim/Poddubnoe, Kr. Königsberg/Gurjevsk Dist. (3). Subtype 1.2.
6. Grebieten/Okunevo, Kr. Fischhausen/Zelenogradsk Dist. (2). Subtypes 1.1 and 1.2.
7. Koddien/Velikolukskoe, Kr. Wehlau/Gvardejsk Dist. (1). Subtype 1.1.
8. [Prussia, Ostpreussen] (1?). Not indicated on the map.
9. Regehnen/Kalinovo, Kr. Fischhausen/Zelenogradsk Dist. (1). Subtype 1.1.
10. Ringels/Iskrovo, Kr. Fischhausen/Zelenogradsk Dist. (1). Subtype 1.2.
11. Tilsit-Spliter, Kr. Tilsit/Sovetsk City (2). Subtype 1.2.
12. Warengen/Kotelnikovo, Kr. Fischhausen/Zelenogradsk Dist. (1). Subtype 1.1.
13. Willkühnen/Golovenskoe, Kr. Königsberg/Gvardejsk Dist. (1). Subtype 1.2.

Lithuania

14. Adakavas, Tauragė Dist. (1). Subtype 1.2b.
15. Gintautai (Palaidžia), Biržai Dist. (1). Subtype 1.2a.
16. Glaušiai, Kėdainiai Dist. (1). Subtype 1.2c.
17. Gudai/Gudden, Šilutė Dist./Kr. Tilsit (1). Subtype 1.2a.
18. Linkuva, Pakruojis Dist. (2). Subtype 1.2c.
19. [Lithuania] (1). Not indicated on the map.
20. Palumpiai/Polompen, Pagėgiai Mun./Kr. Tilsit (1). Subtype 1.2a.

21. Paragaudis, Šilalė Dist. (3). Subtypes 1.2a and 1.2b.
22. Paventė, Mažeikiai Dist. (1). Subtype 1.2b.
23. Plateliai (Dvarlaukis), Plungė Dist. (1). Subtype 1.2a.
24. Rambynas/Rombinus, Šilutė Dist./Kr. Tilsit (1). Subtype 1.2a.
25. Šilutė/Heydekrug, Šilutė Dist./Kr. Heydekrug (1). Subtype 1.2a.
26. Vilkų kampas, Šilutė Dist. (1). Subtype 1.2a.

Latvia

27. Auciems, Pārgauja Mun. (1). Subtype 1.3.
28. Makašānu Salenieki, Madona Mun. (1). Subtype 1.3.
29. Skare, Auce Mun. (1). Subtype 1.2a.

Estonia

30. Jäbara C, Lüganuse Par. (1). Subtype 1.3.
31. Liimala, Lüganuse Par. (1). Subtype 1.3.
32. Mustmätta, Lüganuse Par. (2). Subtype 1.3.

Finland

33. Mäeksmäki, Nousiainen Mun. (1). Subtype 1.3.
34. Penttala, Nakkila Mun. (3). Subtype 1.3.
35. Perttilä, Isokyrö Dist. (1). Subtype 1.2.
36. Sonkkila, Laitila Mun. (1). Subtype 1.3.

The application and evaluation of remote sensing techniques to household archaeology on the Northwest Coast

William T.D. Wadsworth (*Institute of Prairie and Indigenous Archaeology, University of Alberta*), Andrew Martindale (*University of British Columbia*), Colin Grier (*Washington State University*) & Kisha Supernant (*Institute of Prairie and Indigenous Archaeology, University of Alberta*)

Abstract

Northwest Coast (NWC) archaeologists have investigated houses and households for almost a century, often combining excavation with ethnographic data to produce anthropological insights into past social organization. However, the complete excavation of NWC houses has been rare due to the complexity of excavating through heterogenous anthropogenic shell-bearing matrices (shell middens), and a shift away from large-scale excavation. Archaeologists have embraced ground penetrating radar (GPR) and other remote sensing technologies as a more efficient method for exploring subsurface spatial patterns in the archaeological record, but these have not been widely applied on the Northwest Coast of North America, in part because a systematic methodological strategy for evaluating results is lacking.

We propose that a refined application of geophysical techniques to Northwest Coast architectural sites could accelerate several important research directions. Here, we present a case study from the Prince Rupert Harbour (PRH) region to evaluate the efficacy of this new research program and demonstrate its utility. The PRH region, territory of the Tsimshian peoples, has been an area of intensive habitation for millennia. The Tsimshian built monumental winter villages comprised of up to 40 or more large plankhouses situated in massive shell terraces. Many of these village sites have been systematically mapped and inventoried for over five decades, though few house interior patterns have been accumulated in part because of the logistical challenges of subsurface investigation in deep shell-bearing sites. Here we present our efforts to resolve architectural patterns within one house depression feature (House 16) at site GbTo-34 (Kitandach) using subsurface geophysical techniques accompanied by ground truthing using low-impact percussion core testing. We assess and discuss these methods in relation to developing a statistically robust feature confidence index to predict the identifying patterns of subsurface archaeological features from geophysical signals. Finally, we situate our ongoing efforts

in relation to anthropological investigation of NWC households and the interests of First Nations in documenting and preserving their heritage.

Keywords

Remote sensing; ground penetrating radar; household archaeology; Northwest Coast of North America; ground truthing; feature confidence index

1. Introduction

Critical anthropological insights into the past economic, social, and political practices of Indigenous peoples of the Northwest Coast have come through analyses of the archaeological remains of their dwellings (e.g., Ames 2006; Coupland 2003; Coupland et al. 2009; Grier 2006a; Lepofsky et al. 2009; Martindale 2006; Matson 2003; Samuels 2006; Schaepe 2009; Sobel et al. 2006). Over much of the Holocene, the main dwelling employed was the large, post-and-beam, cedar-planked longhouse, referred to by archaeologists as a plankhouse. Plankhouses are complex, large-scale features that are challenging to excavate, and when excavated produce vast amounts of materials and data that must be managed and curated. For example, Tsimshian plankhouses on the northern Northwest Coast are built on massive anthropogenic shell terraces often in excess of 4 m deep; excavation of these requires substantial stepping to maintain worker safety and to avoid collapse of the shell matrix. As such, the number of excavated plankhouses has been limited, resulting in a small number of intensive house excavations providing the bulk of our archaeological knowledge concerning plankhouses across the Northwest Coast.

Even when excavation is feasible, it is destructive. This destruction runs contrary to the ethic of heritage conservation, as it is inconsistent with the overarching goal of preserving the archaeological record. It also stands against the values of many Indigenous communities who want no disturbance of their ancient places and ancestors (e.g., McLay 2008; Supernant 2018). Remote sensing offers an alternative way to acquire data on plankhouses without excavation. While remote sensing does not produce a comparable level of detail to traditional excavation, the benefits are clear. Ground-penetrating radar (GPR) appears well suited to locating major architectural components – a critical set of spatial data for the reconstruction of household and village-level organization. Such data can also be valuable for devising a sampling strategy for subsurface testing and excavation when it is undertaken, maximizing information return for the least excavation effort.

In the Prince Rupert Harbour (PRH) region of the northern British Columbia coast, houses and even entire villages often have well preserved surface expression. House structures were typically bounded by ridges of shell that demarcated the extent of the house footprint at the time house occupation ceased (Archer 2001; Letham et al. 2017, 2020; Martindale et al. 2009). Research suggests that the original perimeter of the structure can be estimated by the midpoint between the upper and lower slope breaks of the depression that forms after the walls are removed or deteriorate and surrounding shell ridges slump (Archer 2001). Although there is evidence of changes in the relationship between the surface contour and the underlying houses older than several millennia, the correlation remains strong in structures that date to the last few thousand years (Martindale et al. 2017). Accordingly, house interior space can be mapped and investigated with some confidence about the boundaries of the structure. In this situation two types of data can be readily sought through remote sensing. First, the layout of major interior features such as hearths, rafter support post holes and storage pits can be mapped. The edge of floor areas can also potentially be mapped by detecting transitions from house floor deposits to exterior shell ridges and terracing. Second, multiple episodes of house occupation, typically represented by superimposed floor deposits and stacked features, can be identified. With these two types of data (horizontal and vertical), it is feasible to reconstruct aspects of the spatial organization and chronological dimensions of house occupations. This is the methodological focus of our remote sensing study at GbTo-34.

However, in many regions of the Northwest Coast, surface expression of ancient houses and villages is often lacking. The Salish Sea of southern British Columbia is one such region where the remains of plankhouses are not typically visible on the surface. There are many potential reasons for this, but the net result is that there are very few sites that can be corroborated archaeologically as villages (i.e., sites with plankhouses) through surface inspection alone. Extensive shell-bearing sites, many with anthropogenically-constructed shell terraces, are common, and a significant proportion of these likely held large wooden plankhouses. However, it is difficult to ascertain the number, size, and orientation of houses within the site, and map their internal organization. Acquiring data to determine where houses were located within these large expanses of shell-bearing deposits is an important step towards reconstructing community patterns and household organization in the Salish Sea.

While both the PRH and Salish Sea regions present distinct challenges for remote sensing, it is clear that we cannot rely solely on traditional excavation methods to generate the requisite sample of village plans and house interior maps to fully document historical trends in household and community organization and change. If we are to put the Northwest Coast on a solid empirical footing archaeologically, and substantially increase the sample of house and village plans available to address big-picture questions concerning past lifeways, we must be innovative methodologically. One potential solution we have been pursuing is the application of ground-penetrating radar (GPR) supplemented by other near-surface remote sensing techniques, such as magnetic gradiometry (Conyers 2018). In this paper, we briefly describe the methodology we are developing and testing, which focuses on geophysical visualization and ground truthing of houses with identifiable surface expression in the Prince Rupert Harbour region. We present preliminary results that evaluate the utility of this approach for archaeological prospection and mapping in Northwest Coast plankhouse contexts.

2. The Importance of Houses and Households in Northwest Coast Societies

After a long history of excavating deeply into shell-bearing sites for the purpose of reconstructing culture histories and artifact sequences, Northwest Coast archaeologists have turned in the last few decades to household-focused archaeology — that is, to excavations designed to expose significant portions of ancient houses and reconstruct the spatial and social organization of its inhabitants. Driven by ethnographic descriptions of large cedar plankhouse dwellings, the objective has been to reconstruct activities that took place and socioeconomic relations that obtained within these monumental structures. Ancient plankhouses typically have floor areas between 50 and 200 square meters, but can measure over 400 square meters in size (Coupland 2003; Grier and Kim 2012; Lepofsky et al. 2009; Martindale 1999; Matson 2003).

It is critical to have these data on houses and villages to better understand spatial organization in these locations. Large cedar plankhouses were the setting for a variety of fundamental daily tasks, but also the locus of a range of economic, social, and political interactions (Coupland 2006; Grier 2006b). On the Northwest Coast, large households were central institutions that structured many practices both locally and across regions (Ames 2006; Coupland et al. 2009; Grier 2003; Hajda 1994; Suttles 1991). Their changing form also supports many theories and explanations for culture change in the region (e.g., Coupland 1996; Coupland et al. 2009; Grier and Kim 2012; Lepofsky et al. 2009; Matson 2003; Schaepe 2009). Large households have typically been seen as the economic engines of social complexity, central to the emergence of a storage-based surplus economy. Permanent villages are viewed as the hallmark of a settled way of life, involving more institutionalized land tenure systems (Grier 2014; Letham et al. 2020). Village complexes with extensive terraforming and monumental construction reflect long-standing connections to keystone places (Grier et al. 2017; Letham et al. 2020; Lepofsky et al. 2017). Throughout the Northwest Coast, houses were a spatial manifestation of the complex and enduring interactions within and between foundational social and legal entities, such as the wilnat'aał, or extended family matriline, in the Tsimshian area (Martindale et al. 2017).

Despite the small sample of excavated houses across the coast, recurring patterns in their layout have been documented in both ethnohistoric descriptions (e.g., Suttles 1990, 1991) and through archaeological excavation (Ames 2006; Coupland et al. 2009; Grier 2006b; Lepofsky et al. 2009). The framework of Tsimshian houses consisted of four plank-clad walls supported by upright posts, enclosing an interior smaller quadrangle of four major posts. The latter supported a gable roof beams and roofing planks. In northern regions of the coast, the layout of rafter support posts varies between sub-regions and presumably cultural communities (MacDonald 1983). The location and orientation of the wall and roof posts indicate both the type of superstructure and the overall dimensions of the house. Salish houses differed by having both a shed roof design rather than a gable roof, and by their length, which was often many times their width (Grier 2006a; Matson 2003; Suttles 1991). In essence, Salish houses were composed of a series of separate house compartments lined end to end. This architectural strategy reflects the flexible size and composition of the household, which was determined by cognatic bilateral descent (i.e., it was composed of both patrilineal and matrilineal relations and membership that was negotiable)(Barnett 1955; Suttles 1991). Northern social structure was more rigid and defined by patrilocality (women live with their husbands) and avunculocality (men live with their uncles), creating a household focused on a single matrilineally-related group of men, their spouses, and nephews. The northern house design, like the northern social household, was less flexible than its Salish counterpart (Suttles 1991).

However, house forms in both regions are composed of similar recurring spatial sub-units. Various “zones” within the house reflect different activity areas, including a living/sleeping area (or “bench zone”) around the interior perimeter, areas of open floor space (the “traffic zone”), and domestic activity space in and around hearth features (Grier 2006a; McDonald 1983; Samuels 2006). The house interior was essentially an open hall, with limited permanent partitioning. Hearth features, both smaller domestic fire spots associated with individual families and larger collective or ceremonial hearths located more centrally, most clearly define the organization of space within the house interior. Archaeological examples regularly contain all these elements, illustrating the organization of large, multi-family households in space and, since most houses appear to have been occupied for several centuries, over time (Ames 2006; Coupland et al. 2009; Grier 2006a).

Hearth arrangements provide an important window into the social relations of families within households. Coupland et al. (2009) underscore this point in their coast-wide analysis of houses, advancing the idea that the presence of a central hearth reflects a strong ethic of communalism and integration of the household. Conversely, a series of smaller, spatially distributed hearths reflect less integration of individual families within the overarching household. In the Coast Salish area houses appear less integrated around a central hearth. The typical arrangement of multiple domestic hearths in the Coast Salish shed roof house type, in contrast to the large central hearth evident in other areas of the coast, reflects higher levels of autonomy for individual families in economic, social, and political practices (Grier 2006a; Matson 2003). The northern house design also embodies declarations of authority by the leader of the household. As such, house fronts are used as canvases to project the key iconography of crests (ayuuks) of the matriline, which point to its history (adawx) and legal rights. The central hearth and interior of the building also play a role in this authority by acting as key elements of feasts hosted by the house to perform and legitimate its history and legal rights. Higher ranking leaders and chiefs have larger houses in order to host larger feasts (Coupland 2006).

Seeing hearths and other architectural features as not simply functional, but instead reflective of social practices and relationships, is a poignant example of how thinking about households transforms the archaeology of houses into an enterprise that connects to larger issues in Northwest Coast history. Spatial organization of the major architectural elements within houses and villages is a key dataset in unpacking these complex social dynamics. However, they are time consuming to resolve through excavation, hence the value of a test of the capabilities of remote sensing to accurately and precisely define architectural elements. As we have argued, villages and houses, and the social practices they embody, are central to tackling critical questions in Northwest Coast archaeology and for theorizing social change. With an enhanced capacity to map houses and villages, we anticipate significant advances in several current themes in Northwest Coast archaeology, as outlined below:

Research Direction 1. The emergence of settled village life, including the use of large houses and their arrangement into substantial villages, is inextricably connected to the emergence of social complexity in Northwest Coast scholarship (Matson and Coupland 1995). Social complexity, as typically construed, includes the use of large houses, the emergence of settled villages, resource ownership, and sustained social inequalities (Ames and Maschner 1999; Matson and Coupland 1995). While most Northwest Coast archaeologists decreasingly value the aim of developing a coast-wide, prime mover explanations for such transformative changes, the changing organization of houses and villages remains central to understanding Northwest Coast histories. Household theory provides a framework for interpreting household change in relation to emerging new socioeconomic circumstances, and as such provides a window to investigate change over time (Ames 2006; Grier and Kim 2012; Coupland 1996).

Research Direction 2. Houses are, as Marshall (2006) has argued, a foundation of domesticated society, in which the built environment (and specifically house architecture) is seen as playing a critical role in shaping cultural practices spatially and socially. Such perspectives connect the use of long-standing habitation locations to the construction of place physically and conceptually, and emphasize the connection between place, land tenure, ownership, and property (Grier 2006b; Martindale et al. 2017; Schaepe 2009; Thom 2005). Houses are therefore not simply reflective of an adaptation or strategy, but rather recursively shape social practices.

Research Direction 3. Houses and villages were at the center of constructed landscapes on the Northwest Coast, and the places around which monumental investments in production features were made. Investments in large scale production features such as clam gardens, wetland features, and fish weirs, along with shell dikes and house sites themselves, changed the way in which physical resources were mobilized, and the social relations that attended such practices (Grier 2014; Grier et al. 2017; Letham et al. 2020; Mathews and Turner 2017). These large complexes of features are typically clustered around long-standing village sites (Grier 2014; Letham et al. 2020). Such terraforming has been argued to have been a catalyst for the emergence of ownership and associated mechanisms of resource control that were employed to regulate access and harvesting cycles. Households and villages were the scales at which such practices likely emerged and were sustained.

Research Direction 4. The distribution of village sites across a landscape provides an important indicator of how regional-scale interactions were organized. It is clear from both ethnographic (Barnett 1955; Suttles 1960; Thom 2005) and archaeological data (e.g., Grier 2003; Mackie 2003; Martindale et al. 2017; Supernant and Cookson 2014) that site positioning decisions were made on a regional scale and changed through time. Resource gathering can be thought of as involving "social foraging" — the idea that many resources accessed outside one's own village territory were acquired through social negotiation and made possible through existing social ties. As the spatial organization of the household represents social relationships amongst its members, settlement patterns reflect the relationships among households and villages across a landscape.

Research Direction 5. A sufficient sample of houses and villages in their anthropogenic and geological context is a necessary data set for the evaluation of house and community variability and predictive modelling of site locations. Differences in house and village form are frequently invoked as being culturally and historically meaningful, but the empirical basis of for establishing difference and similarity is generally qualitative rather than quantitative. More spatial data allows for better evaluation of similarity and difference. Similarly, site location prediction has become a key goal of heritage legislators and the Cultural Resource Management (CRM) industry, who seek to better evaluate the likelihood of encountering heritage sites on the landscape (Miller 2018). A richer empirical data base of spatial metrics at a variety of scales of practice permits improved predictive modelling.

Each of these important directions in Northwest Coast research will be significantly enhanced by having a larger sample of house and village plans with which to work. The key therefore is to develop a methodology for significantly increasing our sample of house and village plans without large-scale, destructive excavations. Geophysical techniques offer this possibility as it is the hearths, floors, postholes, pits and other house features that are potentially identifiable with geophysical methods such as ground-penetrating radar, allowing access to patterning in house architecture without excavation. Remote sensing provides a desirable opportunity to increase sample size dramatically while avoiding the destruction of heritage sites.

3. Geophysics on the Northwest Coast: Possibilities and Prospects

Ground-penetrating Radar (GPR) is an active remote sensing technique that transmits radar waves into the ground and records the time and amplitude of the returned signal (Conyers 2013; Goodman and Piro 2013). Data are collected along survey lines and can be rendered as profiles in visualization software. Through post-processing techniques, these profiles can be interpolated to create plan view maps at varying depths. These interpolations can also be converted to 3D volumes for the visualization of subsurface features in multiple dimensions (Conyers 2018). Compared to other geophysical techniques, GPR has the advantage of real-world depth analysis and 3D imaging of targets rather than strictly forward modelling (Conyers 2018; Sturm and Crown 2015). GPR has been successfully applied to diverse contexts and problems in archaeology, well-described in a variety of major synthetic works (e.g., Campana and Piro 2009; Conyers 2013, 2016, 2018; Goodman and Piro 2013; Johnson 2006; Oswin 2009; Schmidt et al. 2015; Wiseman and El-Baz 2007). It has been successful primarily in areas where archaeological features contrast dramatically with relatively homogenous background matrices, as when stone architecture is present in sand. It has also been applied at a landscape scale (e.g., Campana and Piro 2009), as with recent investigations in and around the well-known site of Stonehenge. There, remote sensing surveys have revealed additional buried stone features as well as more subtle features such as pit arrangements and wooden henge-like structures made of perishable materials, not unlike features found in Northwest Coast sites (Gaffney et al. 2012).

Domestic architectural targets (i.e., houses) involve changes between horizontally-oriented strata, large and potentially complex yet discrete features with vertically-oriented interfaces, and arrangements of what might be considered point targets (objects such as rocks). Success has been achieved in GPR imaging of similarly perishable architecture and features elsewhere. For example, Kofun-period pit and surface structures from 7th century Japan have been clearly identified after their burial by volcanic ash (Tohge et al. 1998). Volcanic ash, due to its properties for conducting GPR waves, offers a productive depositional context for GPR. On the Northwest Coast, most targets pertaining to architecture are embedded in a heterogenous matrix of shell and other complex anthropogenic deposits (Dalan 1992; McDonald 2002). While shell-bearing deposits have been investigated elsewhere in North America with some success (Miller et al. 2018; Thompson et al. 2004; Thompson and Pluckhahn 2010), the reflective complexity of the shell matrix and its engineerable plasticity present additional problems. Shell matrices allow architectural elements to be removed, rebuilt and relocated with ease, creating the possibility of architectural features overlapping. Northwest Coast plank houses were regularly inhabited, refurbished, and re-organized spatially over as many as three or four centuries, creating complex superimposed spatial patterns (Ames et al. 1992; Grier 2006a; Patton 2011). Such complexities have made even traditional house excavations challenging, and so potentially present significant difficulties for associating GPR signals with discrete architectural elements and contemporaneous architectural patterns.

On the Northwest Coast, GPR applications have been limited and mostly applied to human burial contexts (e.g., Daniel 2015), and only occasionally focusing on other types of targets such as earthen pit-house features (e.g., Conyers 2007: 341-342; Dojack 2012a) and coastal plank houses (e.g., Cross 1996; Dojack 2011, 2012b; McDonald 2002). Work led by one of us (Martindale) has offered perhaps the most specific methodology for locating and evaluating GPR signals potentially indicative of archaeological burials in the region, involving the use of a "confidence index" (see Daniel 2015). This approach consisted of generating an objectively-derived and reproducible value between 0 and 1 that stipulates the degree of conformance between an anomaly and a known archaeological feature. Such an approach provides for the systematic assessment and interpretation of GPR anomalies. In the study provided by Daniel (2015), no ground truthing was possible given the sensitive nature of the GPR targets (i.e., human burials). In our work presented here, we carry this notion of prediction forward, outlining initial steps toward a multivariate predictive model, validated by minimally-invasive ground truthing, that can be used in a range of Northwest Coast depositional contexts.

Archaeological remote sensing projects elsewhere in North America have had success in areas where construction and deposition processes were broadly analogous to Northwest Coast archaeological sites. On the western Florida coast, for example, Thompson et al. (2014) have used GPR to map subsurface stratigraphic relationships related to mound construction at the Pineland site complex. Their survey provided insights into the cultural and natural formation processes of the mound complex and revealed a series of previously unidentified small and large architectural features. Similar investigations have been undertaken on earthen mounds in the US southeast, where Bigman and Lanzarone (2014) were able to effectively map the subsurface of the central portions of Ocmulgee Mound A in Georgia. In a similar vein, Gamble (2017) has utilized GPR to help establish that Chumash mounds in southern California were in fact monumental constructions. Like these sites, the archaeological record of the Northwest Coast includes large-scale mound constructions and production features (e.g., clam gardens, freshwater wetland gardens, fish weirs), house sites, defensive structures, and shell dikes and ridges (Grier et al. 2017; Martindale et al. 2017).

To overcome the many potentially confounding problems of these complex archaeological situations, remote sensing surveys can mobilize multiple techniques to aid interpretation (Conyers et al. 2018; Gaffney et al. 2015; Kvamme 2003a). Our investigations presented below couple GPR survey with magnetic gradiometry, as it has been shown in other contexts to aid site and landscape interpretation (e.g., Conyers 2018; Gaffney and Gater 2003; Kvamme 2003b; Wadsworth et al. 2020). Magnetic gradiometry is a passive remote sensing technique that records local variation in magnetic fields using two sensors (Kvamme 2006). The top sensor records the overall magnetic field and the bottom sensor records the near-surface magnetic field. Subtracting the overall field from the near-surface field generates a 2D magnetic gradient map of the site, with 'anomalies' potentially representing features with significant variation in magnetic susceptibility from the background, including hearths (e.g., Dolan et al. 2017).

The number of fully reported and/or published remote sensing studies of Northwest Coast plankhouses are few, but applications of magnetometry and other geophysical technique such as resistivity have clearly been illuminating. Matson's early work at Shingle Point on Valdes Island (Matson et al. 1999) involved resistivity survey, completed by Guy Cross (Cross 1995), illustrating potential feature patterning inside a precontact Salish plank house at Shingle Point on Valdes Island (Matson 2003; Matson et al. 1999). Geophysical survey was followed by extensive excavations, resulting in the entirety of a plank house compartment being subsequently excavated and ground truthed (Matson 2003). Two decades later, Dolan et al. (2017) applied magnetometry at the nearby Dionisio Point village (DgRv-3), where significant excavation has taken place over the last 20 years (Grier 2003, 2006a, 2014). Magnetic gradiometric survey, completed by a team from the Center for Advanced Spatial Technologies at the University of Arkansas, was successful in delineating major activity areas within plankhouses at the village site (Dolan et al. 2017). It was also successful in identifying the patterning of combustion features (i.e., hearths) within houses. Dalan (1992) provides description of early use of electrical resistivity, investigating site formation processes at a large shell-bearing site at British Camp in the San Juan Islands of Washington state. Her work revealed that the large shell-bearing deposits accumulated vertically and slowly, and prograded seaward from the shoreline over time. Other geophysically-driven projects in areas adjacent to the Northwest Coast have shed important light on house form and village structure, as exemplified by a magnetic gradiometry and conductivity survey at the Bridge River site (EeR-14) in the interior plateau of British Columbia (Prentiss et al. 2008).

In our view, remote sensing surveys of house remains are more likely to provide insights when guided by and evaluated against a model that expresses a typical or expected spatial organization and layout of houses (e.g., Matson 2003; Prentiss et al. 2008) and the geophysical properties of features they contain (Conyers 2016). As discussed above, the shed roof house found in the Coast Salish region has a unique spatial footprint and interior signature, based around multiple individual rather than one central hearth area, and incorporating lines of rafter support uprights along the front and rear walls. Conversely, the Tsimshian plankhouse consists typically of four large roof posts, a central hearth, and upright support posts for the walls. Excavations in coastal and interior Tsimshian settings demonstrate that house builders valued symmetry, recurring spatial distances and proportions, and right angles (Coupland et al. 2009; Martindale 1999). Yet it is important to consider that houses and house deposits were altered and reworked over time through activities such as sequential house rebuilding, floor rejuvenations, pit and cellar excavations, and shell terrace construction (Martindale 1999). Moreover, archaeological research has shown that not all houses will or should conform to an ideal template (e.g., Coupland et al. 2009; Grier 2006a; Matson 2003; Martindale 2006) and geophysical investigations must accommodate that variability.

Nonetheless, an expected model offers a frame of reference in which to situate identified features and measure potential variation, and the application of a house spatial model to geophysical survey results will be critical. In the Salish area, the work conducted at Dionisio Point (Dolan et al. 2017) took this approach. Distinct zones of activity within houses were posited, transitions between interior floor and exterior areas were explicitly demarcated and expected hearth locations were identified, drawing on previous archaeological investigations of shed roof houses (e.g., Grier 2006a; Matson 2003; Samuels 2006). Expected magnetic signatures were posited for areas of the house based on their known depositional characteristics and were compared to collected geophysical survey data. Strong concordance with expectations was found between house areas and magnetic signals (Dolan et al. 2017).

Work at the McNichol Creek site (GcTo-6) in the Tsimshian region provides a similar case study from a northern region of the Northwest Coast (Cross 1996). Here, combined GPR, induced electromagnetic conductivity (EMC), and ambient magnetic field surveys were conducted within five house depressions to resolve large architectural features including hearths, post molds, and occupational surfaces (house floors). Cross identified several potentially confounding factors in the subsurface that might obscure the expected patterning of architecture, including buried metal and deadfall logs within the 0.5 to 1.25

m of overburden. The GPR distinguished occupational zones located near the surface from adjacent space and allowed identification of major stratigraphic breaks within and outside of the depressions. Both magnetometry and GPR identified appropriately-sized anomalies in the expected position of major hearths and GPR locations of potential major post molds. Overall, the pioneering work of Cross (1996) demonstrated (1) the utility of remote sensing in northern contexts overall, (2) the value of alternate methods to assess the nature of subsurface anomalies, (3) the importance of both signal character and anomaly dimensions and location for the identification of architectural elements, and (4) that replicating expected spatial patterns in multiple houses provides added confidence in the results.

While the complexity of Northwest Coast sites and the nature of their deposits and features present challenges for remote sensing methodologies, the success of the limited number of studies that have been conducted, particularly when coupled with studies in other areas of the world with similarly complicated deposits and comparable archaeological objectives, attests to the potential for remote sensing to reveal household, village, and settlement patterns on the Northwest Coast.

4. Study Area

The present study is situated in Prince Rupert Harbour (PRH) on British Columbia's northern coast (Figure 1). Here, under high annual precipitation (+3 m) and dense forest, the Coast Tsimshian have lived and built their monumental winter villages for millennia (Ames and Martindale 2014). The ancestors of the modern Tsimshian had a highly specialized, yet diverse marine-based economy based on shellfish, salmon, eulachon, herring, and a suite of other resources obtained from both sea and land. Intensive harvesting of shellfish led to the creation of dense shell matrices in and around their village sites. Villages were occupied year-round, though people were most sedentary in winter, and the winter villages in PRH appear to have denser shell matrices than elsewhere on the NWC (Ames and Martindale 2014).

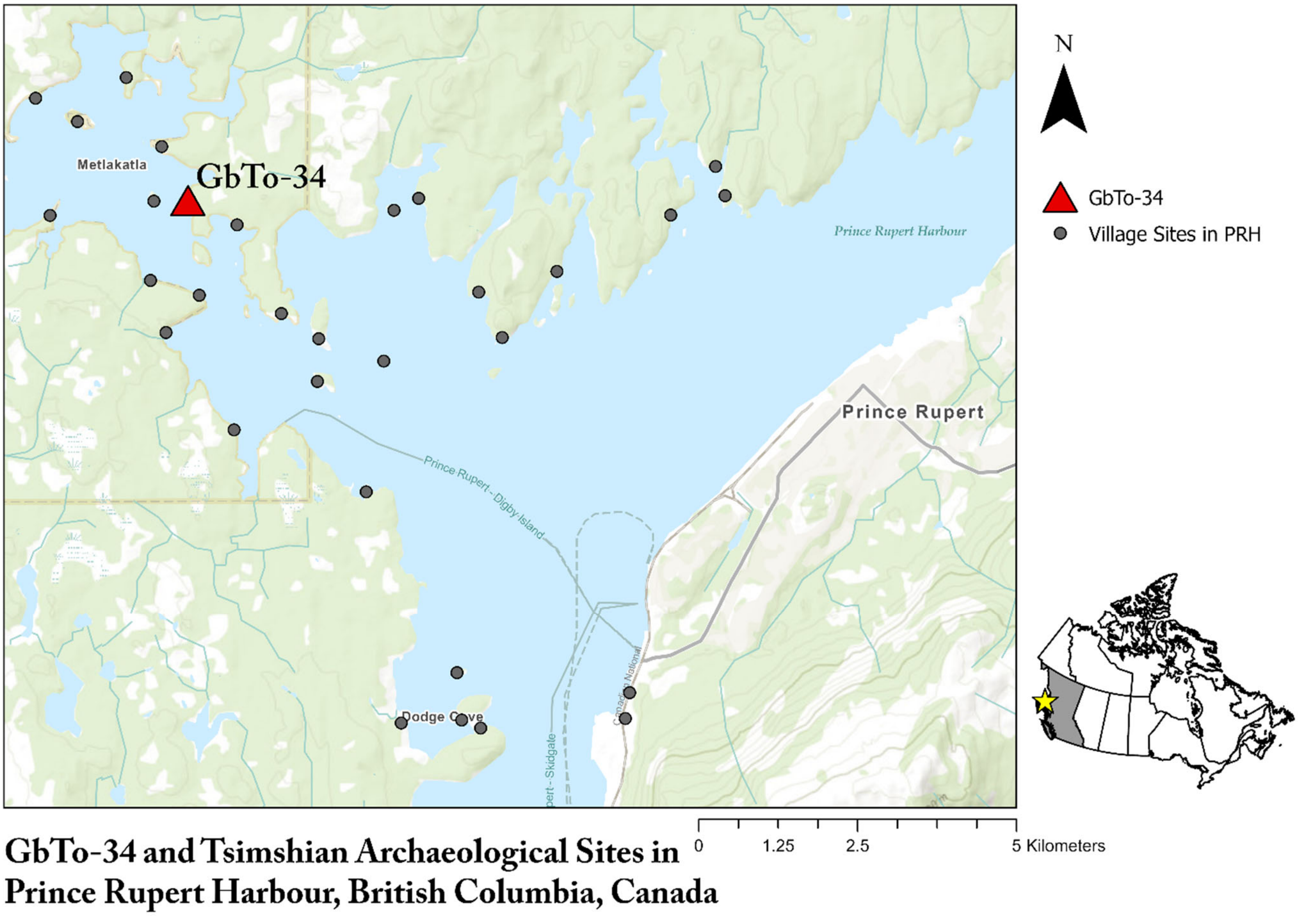

Figure 1. Regional map of Prince Rupert Harbour, British Columbia with GbTo-34 (Δ) and other Tsimshian archaeological village sites (○) indicated. Created in ArcGIS Pro using sources from: Esri, Airbus DS, USGS, NGA, NASA, CGIAR, N Robinson, NCEAS, NLS, OS, NMA, Geodatastyrelsen, Rijkswaterstaat, GSA, Geoland, FEMA, Intermap and the GIS user community, NRCan, Esri Canada, and Canadian Community Maps contributors, Esri Canada.

Our investigations focused on one of these winter villages, Kitandach (GbTo-34), a large coastal village site in PRH. The site has been the subject of significant archaeological investigation, and represents one of the few consistently occupied sites during the PRH Middle period (1000-3500 BP)(Cookson 2013; Edinborough et al. 2017; Letham et al. 2017; MacDonald and Inglis 1981). The site topography consists of large shell ridges that occur across the site and rise up to 4 m (Letham et al. 2017). Between the shore and the furthest inland shell ridge are two large stepped terraces, each with a row of house depressions. In total, the site has three house rows and 17 visible house depressions, although there may be an additional front row of houses truncated by erosion (Figure 2). Radiocarbon dates for the site span the last 5000+ years of history, with median dates that range from 313 to 5721 cal BP (Edinborough et al. 2016; Letham et al. 2017). The average house depression size is 55.8 square meters, and the site follows the typical village pattern of larger (more prominent) houses in the front-center position (Archer 2001; Coupland 2006; Letham et al. 2017).The southern portion of the site was impacted by European-introduced gardening (potato farming) after contact, resulting in damage to portions of the site.

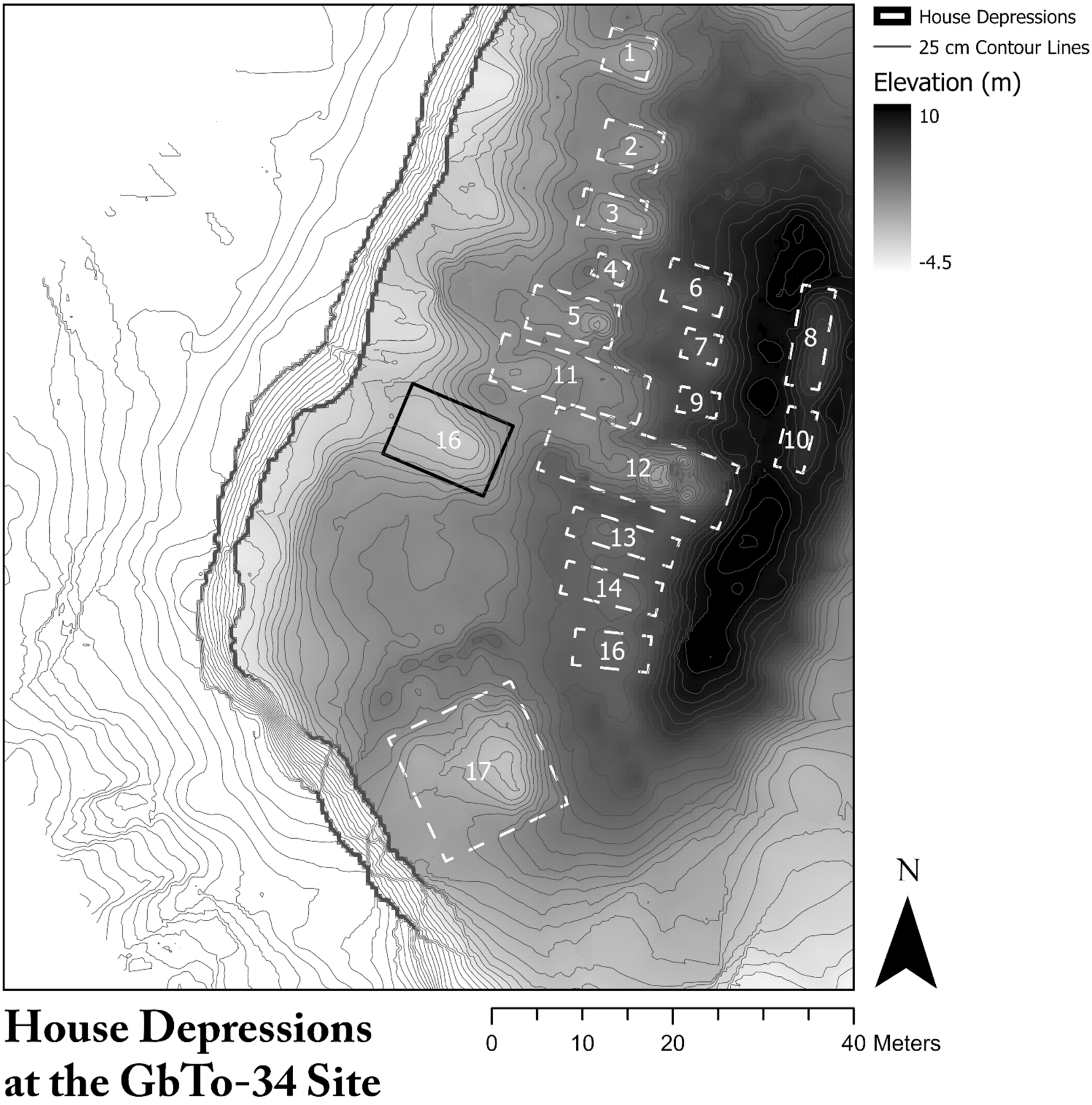

Figure 2. Map of the Kitandach Site (GbTo-34) with house depressions outlined and numbered. The depression investigated in this paper, House 16, is outlined with a solid black rectangle, while the others have dashed outlines. The map of house depressions was modified from the original drawings by David Archer (2001) and published reproductions in Letham et al. (2017). Elevation data by Kisha Supernant. Figure was created using ArcGIS Pro.

In 1971 the largest plankhouse at GbTo-34 was excavated by Richard Inglis and a team from the Canadian National Museum (House 17 in Figure 2)(MacDonald and Inglis 1981). Although his reports on the site hold limited utility for the present study, they contain a list of artifacts found in the house depression and a pH analysis of the soil, which was found to be relatively neutral. Given the size and anomalous shape of House 17, it is possible that it postdates the other house depressions, which represent an earlier village component (Letham et al. 2017). However, the site dates come primarily from the shell terrace matrix, which may not accurately reflect the dates of occupied houses. More recently, Kitandach was systematically mapped, cored, and intensively radiocarbon dated by Letham and colleagues (Letham et al. 2017). From this work it was determined that shell deposits comprised a subsurface area of 8200 square meters across the site. The extensive previous research at the site allows for geophysical data to be compared to existing archaeological information. Specifically, House 16 at Kitandach was chosen to test the geophysical methods, as it had yet to be archaeologically investigated in any detail.

House 16 is a large house depression situated at the 'front' of the village, that is, in the first intact row along the shore. As such, House 16 is at high risk due of coastal erosion, and shell continues to erode from the shoreface in front of the depression, making its investigation more urgent than others. Being closest to the shore also offered several advantages for geophysical survey, including accessibility to the survey area and requiring less vegetation clearing. Despite these advantages, the survey site was not clear of obstructions, and significant effort was required in closely cutting the small saplings and removing the deadfall to allow for the geophysical surveys to run unobstructed, following Cross's (1996) protocols. Fortunately, no significant trees had regrown within the house depression. Percussion coring in House 16 during the 2019 season (discussed further below) has provided a detailed view of its soils, which are comprised of a top humic layer, followed by various sandy/shell-rich soil layers.

4.1. Methods

In the summer of 2019, GPR and magnetic gradiometric surveys were conducted at House 16, covering the depression and several meters beyond its evident extent (Figure 3). A grid of 10 x 14 m was staked out using non-magnetic tapes and tent pegs. The GPR survey was conducted using a GSSI SIR 3000 GPR console with a 400 MHz center frequency antenna. During the same summer, surveys at other sites around Prince Rupert Harbour helped us to establish a relative dielectric constant range of 20-23 (Wadsworth 2020). Knowing this and the depth of the deposits, the range was set to 90 ns and samples were to set to 1024 to ideally capture the entirety of the house deposit over the area of interest. Gains were set automatically in-field and were consistently used over the course of the survey. To maximize resolution of the archaeological features, a transect spacing of 25 cm was used. The same GPR grid was surveyed unidirectionally in both the x and y directions. Given the substantial topographic variation of the house depression when moving from external ridges to interior floor areas, the ground-penetrating radar data was post-corrected for surface elevational differences.

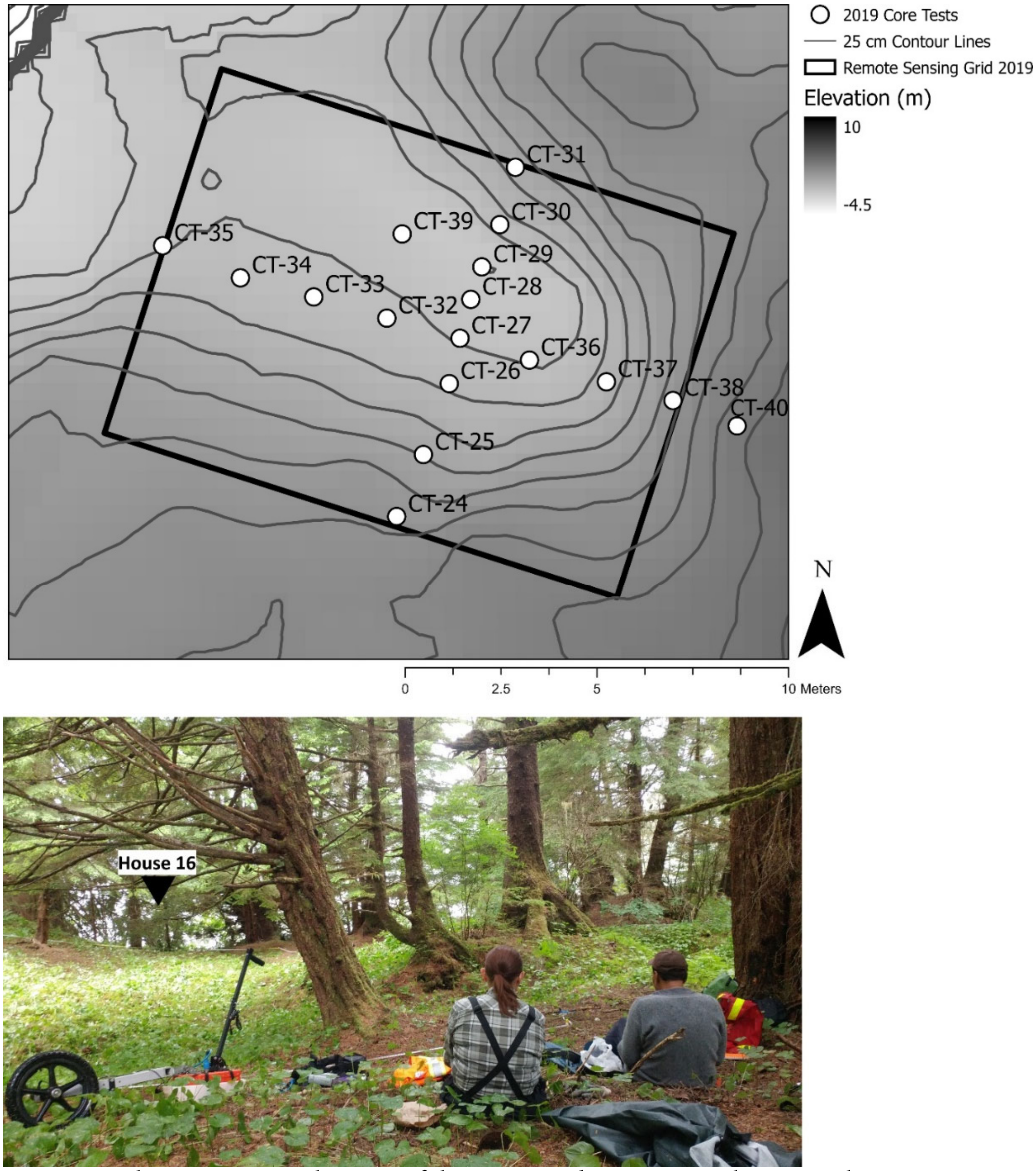

Figure 3. Top: Close-up topographic map of the House 16 depression at GbTo-34 with 25 cm contour intervals. The black rectangle represents the georeferenced remote sensing grid over the house depression, and white circles are core test locations (with abbreviated name/core number). Bottom: View from the back of House 16 looking over the depression towards the shore. Picture shows the cleared House 16 ready for GPR survey. Kisha Supernant (University of Alberta) and Steve Dennis (Lax Kw'alaams) pictured. Photo by William Wadsworth.

The magnetic gradiometry survey was conducted using a GEM Systems GSM-19 Overhauser magnetometer. Magnetic data was collected in survey transects with sensors set to a height of 15 cm and 70 cm above the ground. An AC filter of 60 Hz was used, and cycle time was set to 0.2 seconds. While this equipment collects data using time rather than distance, equipment parameters were set to input manual xy grid markers, which the magnetometer uses to space the readings. The machine was autotuned, and 'zeroed' away from the archaeological site. Like the GPR survey, the magnetic survey was conducted along 25 cm transects in 'walk grad' mode and in both x and y directions. Unlike the GPR survey, however, transects in each grid were conducted bidirectionally (that is, in a zigzag pattern). In both our GPR and magnetic gradiometry surveys in the y direction effectively duplicated the x direction data. However, both directions will be drawn upon to communicate results.

Prior to processing, both the GPR radargrams and timeslice data were corrected for topographic variation as follows. In *ArcGIS Pro*, elevation data from House 16 was sampled from high-density topographic maps produced in previous years of the project (Letham et al.. 2017). To convert two-way time to depth, a dielectric constant of 21 was determined for this specific site using hyperbola fitting analysis. GPR profile analysis and basic processing (time-zeroing and background removal) took place in *GPR Viewer*, before being 'sliced' into 2 ns timeslices (approximately 5 cm thick) using *GPR-SLICE* . This thinness was necessary as thicker timeslices seemed to obscure the complicated feature deposits. Following the creation of these timeslices, the data was then exported and visualized as amplitude maps in *Surfer 18*. An inventory of potential features was created during the profile analysis stage of GPR processing and aided the interpretation of elevation-corrected amplitude maps. The magnetic gradiometry data also underwent basic processing. Zero-mean traversing and de-spiking corrections were applied to the data using *Snuffler.* The data was then exported and visualized as a magnetic gradient map in *Surfer 18*. Using the same program, profiles from across the house depression were sampled and analyzed in conjunction with the GPR and core data. Some uninterpreted data (without annotations) from these methods are presented in Figure 4.

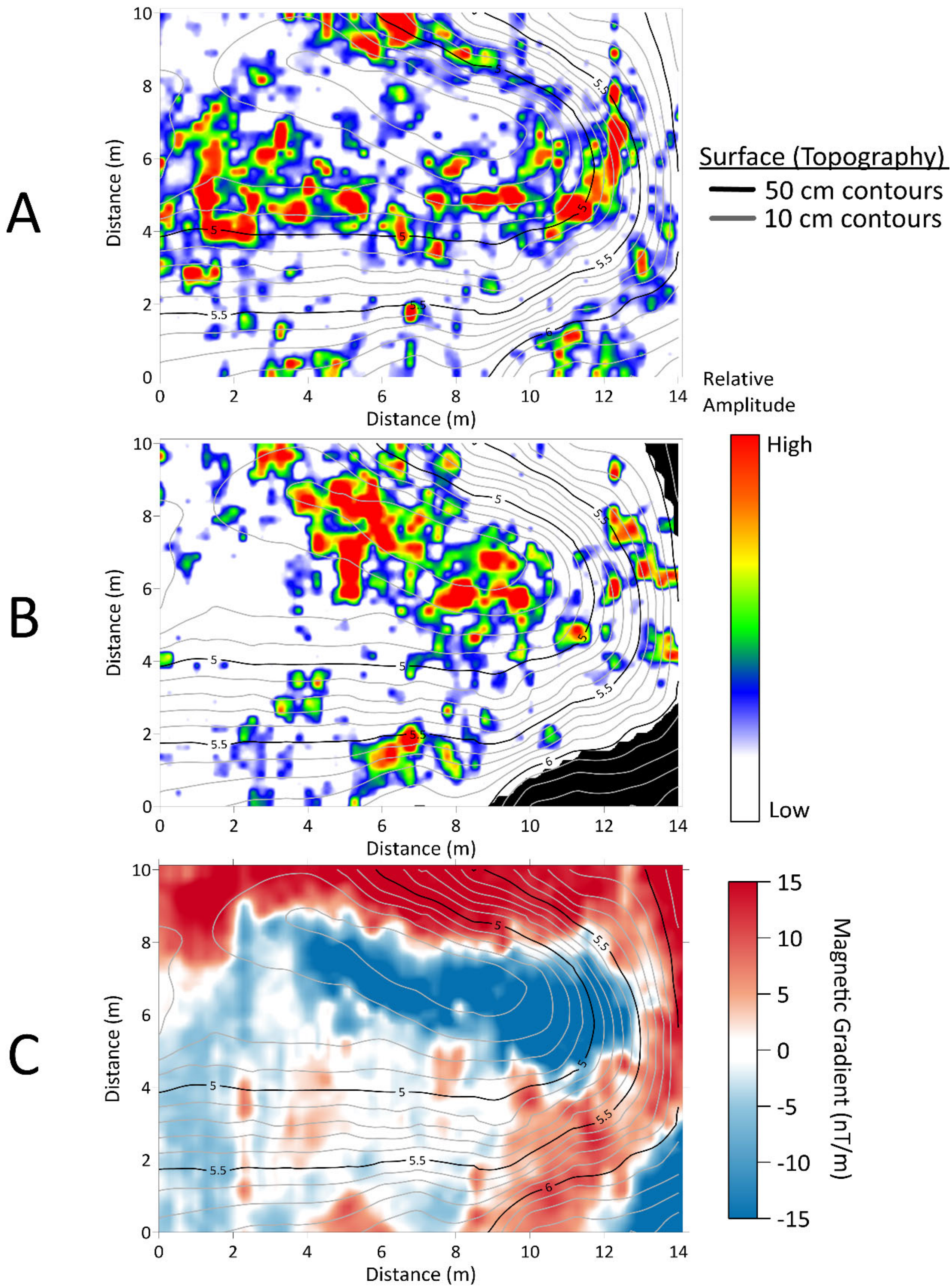

Figure 4. Uninterpreted GPR and magnetic gradiometry data with topographic contours superimposed. A: Elevation corrected timeslice from potential occupation surface around 220 cm DBD. B: Timeslice from a deeper potential occupation/ feature layer at approximately 270 cm. C: Zero-mean corrected and de-spiked magnetic gradiometry data from House 16 (on a scale of -15 to 15 nT/m). Strong magnetic signatures were present across the depression and are likely indicative of features.

The results of these processed geophysical surveys were then used to identify potential house architectural features, characterize their size and orientation, and identify an initial set of features, primarily the possible central hearths, for ground truthing with percussion coring. Hearths are expected to be indicated by layers of dark sand/soil layers, containing charcoal and plant materials, and situated in occupation surfaces interspersed between shell layers (Martindale 1999; Ruggles 2007). Percussion core samples were obtained in a crosscut pattern across the house depression every 1 to 2 m, with additional judgmental sampling in the center of the house area (Figure 3). Finally, each of the remote sensing survey grid corners and core sample locations were georeferenced using either a Leica G15 RTK GNSS or Leica total station and imported into *ArcGIS Pro* for analysis.

5. Results

5.1. Ground-penetrating Radar

A number of general conclusions about how radar reacts to PRH environments were drawn during the 2019 season that help make sense of the House 16 data (Wadsworth 2020). First, the higher water content in the soil slows radar wave velocity, which results in fewer (due to poor energy penetration/reflection) and laterally defined diffraction hyperbolae (Conyers 2016). Second, the variation between different shell layers appears to correlate to variation in moisture content and the dielectric constant between layers, creating differences in radar velocity and the overall signal. Moisture retention is a result of high organic content/lower shell content and particle size. Overall, GPR distinguishes localized features such as post-molds and hearths that have both planar and vertical interfaces and differences between horizontally layered stratigraphic planes of different composition. Point-source reflections found within these deposits are possibly linked to the heterogeneity of both features and occupational zones within the shell matrix.

Rather than discussing the GPR results in terms of a relative depth, the following reflection depths were calculated to be on a scale comparable to the coring data. The timeslice depths had to be rectified by approximately 30 cm to be in line with the percussion coring datum (the highest core, CT-2019-38), the timeslices that exceeded this height were excluded from analysis, as were other cores beyond the house margin. The result of this procedure generated depth-below-datum (DBD) depths that are directly comparable between the GPR and the coring data as summarized below.

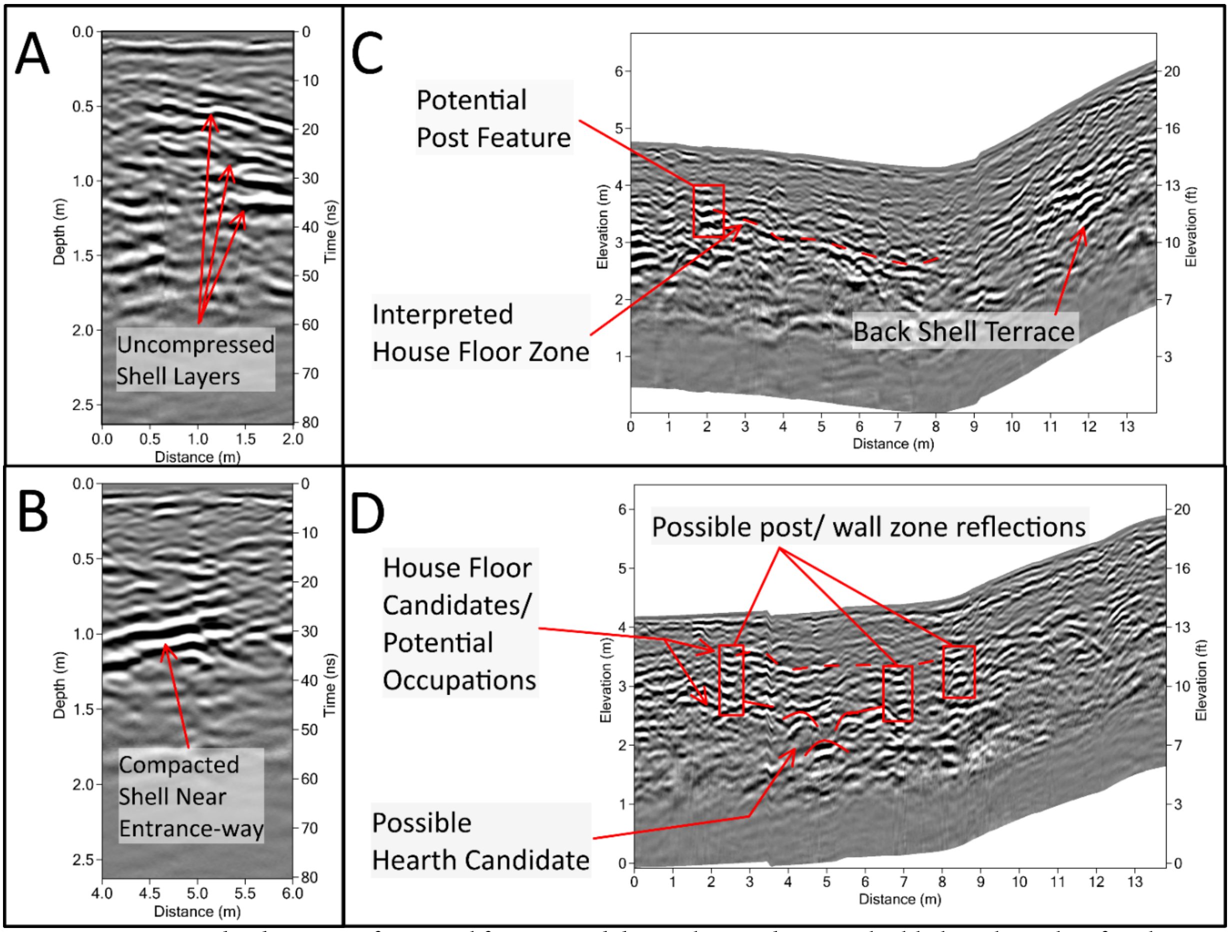

Figure 5. Interpreted radargrams of potential feature candidates. These radargrams highlight only a select few that are pertinent for the present study. A: Overlapping and stacked uncompressed shell layers from the shell ridges around the house depression. B: Compacted shell/occupation layers near entranceway of house. Similar reflective features interpreted as house floors within the interior of the house. C: Radargram crosscutting House 16 (in the y direction) with examples of interpreted post features, potential occupation layer, and transition to shell terrace. D: Radargram from the y direction showing multiple identified post reflections, two potential occupation layers, and a hearth candidate.

Prior to discussing GPR features within the house depression, it is important to consider the perimeter. GPR results indicate that the outer ring of the house depression largely consisted of overlapping highly reflective layers (Figure 5: A), which were determined to be part of the shell matrix. These features also conformed well to the topography around the 'sides' and 'back' of the house depression, however the layers seemed to converge toward the front (Figure 5: A and B; Figure 6). This can be interpreted as the result of entrance way construction and possible compaction due to increased foot traffic. Potential features were also identified beyond the house margin but were excluded from the present analysis of internal house components.

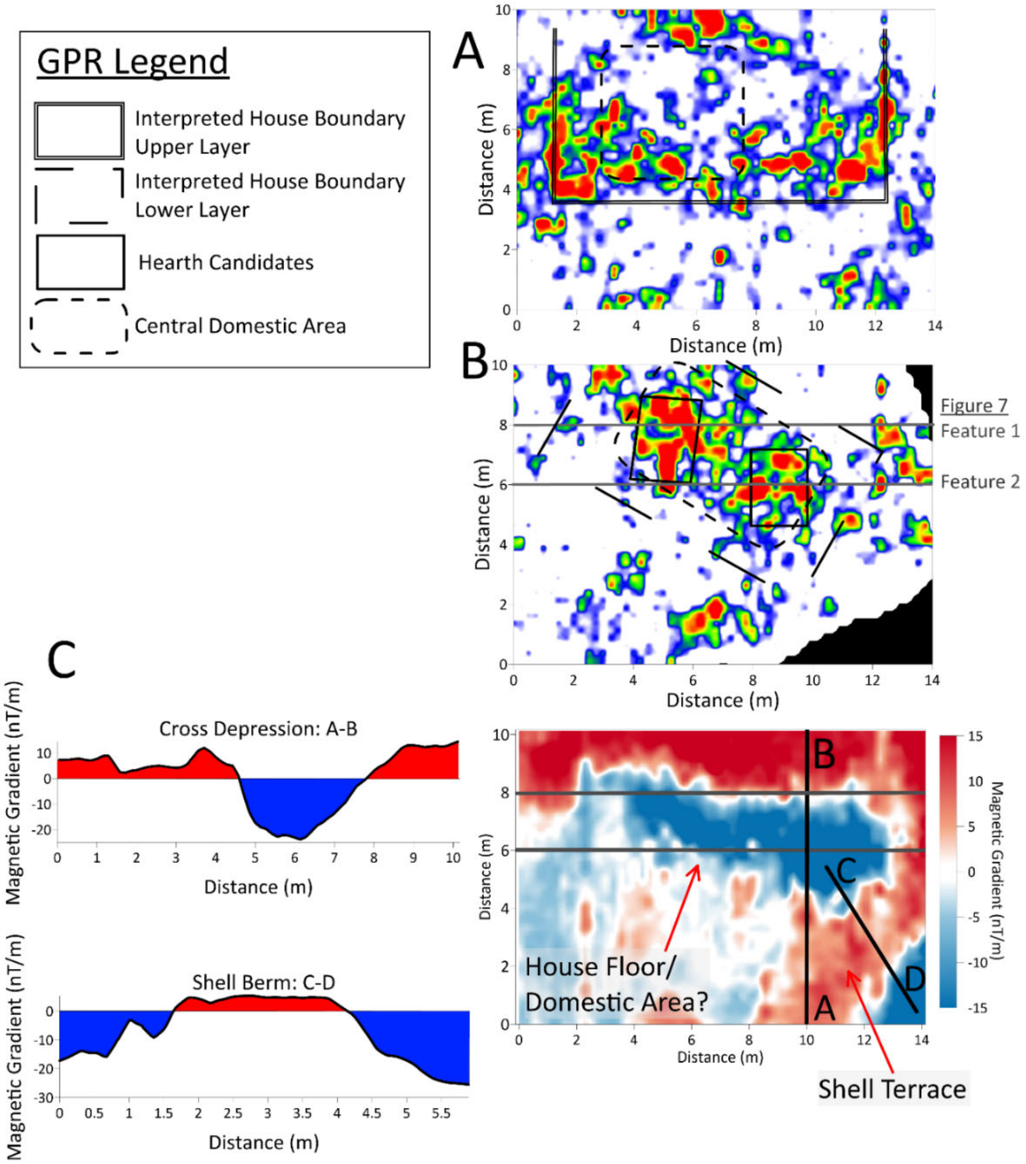

Figure 6. Emerging interpretation of House 16. A: GPR timeslice from 220 cm DBD. Linear reflections may represent the boundary between house and shell berms or wall zones. Three of these boundaries were interpreted (double solid line) and connect to two possible post reflections. The interior interpreted 'domestic area' is represented in deeper layers but is relatively absent in this layer with many reflections occurring between this area and the house boundary (house perimeter). B: Two large (approximately 2 x 2 m) features were located in the elevation-corrected profiles and are seen here in a GPR timeslice from 270 cm DBD (indicated by solid squares). Two GPR and magnetic profiles crossing these potential features are highlighted in Figure 7. While boundaries are not as clear as upper layers, the central area around the features seems to be a higher amplitude area compared to the rest of the grid, and boundaries were based on the size of the upper components. C: Profiles taken from the magnetic gradiometry data appear here and in Figure 7, and are plotted here on the house spatial plan. Magnetic profiles clearly demonstrate the inferred change between 'inside' and 'outside' the house, with the shell ridges forming the depression being positively magnetic and the interior depression itself negative. Potential features in the magnetic data are noted.

Following the archaeological model for Tsimshian plankhouses, profile and timeslice analysis attempted to identify reflection 'candidates' for house floors, large interior roof posts, wall support posts, walls, and central hearths (Figure 5: C and D; Figure 6). The majority of potential features identified occurred near the center of the house depression at around 2 to 3 m DBD. Above this, the subsurface appeared to consist of fill layers over the house deposit. Highly reflective boundaries possibly related to stratigraphic breaks were found within this zone. However at times, these linear reflections disappeared or were disjointed in profile. It was hypothesized that these GPR reflections might be related to 'house floor zones' and two potential candidates were identified at approximately 220 to 235 and 255 to 270 cm DBD. In some areas these two distinct zones appeared to converge, but in others they were discrete features. Within these zones potential features were identified, but between these zones the reflections were less clear. While an occupational surface (i.e. the floor of a house) may be expressed as a singular sedimentological component, it is more likely to be a heterogenous vertical zone in that includes impacts the subfloor, the floor itself, and material traces on top of the floor. Heterogeneity also extends laterally, with different parts of the floor demarcated by features, activity areas and varying interstitial spaces. This vertical and horizontal material variation likely creates complex GPR reflections. Thus, an occupational floor might be more appropriately thought of as a horizontal zone of heterogeneity punctuated by reflective features of different forms within a more homogenous matrix.

Within the identified upper layer (220 to 235 cm), possible post and linear radar reflections were identified. These identified post reflections appear to be up to 50 x 50 cm when viewed in profile. While it is tempting to speculate these large post and linear reflections might be corner posts and walls, it is a more conservative to suggest these represent the boundaries between shell and house matrix, at least until more data are obtained. This caution was supported by the realization that, when examined in profile, these linear reflections do not produce a line of point-source reflections (as one would expect from a wall) but are a more reflective layer abutting the shell matrix. Further, only three house boundaries could be identified, with the fourth being possibly obscured by the north shell berm. From these interpreted boundaries the house area is approximately 6 x 11 m. Boundaries identified in this upper layer allowed for this preliminary interpretation of house size and shape to be obtained, however these same potential features were not identified in the lower layer (255 to 270 cm DBD). It is also interesting to note that the shape of these boundaries conform well with the surface topography. Furthermore, inside the interpreted perimeter of these boundaries is a layer of small point-source reflections that may be related to artifacts related to the living area inside the house, though this has not been confirmed through excavation.

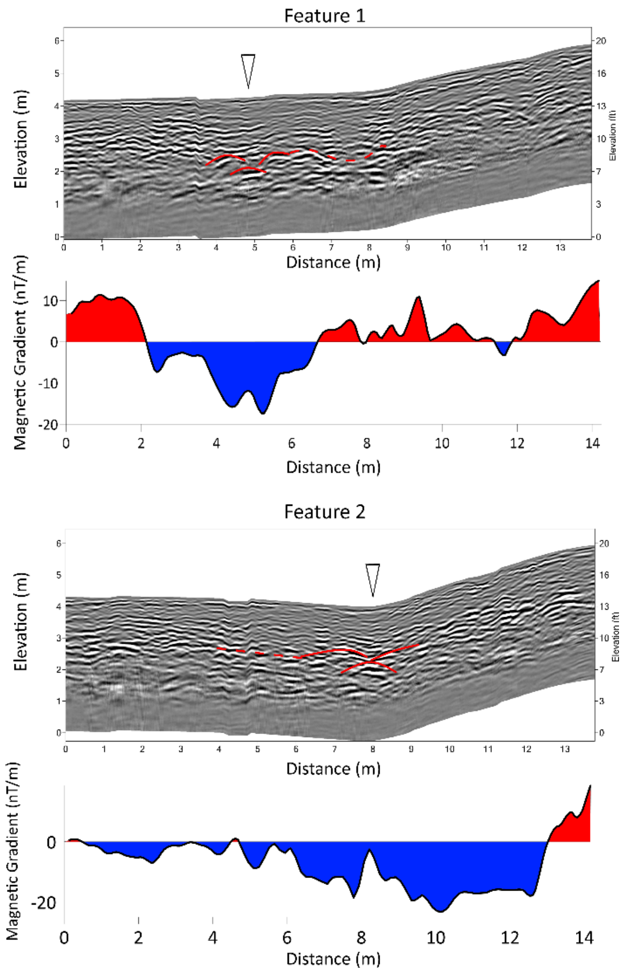

Figure 7. GPR and Magnetic Profiles from two interior feature candidates in the center of House 16 (approximately 270 cm DBD). GPR 'bow-tie' reflections identified in the profile as potential basin-shaped features correspond with magnetic lows (-15 to -20 nT/m), with certain areas not directly over the features being more moderately negative/positive. Roughly continuous radar reflections were found across this layer connecting the features. Currently it is suspected that these features are hearths. GPR annotations do not capture the full range of features in the profiles, but specifically highlight the identified bowtie reflections connected to potential occupation surface.

Candidates for central hearth features were also found in both potential occupation layers (Figure 6). GPR profile analysis identified large 'bow-tie' reflections characteristic of 1.5 to 2 m synclinal features (in both directions). In the upper layer only one such feature was identified, but was located more towards the front/shore than center of the house. Two obvious and large bow-tie reflections were found in the 'floor' of the lower layer (approximately 270 cm DBD) (Figure 7). These were large and roughly rectangular in shape and appeared to have an internal structure. These features were separated 1.5 m apart and were connected to the identified potential surface. Around these potential features many point-source GPR reflections were present. Beneath this lower layer, the GPR signal largely attenuates.

5.2. Magnetic Gradiometry

The magnetic data used to augment the GPR survey provided interesting results that helped characterize potential features (Figure 6 and Figure 7). First, the shell matrices surrounding the house depression were strong positive magnetic anomalies which correlated well with surface topography. While originally much stronger magnetic values prior to de-spiking, shell matrices were determined to have a magnetic gradient of about +5 to +15 nT/m. These high positive values make sense given the immense amount of organic content in these shell matrices (Campana and Piro 2009). When profiled across, the magnetic values also seem to form 'ridges' or normal curves with the highest magnetic values occurring at the center and lessening toward its edges, perhaps indicating organic density.

Within the center of the depression, magnetic lows were mostly found. These magnetic values also appeared to have a rectilinear character to them. The most negative magnetic values were found at the very center of the house depression and corresponded directly with the potential hearth features identified at 270 cm DBD (Figure 7). When the magnetic profiles were sampled along these bow-tie radar reflections, magnetic values of -10 to -20 nT/m corresponded directly with the features. This is interesting as the upper 'hearth' candidate, while negative, is less magnetically striking.

Many other features appear to be present in the magnetic data, both small positive and negative anomalies. These have yet to be investigated in great depth, however, and no strong dipoles were found, limiting forward modelling potential. As previously mentioned, the magnetic gradiometry survey was chosen to augment the GPR survey as a secondary technique, and as such, its survey methodology is being developed. It is quite possible that with more refined application in the future, more dipoles can be discovered/modelled and anomalies better characterized.

Overall, there appears to be concordance between the GPR and magnetic data. However, to prevent self-affirming interpretations, we hope to follow each line of inquiry to its completion before combining the datasets. Above, a potential geophysical template with limited *a priori* feature interpretations was described. Following the presentation and interpretation of percussion coring data collected from House 16, all three lines of evidence are combined to form interpretation models.

5.3. Ground Truthing with Percussion Coring

Percussion coring was developed by Cannon (2000) as a method of sampling basal components from shell matrix sites for radiocarbon dating. It was subsequently applied to mapping subsurface stratigraphy (Martindale et al. 2009), lithographic analysis of subsurface components (Pluckhahn et al. 2015), and site development metrics (Letham et al. 2017). In each case, researchers demonstrated the potential of this method for more refined stratigraphic assessment. The method is straightforward. A cylindrical hollow bit containing a plastic sample sleeve that is 3 or 4 feet (91.5 or 123 cm) long by 1' (2.5 cm) in diameter is hammered into the subsurface, reaching sample depths of over 5 m. The core sampler (we used an ESP Plus Subsurface Probe) captures stratigraphic integrity of the subsurface but distorts stratigraphic relationships by compression. Currently, we do not have any data on the relative compression effect on different kinds of stratigraphic components, so a single expansion factor is applied to each sample tube results. Samples are mapped into layers by a series of lithological traits including composition, particle size and range, compaction, color, and estimated shell and charcoal fraction. The results are tabulated and presented as standardized charts in *Strater 5*, which can also be used to create hypothesized projections of horizontal stratigraphy across adjacent cores based on stratigraphic similarity and difference.

Here, we compare a series of closely spaced percussion core tests (1 to 2 m apart) arranged in perpendicular transects along the major axes of the H16 house depression at GbTo-34. Coring inside the known house depression provides one certainty for our analysis: there is likely an occupational surface in the upper component of these cores associated with house occupation prior to abandonment. The purpose of the core analysis was to identify the lithological and stratigraphic candidates for this occupational surface and its constituent features for comparison to the remote sensing interpretations, representing an initial attempt at ground truthing. The advantage of coring is its speed, efficiency, and minimal destruction of the archaeological site. The challenges of this application of coring is that occupational surfaces within structures in NWC shell terraces are complex and heterogenous. The horizontal sample of stratigraphic results within the core diameter (2.5 cm) may not be sufficient to locate recurring patterns associated with the complex patterns of house floors. A smaller interval in core locations decreases the efficiency of coring as a ground truthing method; if percussion coring is useful as a ground truthing tool for remote sensing it ideally will be effective at this intensity and scale of data collection.

Despite the heterogeneity of occupational surfaces and the complexity of shell terrace formation, our expectation is that some surfaces would be visible in some form in percussion cores. Occupational surfaces represent a suite of recurring properties that include increased compaction, higher levels of smaller sediment particles (silts, clays and sands), higher concentrations of charcoal, lower concentrations of shell, and higher organic components visible as darker sediments. Preliminary assessment of the 2019 House 16 core results suggests that there is a pattern of three layers within any house floor: a lower component with larger particle sizes, lower organic and charcoal content and high compaction (this seems to be a subfloor response to use of the floor), a middle layer with high compaction, small particle size, high charcoal content, and varied composition and colour (this is the floor proper), and an upper component with larger particle size, low shell content, low compaction, and high charcoal content that is of variable thickness (this represents the contents on the surface of the floor). In contrast, shell terraces that are not part of occupational surfaces tend to have high shell content, low to very low compaction, large particle sizes, and low content of charcoal and fine particles.

In addition to sedimentological traits, specific archaeological features can be identified in cores from their major sedimentological components, most notably hearths. Core CT-2019-028 (Figure 8), located near the center of the depression, contained two thick charcoal layers at about 210 cm and 270 cm below the reference datum (the ground surface at CT-2019-038). Thick lenses of charcoal in this context are positive evidence of hearth features, which we expect to see in the center of each house. That two such features are stacked in approximately the same horizontal position, suggests that houses are rebuilt in the same location, a pattern visible in other locations in the region (Patton 2011).

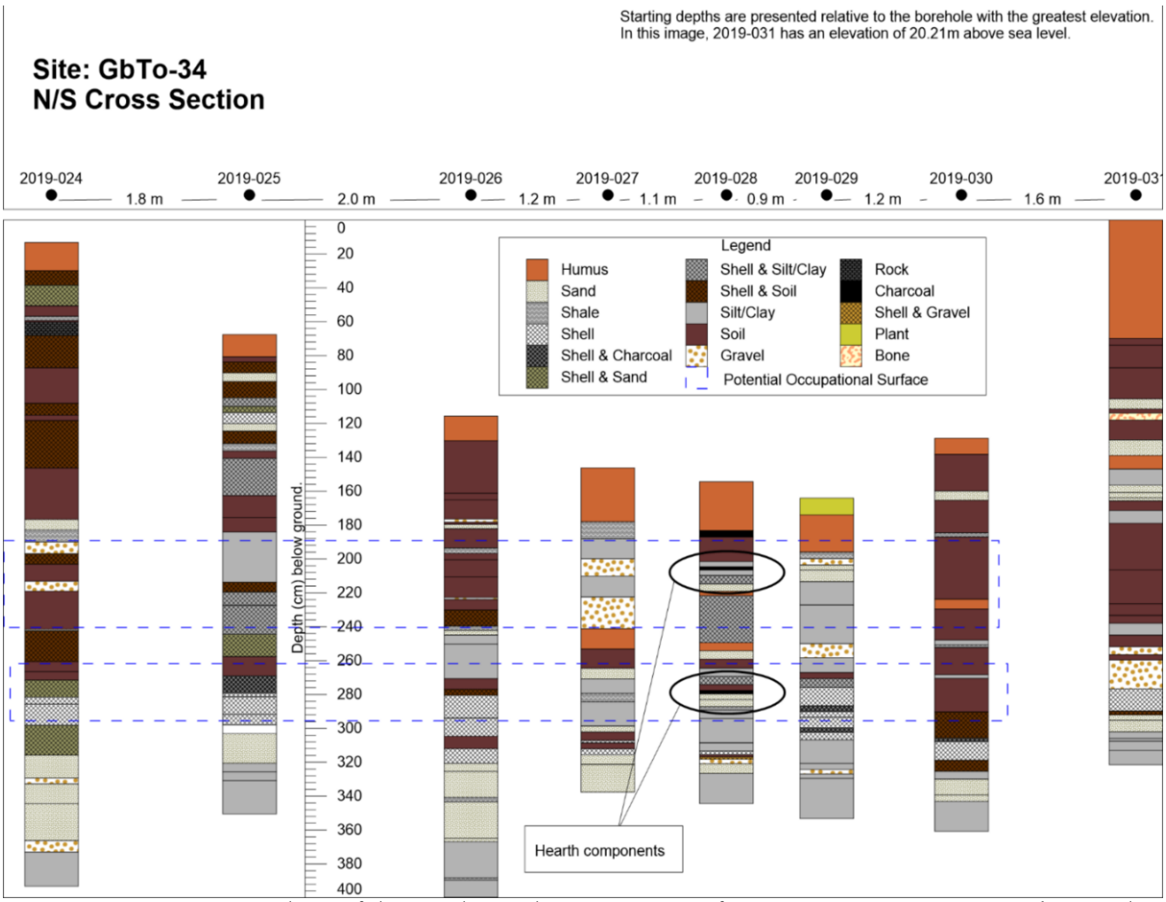

Figure 8. Percussion core analysis of the North-South cross section of House 16. Cores are arranged on a relative scale to the most elevated core (CT 2019-031). Two potential occupation surfaces, approximately 190 to 240 cm and 260 to 290 cm were identified based on several characteristics. Two hearth components were specifically identified within these potential layers in CT-2019-028 from thick charcoal lenses. This core is directly adjacent to GPR Feature 2 (Figures 5 and 6) and the lenses occur at similar depths.

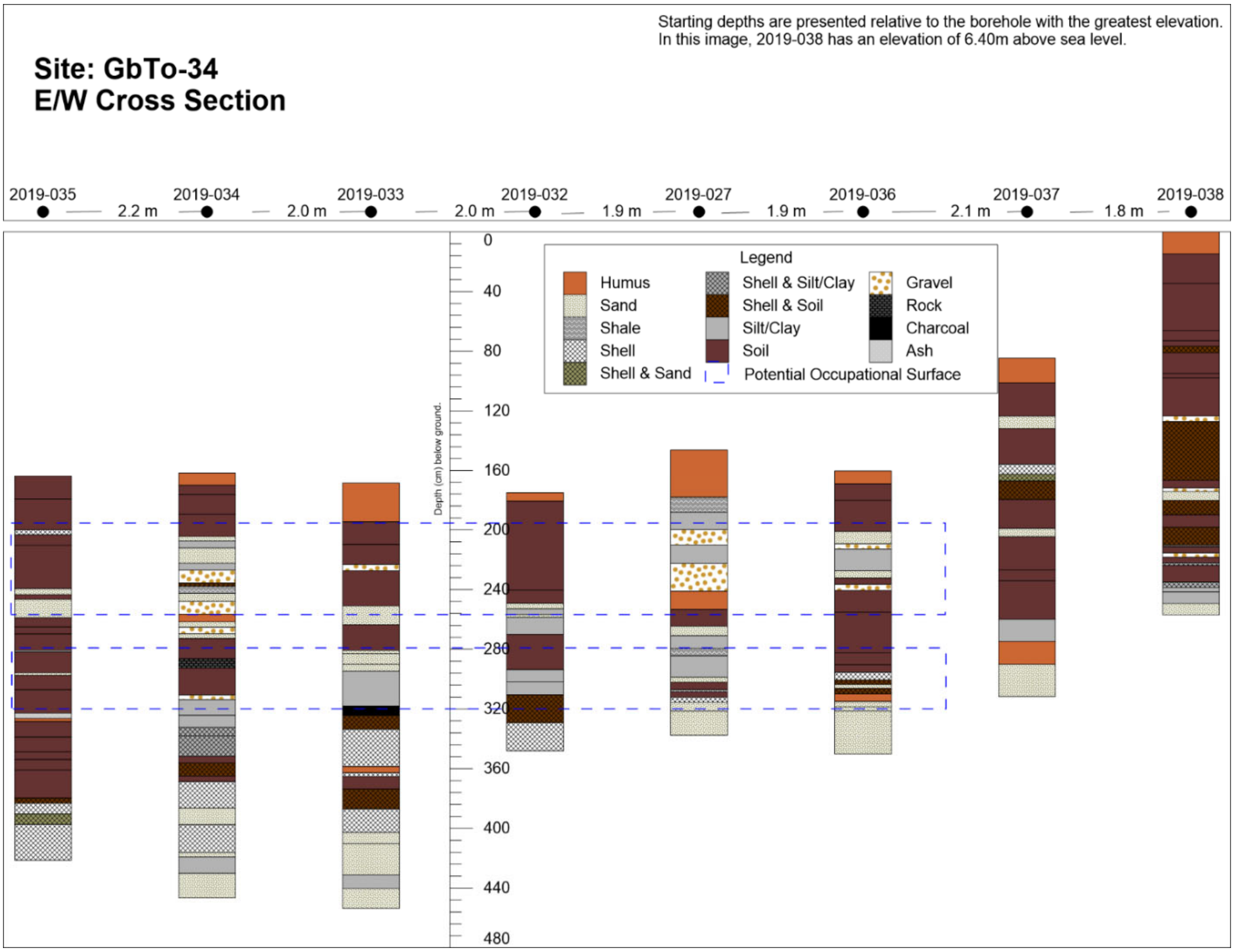

Figure 9. Percussion core schematic of the East-West cross section of House 16. Cores are arranged on a relative scale to the most elevated core in the profile (CT 2019-038). Two potential occupation surfaces were again seen in this profile, approximately 200 to 250 cm and 280 to 320 cm. These were deemed corroborative of the GPR and N-S core cross sections, which also identified occupation layers at these depths.

Occupational surfaces are visible in excavation as horizontally arranged zones of predictable difference within a house (Martindale et al. 2017). Figures 8 and 9 show the cores from House 16 (see Figure 3) presented as lithological schematics, using the program *Strater 5*. These have been rectified in both vertical and horizonal positions for each core, although the two scales are different. The result is a sequence of stratigraphic components within each core and visible patterns between cores. Note for example, the relatively horizontal sand and silt/clay layers at the base of each core representing the beach veneer beneath the site, and the dense shell layers above this perhaps representing shell terraceing related to village construction (Letham et al. 2020). These cores contain many layers from 2 and 4 m depth, more towards the edge of the house depression, where the cores primarily sampled deep shell-bearing deposits. The percussion method distorts some stratigraphic positions within each 3’ (91.5 cm) segment. However, using the hearth components as a reference, we can identify two candidates for occupational components based on the principles of content and relative heterogeneity noted above. These are visible in the N-S profile at 190 to 240 cm below datum and at 260 to 290 cm below datum. These components are less visible at the edges of the transect, where the floor is transitions to exterior shell terracing. The E-W profile shows the perpendicular transect (i.e. along the long axis of the house, front to back). Although not as clear, both potential occupational surfaces are identifiable at approximately the same depth. Note that the surfaces in the E-W transect profile appear to slope to the west (left in Figure 9), as would be expected from the back to front of the house. While there is still work to do on defining the positive characters of occupational surfaces and house floors in NWC shell terrace-based houses as they may be gleaned through percussion coring, these results revealed candidates for features that are consistent with remote sensing data.

6. Discussion: From Observation to Prediction

Mobilizing 3D GPR data is a challenging but a worthwhile endeavor that benefits from an iterative approach sensitive to both obvious and subtle signals produced from remote sensing (Conyers *et al.*. 2019). Similar research from projects around the globe have shown that 1) no one method of investigation can provide a complete interpretation of the subsurface in complex contexts, 2) interpretations evolve over time with refined techniques and increased sample sizes, especially in contexts that are ground truthed, and 3) macro spatial patterns hypothesized from ethnographic and archaeological data provide useful test scenarios (e.g., Conyers et al. 2018, 2019; St Pierre et al. 2019). This study has followed a similar approach, taking caution to not over-process data or over-interpret results. Like many archaeological features the world over, plankhouses on the Northwest Coast varied in size, shape, and function over time, creating difficulties for straightforward archaeological and geophysical interpretation. These challenges and the paucity of comparative geophysics research on the northern Northwest Coast similarly tempers our interpretive framework.

Our feature interpretations from the geophysical and ground truthing results are summarized in Table 1. Previous geophysical work at the McNichol Creek (GcTo-3) site in PRH helps to corroborate our interpretation of the features in House 16 (Cross 1996). Although Cross's work reflects a time in which GPR was initially being incorporated into archaeology, it generated data from within similar house depressions. While lacking equipment and software available today to produce detailed profile and amplitude maps, Cross (1996) noted evidence for an internal floor structure within the house depressions. These correspond well to the higher amplitude layers found in the 2019 data from Kitandach. Somewhat more comparably, Cross (1996) conducted magnetometry surveys over the house depressions and found that the centers produced roughly rectangular and magnetically low (-10 to -20 nT/m) signatures. He suspected these were likely negative due to concentrations of fire-altered rock and soil, an interpretation similar to the 2019 identification of hearths/domestic areas from negative magnetic values. While not replicated in the present study, Cross (1996) also collected conductivity data and found readings to be low (2 to 3 ms/m) in the center of the depressions, but suspected this was most likely the compaction of the high activity area.

Geophysical work conducted by other researchers in similar archaeological contexts helps to bolster these observations and interpretations. In coastal California, Arnold *et al..* (1997) used GPR and magnetic techniques to survey Chumash houses within dense shell-bearing deposits. Like the data from House 16 at Kitandach, house areas were identified as gaps in amplitudes bounded by linear anomalies, and had a very slight 2 to 3 cm reflective floor identified in profile. Similarly, these internal areas appeared as magnetic lows (Arnold et al. 1997). In the interior of British Columbia Prentiss *et al..* (2008) found the lowest negative values within pithouses to be associated with hearths and archaeological deposits of charcoal, fire-cracked rock, and burnt bone. Their results emphasize an important point, that while hearths are typically associated with positive signatures (Conyers 2018; Dolan et al. 2017), magnetic signatures are dependent on how hearths are constructed. Floors and central hearths were likely rejuvenated regularly and comprised of various burnt soils and sands (Martindale 1999), not large amounts of positively magnetic rocks. It is entirely possible that the central domestic area of the house would appear as magnetically negative. Finally, both posts and shell-bearing sites have been well-documented through remote sensing techniques and the results presented here illustrate similar characteristics (e.g. Arnold et al. 1997; Conyers 2018; Thompson 2015).

Expected Archaeological Zone/Feature			2019 Results/Interpretation		
Areas	Features	Archaeological Description	Ground-penetrating Radar	Magnetic Gradiometry	Percussion Core Testing
Central Domestic Area	Hearths	Basin-shaped/ synclinal depressions, regularly cleaned. Concentric layers of fire-reddened soil, ash/charcoal/sandy matrix, covered by a layer of sand with lesser amounts of charcoal (Martindale 1999: 231-234)	Size/ Shape-derived. Large 2 x 2 m 'bow-tie' shaped reflections located center-back of houses.	Low negative signatures (-15 to -20 nT/m). Spreading over center-back of house.	Core contained layers of burned sand and pieces of charcoal at the expected feature depths determined by GPR
	Domestic artifacts	Appear on the surface of house floors, such as, lithic 'cookstones'.	Point-source reflections on interpreted floor, possibly large artifacts (likely lithics)	Not directly observed- small positive and dipole anomalies appear within magnetic lows, not as consistent	Not observed

	House floor	Soil change, and very compacted. Lowest cultural feature at sites.	Compact reflective layers roughly fitting surface depression	Predominantly negative or neutral magnetic readings	Increased compaction sometimes noted, as well as presence of charcoal and shell.
Sleeping/Living Area	Benches and Artifacts	Either identified as physical constructions or by linear post pattern with accumulated material artifacts, known as a “bench midden” (Martindale 1999: 231).	Lots of point-source reflections, highly reflective areas around perimeter of the identified house boundaries	See Domestic Artifacts-Mag. Some areas within the house have a higher positive signal.	Some fine burnt and waterlogged wood remains in perimeter zone (CT-33). Otherwise not observed.
Traffic/Open Space Area	Compacted areas	Thought to be similar to highly compacted house floor	Not differentiated from other 'house floor' reflections (see domestic area). Other sites showed higher compaction of shell between houses, suspected to be due to foot	Not directly observed	See House Floor.

			traffic (Wadsworth 2020)		
House Boundaries/Outside	Posts/Post Molds	Corner posts were 60-70cm at GbTh-4 (Martindale 1999: 227). Rocks are found in their base. Smaller posts are under 50 cm in diameter.	Large post reflections (50 x 50 cm) with high amplitude found regularly spaced near boundaries in house depression. Smaller posts may be confused with other pit features and were excluded from interpretation.	Not directly observed. Perhaps only the molds remain.	Core 27 had copious amounts of gravel and clay at the occupation layers. May represent a post mold. Not yet determined.
	Shell berms with artifacts and inclusions	Huge deposits of shell, varying in compaction, density and fragmentation.	Complicated dipping/overlapping, highly reflective layers and noise, point-source reflections and other features appear to be inside these shell matrices	Strong positive magnetic anomalies (5 to 10 nT/m) that surround the house depression	Large amounts of shell in Core

Our results are consistent with other geophysical case studies, and the geophysical interpretations of house features also correspond well to percussion core testing. The distinction between occupational and non-occupational layers was clear in the percussion cores, with occupation surfaces being characterized by three sublayers in a house floor 'sequence'. Two candidates for these house floors were identified at around 190 to 240 cm and 260 to 290 cm, which correlate with two potential occupation layers seen in the GPR at 220 to 235 cm and 255 to 270 cm. Two superimposed candidates for hearths were identified as thick lenses of charcoal in cores in the same area as potential hearth features visible in the GPR and magnetic gradiometer results. We were however, unable to locate or visualize any obvious house posts with this same analytical strategy, Shell ridges surrounding the house were readily identified, being comprised of substantial dense shell deposits. Beneath the deepest identified occupation layer, shell and silt/clay layers can be interpreted as part of the underlying beach to overlying village/shell-terrace transformation. While the coring data from House 16 has illustrated the utility of combining low impact ground truthing approaches with geophysical survey strategies, the next stage of research will be to simplify lithographic sequences in the cores and construct profiles so they can be more directly compared with GPR data.

6.1. Two Models for House 16

Even when employing wide-area excavation methods, the complex, often shell-rich house features typical of the Northwest Coast are challenging to reconstruct, owing to the centuries of habitation, refurbishment, and reconstruction they reflect (Ames et al. 1992; Grier 2006a). Architectural elements were removed, rebuilt, and relocated frequently over the lifespan of a house, which can produce overlapping and stacked features, as well as mixed layers in the stratigraphy. Remote sensing offers an expedited way to view the subsurface, though application of these techniques does not necessarily simplify the interpretive complexities. With this caveat in mind, we propose two potential interpretive models of House 16 gleaned from our 2019 surveys.

One possible explanation for the data we gathered from House 16 is that occupation of one large Tsimshian house generated all the identified features between 2 and 3 m DBD. Given that houses were rebuilt and refurbished in place, it is possible that the upper deposits were either built over the existing lower features or represent a continued expression of them. The dimensions of the house are drawn from the upper deposits, being approximately 6 x 11 m with the long axis facing perpendicular to the shore). The perimeter of the living zones were contained within this area, with the largest hearths set in the center of what is now the house depression. In this interpretation, centuries of re-use and refurbishment created overlapping internal 'floor' layers and artifacts. This might partially explain why the lower identified hearth features generated a much stronger magnetic anomaly than the upper

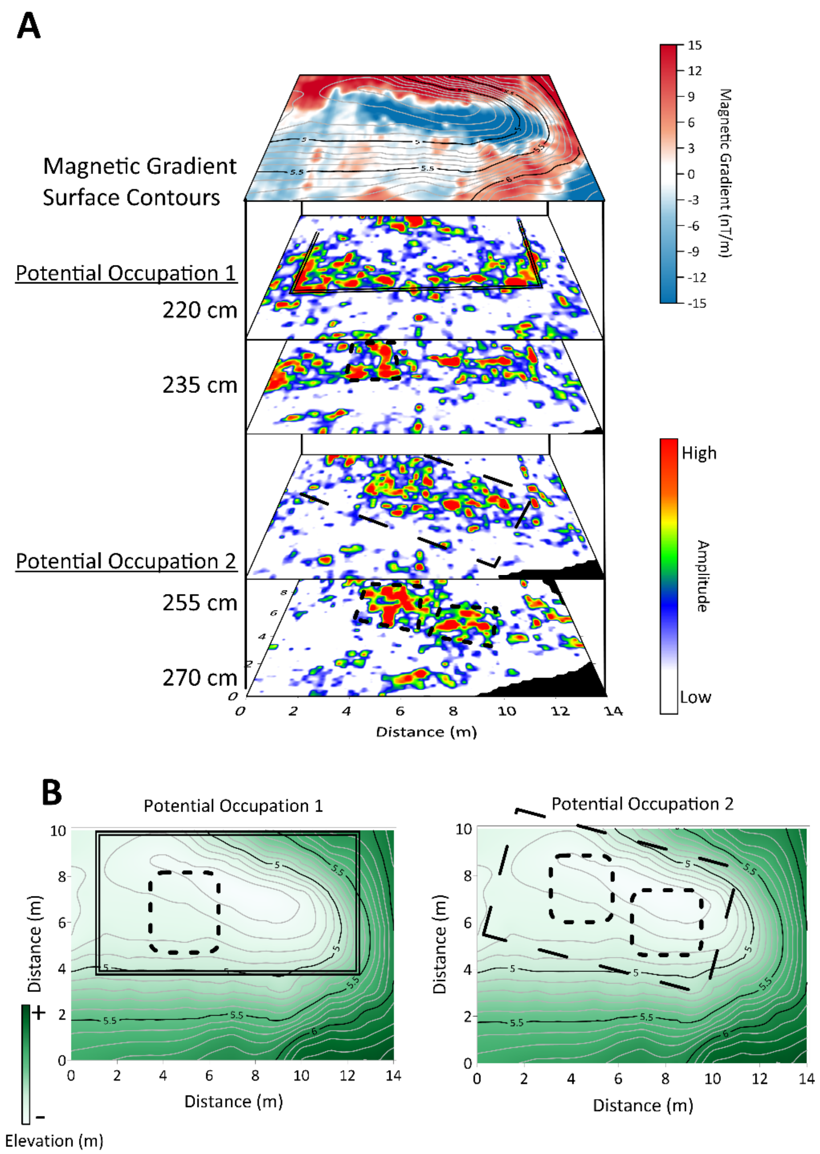

Figure 10. Proposed 'Two House' Interpretation from the geophysical data. A: Stacked remote sensing interpretations. B: Potential Occupation interpretations overlaid on the surface topography of House 16. Potential Occupation 1 (approximately 220 to 235 cm) showed very clear boundaries (double solid line) and perimeter reflections perhaps representing a living area. However, the hearth features (dotted squares) located in these layers are not as central and not as magnetically negative as the lower occupation. Potential occupation 2 (approximately 255 to 270 cm) showed a very clear central domestic area (with strong correlation between GPR, Magnetics, and core data concerning the identification of hearths), but did not show as clear boundaries and a hypothetical shape (dashed house boundary) was determined largely from the transition between high to low amplitudes and size of the upper house boundary.

layers, as well as the lack of a definitive lower house interior to shell-bearing deposit transition. Standing against this interpretation is that both the coring data and the GPR data show two discrete occupation layers/transitions. Yet, the idea of a “floor zone” as characteristic of house interior space rather than discrete, identifiable floors was advanced by Grier (2006a) for House 2 at Dionisio Point and Samuels (2006) at Ozette, and so has been recognized in shed roof houses to the south. Some house depressions in the Tsimshian zone are over 2 m deep, suggesting that a considerable volume of material had built up around the perimeter prior to abandonment. Part of our future work will include detailed radiocarbon dating of potential house features and both interior and exterior deposits to better describe their occupational histories.

The alternative model, and the one we presently favor, is the interpretation that two discrete occupations generated by two distinct houses exist within the depression (Figure 10). This model is chiefly supported by the GPR and coring data that recorded a 20 to 25 cm stratigraphic difference between identified occupation layers and potential features in each. This would also explain why the surface topography better matches the boundaries of the more recent upper occupation compared to the lower occupation, which appears to angle slightly more towards the north. Differences in house construction may also partially explain differences seen between geophysical signals and the surface topography (such as the very strong negative magnetic values). The biggest problem with the two-house interpretation is that the house boundaries were not as convincingly identified in the lower occupation, and so the exact perimeter of the house cannot be established. Instead, the house area was estimated from the apparent angle and higher amplitudes of the domestic area, coupled with existing information ideas about Tsimshian houses (see dotted outline Figure 9:B). There is archaeological excavation data from Tsimshian territory that could support either model, from at GbTo-77 (Patton 2011) and GcTr-8 (Martindale et al. 2009), suggesting additional work and methodological approaches are warranted.

One direction we see as critical for putting varying or contrasting interpretations of geophysical data on solid ground is the pursuit of a predictive model to confidently and objectively assign archaeological identities to geophysically-observed features. Following its initial proposal by Daniel (2015), we have begun working on the architecture of a ‘Feature Confidence Index’. This methodological strategy involves explicitly establishing the expected geophysical attributes for known/expected plankhouse architectural features, and how they should appear in remote sensing surveys. Surveys can be conducted, predictions made, and expectations then compared to actual archaeological features through ground truthing tests, which may including low-impact percussion coring as employed here, but also shovel testing, excavation, and the mapping of profiles in erosion exposures. The development of a multivariate model that incorporates an array individual traits, and which quantifies the relative influence of each trait on overall predictive confidence can be generated, and ten applied in new contexts. This allows for improved quantification of the confidence with which we can predict the identity of an archaeological feature using its geophysical characteristics, and vice versa. To do this, we need to think expansively in terms of what attributes of features (geophysical or archaeological) may be useful in defining feature identities. A recent paper by Trinks and Hinterleitner (2020) presented a similar attribute based GPR analysis using a variable they call 'coherence,', which refers to the consistency of amplitude variations within features across space in a survey grid. Such a measure gets us beyond considering solely points of amplitude variation as data. Their methodology statistically quantified equivalence of amplitude, phase shift, and frequency content between and across GPR traces, offering several new ways to mobilize GPR data (Trinks and Hinterleitner 2020). Being able to develop a similarly creative set of variables for Northwest Coast plankhouse contexts for incorporation into a confidence index is another instance of the methodological creativity that will be required to move from interpretation to prediction in geophysics and remote sensing.

Finally, it is important to keep in mind why we are conducting this low impact methodology in the first place. Conducting archaeological research in North America is almost always focused on Indigenous pasts (Supernant 2018). The PRH project is a collaborative research project, and explicitly incorporates the goals of the Coast Tsimshian communities of Lax Kw'alaams and Metlakatla, who desire non-invasive alternatives to traditional archaeological techniques. Building confidence in the application of remote sensing techniques can advance archaeological goals while furthering community objectives. Accurate and precise descriptions of house and village settlements through archaeology are increasingly valuable as Indigenous communities preserve their material heritage, seek redress for damage to that heritage, and utilize heritage data in legal claims for rights and title.

7. Conclusions & Prospects for NWC Archaeology

The Northwest Coast, as with other heavily vegetated and wet/clay-rich archaeological regions with predominantly perishable architecture and material culture, may appear to offer less than a favorable environment for the application of remote sensing techniques (see McLay et al. 2009: 21). However, advances in the technology, new strategies for its application, and more rigorous avenues for interpretation are continually opening new possibilities for overcoming its confounding aspects (Conyers 2013). While the results of this study have clearly identified challenges for incorporating these techniques on the Northwest Coast, we have also shown its utility for identifying features, occupation zones, and house spatial organization in northern NWC houses, adding to the pioneering work of Cross

(1996) at McNichol Creek. Both the GPR and magnetic gradiometry surveys provided high quality and interpretable data that allowed for the potential identification of features and the delineation of more general areas/zones, house boundaries, and the transition to exterior shell ridges/mounds. Both surveys contributed to information about form and composition. GPR was particularly useful at locating house and feature form and depth and magnetics was particularly useful for identifying and characterizing its features and deposits. Together these two techniques provided significant resolution to house interior organization, especially when combined with previous archaeological research (Figure 11). While our methodologies are still developing, geophysical survey at House 16 has seemingly identified multiple occupations within a single house depression – an observation critical for establishing the nature of plankhouse occupations. This interpretation was supported by our percussion coring analysis, and will be evaluated independently through future radiocarbon dating.

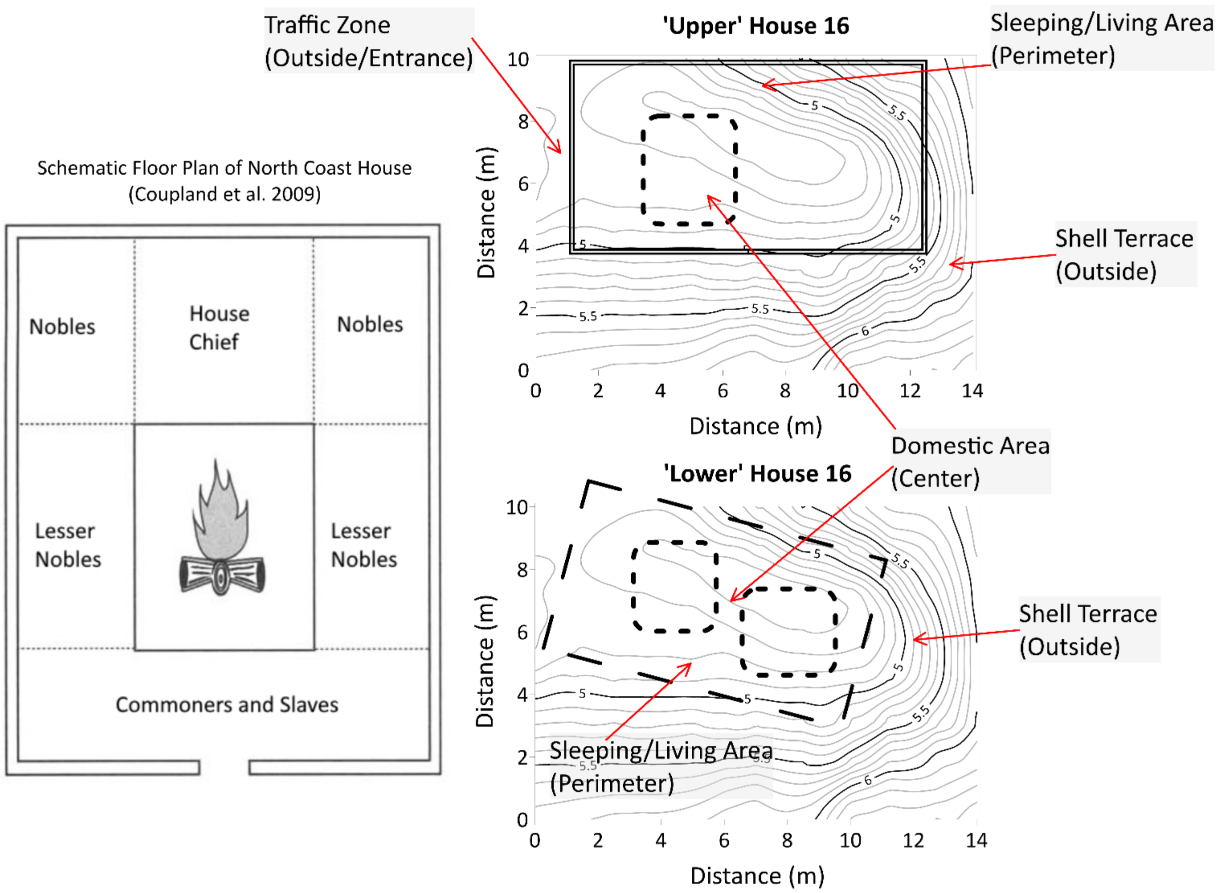

Figure 11. Comparative schematic diagrams between published knowledge of Northern Coast houses (from Coupland et al. 2009) and the interpretations created for the upper and lower House 16 occupations. Utilizing a broad schema of 'zones' within houses (e.g., Samuels 2006), archaeological/ethnographic knowledge can begin to be 'mapped' on to these remote sensing surveys.

Overall, our application of geophysics on the northern NWC illustrates promise for advancing current and long-standing research objectives in the archaeology of the Pacific Northwest. Expedient survey and dating of large houses can provide critical data for addressing the major research directions we have outlined that rely on data concerning house and village organization, and the relationship of changing households and communities to broader currents of Northwest Coast histories. Moreover, our survey of House 16 clearly demonstrates the potential for remote sensing to contribute information about the nature of constructed landscapes, including mapping the monumental shell terraces that form village sites, and the extent of use of shell matrix in construction efforts such as shell dikes and engineered wetlands (e.g., Grier et al. 2009; Grier 2014; Grier et al. 2017). Such expansive practices are particularly difficult to address with conventional archaeological techniques.

The houses at Kitandach remain visible on the surface, aiding strategies for collecting intrahouse data, but many large shell-bearing sites do not offer a similar opportunity. As we highlighted for Coast Salish region, many large sites that likely contain the remains of plankhouses show no visible signs of these on the surface. The capacity to identify buried houses and thus locate communities will allow for better documentation of the regional distribution of village sites. In conjunction with large-scale regional remote sensing investigations (such as LiDAR-based survey), our prospects for addressing questions concerning regional interactions, the distribution of resource gathering places, and, more broadly, changes in regional settlement patterning through time (e.g. Letham et al.. 2017; Martindale et al. 2017; Supernant and Cookson 2014) are significantly increased. While technically challenging, these remote sensing applications can mobilize and build on the immense amount of archaeological and ethnographic information available from almost a century of research (Figure 11). In this way the Northwest Coast provides an ideal setting for remote sensing to investigate the big-picture anthropological questions that we have outlined. Northwest Coast research can productively contribute to the growing body of studies that are bridging the gap between anthropological questions and remote sensing methodologies (e.g. Conyers 2018; Kvamme 2003b; St Pierre et al. 2019; Thompson 2015; Thompson et al. 2011).

An overarching goal of our work is for archaeologists to be able to offer concrete and defensible interpretations concerning the nature of heritage sites, providing a firmer footing on which to protect heritage sites by and for Indigenous communities. Developing a strategy for obtaining the most critical information, such as the location of villages, in a non-invasive way serves the ends of all stakeholders in heritage conservation. Implementing such a tool will not only change how researchers approach household archaeology on the Northwest Coast but also how we approach endangered sites in PRH and elsewhere.

8. Acknowledgments

This work was conducted in partnership with and through the support of the Lax Kw'alaams and Metlakatla First Nations. We are grateful to these communities for their willingness to work in partnership with us and for permission to work in their territory. The geophysical equipment used in this study was generously provided by the Baikal Archaeology Project. This research was made possible through generous financial support of a number of institutions, including the Social Sciences and Humanities Research Council of Canada (Grant # 435-2018-0455) and the University of British Columbia. We are also particularly grateful for the numerous collaborators, volunteers, and community members that have helped make the PRH Archaeology Project possible. We specifically thank Bryn Letham, Katherine Patton, Steven Dennis, and Gary Coupland for help in the field. We are grateful to Evie Bell for her laboratory work on the percussion cores and Eric Simons for his review of a draft of this paper. We are all indebted to the late Kenneth M. Ames for his profound scholarship and for guiding our interest in architecture.

9. References

Ames, K.M. 2006. Thinking about Household Archaeology on the Northwest Coast, in E.A. Sobel, D.A. Trieu Gahr and K.M. Ames (eds) *Household Archaeology on the Northwest Coast*: 16–36. Ann Arbor: International Monographs in Prehistory.

Ames, K.M. and A. Martindale. 2014. Rope bridges and cables: a synthesis of Prince Rupert Harbour archaeology. *Canadian Journal of Archaeology* 38: 140–178.

Ames, K M. and H.D.G. Maschner. 1999. *Peoples of the Northwest Coast: Their Archaeology and History*. London: Thames and Hudson.

Ames, K.M., D.F. Raetz, S. Hamilton and C. McAfee. 1992. Household archaeology of a southern Northwest Coast plank house. *Journal of Field Archaeology* 19: 275–290.

Archer, D.J.W. 2001. Village patterns and the emergence of ranked society in the Prince Rupert area, in J.S. Cybulski (ed) *Perspectives on Northwest Coast Prehistory*: 203-222. Ottawa: Canadian Museum of Civilization.

Arnold, J.E., E.L. Ambos and D.O. Larson. 1997. Geophysical surveys of stratigraphically complex island California sites: New implications for household archaeology. *Antiquity* 71(271): 157–168.

Barnett, H.G. 1955. *The Coast Salish of British Columbia*. Eugene: University of Oregon Press.

Bigman, D.P. and P.M. Lanzarone. 2014. Investigating construction history, labour investment and social change at Ocmulgee National Monument's Mound A, Georgia, USA, using ground penetrating radar. *Archaeological Prospection* 21: 213–224.

Campana, S. and S. Piro (eds). 2009. *Seeing the Unseen: Geophysics and Landscape Archaeology.* London: CRC Press.

Cannon, A. 2000. Settlement and sea levels on the Central Coast of British Columbia: evidence from shell midden cores. *American Antiquity* 65: 67–78.

Cheetham, P.N. 2008. Noninvasive subsurface mapping techniques, satellite and aerial imagery in landscape archaeology, in B. David and J. Thomas (eds) *Handbook of Landscape Archaeology*: 562–578. Walnut Creek, CA: Left Coast Press.

Conyers, L.B. 2007. Ground-penetrating radar for archaeological mapping, in J. Wiseman and F. El-Baz (eds) *Remote Sensing in Archaeology*: 329–344. New York: Springer.

Conyers, L.B. 2013. *Ground-Penetrating Radar for Archaeology*. Latham, MD: Alta Mira Press.

Conyers, L.B. 2016. *Ground-Penetrating Radar for Geoarchaeology*. Chichester: Wiley Blackwell.

Conyers, L.B. 2018. *Ground-Penetrating Radar and Magnetometry for Buried Landscape Analysis*. Cham, Switzerland: Springer International Publishing.

Conyers, L.B., E.J. St Pierre, M.J. Sutton and C. Walker. 2018. Integration of GPR and magnetics to study the interior features and history of earth mounds, Mapoon, Queensland, Australia. *Archaeological Prospection* 26: 3–12.

Conyers, L.B., M.J. Sutton and E. St Pierre. 2019. Dissecting and interpreting a three-dimensional ground-penetrating radar dataset: An example from Northern Australia. *Sensors* 19, 1239. DOI:10.3390/s19051239.

Cookson, C. 2013. *An Analysis of Site Selection Behaviours and Landscape Use in the Prince Rupert Harbour Area.* Unpublished Masters thesis, University of Alberta.

Coupland, G. 1996. This old house: cultural complexity and household stability on the northern Northwest Coast of North America, in J. Arnold (ed) *Emergent Complexity: The Evolution of Intermediate Societies*: 74–90. Ann Arbor: International Monographs in Prehistory.

Coupland, G. 2003. Preliminary analysis of socioeconomic organization at the McNichol Creek site, British Columbia, in R.G. Matson, G. Coupland and Q. Mackie (eds) *Emerging from the Mist: Studies in Northwest Coast Culture History*: 152–169. Vancouver: UBC Press.

Coupland, G. 2006. A Chief's house speaks: communicating power on the northern Northwest Coast, in E.A. Sobel, D.A. Trieu Gahr, and K.M. Ames (eds) *Household Archaeology on the Northwest Coast*: 80-96. Ann Arbor, International Monographs in Prehistory, Ann Arbor.

Coupland, G., T. Clark and A. Palmer. 2009. Hierarchy, communalism, and the spatial order of Northwest Coast plank houses: a comparative study. *American Antiquity* 74: 77–106.

Cross, G. 1995. Archaeological Remote Sensing: Shingle Point Site, Valdes Island, BC. Burnaby, BC: Golder Associates.

Cross, G. 1996. Report on Archaeological Remote Sensing, McNichol Creek Site, GcTo-6, Prince Rupert Harbour, BC. Burnaby, BC: Golder Associates.

Dalan, R.A., J.M. Musser and J.K. Stein. 1992. Geophysical exploration of the shell midden, in J.K. Stein (ed) *Deciphering a Shell Midden*: 43-60. New York: Academic Press.

Daniel, S.E. 2015. Ground Penetrating Radar Applied: A Model for Quantifying Interpretation of Human Burials in Historical Contexts. Unpublished Masters thesis, University of British Columbia.

Dolan, P., C. Grier, C. Markussen and K. Simon. 2017. Magnetic gradient survey of the Marpole period Dionisio Point (DgRv-003) plankhouse village, Northwest Coast of North America. *Journal of Field Archaeology* 42: 437–449.

Dojack, Lisa (2011) Dionisio Point GPR Survey (DgRv-3 & DgRv-6): 2011 GPR Results. Unpublished Report, Northwest Coast Archaeology Laboratory, Washington State University.

Dojack, Lisa (2012a) Assessing the Utility of Ground Penetrating Radar in Archaeology on the Northwest Coast: The 'New Wave', 'All Snell', or 'It Just Hertz'? Unpublished Masters Thesis, The University of British Columbia.

Dojack, Lisa (2012b) Dionisio Point GPR Survey (DgRv-3 & DgRv-6): 2012 GPR Results. Unpublished Report, Northwest Coast Archaeology Laboratory, Washington State University.

Edinborough, K., A. Martindale, G. Cook, K. Supernant and K.M. Ames. 2016. A marine reservoir effect ΔR value for Kitandach in Prince Rupert Harbour, British Columbia, Canada. *Radiocarbon* 58: 885–891.

Edinborough, K, M. Porčić, A. Martindale, T.J. Brown, K. Supernant, and K.M Ames. 2017. Radiocarbon test for demographic events in written and oral history. *Proceedings of the National Academy of Sciences* 114(47): 12436–12441.

Gamble, L.H. 2017. Feasting, ritual practices, social memory, and persistent places: new interpretations of shell mounds in southern California. *American Antiquity* 82: 427–451.

Gaffney, C. V. Gaffney, W. Neubauer, E. Baldwin, H. Chapman, P. Garwood, H. Moulden, T. Sparrow, R. Bates, K. Locker, A. Hinterleitner, I. Trinks, E. Nau, T. Zitz, S. Floery, G. Verhoeven, M. Doneus. 2012. The Stonehenge Hidden Landscapes Project. *Archaeological Prospection* 19: 147–155.

Gaffney, C. and J. Gater. 2003. *Revealing the Buried Past: Geophysics for Archaeologists*. Shroud, UK: Tempus Publishing.

Gaffney, C., C. Harris, F. Pope-Carter, J. Bonsall, R. Fry and A. Parkyn. 2015. Still searching for graves: An analytical strategy for interpreting geophysical data used in the search for "unmarked" graves. *Near Surface Geophysics* 13: 557–569.

Goodman, D. and S. Piro. 2013. *GPR Remote Sensing in Archaeology*. London: Springer.

Grier, C. 2003. Dimensions of regional interaction in the prehistoric Gulf of Georgia, in R.G. Matson, G. Coupland and Q. Mackie (eds) *Emerging from the Mist: Studies in Northwest Coast Culture History*: 170–187. Vancouver: UBC Press.

Grier, C. 2006a. Temporality in Northwest Coast households, in E.A. Sobel, D.A. Trieu Gahr and K.M. Ames (eds) *Household Archaeology on the Northwest Coast*: 97-119. Ann Arbor: International Monographs in Prehistory.

Grier, C., 2006b. Political dimensions of monumental residences on the Northwest Coast of North America, in J.J. Christie and P.J. Sarro (eds) *Palaces and Power in the Americas: From Peru to the Northwest Coast*: 141–165. Austin: University of Texas Press.

Grier, C. 2014. Landscape construction, ownership and social change in the Southern Gulf Islands of British Columbia. *Canadian Journal of Archaeology* 38: 211–249.

Grier, C., B. Angelbeck and E. McLay. 2017. Terraforming and monumentality as long-term social practice in the Salish Sea region of the Northwest Coast of North America. *Hunter Gatherer Research* 3(1): 107–132.

Grier, C. and J. Kim. 2012. Resource control and the development of political economies in small-scale societies: contrasting prehistoric southwestern Korea and the Coast Salish region of northwestern North America. *Journal of Anthropological Research* 68: 1–34.

Hajda, Y. 1994. Notes on Indian houses of the Wappato Valley. *Northwest Anthropological. Research Notes* 28: 177–188.

Johnson, J.K. (ed). 2005. *Remote Sensing in Archaeology: An Explicitly North American Perspective*. Tuscaloosa: The University of Alabama Press.

Kvamme, K.L. 2003a. Multidimensional prospecting in North American Great Plains village sites. *Archaeological Prospection* 10(2): 131–142.

Kvamme, K.L. 2003b. Geophysical surveys as landscape archaeology. *American Antiquity* 68: 435–457.

Kvamme, K.L. 2006. Magnetometry: nature's gift to archaeology, in J.K. Johnson (ed) *Remote sensing in archaeology: an explicitly North American perspective*: 205–233. Tuscaloosa: University Alabama Press.

Lepofsky, D., C. Geralda Armstrong, S. Greening, J. Jackley, J. Carpenter, B. Guernsey, D. Mathews and N.J. Turner. 2017. Historical ecology of cultural keystone places of the Northwest Coast. *American Anthropologist* 119: 448–463.

Lepofsky, D., D.M. Schaepe, A.P. Graesch, M. Lenert, P. Ormerod, K. Thor Carlson, J.E. Arnold, M. Blake, P. Moore and J.J. Clague. 2009. Exploring Sto:Lo-Coast Salish interaction and identity in ancient houses and settlements in the Fraser Valley, British Columbia. *American Antiquity* 74: 595–626.

Letham, B., A. Martindale and K.M Ames. 2020. Endowment, investment, and the transforming coast : long-term human-environment interactions and territorial proprietorship in the Prince Rupert Harbour, Canada. *Journal of Anthropological Archaeology* 59(April): 101179. DOI:10.1016/j.jaa.2020.101179.

Letham, B., A. Martindale, K. Supernant, T.J. Brown, J.S. Cybulski and K.M Ames. 2017. Assessing the scale and pace of large shell-bearing site occupation in the Prince Rupert Harbour area, British Columbia. *The Journal of Island and Coastal Archaeology* 14(2): 163-197.

MacDonald, G.F. 1983. *Haida Monumental Art*. Vancouver: UBC Press.

MacDonald, G.F and R.I. Inglis. 1981. An overview of the North Coast Prehistory Project (1966-1980). *BC Studies* 48: 37–63.

Mackie, Quentin (2003) Location-allocation modelling of shell midden distribution on the west coast of Vancouver Island, in R.G. Matson, G. Coupland and Q. Mackie (eds) *Emerging from the Mist: Studies in Northwest Coast Culture History*: 260–288. Vancouver: UBC Press..

Marshall, Y. 2006. Houses and domestication on the Northwest Coast, in E.A. Sobel, D.A. Trieu Gahr and K.M. Ames (eds) *Household Archaeology on the Northwest Coast*: 37-56. Ann Arbor: International Monographs in Prehistory.

Martindale, A. 1999. The River of Mist: Cultural Change in the Tsimshian Past. Unpublished PhD dissertation, University of Toronto.

Martindale, A. 2006. Tsimshian houses and households through the Contact Period, in E.A. Sobel, D.A. Trieu Gahr and K.M. Ames (eds) *Household Archaeology on the Northwest Coast*: 140-158. Ann Arbor: International Monographs in Prehistory.

Martindale, A., B. Letham, D. McLaren, D. Archer, M. Burchell and B.R. Schöne. 2009. Mapping of subsurface shell midden components through percussion coring: examples from the Dundas Islands. *Journal of Archaeological Science* 36(7): 1565–1575.

Martindale, A., S. Marsden, K. Patton, A. Ruggles, B. Letham, K. Supernant, D. Archer, D. McLaren and K.M. Ames. 2017. The role of small villages in northern Tsimshian territory from oral and archaeological records. *Journal of Social Archaeology* 17: 285–325.

Matson, R.G. and G. Coupland. 1995. *The Prehistory of the Northwest Coast*. New York: Academic Press.

Mathews, D. and N.J. Turner. 2017. Ocean cultures: Northwest Coast ecosystems and Indigenous management systems, in P.S. Levin and M. Poe (eds) *Conservation for the Anthropocene Ocean: Interdisciplinary Science in Support of Nature and People*: 169-206. New York: Academic Press.

Matson, R.G. 2003. The Coast Salish House: Lessons from Shingle Point, Valdes Island, British Columbia in R.G. Matson, G. Coupland and Q. Mackie (eds) *Emerging from the Mist: Studies in Northwest Coast Culture History*: 76-104. Vancouver: UBC Press.

Matson, R.G. and G. Coupland. 1995. *The Prehistory of the Northwest Coast*. New York: Academic Press.

Matson, R.G., J. Green and E. McLay. 1999. Houses and Households in the Gulf of Georgia: Archaeological Investigations of Shingle Point (DgRv 2), Valdes Island, British Columbia. Victoria BC: Unpublished report 1996-064 on file at the BC Archaeology Branch.

McDonald, K.L. 2002. Archaeological Applications of Magnetometry and Ground Penetrating Radar on Flood Plains of the Pacific Northwest. Unpublished Masters Thesis, Portland State University.

McLay, Eric. D. Brown, N. Oakes and L. Oliver. 2009. Archaeological investigations of ground penetrating radar mapping at Somenos Creek (DeRw-018), BC. Victoria BC: Unpublished report 2006-393 on file at the BC Archaeology Branch.

McLay, E., K. Bannister, L. Joe, B. Thom, and G. Nicholas. 2008. '*A'lhut Tu Tet Sul'hweentst* [Respecting the Ancestors]: understanding Hul'q'umi'num heritage laws and concerns for the protection of archaeological heritage, in C. Bell and V. Napoleon (eds) *First Nations Cultural Heritage and the Law: Case Studies, Voices, and Perspectives*: 150-202. Vancouver: UBC Press.

Miller, J.F, A.R. Kelley, J.T. Kelley, D.F. Belknap and A.E. Spiess. 2018. Ground-penetrating radar as a cultural resource management tool for assessment of eroding shell middens. *Conservation and Management of Archaeological* Sites 20: 199–214.

Oswin, J. 2009. *A Field Guide to Geophysics In Archaeology.* London: Springer.

Patton, K. 2011. Reconstructing Houses: Early Village Social Organization in Prince Rupert, British Columbia. Unpublished PhD dissertation, University of Toronto.

Pluckhahn, T.J., V.D. Thompson and A. Cherkinsky. 2015. The temporality of shell-bearing landscapes at Crystal River, Florida. *Journal of Anthropological Archaeology* 37: 19-36.

Prentiss, A.M., G. Cross, T.A. Foor, M. Hogan, D. Markle and D.S. Clarke. 2008. Evolution of a Late Prehistoric winter village on the Interior Plateau of British Columbia: geophysical investigations, radiocarbon dating, and spatial analysis of the Bridge River site. *American Antiquity* 73: 59–81.

Ruggles, A.J. 2007. Is Home Where the Hearth Is?: Evidence for an Early Non-domestic Structure on the Dundas Islands of North Coastal British Columbia. Unpublished Masters thesis, University of British Columbia.

Samuels, Stephan R. 2006. Ozette household production, in E.A. Sobel, D.A. Trieu Gahr and K.M. Ames (eds) *Household Archaeology on the Northwest Coast*: 200-232. Ann Arbor: International Monographs in Prehistory.

Schaepe, D.M 2009. Pre-Colonial Sto:Lo-Coast Salish Community Organization: An Archaeological Study. Unpublished PhD Dissertation, University of British Columbia.

Schmidt, A., P. Linford, N. Linford, A. David, C. Gaffney, A. Sarris and J. Fassbinder. 2015. EAC Guidelines for the Use of Geophysics in Archaeology: Questions to Ask and Points to Consider [EAC Guidelines 2]. Namur Belgium: University of Bradford.

Sobel, E.A. 2006. Household prestige and obsidian use in the Lower Columbia River Valley: implications regarding prestige and exchange networks on the Northwest Coast, in E.A. Sobel, D.A. Trieu Gahr and K.M. Ames (eds) *Household Archaeology on the Northwest Coast*: 159-199. Ann Arbor: International Monographs in Prehistory.

St Pierre, E., L.B. Conyers, M.J. Sutton, P. Mitchell, C. Walker and D. Nicholls. 2019. Reimagining life and death: results and interpretation of geophysical and ethnohistorical investigations of earth mounds, Mapoon, Cape York Peninsula, Queensland, Australia. *Archaeology in Oceania* 54: 90–106.

Sturm, J.O. and P.L. Crown. 2015. Micro-scale mapping using ground-penetrating radar. *Advances in Archaeological Practice* 3: 124–135.

Supernant, K. 2018. Reconciling the past for the future: the next 50 years of Canadian archaeology in the post-TRC era. *Canadian Journal of Archaeology* 153: 144–153.

Supernant, K. and C. Cookson. 2014. Mapping social cohesion in Prince Rupert Harbour, BC : a social application of GIS to the archaeology of the Northwest Coast. *Canadian Journal of Archaeology* 38: 179–210.

Suttles, W. 1960. Affinal ties, subsistence, and prestige among the Coast Salish. *American Anthropologist* 62: 296-305.

Suttles, W. 1990. Introduction, in W. Suttles (ed) *Handbook of North American Indians, vol. 7: Northwest Coast*: 1-15. Washington, DC: Smithsonian Institution.

Suttles, W. 1991. The shed-roof house, in R.K. Wright (ed) *A Time of Gathering: Native Heritage in Washington State*: 212–222. Seattle University of Washington Press.

Thom, B. 2005. Coast Salish Senses of Place: Dwelling, Meaning, Power, Property and Territory in the Coast Salish World. Unpublished PhD dissertation, McGill University.

Tohge, M., F. Karube, M. Kobayashi, A. Tanaka and K. Ishii. 1998. The use of ground penetrating radar to map an ancient village buried by volcanic eruptions. *Journal of Applied Geophysics* 40(1–3): 49–58.

Thompson, J.R. 2015. *Anthropological Research Framing for Archaeological Geophysics: Material Signatures of Past Human Behavior*. Lanham: Rowman & Littlefield.

Thompson, V.D., P.J. Arnold III, T.J. Pluckhahn and A.M. Vanderwarker. 2011. Situating remote sensing in anthropological archaeology. *Archaeological Prospection* 18(3): 195–213.

Thompson, V.D., W.H. Marquardt and K.J. Walker. 2014. A remote sensing perspective on shoreline modification, canal construction and household trajectories at Pineland along Florida's southwestern Gulf Coast. *Archaeological Prospection* 21: 59–73.

Thompson, V.D. and T.J. Pluckhahn. 2010. History, complex hunter-gatherers, and the mounds and monuments of crystal river, Florida, USA: a geophysical perspective. *Journal of Island and Coastal Archaeology* 5(1): 33–51.

Thompson, V.D., M.D. Reynolds, B. Haley, R. Jefferies, J.K, Johnson and L. Humphries. 2004. The Sapelo Shell Ring Complex: shallow geophysics on a Georgia sea island. *Southeastern Archaeology* 23: 192–201.

Trinks, I. and A. Hinterleitner. 2020. Beyond amplitudes: multi-trace coherence analysis for ground-penetrating radar data imaging. *Remote Sensing* 12(1583): 1–20.

Wadsworth, W.T.D., C.-G. Bank, K. Patton and D. Doroszenko. 2020. Forgotten souls of the Dawn Settlement : a multi-component geophysical survey of unmarked graves at the British American Institute Cemetery. *Historical Archaeology* 54(3): 1–47.

Wadsworth, W.T.D. 2020. Above, Beneath, and Within: Collaborative and Community-Driven Archaeological Remote Sensing Research in Canada. Unpublished Masters Thesis, University of Alberta.

Wiseman, J. and F. El-Baz (eds). 2007. *Remote Sensing in Archaeology.* New York: Springer.

10. Software Used

ESRI. 2020. ArcGIS Pro. Redlands, CA.

Geophysical Archaeometry Laboratory Inc. 2020. GPR-SLICE. Woodland Hills, CA.

Golden Software LLC. 2020. Strater. Golden, CO.

Golden Software LLC. 2020. Surfer. Golden, CO.

Staveley, David. 2019. Snuffler. Sussex, UK.

11. Author Biographies

William T.D. Wadsworth, Institute of Prairie and Indigenous Archaeology, University of Alberta

William Wadsworth is a PhD student in the Department of Anthropology at the University of Alberta, specializing in the application of geophysics/remote sensing techniques to Canadian archaeology, primarily at the request of Indigenous communities on projects that matter to them. Using community-driven and collaborative approaches to the past, he has had the opportunity to work on diverse North American archaeological sites representing different time periods and cultures. Most recently, his research has centered on the use of Indigenous methodologies to reconceptualize archaeological remote sensing for its application in anthropological frameworks and questions. Currently, he is an active collaborator on two larger archaeological projects attempting to locate ancient villages and homelands for Tsimshian (University of British Columbia) and Métis (University of Alberta) communities. His masters and doctoral research have been funded by SSHRC Canada Graduate Scholarships. His research interests include Indigenous archaeology, landscape archaeology, GIS, geophysics, remote sensing and locating unmarked graves.

Andrew Martindale, University of British Columbia

Andrew Martindale is an archaeologist in the Department of Anthropology at the University of British Columbia. His research focuses on the histories of indigenous peoples of the Northwest Coast of North America, specifically that of Tsimshian and Musqueam communities. His work explores the archaeology and ethnohistory of cultural contact and colonialism, space-syntax analysis of architecture and households, the use of Indigenous oral records in archaeology, and the role and interpretation of archaeological data in Canadian jurisprudence, especially its implications for aboriginal rights and titles.

Colin Grier, Washington State University

Colin Grier is an Associate Professor in the Department of Anthropology at Washington State University (Vancouver). His archaeological research concerns complex hunter-gatherer-fisher societies worldwide, with a particular emphasis on reconstructing the ancient and recent histories and past practices of peoples of the Northwest Coast of North America. He is particularly concerned with elucidating alternate forms of political and social organization that can promote sustainable economies, including decentralized forms of resource control. His recent publications relate to monumentality and terraforming practices amongst hunter-gatherer-fisher societies, documenting the extent to which these societies actively constructed their landscapes for social, economic and political ends. His current field research, funded by the US National Science Foundation, involves using geophysical methods to map subsurface plankhouse architecture so as to better illuminate changing household and community organization in the Salish Sea region of the west coast of North America.

Kisha Supernant, Institute of Prairie and Indigenous Archaeology, University of Alberta

Kisha Supernant is Métis, Director of the Institute of Prairie and Indigenous Archaeology, and an Associate Professor of Anthropology at the University of Alberta. An award-winning teacher, researcher, and writer, her research interests include the relationship between cultural identities, landscapes, and the use of space, Métis archaeology, decolonization, and heart-centered archaeological practice. Her research with Indigenous communities in western Canada explores how archaeologists and communities can build collaborative research relationships. She leads Exploring Métis Identity Through Archaeology (EMITA), a collaborative research project which takes a relational approach to exploring the material past of Métis communities, including her own family, in western Canada. She is currently a co-investigator on Cartographies of Deep Time, a recently funded SSHRC Insight Grant project that explores the complexities of history and different ways of knowing with Tsimshian communities in British Columbia. Recently, she has been increasingly engaged in using remote sensing technologies to locate and protect unmarked burials at the request of First Nations communities in Alberta and Saskatchewan. She has published in local and international journals on GIS in archaeology, collaborative archaeological practice, Métis archaeology, and indigenous archaeology in the post-TRC era.